AARHUS
UNIVERSITY

New Resorption Pathways in Polycaprolactone Degradation; roles of Mononuclear and Multinucleated Giant Cells

PhD dissertation

Halldór Bjarki Einarsson

Health
Aarhus University
2015

Dedicated to the loving memory of
Pétur Davíð

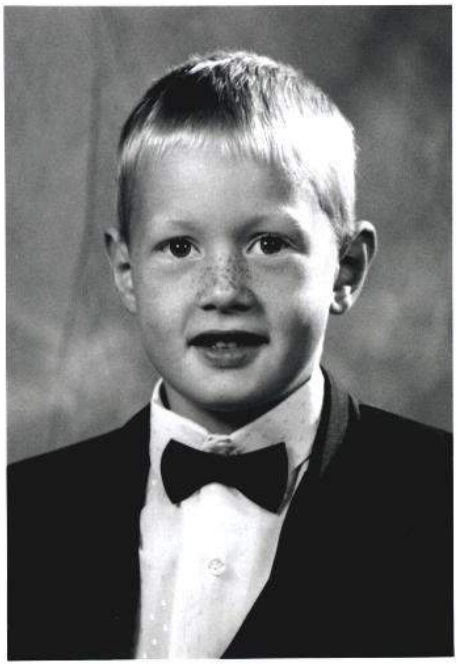

1990-1999

The science of matter

"All matter originates and exists only by virtue of a force which brings the particle of an atom to vibration and holds this most minute solar system of the atom together. We must assume behind this force the existence of a conscious and intelligent mind. This mind is the matrix of all matter."

- Max Planck, 1858-1947

Main supervisor
Professor Cody Eric Bünger, MD, DMSc
Department of Orthopaedics, Spine Unit
Aarhus University Hospital
Denmark

Co-supervisor
Professor Thomas Vorup-Jensen, MSc, PhD, DMSc
Department of Biomedicine, Aarhus University
Denmark

Principal investigator
Halldór Bjarki Einarsson, MD
Department of Orthopaedics, Spine Unit
Aarhus University Hospital
Denmark

Public Defence (*viva*)
Date & time: June 19th 2015 14 p.m.
Venue: K-auditorium, Institute of Pathology
Aarhus University Hospital, builing 7
Nørrebrogade 44
8000 Aarhus C
Denmark

Correspondence
Halldór Bjarki Einarsson, MD
Orthopaedic Research Laboratory
Aarhus University Hospital, KH
Nørrebrogade 44, Building 1A
8000 Aarhus C, Denmark
E-mail: hbe@clin.au.dk
Tel: +45-5040 3839

Assessment committee
Professor Stuart B. Goodman, MD, PhD, FRCSC, FACS, FBSE
Department of Orthopaedic Surgery & Bioengineering
Stanford University School of Medicine
Stanford, California
USA

Dr. Marco N. Helder, MSc, PhD, director of STEGA
Department of Orthopaedic Surgery
Institute for Regenerative Medicine
VU University Medical Center
Amsterdam, North Holland
The Netherlands

Chairman
Professor Thorsten Ingemann Hansen, MD, DMSc
Department of Public Health
Aarhus University
Denmark

Viva
Chairman
Professor Stephen Jacques Hamilton-Dutoit
MD, FRCPath. Institute of Pathology
Aarhus University Hospital
Denmark

Contents

Work of writing & list of papers

The work described in this PhD dissertation was carried out at the Spinal Unit Aarhus University Hospital, Department of Biomedicine, Aarhus University and Yale University School of Medicine. In addition, the Graduate School's integrated MD/PhD program at Aarhus University (GP Biomedicine) was followed. The PhD dissertation is based on a monograph with incorporated seven inter-connected studies. Supplementary work performed during the course of the MD/PhD program is included under appendix. A summary with declaration concerning the monograph has been signed by the PhD student and the main supervisor.

Monograph *New Resorption Pathways in Polycaprolactone Degradation; roles of Mononuclear and Multinucleated Giant Cells*

Supplementary work

Paper 1 *Cui W, Cuartas E, Ke J, Zhang Q, Einarsson HB, Sedgwick JD, Li J, Vignery A. CD200 and its receptor, CD200R, modulate bone mass via the differentiation of osteoclasts. Proc Natl Acad Sci USA. 2007; 104(36): 14436-41*

Paper 2 *Greisen SR, Einarsson HB, Hvid M, Hauge E, Deleuran B, Kragstrup TW. Spontaneous generation of functional osteoclasts from synovial fluid mononuclear cells as a model of inflammatory osteoclastogenesis. Manuscript submitted; Acta Pathologica, Microbiologica et Immunologica Scandinavica*

Paper 3 *Jalilian B, Christiansen SH, Einarsson HB, Mehdi R, Petersen E, Vorup-Jensen T. Properties and prospects of adjuvants in influenza vaccination - messy precipitates or blessed opportunities? Molecular and Cellular Therapies, 2013 Vol. 1,2*

Paper 4 *Jalilian B, Einarsson HB, Vorup-Jensen T. Glatiramer acetate in treatment of multiple sclerosis: a toolbox of random co-polymers for targeting inflammatory mechanisms of both the innate and adaptive immune system? Int J Mol Sci. 2012; 13(11): 14579-605*

Acknowledgements

In “going for it” with all my capacity, strength, and sagacity, I’m most grateful to Aarhus University, the supervisors, and the people who gave me this opportunity, believed in the project, and gave their solid support at every step of the way. Just as life goes in general, not all things went safely and smoothly throughout this path. In spite of my many failures during the PhD journey, they didn’t determine the end result, because formed by reactions to those many mistakes, and with the willingness of harness, I came through more open-minded. That is thanks to all of my friends and family, my dear lab mates, and Pétur Davíð, who taught me how to conquer fear.

Project funding

Gratefully received from The Lundbeck Foundation Nanomedicine Centre for Individualized Management of Tissue Damage and Regeneration, The Danish Rheumatism Association (stipendium nr. R67-A994), AP Møller fund for Icelandic students (Dansk-Islandsk samfund), Fabrikant Einar Willumsens Mindelegat (nr. jkc/bl 800.211) and from Aarhus University.

Abbreviations

ANOVA	analysis of variance
APC	allophycocyanin
BSA	bovine serum albumin
$CaCl_2$	calcium chloride
CCR5	chemokine (C-C motif) receptor 5
CD	cluster of differentiation
CD/m^2	candela per square metre
CI	confidence interval
CXCR4	chemokine (C-X-C motif) receptor 4
DAPI	4' 6-diamidino-2-phenylindole dihydrochloride
DC-STAMP	that dendritic cell-specific transmembrane protein
Delta H	change in enthalpy
Delta G	change in Gibbs free energy
DMA	dynamic mechanical analysis
E''	loss modulus
E'	storage modulus
EDTA	ethylenediaminetetraacetic acid
ELISA	enzyme-linked immunosorbent assay
Eu^{3+}	oxidation state +3 of europium
FACS	fluorescence-activated cell sorting
F-beads	fluorescent carboxyl polymer microspheres
FBGCs	foreign body giant cells
FCS	fetal calf serum
FITC	fluorescein isothiocyanate
FSC	forward scatter
HCl	hydrogen chloride
HIV	human immunodeficiency virus
HSV	herpes simplex virus
HV	high voltage
IFN-γ	interferon gamma
Ig	immunoglobulin
IL	interleukin
K	degradation rate constant
KIM127	IgG1 mAbs against CD18 from hybridoma cell lines CRL-2838
KIM185	IgG1 mAbs against CD18 from hybridoma cell lines CRL-2839
LVD	low voltage detector
mAbs	monoclonal antibodies
MAC	membrane attack complex
M-CSF	macrophage colony stimulating factor
$MgCl_2$	magnesium chloride
MMA	methylmethacrylate
M_n	molecular weight
M_n°	initial molecular weight
MNC	mononuclear cells
MNGCs	multinucleated giant cells
MSC	mesenchymal stem cells
MTT	methylthiazolyldiphenyl-tetrazolium bromide
NaCl	sodium chloride
NaOH	sodium hydroxide

NK cells	natural killer cells
NSE	non-specific esterase
OPG	osteoprotegerin
OPN	ostepontin
PBS	phosphate buffered saline
PC7	phycoerythrin cyanin 7
PCL	poly(ε-caprolactone)
PE	phycoerythrin
PMNCs	peripheral blood mononuclear cells
QQ	quantile-quantile
R^2	coefficient of determination
RANK	receptor activator of nuclear factor-kappa B
RANK-L	receptor activator of nuclear factor-kappa B ligand
RGD	amino-acid sequence motif Arg-Gly-Asp
RPM	rotation per minute
SEE	standard error of the estimate
SEM	scanning electron microscopy
siRNAs	small interfering ribonucleic acid
sMAC	soluble membrane attack complex
SSC	side scatter
TBS	tris-buffered saline
TCR	T cell receptor
TFE	2,2,2-Trifluoroethanol
TGF-β3	transforming growth factor beta 3
TRAP	tartrate resistant acid phosphatase
TRIFMA	time-resolved immunofluorimetic assay
WD	working distance
αMEM	alpha minimum essential medium

Summary

Prerequisite for scaffold tissue engineering is to establish knowledge about host reactions toward the individual components. Exogenous antigens are defined as molecules that can specifically evoke immune response, however these are generally recognized as being proteins or polysaccharides of microbial or "non-self" origin. Introduction or insertion of foreign body materials into the organism leads often to cell fusion of mononuclear cells, in addition to formation of syncytial giant cells (foreign body giant cells). As an attempt to find an answer to the above raised consideration, poly-caprolactone (PCL) was used in the present project, which chemical composition consists of repeating $C_6H_{10}O_2$ monomers bound by ester-linkage. This polyester has previously been suggested as a promising template of choice for tissue regeneration hence restoration of tissue function via seeded mesenchymal stem cells (MSC) on the template. Furthermore, template functionalization is another tissue engineering approach often applied as an attempt to control the genesis of specific and desired tissue type. Increased cell performance as well as the formation of cartilage or bone tissue in a 3D microenvironment by trans-differentiation of MSC to chondrocytes and osteoblasts has previously been discovered. It is based on polymorphism in the population that the challenge arises regarding development of a prominent and individualized tissue engineered template. Precisely due to this perspective, in conjunction with the results already published and the great social significance of this source of research, the major purpose of the present project was to investigate the effect of cell fusion and thus the effect of syncytial giant cells on PCL. This project has led to new knowledge within the field of regenerative medicine, as the results indicate that osteoclast-like cells mediate degradation of PCL via phagocytosis. In addition, the findings from this project suggest that PCL can act as an antigen. This in all probability is explained by the observed increased β_2-integrin shedding and the complement activation, which the author suggests supports the final conclusion: that phagocytosis occurs after PCL opsonization via complement component surface coating. Other results considered to rationalize the idea that PCL provoke immunological reactions, are the additional cell fusion findings, differentiation of mononuclear cells into osteoclast-like cells and their increased phagocytic capabilities in the presence of T cells.

Danish summary / Dansk resumé

Et fundamentalt led i forbindelse med undersøgelse af de antagede biokompatible vævsskabeloner inden brug til vævsrekonstruktion med det formål at genoprette normale vævsfunktion fx efter vævsskade, vedrører skabelonens potentiale evne til at fremkalde immunologiske reaktioner. Eksogene antigener defineres som molekyler, der netop kan fremkalde immunrespons, men disse er normalt anerkendte som værende proteiner eller polysakkardier af mikrobiel eller "fremmed" oprindelse. Introduktion eller indføring af fremmedmaterialer i organismen medfører cellefusion af mononukleære celler samt dannelsen af syncytiale kæmpeceller. I projektet blev der anvendt polyesterskabelon, hvis kemiske sammensætning består af gentagende $C_6H_{10}O_2$ monomerer linket vha. esterbindinger dvs. polycaprolactone (PCL) og som tidligere har været foreslået som et lovende skabelonvalg for vævsregeneration til genoprettelsen af vævsfunktion via skabelonens påførte mesenkymale stamceller (MSC). Endvidere vælger man ofte ved denne form for vævsteknologi at funktionalisere disse vævsregenerationsskabeloner mhp. at danne et grundlag for kontrolleret vævsgenese. Øget celle-ydeevne samt dannelse af knoglevæv i et 3D-mikromiljø fremgår af tidligere opdagelser om trans-differentiering af MSC til kondrocytter og osteoblaster. Det er på baggrund af polymorfismen i befolkningen, at udfordringerne opstår mhp. udvikling af den mest prominente og individualiserede vævsskabelon. Netop det perspektiv, sammenholdt med de allerede opnåede resultater og den store samfundsmæssige betydning, har medført det hermed præsenterede projekt, hvor formålet har været at undersøge effekten af cellefusion og dermed effekten af syncytiale kæmpeceller på skabelonen. Projektet har ført til ny viden inden for regenerativ medicin, idet resultaterne indikerer, at osteoklast-lignende celler medierer degradering af skabelonen via fagocytose. Endvidere antyder fundene, at materialet PCL i en vis forstand virker som et antigen. Det forklares formentlig af den øgede β_2-integrin ekspression og shedding samt af den observerede komplementaktivering, der også understøtter den endelige konklusion: at fagocytosen først kan opstå efter PCL-opsonisering via komplementkomponenternes overflade-beklædning. Øvrige resultater der rationaliserer idéen om, at PCL fremprovokerer immunologiske reaktioner, er yderlige cellefusionopdagelsen, uddifferentieringen af de mononukleære celler til osteoclast-lignende celler samt øget fagocytoseevne af disse celler i forbindelse med tilstede-værelsen af T-lymfocytter.

1. Introduction

1.1 Historical background

In 1665 Robert Hooke, an English natural philosopher, architect and mathematician, was the first to discover the cell. Hooke had a passion for science and with his microscope, originally constructed by Christopher White in London he observed, characterized and described through his drawings the basic cell structure of a cork. This finding was published in his book Micrographia, among other important observations and investigations, for instance fossilized woods, leading him to draw the conclusion that fossilized objects are the remains of living organisms. Hooke's observation of the cell was a major scientific breakthrough and along with improved magnifying glass lenses the foundation for the cell theory was established. The contributions to basic cell biology by Theodor Schwann, Antonie van Leeuwenhoek, Matthias Jakob Schleiden and Rudolf Virchow from the 16th to 18th century, were in addition an important step forward to the notion that the cell governs the basics of life, as later indicated by the cell theory. In nearly all undergraduate textbooks on cell biology, the reader is introduced to the cell as the basic unit of life with one nucleus, cell organelles and cytoplasm surrounded by a cell membrane associated with anchored proteins. The ancestors to this basic unit are the prokaryotes, cells without a nucleus. Another typical example for enucleated cells, are the red blood cells. Multinucleated cells however, are rarely mentioned as another exception from the basic cell structure. These polykaryons or multinucleated giant cells (MNGCs) can be found in placenta, skeletal muscles and in bone. Occurrence elsewhere is abnormal (1).

1.2 Cell fusion

Regardless of cell origin, the cell fusion process is dependent on survival of the progenitor cells, differentiation of precursors and degree of activation in addition to fusion protein expression. Cell fusion between two or more eukaryotic cells and its mechanisms have been discovered and described for various normal homeostatic conditions. The most well-known example, from early life development, is the fusion of an oocyte and spermatozoa. After fertilization and by the 8th day of development, the blastocyst is partially embedded within the endometrial stroma and its

trophoblast has differentiated into two layers. The inner layer is composed of mononuclear cells (MNCs) i.e. the cytotropoblast and the outer layer of a multinucleated zone. It is this multinucleated zone, which over the course of embryonic development loses its individual cell membrane barriers that penetrates deep into the surrounding stromal tissue. This form of penetration, or erosion of the associated endothelial lining cells of maternal capillaries within the stromal tissue, represents the early stage of placenta formation. The MNGCs provide the placenta various life supporting endocrine properties, ensuring maintenance of the corpus luteum until termination of the fourth mouth of development, through the production of human chorionic gonadotropin, production of progesterone, leptin and human placental lactogen. During the process of embryogenesis, a significant portion of the muscular system develops after fusion of paraxial mesodermal derived myoblasts, into characteristic multinucleated cells. These most often extremely extended multinucleated skeletal muscle cells are cylindrical in shape, hence they often are termed muscle fibers, where individual fibers are separated from each other by their sarcolemma. It is through clustering of these muscle fibers, the connection to the nervous system (where individual fibers receive fine-tuned motor stimulation), their above described morphology and intracellular expression of actin and myocin, as well as through their reserve of calcium ions within the sarcoplasmic reticlulum, that body movement is primarily controlled. Yet another example of MNGCs within the organism, are osteoclasts (figure 1) which are reported to derive from circulating peripheral blood monocytes. It is at the location of bone microenvironment, that these monocytes through regulation of osteoprotegerin, receptor activator of nuclear factor-kappa B and its ligand (called the OPG-RANK-RANK-L system), that a physiological foundation for formation of these MNGCs is created. In addition, a certain pre-cursor cell density at this location, is thought to be a key factor for the occurrence of fusion, prior to differentiation into fully functionalized osteoclasts, which are able to resorb bone.

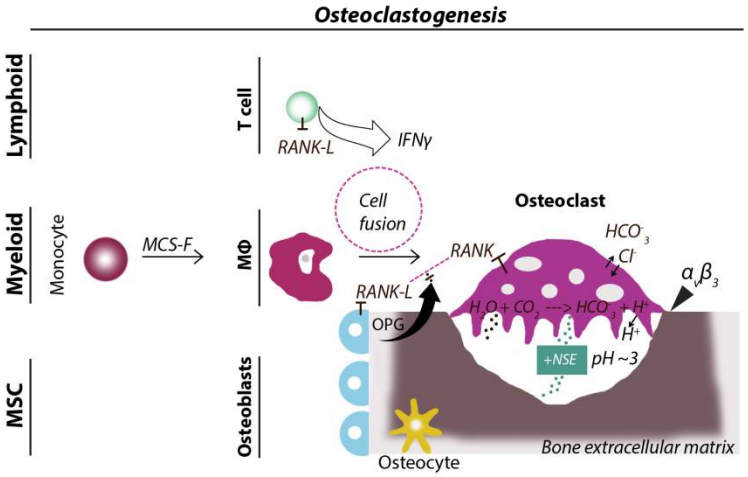

Figure 1: The bone remodeling unit and basics steps of osteoclast formation. Osteoclast and osteoblast activity is coordinated by a number of well-described hormones and paracrine signal molecules to maintain bone remodeling and homeostasis. Many of these signal molecules and corresponding receptor are already being targeted by commercial drugs. Osteoclasts are MNGCs that reabsorb bone. They are derived from haematopoietic pro-genitor cells of the myeloid cell type that gives rise to both the monocyte-macrophage lineage and the osteoclast lineage (2). These pre-cursor cells form mature osteoclasts upon fusion and multinucleation, and play a key role in the remodeling process; a process which relies on complex 3D interactions between the bone matrix, bone-forming osteoblasts, and bone-degrading osteoclasts (2, 3). The central machinery set in motion for induction of osteoclastogenesis is fusion of macrophages and the RANK-L/RANK/OPG system (4). This refers to a crosstalk between two tissue types originating from two different stem cells and germ layers (5), i.e. the immune system and bone tissue (osteoimmunology).

1.3 Endogenous induced cell fusion

Back in 1838, Rudolf Virchow's German and doctoral advisor at the Charité University Hospital in Berlin, Dr. Johannes Peter Müller, was the first scientist to discover cell fusion and polykaryocytosis associated with neoplasms. Since then, cell fusion and the formation of MNGCs has been detected in many types of cancers, often resembling Warthin-Finkeldey cells, first described by Warthin and Finkeldey in 1931 (6). Some sixty years later Kamel *et al.* came up with some interesting findings, showing Warthin-Finkeldey cells expressing CD3 (7). Their observations have in other words shifted our novel understanding and focus, which concentrates on haematopoietic progenitor cells of the myeloid type lineage as the primary source of origin for the formation of MNGCs in a pathological condition. In their paper, Warthin-Finkeldey cells are revealed to derive from T cell precursors, based upon the above mentioned marker, hence the genesis of these cells occurs upon the multi-nucleation of haematopoietic progenitor cells of the lymphoid lineage. Fused lymphocytes have in addition been identified in the systemic autoimmune disease lupus erythematosus (8). Other, more

infrequent diseases however, i.e. Langerhans cell histiocytosis (9), Wegener's granulomatosis, Sarcoidosis and idiopathic giant cell myocarditis, Horton Disease, Kimura disease (10), Xanthoma, Xanthogranuloma and fat necrosis (Touton giant cells), reveals similar giant cell pathohistology. For many of these endogenous induced cell fusions, giant cells of the same phenotype are observed as for the exogenous induced cell fusions (Langhans giant cells).

1.4 Exogenous induced cell fusion

The fusion reaction phenomenon between a viral pathogen and a host cell is most often acknowledged as an example of virulence evolution. It in other words enables the pathogens to hide from the host immune response and keeps them at a latent stage within a syncytium. Major infectious diseases like measles, mumps, croup and infant bronchiolitis are associated with the paramyxoviruses, and their shared pathogenic properties among others are MNGC-formations or syncytium (hence the terminology respiratory syncytial virus for infant bronchiolitis). Entry of viruses to a host cell via viral-cell fusion is best described by human immunodeficiency virus (HIV), which has a virus tropism for T cells expressing the CD4 antigen and cells of the macrophages lineage (monocytes and kupffer cells, representing over 80% of the tissue macrophages within the human organism, and the remaining 20% being tissue macrophages like microglia cells of the brain (11), alveolar and peritoneal macrophages, osteoclasts and dendritic cells of the skin). After binding of HIV gp120 to CD4 and its co-receptor (chemokine receptor) on the target cell, the virion-cell-membrane fusion is mediated by the binding of HIV gp41 to CD4 and its co-receptor (fusin) resulting in a release of the viral nucleocapsid into the target cytoplasm. The macrophage lineage cells express both the CCR5 and CXCR4 chemokine receptors, hence they can be potentially infected by both M- and T-tropic virions. Additional examples of viruses, able to cause membrane fusion, are orthomyxoviruses or influenza virus type A, B and C. The viral hemagglutinin, a glycoprotein expressed and anchored on the virion envelope, binds to sialic acid-containing receptors on the surface of epithelial cells in the upper respiratory tract. This binding promotes the viral envelope to fuse with the target cell membrane. The author has previously reported a third viral-cell fusion example (12) and by that indicated herpes simplex virus (HSV), whit two different antigen types, leading to fusion between not only virion and target cell, but additionally to

morphological changes of the infected cells, formation of nuclear inclusions bodies and syncytial giant cells. Other herpes family virions like e.g. varicella-zoster can moreover trigger fusion of target cells. Since the discovery of the tubercle bacillus by the German physicist Robert Koch in 1882, cell fusion or the formation of MNGCs has been widely recognize, to rise from infection with various bacterial species. In the case of bacterially induced cell fusion, granuloma formation - including fused macrophages within these granulomas - is a histopathological diagnostic criterion for tuberculosis (13). The disease pathogenesis is initiated by alveolar macrophage phagocytosis or engulfment of the airborne *mycobacterium tuberculosis bacilli*. In this initial phase the mycobacteria replicates intracellularly and activates $CD4^+$ and $CD8^+$ lymphocytes. The recruitment of T cells to the side of primary infection is regulated by the concentration gradient of the chemotactic factors produced by the characteristic fused macrophages, formed after the engulfment of the mycobacterium. This is the first step in tubercle bacillus induced granuloma formation known as a tubercule. The infected macrophages ultimately get attacked by intact macrophages, leading to their fusion and the formation of Langhans cells, named after the German pathologist Theodor Langhans. Moreover, *Treponema pallidum* causes the venereal disease Syphilis in which Langhans giant cells can be detected. These giant cells are in addition the trademark of other granulomatous and non-infectious diseases, and recently the pathophysiological mechanisms initiating Langhans giant cell formation has been partly recognized by a Japanese research group, as noted below. Granulomas are usually surrounded and infiltrated with T cells. Sakai *et al.* establish a co-culture system and by negatively selecting human monocytes which were stimulated with the Concanavalin A prior to autologous CD3+ cell exposure. Their results, of three independent co-cultures, show a significant increase in Langhans giant cell formation, via the interferon gamma (IFN-γ) stimulation provided by the T cells and signaling processes involving CD40-CD40L interactions. The group observed additionally, that dendritic cell-specific transmembrane protein (DC-STAMP) was involved in the fusion process of Langehans giant cell formation (14). Similar findings have been reported by Yagi *et al.* about DC-STAMP's role for yielding the multinucleation of pre-osteoclasts, the formation of foreign body giant cells (15, 16) and were furthermore reported for various parasitic infections (*Neurocysticercosis* and *Cerebral sparganosis*) (17, 18) and fungal infections (*Candida albicans, Aspergillus, Cryptococci* and *Histoplasma*) (19-23).

1.5 Granuloma formation

The etiology of granulating inflammation is recognized to be both of non-infectious and infectious origin, meaning that granuloma formation is the result of a secondary reaction, seen after various tissue damages, which can be induced both endogenously and exogenously. Histophathological evaluation reveals circular accumulation of macrophages (histocytes or foam cells), and because these cells have phagocytic capabilities, the zone is often referred to as the resoptive zone. Syncytial formations within the zone are common and it is difficult to distinguish individual cell borders from each other. The granulated tissue, surrounding this innermost zone, is composed of fibroblast and T lymphocytes, which is why CD3 expression was investigated in the present project. Healthy tissue, separated from necrotic tissue, resportion of damaged tissue and reparation are among the basic functions of granulomas. Formation of a foreign body granuloma is a common host response directed against foreign material, which has been lodged for any given reason into the human body. Inhalation of foreign macro- and/or microparticles can give rise to granulomatous inflammation in the respiratory tract as well as in the lung parenchyma itself. *Pneumoconiosis* like *asbestosis, silicosis, siderosis* and *anthracosis*, are all work-related illnesses that ultimately can lead to emphysema (24) or irreversible restrictive lung diseases (interstitial pulmonary fibrosis) (25, 26). It is now well documented in the literature that inhaled asbestose fibers, microscopically visible as *ferruginous bodies*, can cause lung cancer (27, 28) - primarily adenocarcinoma and mesothelioma - and that the overall incidence of cancer has increased by factor 3, compared to the background population (29). Since the first discovery of asbestose induced mesothelioma in 1960 (cited by Ribak *et al.*) (30) a call for legislation to prohibit industrial use of these hazardous silicate minerals has seen the daylight in many industrial countries. It is worth noticing that the terminal conditions caused by asbestose fibers are initially launched as a foreign body induced inflammatory reaction. This has been shown *in vitro*, by enzyme-linked immunosorbent assay (ELISA) and detected increased interleukin (IL) 8 production (31), and in an animal model, by revealing MNGCs associated to foreign body asbestose fibers (32). Still, millions of workers worldwide are exposed on a daily basis to foreign materials or particle dust while e.g. manufacturing aluminum, iron and steel, glass, rubber, leather, textiles and plastic. In addition to the airway route of entry, foreign body materials can reach the gastrointestinal tract (33), gain access to the body via systemic administration of a

pharmacological agent or vaccination (34), by injection of biological filler materials for soft tissue augmentation (35-38), trans-dermally by an accident (39) and directly via wound occlusion dressing (40) or suturing (41). Reported as early as in 1974 and although specified as absorbable sutures, by the manufacturers, these sutures can bring forward a foreign body reaction (42). With the increased use of surgical implants and medical devices in humans for the last several decades, aseptic loosening and the etiology of implant failure has been brought to our attention. This has moreover created an opportunity to study the host response to implants more thoroughly and the characteristics of foreign body giant cells (FBGCs) associated to the implants. State of the art implants for stabilizing, supporting and for major augmenting of damaged tissue, in addition to many approved life-supporting medical devices (artificial pacemakers and biosensors) can evidently all induce recruitment and infiltration by macrophages and T lymphocytes at the side of material implantation, and hence trigger accumulation of FBGCs (43-47).

1.6 Integrins & the complement system

Integrins, are heterodimeric proteins consisting of an α- and β-chain (figure 2), with transmembrane and cytoplasmatic domain (48). The external domains of a number of integrins recognize extracellular matrix proteins like ostepontin (OPN) via interaction with specific amino acid motifs. The cytoplasmic domain of these heterodimers associate, in turn, with intracellular molecules particularly those involved in downstream signaling and organization of the cytoskeleton (49). Human osteoclasts express at least three integrins, $\alpha_V\beta_3$, $\alpha_2\beta_1$ and $\alpha_V\beta_1$; $\alpha_V\beta_3$ (figure 1) is also known as the vitronectin receptor, and these integrins are known to mediate cell to extracellular matrix attachment (50). The amino-acid sequence motif Arg-Gly-Asp (RGD) is present in the ligands for certain integrins, and this short sequence can serve as a specific binding site for the integrin. Many matrix proteins, including OPN, contain the RGD sequence (51). Given their capacity to bind extracellular matrix proteins, integrins are likely candidates to mediate osteoclast-bone and osteoclast-grafts substitute attachment. The β_1 and β_2 integrin expression by osteoclast precursors, i.e. monocytes, has been reported to play co-operative role in cell adhesion during the formation of MNGCs (52).

The role of osteoclast β_2-integrin mediated adhesion to bone extracellular matrix nevertheless not been studied. Therefore, this study will focus on the role of β_2-integrins in osteoclast and FBGC adhesion. The aim is to add new dimension to osteoclast research, by mainly using 3D scaffolds for adhesion substrates.

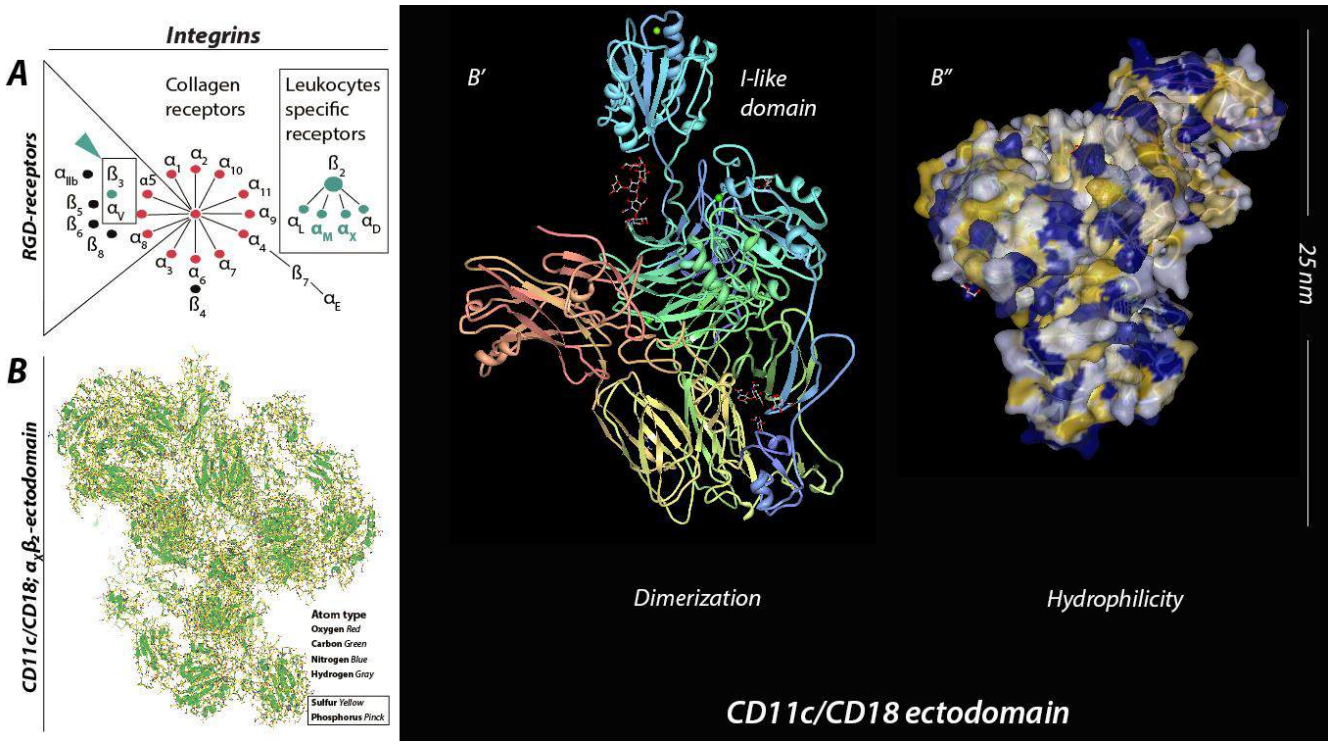

Figure 2: The family of integrin receptors. Integrins represent the major cell surface receptors responsible for attachment of cells to their surrounding extracellular components. Integrins are transmembrane proteins and consist of alpha and beta subunits (αβ heterodimers). For protein ligand interactions, integrins bind to short amino acid sequences and the first characterized sequence was Arg-Gly-Asp; the RGD integrin recognition sequence. (A) Osteoclast $\alpha_v\beta_3$ RGD-receptors (green arrow additionally indicated in figure 1), in addition to leucocyte-specific receptors (the β_2 receptors) are outlined and given a special attention. Complement receptors 3 and 4, known as CR3 (CD11b/CD18; integrin $\alpha_M\beta_2$) and CR4 (CD11c/CD18; integrin $\alpha_X\beta_2$) bind to a large number of non-protein and protein ligands. They all have an I-domain (B') which is important for the ligand binding interaction. (B) CCP4 Molecular Graphics software (University of York, UK) was used after successfully loaded PDB-file (3K6S) for the $\alpha_X\beta_2$ ectodomain from the research laboratory for structural bioinformatics protein database (RCSB PDB). The CCP4 software is intended for analyzing macromolecules and enables visualization of sulfur and phosphorus atoms, hence hypervalency sites and hydrophilicity (B''). The probability for interactions increases with greater valency. The figure is modified from reference (53).

Prior to phagocytic mediated degradation of a foreign body materials, these complement receptors must bind to the involved complement components, after material recognition and opsonization. Activation of the system is triggered via classical, lectin and alternative pathway (figure 3).

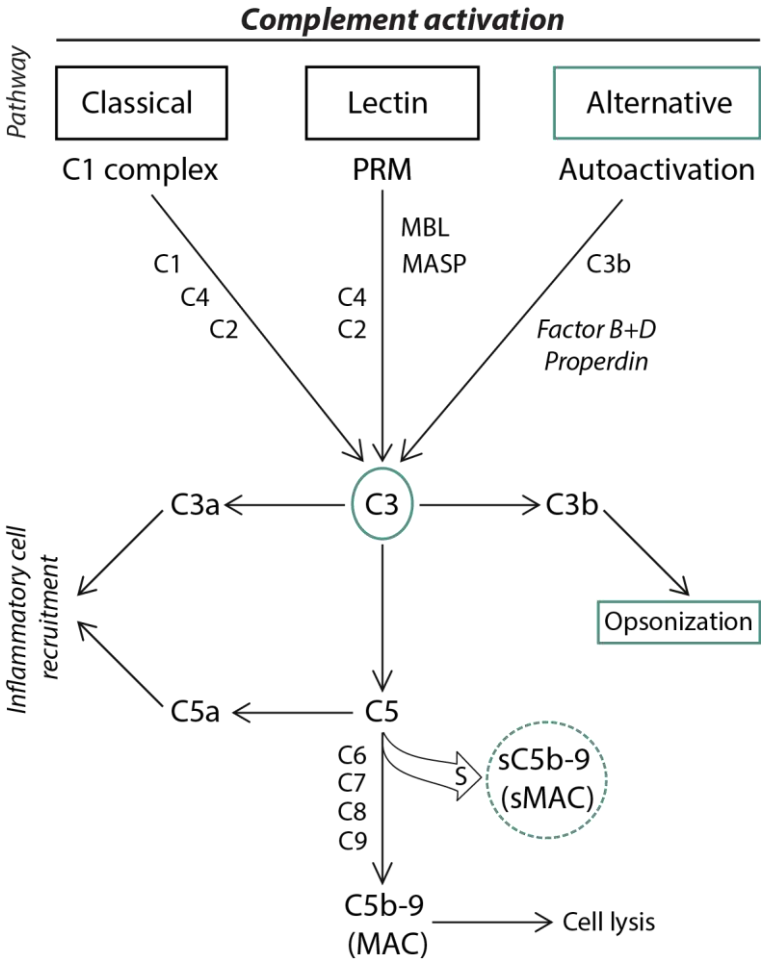

Figure 3: The complement system. This part of the immune system plays a central role in the recognition and opsonization of pathogens and is brought into action once foreign antigens are identified. All three pathways converge on the same reaction, leading to cleavage of the complement component C3 into C3a and C3b fragments. The component C3b then tags pathogens (opsonization) prior to engulfment of the entire pathogen-C3b complex by phagocytes. The final product in the cascade is the formation of membrane attack complex (MAC) which assembles to generate pores in the pathogen membrane leading to lysis. Hence, experimental detection of this end-product reveals complement activation in general. The figure is modified from references (54, 55).

1.7 Osteoclast function in bone tissue engineered alternative

Bone grafts or bone grafts substitutes are frequently needed for the surgical treatment of extensive bone loss or diseased bone tissue caused by; trauma, tumor, infection, degeneration, or congenital abnormalities. Autologous bone graft is currently the only available source of viable bone graft. It is usually harvested from the iliac crest, requiring an additional surgical procedure. Autograft has been the gold standard for the reconstruction of osseous defects by supplying both osteoinductive growth factors, osteogenic cells, and a structural scaffold. Nevertheless, bone autografting is

associated with several drawbacks. First, the availability of autologous bone graft is limited, which precludes its use for surgical procedures requiring extended amounts of bone graft material. Furthermore, the harvesting procedure is associated with donor site morbidity, i.e. pain, neuro-vascular injury, and infection at the harvest site (56-60). Implantation of allogeneic bone is an alternative to bone autografting. Allografts are usually acquired from cadaver bone or femoral heads from patients undergoing hip replacement surgery. One of the disadvantages linked with allografting is the potential risk of HIV transmission and/or transmission other viral or bacterial pathogens (61). Therefore tissue banks routinely screen cadaveric serum, and several physical and chemical methods have been developed for allograft processing (62-69). These methods may however cause reduced osteoinductive capacity of the allograft material, increasing the risk of pain and re-operation as a consequence of graft failure (70-74). The risk of graft infection and host rejection are further limitations of allografting (75, 76). In addition, injectable bone cements, metal-based joint replacement prostheses and metallic bone prostheses are widely used in the clinic as to restore bone defects, and these approaches provide immediate structural support (77-79). Drawbacks include supercritical rapid resorption rates, the potential for thermal necrosis and bone loss around the cement due to stress-shielding (80-83). Several synthetic and naturally occurring biomaterials have been recognized as void fillers for osseous defects for use alone or in combination with bone forming cells (84-94). Many previous studies in bone tissue engineering have focused on bone formation from both mature and marrow-derived osteoblasts on various scaffolds, and these experiments demonstrate that bone can be generated by tissue-engineering techniques (95-97). Osteoconduction, osteoinduction, and remodeling are important events that take place once the constructs have been implanted (98-100). Within the tissue engineering paradigm ”the implanted construct” which includes a scaffold cultured with cells, will eventually ideally convert itself into a tissue morphology mimicking native tissue. This will include bone remodeling, but especially it also includes the degradation and disappearance of the scaffold. Implantation of poly(ε-caprolactone) (PCL) constructs, has been suggested as a promising alternative to state of the art bone tissue repairing techniques, and as a template of choice to support bone regeneration (101). PCL is a linear semi-crystalline polyester and synthesized by ring-opening polymerization of cyclic epsilon caprolactone in the presence of a catalyst (102). PCL is

considered to be biocompatible polyester, known to be biodegradable via abiotic hydrolysis, has a melting point of 55-60˚C and tensile strength of ~23 MPa (103). Hence, PCL is a load-bearing structure, which brings about biomechanical support. In brief, PCL can serve as a template for tissue regeneration if seeded with stem cells, functionalized after additive manufacturing or compartmentalization of essential siRNAs to trigger genesis of specific tissue at the site of implantation and even as a drug delivery vehicle (104, 105).

Prerequisite for scaffold tissue engineering is to establish knowledge about host reactions toward the individual components. Therefore, for the present monograph, potentially provoked immune stimulatory responses to PCL were investigated. The major aim was to study target effects of MNGCs on PCL. The sub-aims of the investigations covered 7 main areas of basic research:

The aims of *in vivo* studies 1-2

1. To qualitatively and quantitatively investigate for granuloma and FBGC formations at the site of PCL implantation
2. To quantitatively investigate the scale of T cell recruitment, to the site of PCL implantation

The aims of *in vitro* study 3-7

3. To investigate differentiation of negatively selected cells of the monocytes-macrophages lineage to osteoclasts on PCL in static cultures
4. To investigate the role of β_2 (CD18) integrins in MNGC-to-PCL adhesion
5. To investigate resorption of PCL constructs by activated osteoclast-like cells and compare the MNGC-mediated resorptive degradation of PCL in monoculture and in a T cell co-culture setting, with the chemical, i.e. the hydrolytic degradation
6. Investigate the potential for complement activation, induced by PCL itself
7. To study PCL's mechanical properties prior to culturing and after cell mediated degradation

This brought forward the following hypothesis, that the degradation of PCL by hydrolysis is further directed by resorption and phagocytosis, mediated by mononuclear and MNGCs.

2. Methodological considerations

2.1 *In vivo* samples

Bioscaffolder (SysEng, Hünxe, Germany) produced 3D/cylinder-shaped (10 x 10 mm) PCL scaffolds (50 kDa, Perstorp, UK), with high porosity (approximately 1000 µm fiber distance and with a 0/105 degree pattern) were produced with the deposition speed of 600 mm/min. Prior to implantation, the scaffolds were sterilized by ethanol exposure at [96%], [70%] and [50%] with the duration time of 30 min. for each sterilization step, followed by rinsing in sterile water and removal of solvents in a vacuum chamber. To increase hydrophilicity of the PCL constructs, scaffolds were treated with 1.25 M NaOH for 16 H:

$$NaOH_{(S)} \xrightarrow[-\Delta H]{H_2O_{(l)}} Na^+_{(aq)} + OH^-_{(aq)}$$

This chemical reaction is an exothermic dissolving process, i.e. the enthalpy of solvation is negative (-ΔH). Hence, it was necessary to cool down the solution to room temperature before the 16 H treatment. This step was followed by neutralization with 1 M HCl for 1 H and rinsing in sterile water. The sodium hydroxide treatment was performed as an attempt to improve MNGC and T cell attachment (referring to the increased hydrophilicity). The theoretical background is that hydroxide ions solutes in the solution act as nucleophiles, meaning that OH^- donates electron to an electrophile to form intermolecular bonds (hydrogen bonds). The potential for hydrogen binding is shown below (green circles)

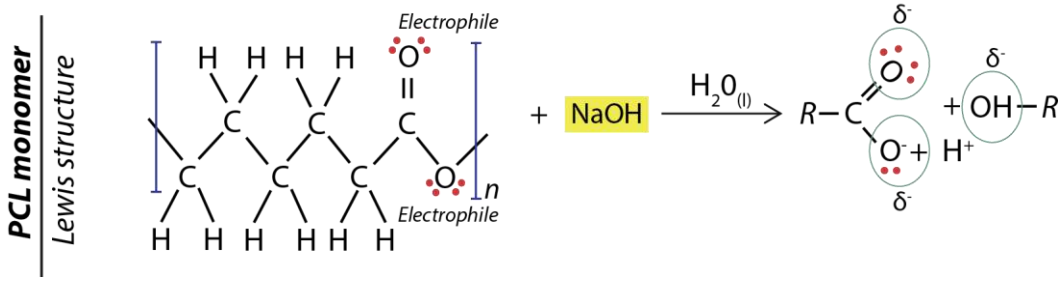

A paired *in vivo* cranial bone defect model study, on eight-month-old female Danish Landrace pigs (*Sus scrofa domesticus*) was launched, to investigate for granuloma formation, macrophage fusion

and/or recruitment of multinucleated giant cells (foreign body giant cells) and T lymphocytes at the site of implantation. Anesthesia, including surgical procedures performed on the animals and post-operative treatment has been described elsewhere (106). The study was approved by the Danish Animal Research Inspectorate and conformed to Danish law (application no. 2012-15-2934-00362). Non-penetrating calvarial bone defects positioned 10 mm apart were created, by using cannulated drill bit, where the 10 x 10 mm cylinder-shaped PCL scaffolds were placed or defects left empty for comparison. PCL scaffold implantation time was eight weeks and after animal euthanization with phenobarbital overdose, resected calvarial bone (kept at -80˚C) were cut in half, dehydrated in ethanol (70%–99%) and embedded in methylmethacrylate (MMA). By microtomy, 7 µm thin slices were made on 2 levels in sagittal plane with 400 µm between all levels, using a microtome (Polycut E, Reichert-Jung, Heidelberg, Germany). Sections were then deacrylated with 2-methoxy-ethyl acetate (Merck-Schuchardt) overnight, followed by rehydration in graded alcohol series (100%, 96%, 75%, 50% and 20% for 5 min. each) and then thoroughly washed with distilled water. The samples were stained with Goldners-Trichrome and for tartrate resistant acid phosphatase (TRAP) separately after rehydration, for detection of non-mineralized and mineralized bone, osteoblasts and osteoclast-like cells. All samples were incubated in citrate buffer (pH 6.0), prior to T cell receptor (TCR) immunostaining, treated with microwaves (1000 W) for 20 min. and allowed to cool at room temperature for 30 min. Bovine serum albumin (BSA) (1%) was used as blocking agent for 30 min. at room temperature. After titration of primary antibodies ranging from 1:100 to 1:1000 and rinse of samples in Tris-buffered saline (TBS; pH 7.6; 0.05 M) containing Tween (0.03%), the most optimal gained concentration of primary antibody, i.e. diluted 1:200 primary anti-CD3 produced in rabbit (product nr. C7930, Sigma-Aldrich), was added to the samples. This step was followed by incubation overnight at 4°C in a wet dark chamber. Negative control staining was obtained by omission of the primary antibody, by using isotype rabbit IgG1 at the same concentration as was used for the primary antibody, with the addition of secondary antibody (see below). For second and third negative controls 1:450 diluted donkey anti-rabbit secondary antibody was used alone or samples left un-stained/treated. This step was followed by wash x 4 in TBS (pH 7.6; 0.05 M) containing Tween (0.03%). The immunostaining was completed by the addition of 1:450 diluted donkey anti-rabbit secondary antibody conjugated with Alexa 488 and the incubation time was 60 min. in wet dark

chamber at room-temperature. Samples were then washed x 4 in TBS (pH 7.6; 0.05 M) containing Tween (0.03%) and placed on Thermo scientific glass plates followed by sealing with cover slips. Samples were kept in dark prior to confocal imaging and the TCR luminance signal (CD/m^2) detected by using ImageJ (National Institutes of Health, MD). For Goldners-Trichrome and TRAP staining, MNGC were counted by using newCAST software version 3.4.1.0 (Visiopharm, Denmark). Detailed description of TRAP staining, real-time polymerase chain reaction and dentin plate assay is listed in paper II (appendix).

2.2 Cell culturing

Peripheral blood mononuclear cells (PMNCs) were isolated from 0.9% NaCl four times diluted leucocyte-rich buffy coats from healthy donors (The Blood Bank, Aarhus, Denmark), by two-step density centrifugation, to reduce the number of thrombocytes, using sucrose polymer Ficoll Paque PLUS (Amersham Pharmacia Biotech AB, Uppsala, Sweden). Initially, cells were centrifuged for 20 min. at 20˚C (180 x *g*), followed by collection of the plasma phase which was discarded and subsequently additional centrifugation step for 20 min. at 380 x *g*. PMNCs from the interphase were carefully harvested, washed x 3 with 4˚C cold phosphate buffered saline (PBS) containing 1 mM ethylenediaminetetraacetic acid (EDTA), counted using hemocytometer and either kept at 4˚C until further processing or cryopreserved at -135°C until later use. Untouched CD14 positive monocytes and untouched CD3 positive T cells were isolated by negative selection, using Dynabeads® Untouched™ Human Monocytes kit (cat. no. 11350D) and Dynabeads® Untouched™ Human T cell kit (cat. no. 11344D) respectively, according to the manufacturer's instructions (Invitrogen, Life Technologies, Paisley, UK). The technique is based on depletion of cells by addition of magnetically labeled antibodies directed against surface antigens on cells that are not of interest such as B cells, NK cells, thrombocytes, dendritic cells, granulocytes and erythrocytes. By this procedure the monocytes and T cells are left untouched, referring to that the cells have not been bound by antibodies during the procedure and therefore not activated which is important for the subsequent *in vitro* analysis. The technique opposes positive selection, where $CD14^+$ monocytes and $CD3^+$ lymphocytes are isolated (two separate experiments) by incubation with magnetically labeled CD14 and CD3-specific antibodies. The drawback of this procedure is that the antibody binding may

activate the cells and induce a change in cell function prior to the requested analysis. To initiate differentiation of the negatively selected monocytes to macrophages, in addition to trigger cell fusion and genesis of multinucleated giant cells, a well-established in-house protocol and partly modified from reference (107) was followed. Culture duration time was 7 days in a cytokine environment containing 25 ng/ml macrophage colony stimulating factor (M-CSF) (cat. no. PHC2044, Invitrogen, Carlsbad, CA), 40 ng/ml receptor activator of nuclear factor kappa-B ligand (RANK-L) (cat.no. PHP0034, Invitrigen, Carlsbad, CA) and 5 ng/ml recombinant human transforming growth factor beta 3 (TGF-β3) (cat.no. 243-B3, R&D Systems, Minneapolis, MN) dissolved in alpha minimum essential medium (αMEM) without nucleosides (cat.no. 22561-021, Invitrogen, Carlsbad, CA) and 10% fetal calf serum (FCS) (Biochrom AG, Germany). Pre-cursor cell density was 3.5 x 10^5 cells/cm^2 ($A = \pi/4 \cdot D^2$) and cells were cultivated either in monoculture (monocytes) or in co-culture with T lymphocytes at the ratio 1:2 in a humidified atmosphere with 5% CO_2 at 37°C and re-fed every second day by semideplation. The use of biological material was approved by the local ethical committee (Scientific Ethical Committee for the Mid-Jutland Region, permission number: 77). Prior to PCL and dentine exposure at the above noted cell density, cell purity was investigated by flow cytometry. The cells were adjusted to a concentration of 1 x 10^6 cells/ml and transferred (as 100 µl cell suspensions) to FACS tubes (Nunc) which were marked unequivocally post addition of antibodies. Cells were stained with biotinylated mouse anti-human IgG1 antibodies against CD14, CD3, CD4, CD8 and CD19 or biotinylated mouse IgG1 isotypic control in combination with streptavidin-FITC (Dako). Conjugated fluorochromes to the antibodies were (named according to the chronological order of the antibodies) APC or PE, APC, PC7 and FITC. This step was followed by brief vortexing (5 sec.) and subsequently incubation (in dark) at room temperature for 30 min. After incubation, the cells were blocked for unspecific binding in PBS with 0.5% (wt/vol) BSA (cat. no. 12659, EMD Biosciences, Inc., San Diego, CA) and 0.09% (wt/vol) sodium azide. Vortexing was then repeated (5 sec.) and samples centrifuged for 5 min. at 20˚C (300 x *g*). After centrifugation the supernatants were discarded and cell pallets gently released, followed by fixation with 350 µl of 1% paraformaldehyde solution per FACS tube (whilst vortexing). Data were collected using FC500 series flow cytometry system (Beckman Coulter, CA) and analyzed by using FlowJo version 9.7.6

(FlowJo LLC, Ashland, OR). The obtained cell purity after the application of magnetic cell separation technique was >95% for both cell types as indicated below.

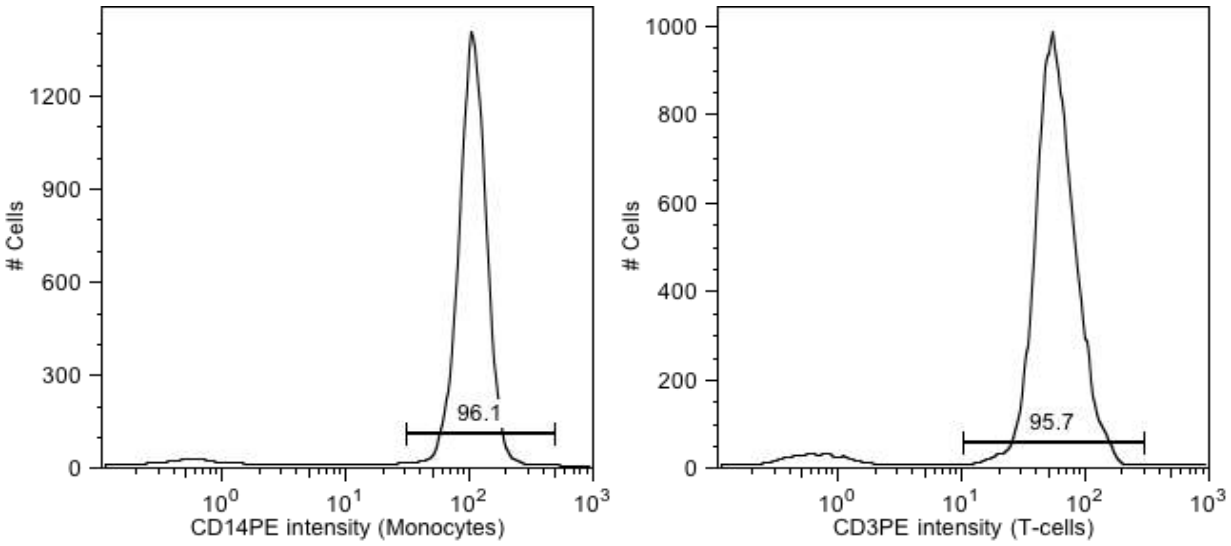

For the present seven interconnected studies, a variety of imaging techniques were used. Cell viability was evaluated after 1:1 Trypan Blue staining and by using optical microscope. For fixed samples with 10% formalin, viability was assessed with fluorescence microscopy imaging after 10 mM Cell Tracker Green staining (Invitrogen) staining and 1 µg/ml Hoechst (Sigma) or 300 nM 4' 6-diamidino-2-phenylindole dihydrochloride (DAPI) nucleic acid (Invitrogen) counterstaining.

2.3 PCL specimen production by electrospinning & molding

PCL solution (Capa™ 6500, 50 kDa, Perstorp, UK) of 30 w/v% in 2,2,2-Trifluoroethanol (TFE) (item no: 91690-100ML, Fluka) was stirred overnight. This step was followed by the addition of 50 µl F-beads (Fluorescent Carboxyl Polymer Microspheres (FC03F), Bangs Laboratories, Inc. IN) to the solution (1 ml volume in total) and stirred for another 5 H. The homogeneous solutions were placed in a 3 ml syringe fitted with a metallic needle of 0.9 mm inner diameter. The syringe was fixed horizontally on the syringe pump (model AL-1000-220Z, World Precision Instruments) and an electrode of high-voltage power supply (Gamma High Voltage Research) was clamped to the metal needle tip. The

flow rate of the polymer solution was 1 ml/H and the applied voltage was 12 kV. The tip-to-collector distance was set to 15 cm and a grounded rotating rim collector (r = 5.1 cm w = 7.3 cm) covered by a piece of clean aluminum foil was used for the fiber collection with a rotary speed of approximately 100 rotation per minute (rpm). Temperature was 21 °C, humidity ranged from 30 to 60% and the spinning time was 1 H. The electrospun fibers were dried under vacuum (Freezone Triad) overnight in order to remove excess solvents. The dried fibers were then soaked in 0.1 mM NaOH for 1 H to increase surface hydrophilicity, followed by rinse in PBS. Afterwards the treated PCL fibers were dried overnight in the freeze drier. The approximately 1 mm thick electrospun PCL fiber membranes (2 cm in diameter) were kept in dark and stored at 4˚C before *in vitro* cell experiments. Samples were then punched out from the membranes by using sterile biopsy punch (Acuderm, FL) with the inner diameter of 7 mm. The punched PCL samples were disinfected with 70% ethanol treatment for 1 H, rinsed in PBS x 2 and air dried in 24 wells Corning® Costar® cell culture plates (Sigma) prior to cell seeding. The fiber morphology was examined by high-resolution scanning electron microscopy (FEI, Nova 600 NanoSEM) at 5 kV. The fibers were placed directly into the SEM chamber without any metal sputtering or coating. As indicated above, an attempt to obtain uniform fiber morphology was performed by adjustment of solution viscosity and adjustment of flow rate, distance between needle and collector during the electrospinning, in addition to adjustment of the applied force. According to Newton's second law of motion, if an object has a constant mass (m), the force is directly proportional to the mass times the acceleration (a):

$$F = m \cdot a$$

Higher acceleration of the jet towards the collector, arising from the Taylor cone was in others words obtained by increasing the applied force (12 kV as previously noted) and it was evident that when the jet was exposed to higher stretching instabilities produced PCL fibers were thinner. The random oriented, electrospun PCL fibers with the incorporated F-beads had a mean diameter of 0.533± 0.246 µm and fiber diameter was based on measurements of 100 fibers, by using the software ImageJ (National Institutes of Health, MD). Pre-cursor cells at the density 3.5 x 10^5 mononuclear cells (MNC)/cm^2 were exposed to PCL fibers at day 1 under sterile conditions. Cell

fusion was triggered by using 25 ng/ml M-CSF, 40 ng/ml RANK-L and 5 ng/ml TGF-β3 dissolved in α-MEM and 10 % FCS as previously described. Medium was semidepleted every second day and post 7 days of culturing preparation prior to confocal imaging required two days. Initially, cells were washed in PBS x 2 for 5-10 min. per washing step, followed by fixation in 3.7% paraformaldehyde for 10 min. at room temperature. After fixation the cells were washed in PBS x 2 (5-10 min.) and blocking obtained by using 1% BSA and mouse IgG (100 µg/ml) dissolved in PBS for 30 min. at room temperature. After titration of primary antibodies (anti-CD18) and gained optimal concentration, KIM185 in addition to KIM127 at the stock concentration 0.98 mg/ml and 0.10 mg/ml respectively, were diluted to 5 µg/ml and added into the samples separately (i.e. run as to separate positive controls). Isotype mouse IgG1 (same concentration as used for primary antibodies) and secondary antibody alone served as negative controls. The incubation time was 24 H at 4°C. This step was followed by PBS wash for 4-10 min. x 4 prior to the 1 H incubation at room temperature for the 1:500 diluted conjugated secondary antibodies with Alexa 488. After the fourth washing step (x 4) in PBS, cell nucleus staining was obtained by the addition of 1X RedDot™2 (Biotium, CA) with the incubation time of 30 min. at room temperature. All samples were then washed x 2 in PBS (5-10 min.) and rinsed in distilled water x 2 before placement of stained PCL constructs with adhered cells on Thermo scientific glass plates, sealed with cover slips. Samples were kept in dark prior to confocal imaging which was performed to enable visual distinguishing between organic and inorganic material. To gain both higher magnification and optical resolution, SEM was used and samples analyzed with low vacuum secondary electron detector (Nova NanoSEM 600, FEI Company). For this purpose samples were washed in PBS x 2 and fixed by using 2.5% Glutaraldehyde in 0.1 M sodium cacodylate buffer (pH 7.4) at 4˚C overnight. As to overcome reduced electrical conductivity the samples were dehydrated in a serially grade ethanol (50- 99%) followed by removal of solvents in vacuum chamber. Release of F-beads incorporated within electrospun PCL fibers, to the microenvironment was investigated by using FACSAria III (BD Biosciences, CA) with 375 nm laser to excite the beads and emission collected in a 450/50 nm filter. From day 1 - 7 the culture medium was collected from the 24 wells (representing samples for the quantification of cell mediated PCL degradation by using FACSAria III as previously noted) and allowed to run for 120 sec. Collected raw data were analyzed by using FlowJo version 9.7.6 (FlowJo

LLC, Ashland, OR). Due to the major challenge of gaining controllable morphology, area and topography precision by electrospinning, the electrospun PCL fibers (figure 4) potential anisotropic behavior in addition to their week and fragile nature as a load bearing structure, compact test specimens for dynamic mechanical analysis were constructed by a molding. To meet the test specimen specific dimensions, the mold composed of aluminum (male-to-female molding concept) with ventilation holes in order to allow escape of trapped air during fabrication. Guidelines from ASTM International, PA (ASTM D638-10) were used for test specimen fabrication. A phase separation, for each sample (0.09 g/specimen of PCL granules) was induced by a heating/cooling cycle, i.e. melting of PCL granules at 100^0C for 15 min. followed by a cooling step at 5^0C for 45 min. The fabricated test specimens were then compared individually to each other, to determine if they had similar properties with regard to young's modulus, tensile stress, yield stress and visual appearance. Dynamic vibration technique with Bose ElectroForce® 3200 Series II instrument (Electro Force Systems Group, Bose Corporation, MN) at room temperature was used to measure Tan delta (δ) for all specimens:

$$\text{Tan}(\delta) = \frac{E''}{E'}$$

Tan (δ) is the relationship between loss modulus (E'') and storage modulus (E'). Loss modulus is the materials ability to dissipate energy that is applied to it (the energy which goes into the material is lost, e.g. when the material is stretched the energy which goes into it is lost and the material will not return to its original shape. Storage modulus i.e. the elastic modulus, is the material's ability to store energy applied to it for future use or to spring back when deformed at the end of a bending process. Test specimens were treated for 3 H in 5 M NaOH solution, followed by disinfection with 70% ethanol for 24 H and PBS wash x 2 and not considered 100 % identical. Hence, baseline measurements were performed for all samples (n=3) prior to MNGC pre-cursors seeding (3.5×10^5 cells/cm^2) in 12 wells Corning® Costar® cell culture plates (Sigma) or exposure to complete medium alone (25 ng/ml M-CSF, 40 ng/ml RANK-L and 5 ng/ml TGF-β3 dissolved in αMEM with 10% FCS) for comparison. Culture duration time was 14 days (humidified atmosphere with 5% CO_2 at 37°C). Low

energy radiation mediated degradation or ultra violet light exposure was avoided throughout the entire period. Tan (δ) was measured by the above noted dynamic mechanical analysis approached and the frequencies applied, ranged from 1-200 Hz. Mean value of amplitude of displacement equaled to 0.10 mm.

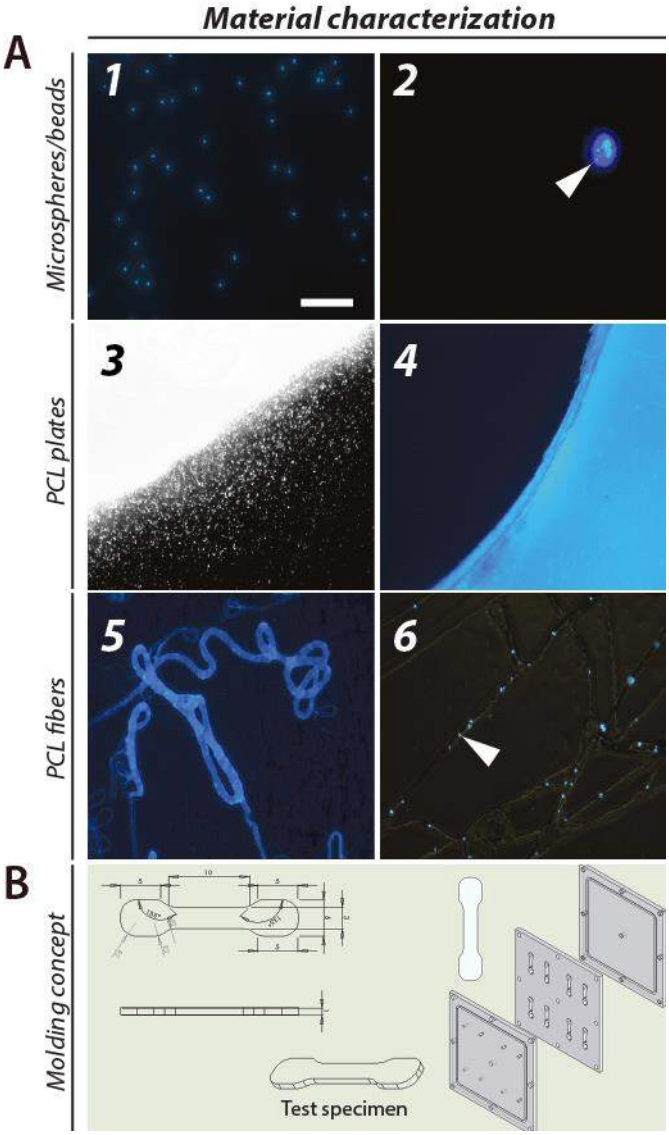

Figure 4: Types of *in vitro* PCL test samples. A pilot study was launched to investigate for phagocytic abilities of the MNGC pre-cursor cells. F-beads in a solution (A1) were engulfed (white arrow) by the negatively selected $CD14^+$ mononuclear cells (A2). Objective x 20, scale bar 10 µm. After having had gained this knowledge PCL test samples were initially produced on a borosilicate glass plate by dissolving 50 KDa PCL granules at 100°C and mixed with 1 µm F-beads at the ratio 1:5. Cells applied were negatively selected monocytes and T cells at the ratio 1:2 and cell purity was detected by flow cytometry. Genesis of osteoclast-like cells was triggered by using osteoclast inductive cytokines. All samples were washed thoroughly before cell seeding with PBS (A3-4). After 7 days of cell culturing in a humidified atmosphere with 5% CO_2 at 37°C the attached cells were trypsinized from the PCL test plates by exposure to 0.25% trypsin and 1 mM EDTA dissolved in PBS at 37°C x 2, followed by vortexing for 5 min and washing step in distilled water. PCL test plates were then characterized by SEM. Gained data from these experiments indicated major artifacts within all test samples. This was due to trapped in air bubbles, making it impossible to differentiate qualitatively between true cell-mediated PCL resorption i.e. creation of surface erosions by the MNGCs from artifacts. Therefore a new full scale study was implemented on electrospun PCL fibers with F-beads (A5-6). Material characterization was evaluated by using epifluorescence microscope prior to cell culturing and after washing x 2 in PBS F-beads were detected within single PCL fibers (white arrow) i.e. no diffusion of F-beads was observed in the microenvironment surrounding the PCL fibers. Post culturing mechanical properties of PCL was investigated for polycaprolactone test specimens produced by molding concept (B) described in more detail in the main text concerning materials and methods.

Preliminary *in vivo* data indicated attachment of osteoclast-like cells to PCL and hence Wang *et al.* previously have shown that osteoclasts are capable of polymeric and metallic particle phagocytosis (108, 109) it was hypothesized that these multinucleated giant cells can mediate degradation of PCL through ester-linkage cleavage, material opsonization and phagocytosis. In the present monograph

these cells are either named osteoclast-like cells or foreign body giant cells (FBGCs), as they govern osteoclastic pheno- and genotype (paper 2) and are capable of foreign body material (PCL) attachment.

2.4 Quantification of sC5b-9 by time-resolved immunofluorometric assays

The potential of complement activation induced by PCL itself was investigated by measuring soluble membrane attack complex (sMAC, i.e. sC5b-9) using time-resolved immunofluorimetic assay (TRIFMA) as previously described (54) . PCL samples composed of 50 kDa PCL particles (~15 mg) and PCL plates (~15 mg) respectively. Particles and plates were run separately for comparison. The applied PCL plates were prepared by dissolving PCL particles at 100°C on a borosilicate glass plate and cooled below -30°C to thermally induce phase separation. After disinfection of PCL samples for 3 H in 70% ethanol the samples were subsequently exposed to 150 µl human serum, followed by incubation overnight at 4°C and 37°C. After incubation, a total volume of 25 µl were used from this sample solution per well, to determine complement activation by using TRIFMA. The initiation of the experiment was performed by coating of microtitre wells with 1 µg/ml mouse anti-human sC5b-9 (Quidel, San Diego, CA), dissolved in PBS i.e. 100 µl/well overnight at 4°C, and blocked with 1 mg BSA/ml PBS for 1 H at room temperature. After wash in PBS x 3 containing 0.05% Tween 20 (PBS/Tw), EDTA serum samples were diluted four fold in PBS/Tw containing 10 mM EDTA (75 µl buffer and 25 µl samples as noted above) and incubated overnight at 4°C. A standard was made from normal human serum and activated by incubation with human IgG-sepharose for 1 H at 37°C. The concentration of sC5b-9 was quantified by comparison with recombinant sC5b-9 (Quidel, A239). Two EDTA serum samples were used as internal controls and wells receiving only buffer as negative controls. Bound sC5b-9 was detected with 0.05 µg biotinylated anti-human C6 antibody (Quidel, A219) for 2 H at room temperature, and was subsequently incubated with 10 ng europium (Eu) labeled streptavidin (Perkin Elmer, MA) in 100 µl PBS/Tw containing 25 µm EDTA for 1 H at room temperature. Bound europium at oxidation state +3 (Eu^{3+}) was detected by the addition of 200 µl of enhancement solution (Perkin Elmer, MA) and reading the time-resolved fluorescence on a DELFIA fluorometer (Victor3, Perkin Elmer, MA). The limit of detection for the sC5b-9 assay was 1

µg/l. The intra- and interassay variations (below 23 and 25% respectively) were calculated by using the formula:

$$\%CV = \frac{s}{\bar{x}} \times 100$$

which enables spreading comparison of two different data sets, by dividing the standard deviation with the mean value, where CV represents the coefficient of variation.

2.5 Quantification of sCD18 by time-resolved immunofluorometric assays

The IgG1 monoclonal antibodies (mAbs) against CD18 were produced by GenScript from the hybridoma cell lines CRL-2839 (KIM185) and CRL-2838 (KIM127) followed by protein A/G purification. The mouse IgG1 isotype (cat. no. M7894; Sigma-Aldrich, St. Louis, MO) was purified from an ascites suspension with protein A/G purification. Biotinylated forms of the antibodies were made by use of Biotin *N*-hydroxysuccinimide ester (cat. no. 14405; Sigma-Aldrich) (110). Measurement of soluble CD18 (sCD18) in supernatants from *in vitro* cell cultures was carried out by TRIFMA as previously described (110). In brief, microtiter wells (FluoroNunc Maxisorp, 437958; Nunc, Roskilde, Denmark) were coated with purified antibodies (2 µg/ml dissolved PBS, pH 7.4) recognizing epitope exposed on human CD18 (KIM185) or mouse IgG1 (100 µl/well). The wells were washed in Tris-buffered saline (TBS)/Tween and blocked by incubation with 200 µl TBS with 1 mg/ml human serum albumin for 1 H at room temperature. After washes, samples of 100 µl heparinized plasma diluted 1:10 and 1:5 or supernatants diluted 1:2 in TBS/Tween with 1 mM $CaCl_2$, 1 mM $MgCl_2$, and 100 µg/ml aggregated human Ig were added to the wells, and the plates were incubated overnight at 4°C. After incubation of the diluted samples, the wells were washed and subsequently incubated with 100 µl biotinylated antibody to CD18 (KIM127). After washing of the wells, Eu^{3+}-conjugated streptavidin was applied and the signals were read by time-resolved fluorometry. Signals from *in vitro* samples were compared against a standard curve made from titrations of plasma from healthy donor controls, followed by R squared measure of goodness of fit. Moreover, after logarithmic transformation, the strength of the linear relationship or the regression between the dependent variable (Eu^{3+}counts per sec.) and the independent variable milliunits

(mU)/ml), was measured by determine the coefficient of determination (R^2), given by regression sum of squares divided by total sum of squares and standard error of the estimate (SEE):

$$R^2 = SS_{Regression}/SS_{Total}$$

$$R^2 = \text{explained variation/total variation}$$

$$SEE = \sqrt{\sum_{i=1}^{n} \hat{E}_i^{\,2}/n\text{-}2}$$

This demonstrates that the standard error of the estimate is the function of square root of the sum of squared errors divided by n - 2. The mathematics refers to the measure of the fit, hence dispersion of the results from the regression line, which in the present case was 99%.

2.6 Statistics

Statistical analysis was performed by using STATA 12 (StataCorp LP, College Station, TX) and GraphPad Prism 5 (GraphPad software Inc., La Jolla, CA). Data was analyzed as one sample from a normal distribution based on paired or unpaired t-test for *in vivo* and *in vitro* observations respectively. Further, when comparing the means of at least three conditions in a particular experiment, were the observations are independent and the populations have a common standard deviation, on-way ANOVA analysis was applied. The assumption of normality was investigated by creating histograms and inverse normal or Quantile-Quantile (QQ) plots for raw data and after logarithmic transformation (figure 5). In the case of non-Gaussian distribution when comparing two populations, a non-parametric Wilcoxon-Mann-Whitney test was used. Statistical significant difference between means is represented by a p value of < 0.05.

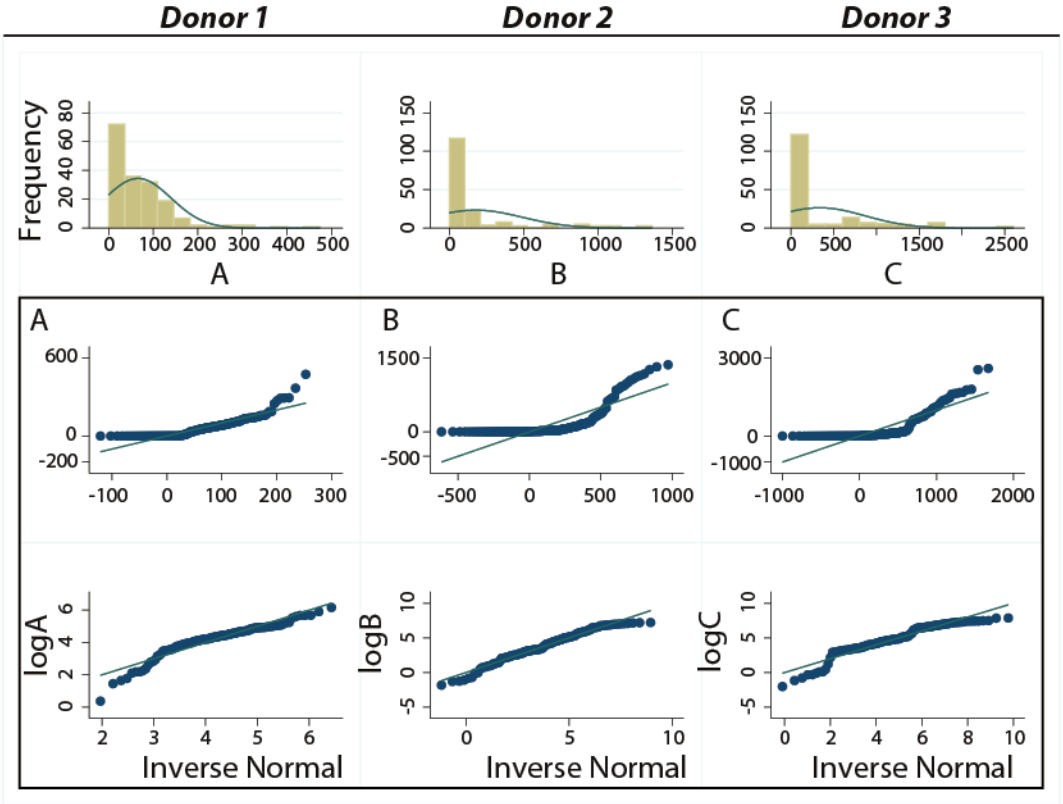

Figure 5: Assumption of normality. Prior to statistical analysis, data were plotted and the assumption for normality checked by creating histograms and QQ-plots by using STATA 12. In this example, raw TRIFMA data set on shedded soluble β_2-integrins have been pooled for statistical analysis. The central data panel (A-C) shows positively skewed data points, not linear and which do not fit a normal distribution. This is classical representation of a biological data set, which as indicated, normally will not follow a perfect bell-shaped curve or Gaussian distribution. The bottom panel illustrates approximately normally distributed set of observations, because the data points follow approximately a straight line after data transformation to a different scale of measurement (logarithmic transformation of positive values). The inverse normal or QQ plots are linear if the data are normally distributed.

3. Summary of studies

This section contains a brief presentation of the most important results. Numerical studies have shown that the formation of multinucleated giant cells is induced by macrophage fusion, a phenomenon supported by the present experimental results.

3.1 Study 1

Formation of a foreign body granulomas and giant cells is a common host response directed against foreign material, which has been lodged for any given reason into the human body. Therefore the question raised was whether implanted PCL scaffolds induce formation of FBGCs

and/or recruitment of T lymphocytes (study 2). A paired study was launched by using a cranial bone defect model in 8-months old female Danish Landrace (n = 3). Samples were collected 8 weeks after surgery, dehydrated in ethanol (70-99%) and embedded in MMA. Then histological analysis was performed on 7 µm thin Goldner's Trichrome and TRAP stained samples. Quantification of FBGCs (intervention vs. control group) was solely made on the basis of MNGCs characteristics and morphology, by using the state of the art stereology software Visiopharm newcast. The results show exclusively a significant difference in FBGCs counts between the two groups (p = 0.0177). Histopathological evaluation (figure 6-7) revealed circular accumulation of macrophages (histocytes or foam cells). Syncytial formations within the center zone of the granulomas were common findings and it was found to be difficult to distinguish individual cell borders from each other.

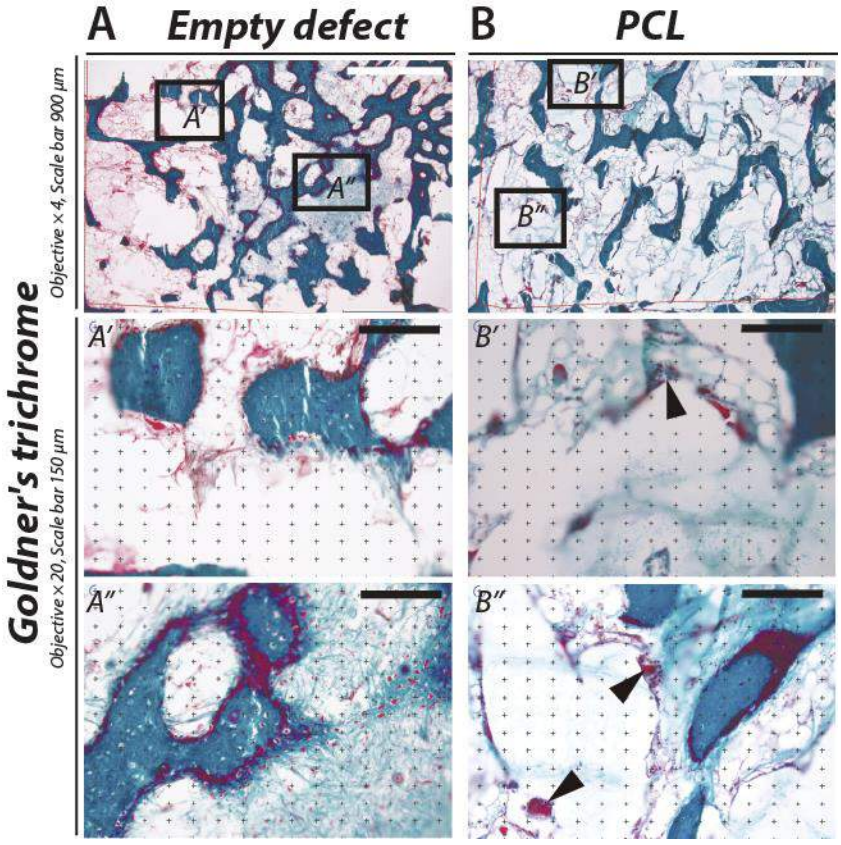

Figure 6: *In vivo* PCL associated FBGCs. Results are gained from a paired porcine calvarial model study, showing light microscopy imaging of empty defects (A) and qualitative comparison of Goldner's trichrome stained *in vivo* samples after 8 weeks of implantation (B). Objectives used and scale bars are indicated to the left. Formation of granuloma-like syncytium and recruitment of multinucleated giant cells, to the site of implanted bioscaffolder produced cylinder-shaped PCL scaffolds, is indicated by black arrows.

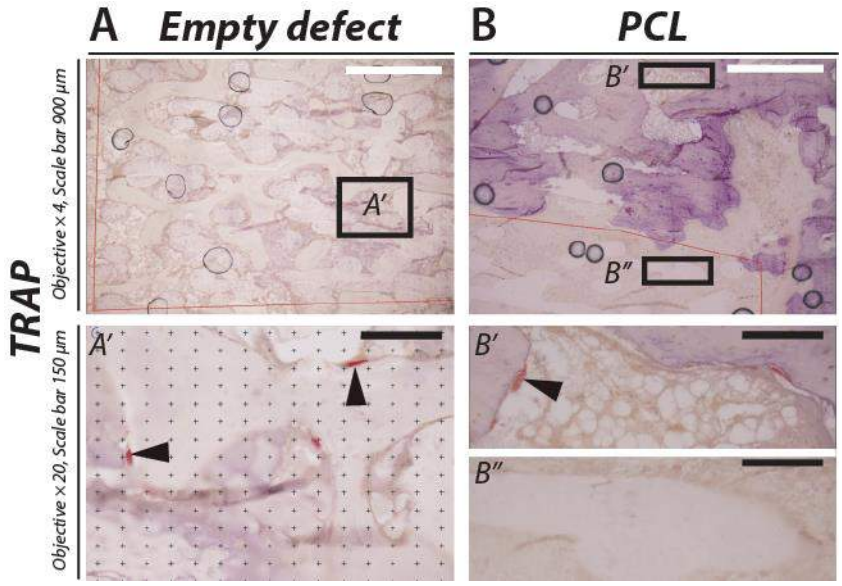

Figure 7: *In vivo* PCL associated TRAP⁺ cells. Representative light microscopy imaging after TRAP staining of empty defects (A), comparted to the outcome after 8 weeks of PCL scaffold implantation (B). Objectives used and scale bars are indicated to the left. From this random field for vision, it can be appreciated that the TRAP⁺ cells are primarily in contact with compact or trabecular bone (black arrows). Other samples showed additionally only sparse number of TRAP⁺ cells in association to PCL implants. The dotted red lines of the first image panel mark the gate prior to quantification of TRAP⁺ cells (see below were *ns* represents non-significant). The same gating strategy was followed for the Goldner's trichrome stained *in vivo* samples shown in previous figure reveling after paired t-test a p value of 0.0177 (***).

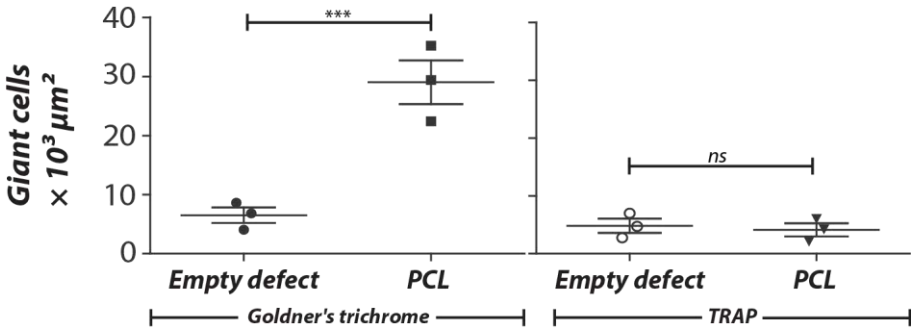

3.2 Study 2

CD3 expression was detected in the surroundings of PCL associated FBGCs i.e. closely related to the innermost zone of the syncytium or the granuloma tissue, suggesting recruitment of T lymphocytes. This was detected by in house modified immunohistochemistry, using porcine anti-CD3 and Alexa 488 conjugated secondary antibodies (figure 8).

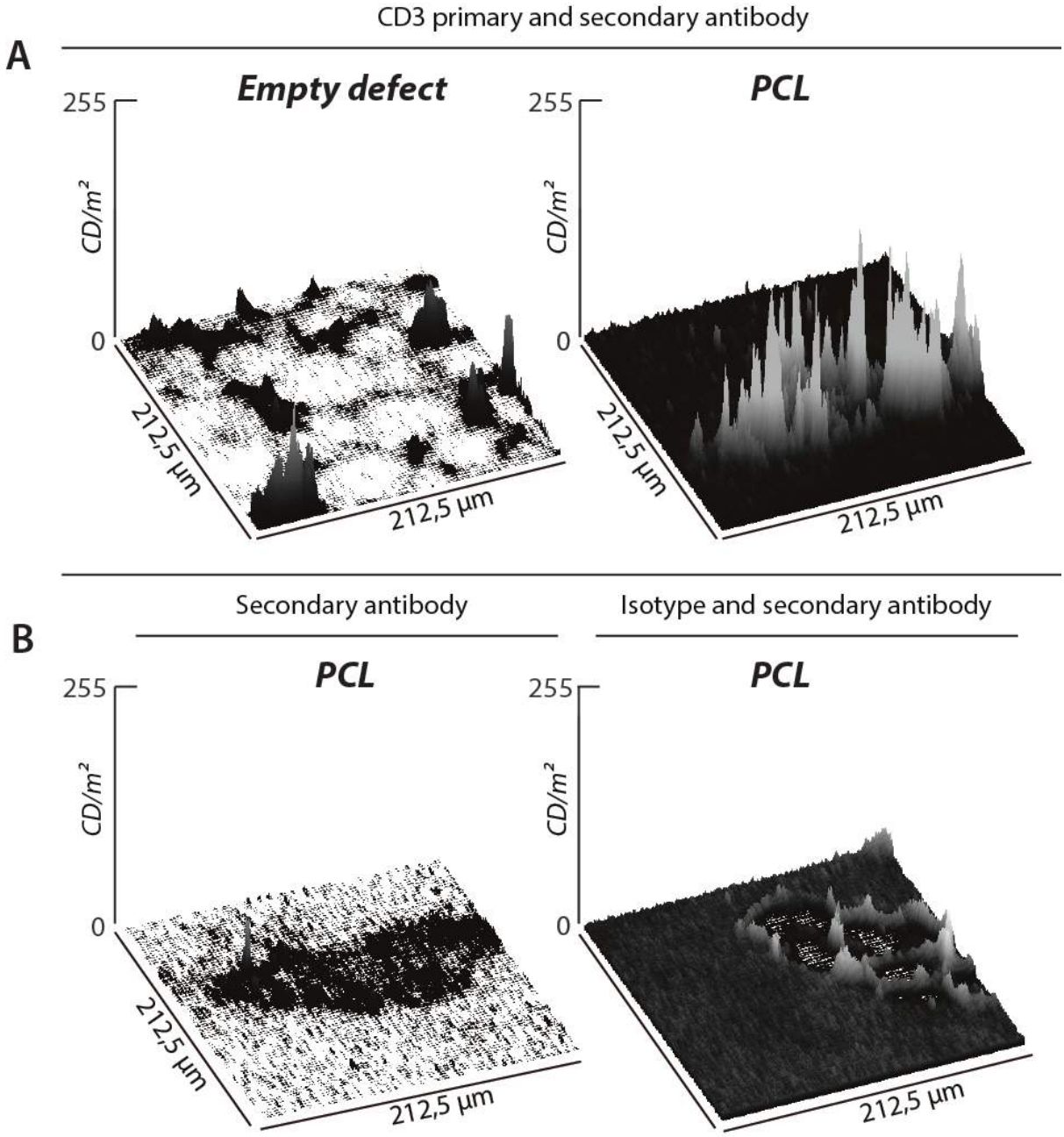

Figure 8: CD3 luminance signal. CD3 luminance semi-quantification was performed x 2 on two separate donors. Signals from empty defect specimens were compared to signals from implanted PCL scaffolds (A) in a paired porcine calvarial model. Non-antibody treated specimens or treated with isotype IgG alone and in combination with secondary antibody in addition to secondary antibody treated specimens only, were used as controls (B). ImageJ was used to generate surface plots from the confocal lms-files for comparison.

3.3 Study 3-7

The main objective by the *in vitro* studies was to investigate PCL degradation by osteoclast-like MNGCs. The hypothesis was that β_2-integrins mediated cell attachment to the polyester, prior to the degradation process itself. The second hypothesis was that phagocytosis plays a crucial role in MNGC mediated degradation of PCL based upon on previous discoveries, showing that $\alpha_M\beta_2$ and $\alpha_X\beta_2$ integrins serve as complement receptors. How these hypotheses were tested will be described and illustrated in the following chapters. First, differentiation of monocytes into MNGCs with osteoclast pheno- and genotype (paper 2) was triggered (figure 9).

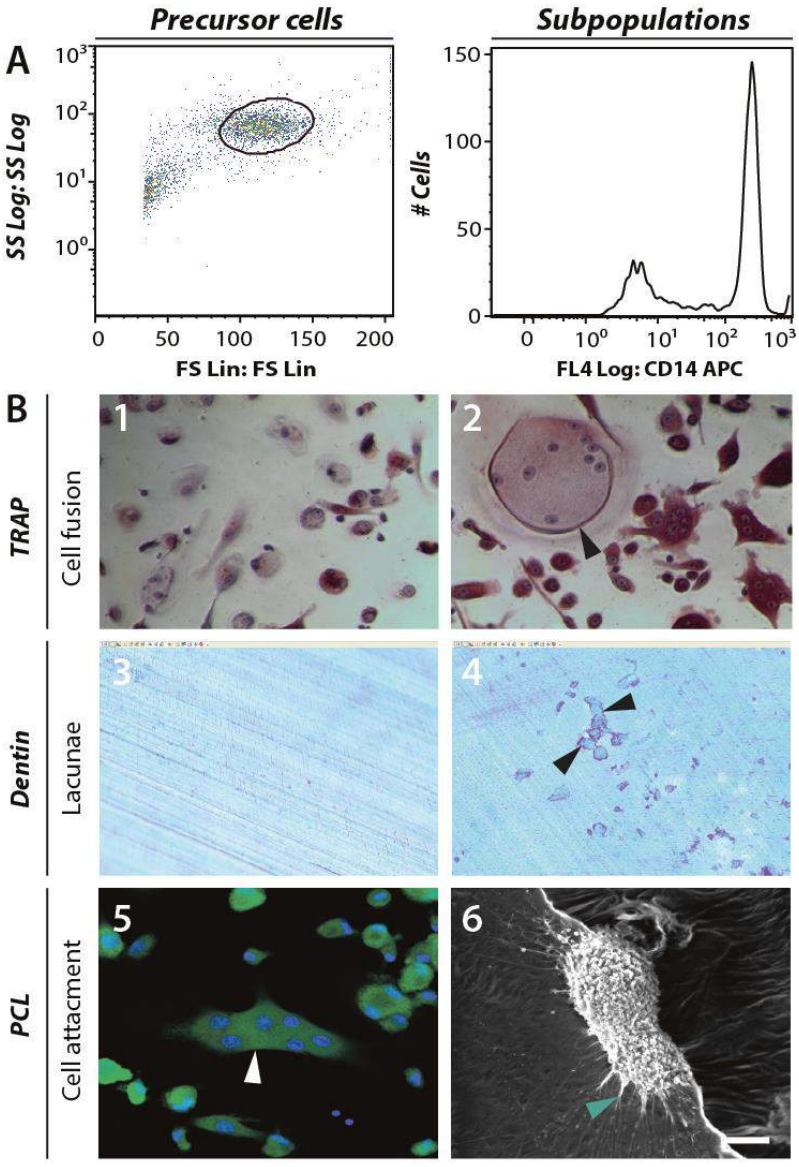

Figure 9: Generation of MNGCs *in vitro*. Osteoclast-like cells were created from mono-nuclear pre-cursors; $CD14^+$ negatively selected monocytes (A). As indicated by the histogram, the pre-cursors were divided into two main subpopulations. Cell density required for cell fusion was $3.5x10^5$ $CD14^+$ cells/cm^2 and multi-nucleation was obtained by stimulation with M-CSF, RANKL and TGFβ3. Fusiogenic density without osteoclastogenic inductive cytokines resulted in zero osteoclastogenesis (B1). When stimulated with M-CSF, RANKL and TGFβ3 classic phenotypic manifestations of $TRAP^+$ osteoclasts were observed (B2). Osteoclast activity or dentin resoptive capacity could not be detected after seven days of culturing for untreated pre-cursors (B3), however when cells treated with M-CSF, RANKL and TGFβ3 lacunae formation was noted (B4). Viability for MNGCs attached to PCL was determined by objective x20 confocal imaging on Cell Tracker Green and DAPI-counterstained cells after 7 days of culturing (B5). By using SEM and low vacuum detector a more detailed visualization (magnification x 8247) of the underlying PCL constructs topography was obtained, showing attachment through pseudopodia projections (green arrow). Magnification x 8247 and scale bar 5 µm (B6).

In osteoimmunology, bone and the immune system share a range of regulatory mechanisms and as indicated by the *in vivo* results upregulation of the stable TCR associated CD3 proteins expressed on the surface of T lymphocytes was detected. T cell effect on the PCL microenvironment was therefore investigated in an *in vitro* co-culture setting with monocytes at the ratio 2:1. As presented by the results below (figure 10), negatively selected T cells ($CD4^+/CD8^+$) enhance osteoclast-like cell activity.

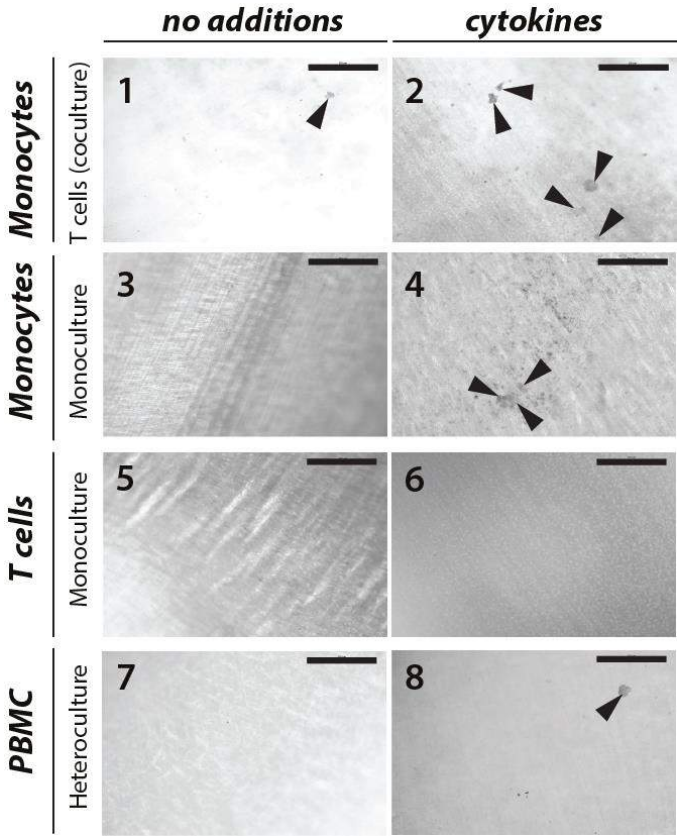

Figure 10: T cell effect on osteoclast-like cell activity. Representative light microscopy imaging of the resorption capacity comparison by osteoclast pre-cursor cells in monoculture and in a T cell co-culture setting. Culture duration time was seven days. Cytokines used were as previously mentioned M-CSF, RANKL and TGFβ3 at the concentration level 25 ng/ml, 40 ng/ml and 5 ng/ml, respectively. No additions refers to a culture setup with αMEM and 10% FCS without the addition of osteoclast inductive cytokines. Black arrows point out lacunae formations which were revealed after trypsinization (subfigures 1 and 2 including 4 and 8). Specification of cell types seeded on dentin plates are marked to the left. Objective × 10 and scale bars equals to 300 µm. Lacunae area was quantified for three separate donors by using the Visiopharm newcast software, followed by one-way ANOVA analysis i.e. repeated measures ANOVA (Tukey).

Monocyte and T cell co-culture vs. same culture setup without any addition of cytokines, reveals mean difference of 484 μm^2 and [20; 947] 95% CI. However, when comparing monocytes and T cell co-culture with monocytes in monoculture, where both cultures had been exposed to osteoclast inductive cytokines, a mean difference of 171 μm^2 was observed with 95% CI of [-292; 634] hence no significant difference detected. Like previously noted, as when comparing the first two conditions in the diagram (next page), significance is moreover seen, i.e. 95% CI 513 [49.5; 976], when comparing co-culture with cytokines vs. monocytes not receiving treatment with osteoclast

inductive cytokines. As expected, significance was furthermore found when comparing the condition monocytes and T cells receiving treatment, with conditions 5-8. * $p < 0.05$ and *ns* equals to non-significance.

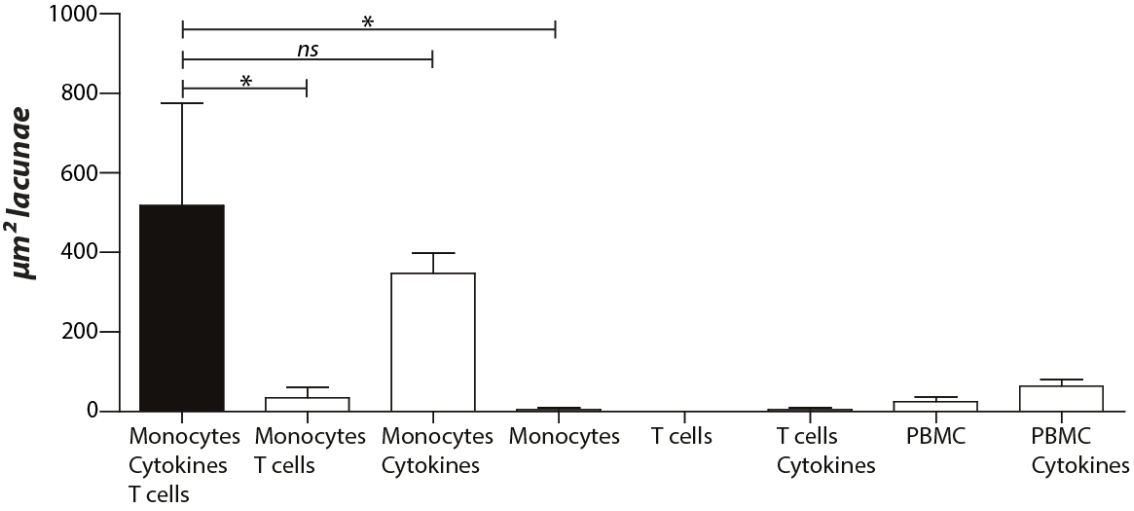

To determine whether PCL is degradable by related MNGCs as were detected in close approximation to the material *in vivo* (foreign body giant cells), monocytes and T cells were seeded on electrospun PCL fibers with incorporated 1 µm F-beads at the ratio 1:5. Same fusiogenic cell density, cytokines and monocyte/T-cell ratio was used as previously described is listed in details under materials and methods. This approach enabled distinguishing between organic and synthetic material by confocal imaging and β_2-integrin detection, in addition to 3D visualization of particle engulfment by the giant cells (figure 11). PCL was found prone to osteoclast-like cell mediated degradation and is here shown to be greatly increased in co-culture setting with T lymphocytes. The degradation proceeds through surface erosion accompanied by release of F-beads into cell media. The supernatants were collected at day 1, 3, 5 and 7 and kept dark prior to flow cytometry analysis for microspheres fluorescence signal detection (Alexa Fluor 350-A). This in house designed approach allowed for measuring the degradation rate. Only F-beads in a solution, at the same density as originally was used for the electrospun fiber production, served as a positive control group. Monocytes attached to PCL, without incorporated F-beads and at the density 3.5×10^5 cells/cm^2 served as a negative control group. The F-beads released from the PCL constructs, during the seven day period of cell culturing, hence exposure to MNGCs and T cells, appeared in the same

gate as was detected for the positive control group (figure 12 and 13). However, the fluorescence intensity (Alexa Fluor 350-A) was greatly reduced and right shifted on the forward scatter, suggesting PCL polymer debris attached to the released particles resulting in signal intensity disturbances. Two different gating strategies were applied for two separate experiments. The path is shown in figure 12 were dead cells and debris was attempted to be gated out, followed by inclusion of events which turned on the side scatter according to the appearance of positive control events. In other words, F-beads release from the PCL constructs (mean counts are shown by the FlowJo generated histograms) was based on events in pre-defined gate, selected around appeared positive signal events detected for the positive control. There were 280 events detected for constructs not exposed to cells, suggesting abiotic hydrolysis, 678 events for constructs exposed to monocytes alone at day 7 (these cells had fused to become giant cells) and 974 events were observed for the condition monocytes (giant cell pre-cursors) in co-culture with T cells. Similar results were obtained for the second donor. The results support previous presented findings (study 3) showing how the resorptive capacity of osteoclast-like cells can be increased, apparently as an effect to T cell co-culturing.

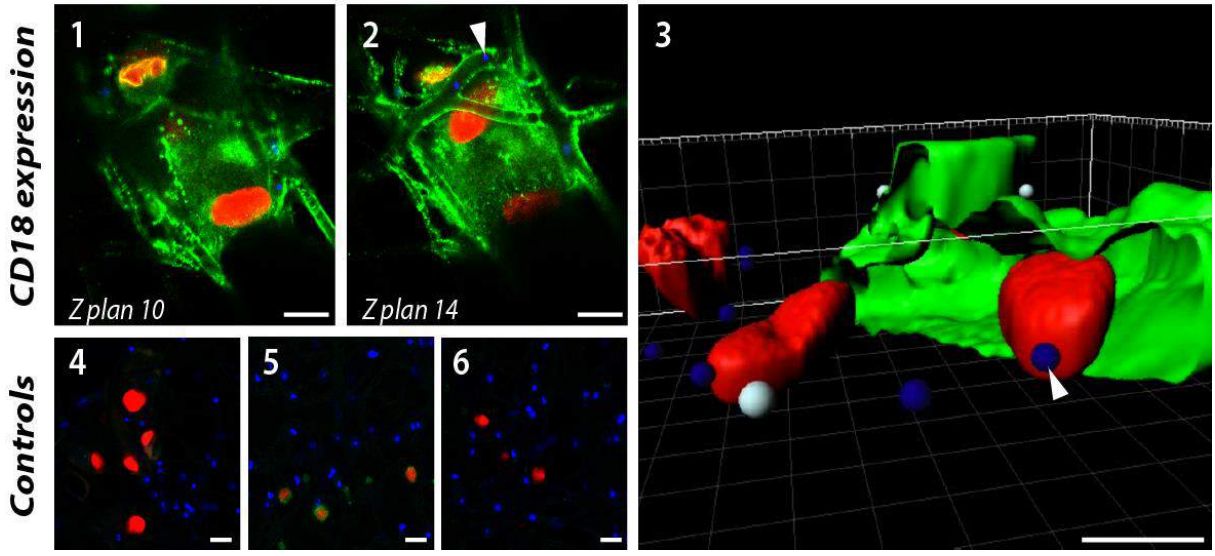

Figure 11: Osteoclast-like cells in PCL foreign body microenvironment. Confocal imaging (objective x 20) revealing plasmalemma β_2-integrin expression of osteoclast-like cells attached to PCL. Z planes are indicated for both subfigures (1-2) and blue particles (white arrows) represents F-beads incorporated within electrospun PCL fibers (2) and after 7 days engulfed F-beads by the osteoclast-like cells (3). Cell nuclei are stained with RedDot™2 (Biotium, CA) and controls included for non-treated specimen (4), isotype primary IgG1 antibody (5) and secondary antibody (6). Scale bars, 10 µm.

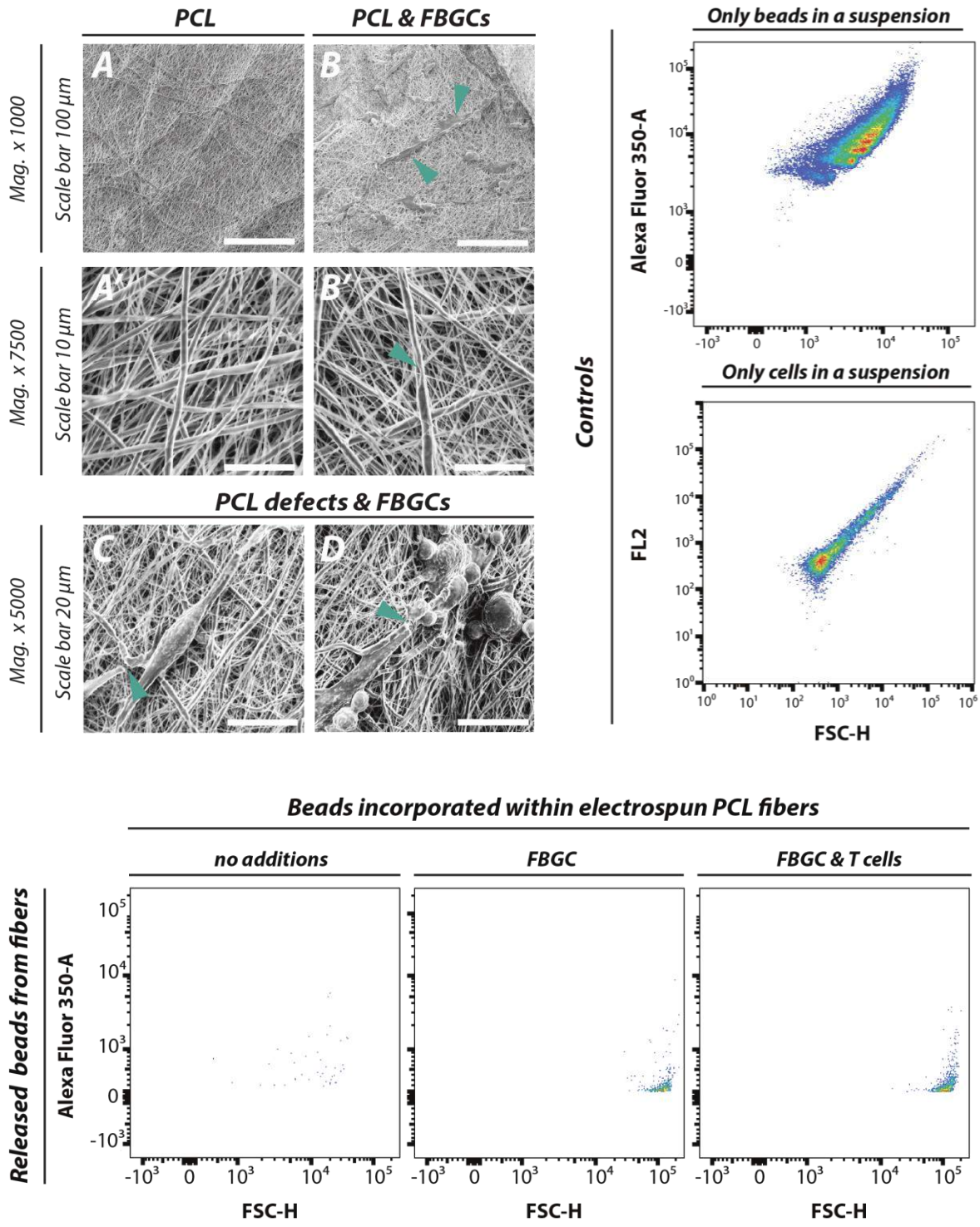

Figure 12: Top left hand subfigures show SEM imaging of PCL fiber surface and foreign body giant cell interactions (LVD, HV 5 kV, tilt 0˚ and WD 5 mm). Magnifications and scale bars are indicated to the left. Controls (A-A'). Green arrows point out cell-to-fiber attachment (B-B'), cell associated fiber-like crack (C) and fissure (D). Control flow cytometry output (to the right) and data on fiber F-beads release (bottom panel) after 7 days of cell mediated PCL degradation.

Figure 13: Verification of primary flow cytometry results. (A) Gating strategy is indicated for all dot plots, showing excluded artifacts (black arrow and events in general below the gating path). The autofluorescence signal tail observed when cells in a suspension are analyzed alone, as can be detected from previous figure (figure 11), has additionally been attempted excluded from the gate and by using side scatter rather than forward side scatter on the x-axis. (B) Total number of events, i.e. released F-beads from the PCL constructs after 7 days of osteoclast-like cell exposure. Green indicate co-culture with T cells, blue a monoculture condition and red no cell-to-PCL exposure, suggesting abiotic hydrolysis of PCL as previously documented. (C) Same variable analyzed as in B, but now showing the mean value from two independent experiments (same colors are used as for the above three mentioned conditions).

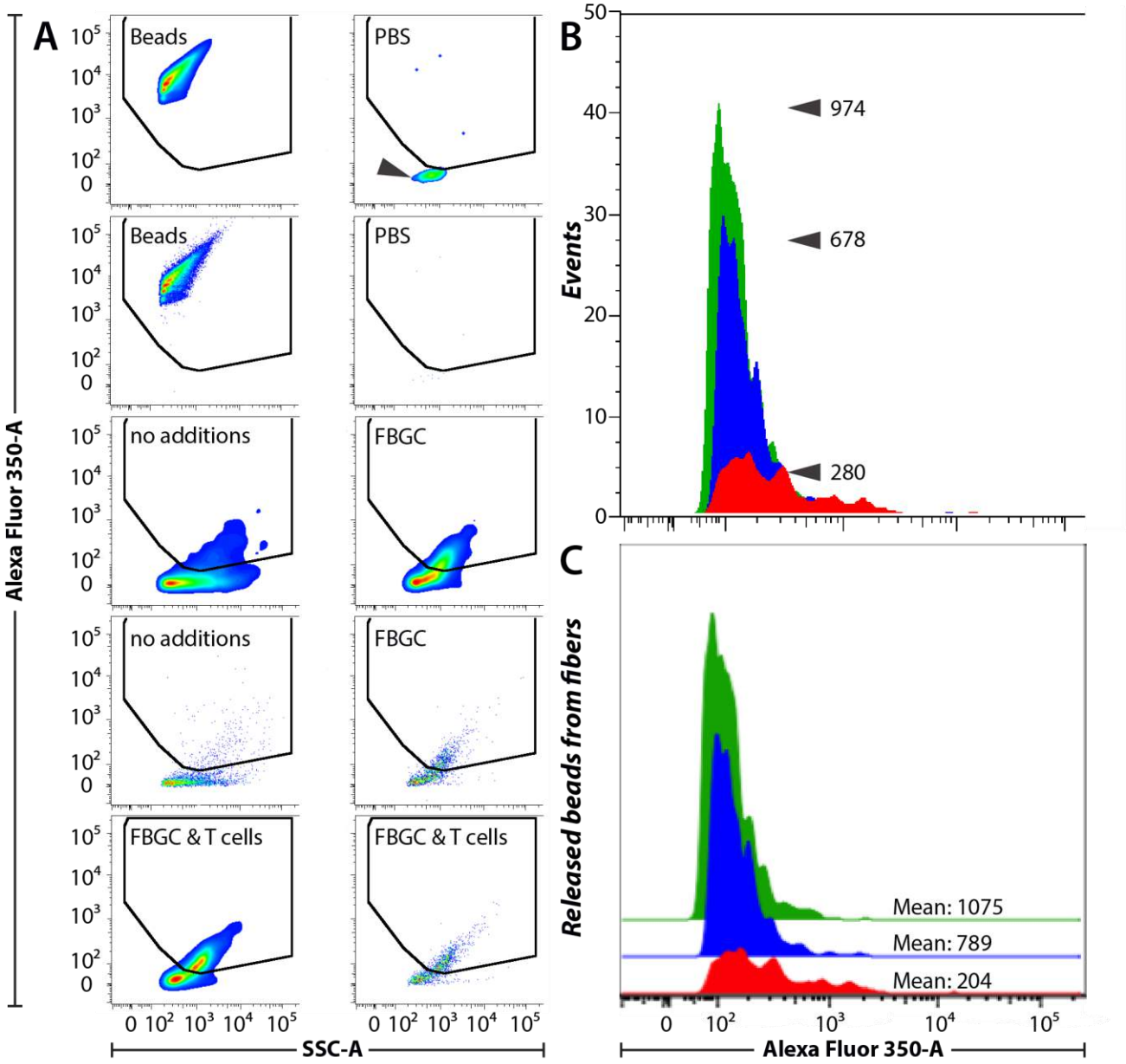

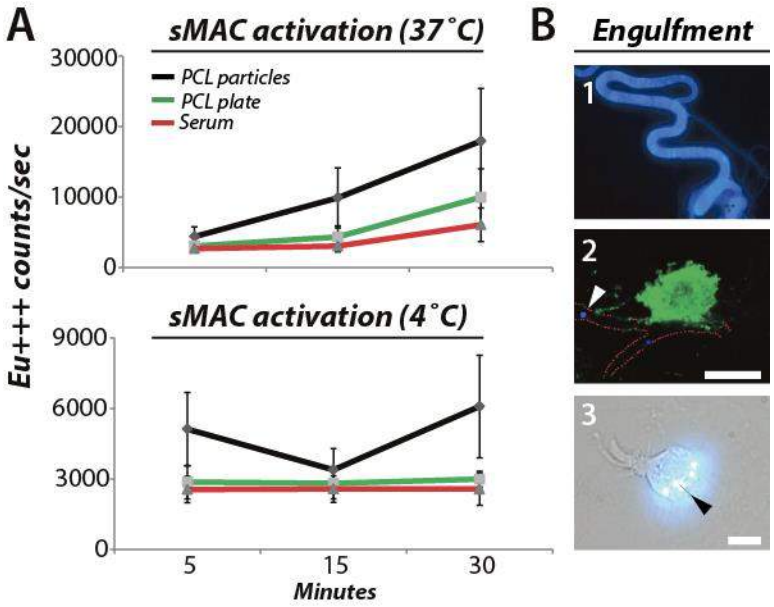

Soluble MAC concentration increases exponentially over time at 37˚C (A) upon PCL to human serum exposure (above), measured by TRIFMA. Qualitative results to the right (B) supporting the hypothesis of complement activation by PCL. Representative epifluorescence imaging of PCL fiber with incorporated F-beads, magnification x 40 and a confocal picture of B_2-integrin positive osteoclast precursor cell attached to PCL fiber (1-2). Migration path towards the F-bead (white arrow) has been attempted indicated by the red dots (2). Below, 2D configuration of engulfed F-beads by osteoclast precursor cell, revealed after trypsinization. Scale bars 10 and 5 µm, added by using ImageJ. 3D-imaging of β_2 integrin positive phagocytic multinucleated osteoclast-like cell is shown in figure 10. In addition, the role β_2 (CD18) integrins in MNGC-to-PCL adhesion was further explored by TRIFMA showing shedding by mononuclear and multinucleated giant cells (osteoclast-like cells) from day 1-7, during cell migration on three different materials. The results demonstrate significantly increased shedding, hence cell migration and activity (ANOVA $p < 0.05$), when the outcome is compared between dentin and the two foreign materials (figure 14).

Figure 14: B_2-integrin shedding for different culture conditions from day 1-7.

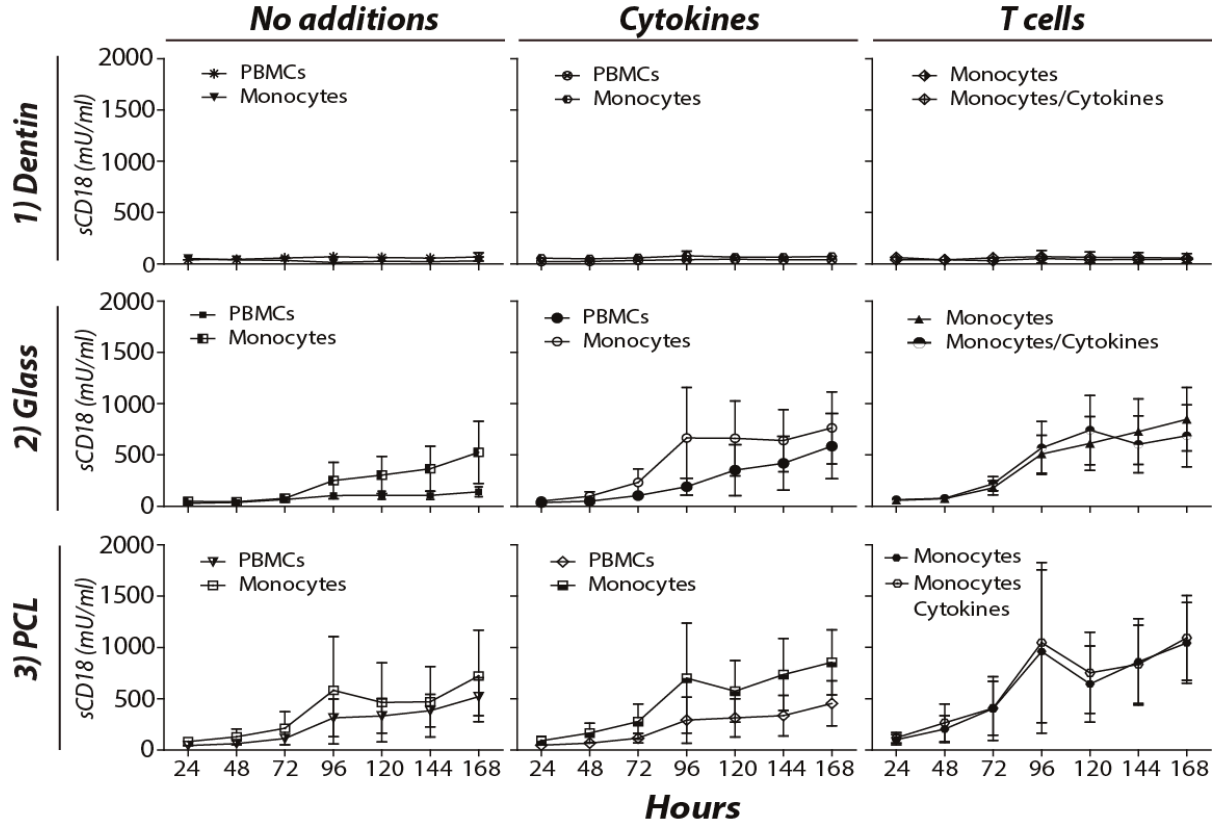

SEM imaging of compact PCL constructs (figure 15 page 48, A1-A3) with LVD, showing osteoclast-like adhesion (A1, magnification x 2655 and scale bar 20 µm), bare or un-seeded PCL constructs prior to DMA without evidence of penetration or pit-formation for comparison (A2, magnification x 500 and scale bar 200 µm). After two weeks of cell culturing followed by trypsinization, scattered PCL defects, as indicated by the green arrows, can be observed by SEM (A3, magnification x 500 and scale bar 200 µm). DMA results below (B) reveal negative baseline TanDelta peak value at 168 Hz for the control PCL group (indicated by the red line) and a right shift with negative peak value at 170 Hz (black line) after two weeks of osteoclast-like cell exposure. The results indicate increased material stiffness. A plausible explanation to these findings is that the giant cells leave trail of adhesion

molecules behind their migration track. Results supporting this consideration are included in subfigures A4 and A5, showing SEM and confocal imaging of giant cell attached to electrospun PCL fiber (A4, magnification x 3000 and scale bar 40 µm) and a positive B_2-integrin signal from the associated PCL fibers (A5). White arrow point out a single left behind F-bead within PCL fiber.

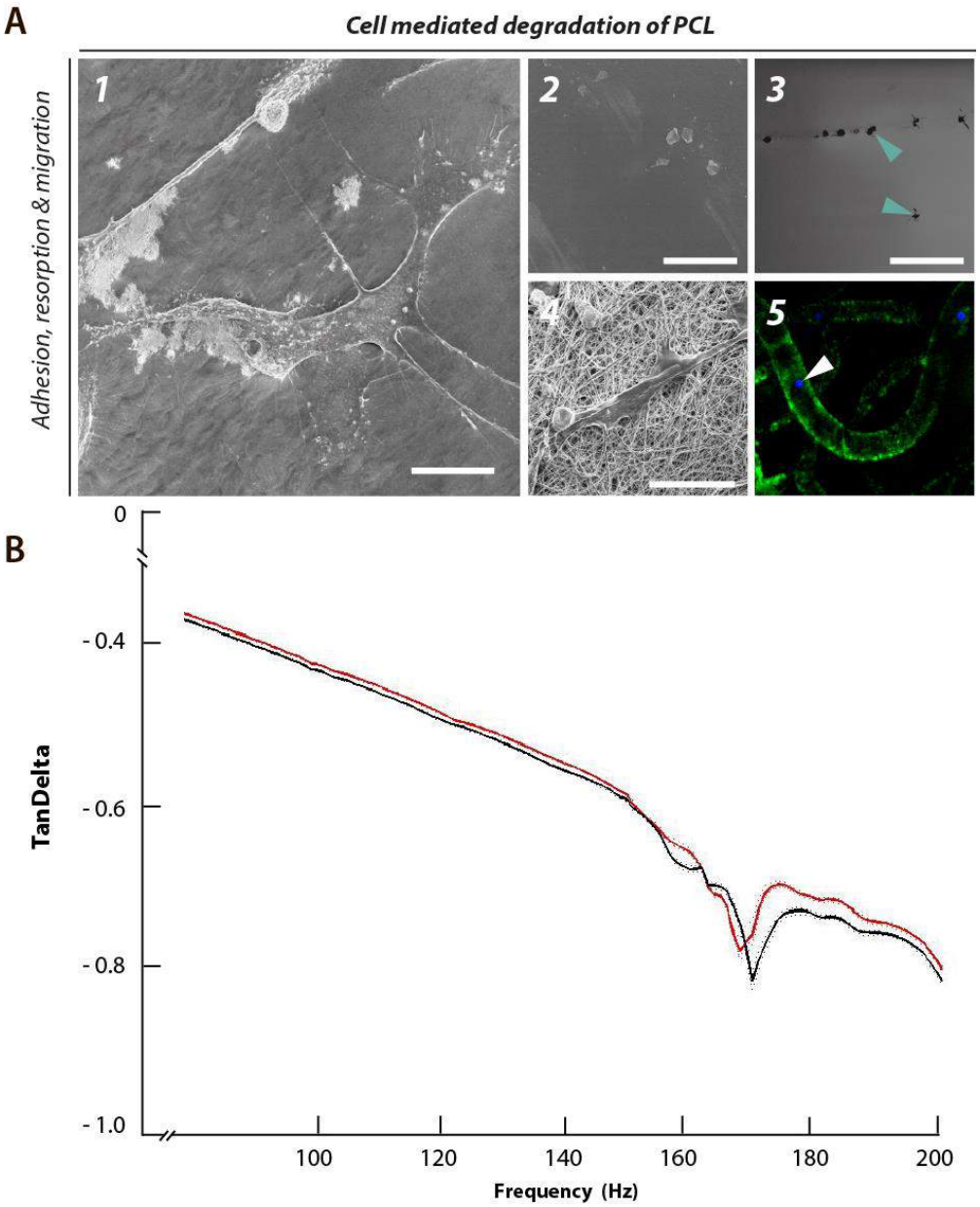

Figure 15: Initial cell mediated PCL degradation (after two weeks) accompanied by increased material stiffness.

4. Discussion of the findings

The presented state of the art methods used for this monograph, the modified in house methodologies and the gained results, provide new knowledge to the field of osteoclast and polyester degradation research. The main findings of the seven interconnected studies indicate that PCL can be degraded by osteoclast-like cells, a process enhanced in the presence of T cells. Moreover, osteoclast-like cells shed B_2-integrins and the shedding increases significantly upon migration on foreign materials like PCL, suggesting increased cell activity. Although not entirely evident, the data point out that the degradation process partly is a result of phagocytosis. Taken the TRIFMA data into account, it is reasonable to address the idea of PCL complement opsonization, followed by B_2-integrin complement receptor binding. Weakening of the PCL constructs is presumably induced by low pH at the subosteoclastic compartment and through the action of non-specific esterase, leading to enzymatic cleave of the ester-linkage between PCL monomers. This form of chemical degradation is considered essential prior to phagocytosis of single PCL fragments additive to the F-beads. PCL fragments adhesive to F-beads is reasoned based on the right lower shift of events detected on the forward site scatter plots, indicating increased particles size (compared to the control group, i.e. only F-beads in a solution) and reduction in fluorescence signaling. As previously noted, cell viability was assessed by Trypan Blue or Cell Tracker Green staining, in addition to Hoechst or DAPI counterstaining. Non-specific esterase activity (NSE, first indicated by figure 1) was therefore indirectly detected by this approach, performed alternatively to the colorimetric Methylthiazolyldiphenyl-tetrazolium bromide (MTT) viability assay, where Quinone reductase activity is indirectly detected by menadiol induced reduction of MTT to a blue formazan dye and can be measured over wavelengths between 550 and 640 nm (111). NSE activity was measured qualitatively, by using the fluorescent dye Cell Tracker Green (5-chloro-methylfluorescein diacetate). The two intracellular reactions of this reagent are shown below, which can react with glutathione:

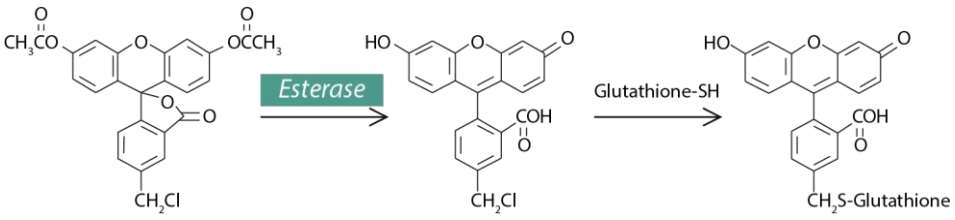

It has previously been reported that the product is non-fluorescent until acted upon by intracellular NSE (112). Although not profoundly published on (two manuscripts found), expression of NSE by osteoclast-like cells has been reported in the literature (113, 114). Based on this knowledge and the present findings, it is considered plausible that the observed osteoclast-like cell mediated degradation of PCL is initiated by esterase release into the microenvironment, followed by catalyzing hydrolysis or cleavage of the ester-linkage between the PCL monomers (figure 16). Addition of external acid is essential for PCL hydrolysis (115), which as in present *in vitro* setting can be achieved by the low pH within the subosteoclastic space. PCL is indeed biodegradable (116) and is easily degraded by microorganisms like *Pencillium oxalium* fungi as recently revealed (117). Weight loss of the polyester constructs was considered a reasonable outcome of the cell mediated degradation, however this effect was not observable after 14 days of cell culturing which is supported by Woodward *et al.* (118) remarking that the reduction in molecular weight (M_n) is determined by the initial molecular weight (M_n°) prior to the degradation process itself, as a function of time (t) and the degradation rate constant (k) according to the kinetic law, indicated by others (119) :

$$M_n = M_n^\circ \exp(-kt)$$

The same research group concluded that the first degradation step involves non-enzymatic and random hydrolysis of the ester-linkage between PCL monomers and that the loss of mechanical strength is additionally a function of time.

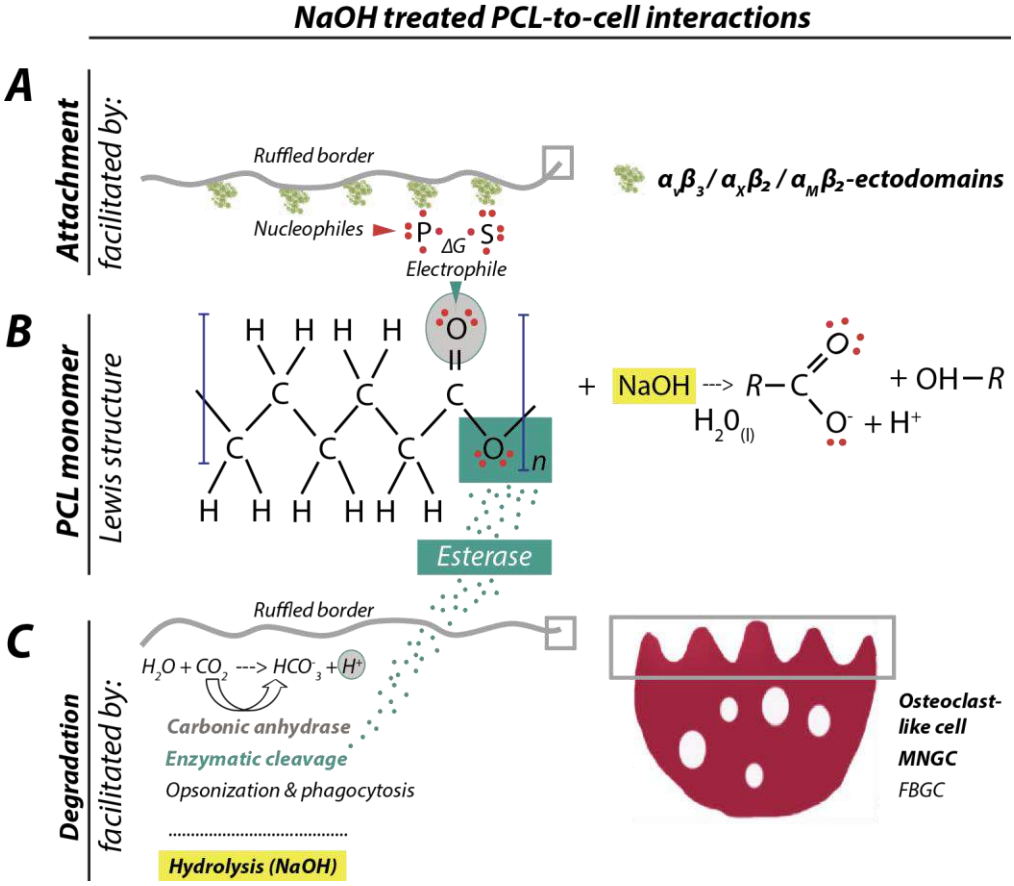

Figure 16: PCL is aliphatic polyester of linear monomers composed of a carbon chain with ester-linkage at every 7th position within a single monomer ($C_6H_{10}O_2$). The number of valence electrons assigned to the ester-linkage and the carbonyl group of the ester compound, after following the octet rule, equals to two and four electrons respectively. Hence, these electrons potentially can participate in the formation of new chemical bounds between PCL and cell synthesized molecules (A-B). Non-enzymatic hydrolysis of PCL, enzyme catalytic degradation by NSE, including low pH value beneath the ruffled border, are factors considered of importance, prior to complement opsonization and phagocytosis of PCL fragments by the phagocytic osteoclast-like cells (C) as indicated by the presented 3D confocal and flow cytometry results.

The chemistry behind PCL and adhesion molecules attraction, can be based on nucleophiles which donate electron to an electrophile to form a chemical bound in a reaction e.g. with protein components, expressed by the cells in the PCL microenvironment. Another plausible explanation is binding via hydroxyl groups formed after the NaOH treatment of PCL, leading to a chemical shift of the monomer, i.e. from a carbonyl group in the compound, associated to the ester-linkage, to a hydroxyl group (figure 16). Ultimately, NaOH treatment leads to a more hydrophilic PCL-surface, at

least partly for the polyester, giving it the capacity of hydrogen bonding sites with another chemical compound; hence the positive charge on the hydrogen atom produces an attraction for the electronegative neighboring atom, typically oxygen (O) or nitrogen (N), e.g. within a protein structure on the cell surface (integrin ectodomains as illustrated in figure 16). Same is theoretically true in the case of PCL opsonization by complement components prior to phagocytosis, indicated by the previously shown results. An exception to the octet rule mentioned above seen for the Lewis structure sketch of a single PCL monomer, applies for phosphorus (P) and sulfate (S). These atoms, in an identical protein structures (integrin ectodomains or complement components) can form an expended octet (more than 8 valence electrons surrounding P and S respectively), i.e. op to 12 e^- (hypervalency, as mentioned in figure 2), which means that the electron pairs can separate from each other and form bonding sides. Covalent binding (electrons shared by nuclei) is added to the atom within the PCL monomer which is most electronegative and according to the periodic table of electronegativity by Pauling scale, oxygen is most electronegative (3.5). In all probability the chemical binding described is spontaneous (negative Gibbs free energy), but it should be noted that the internal/total energy of the system in question (enthalpy) and its disorder (entropy) can't be calculated. A simplified drawing of the ruffled border (A and C), with anchored integrins primarily associated to the sealing zone, is shown above and attempted to be described more in details in figure 1-2 (Introduction) for *wild type* osteoclast. Here the ruffled border is outlined for PCL attached osteoclast-like cells (MNGCs), generated by the present *in vitro* experiments, and for the *in vivo* observed FBGC in close relation to PCL.

5. Conclusions & future perspectives

This monograph provides new information on osteoclasts-like cell activity, resorption and phagocytic capacity. As indicated by the data, their effect on the polyester PCL results ultimately in cell mediated degradation of the material, an effect which is enhanced in the presence of T cells. The results are in an agreement with previously published results, showing lymphocyte mediated fusion of MNGC pre-cursors and that osteoclastogenesis can directly be triggered by activated T cells through the RANK-L/RANK/OPG system (120, 121). Related observations by Takayanagi *et al.*

(122) supporting the notion that osteoclast activity is regulated by the immune system was followed by the introduction of the term osteoimmunology (123).

Apparently, cells of the monocyte-macrophage lineage are capable of degrading PCL. The degradation is further found to be accelerated in the presence of T cells. Such properties are considered important for successful use of PCL in tissue engineering. Future projects, with greater scientific impact and clinical value, are considered to concern advance development of viable and homogenous bone graft substitutes with superior remodeling properties. Interactions and performance of bone forming cells and bone reabsorbing cells with matrix-components, coated to biomaterials like PCL substituting bone grafts, has not been described in detail. Hence, the focus of future experiments is set on a new co-culture setting, with human mesenchymal stem cells and human monocytes (osteoclasts), aiming to investigate differentiation, adhesion and the potential for remodeling on biosynthetic PCL scaffold template, substituting bone grafts.

References

1. Chambers TJ (1978) Multinucleate giant cells. *The Journal of pathology* 126(3):125-148.
2. Teitelbaum SL (2000) Bone resorption by osteoclasts. *Science* 289(5484):1504-1508.
3. Ducy P, Schinke T, & Karsenty G (2000) The osteoblast: a sophisticated fibroblast under central surveillance. *Science* 289(5484):1501-1504.
4. Lacey DL, *et al.* (1998) Osteoprotegerin ligand is a cytokine that regulates osteoclast differentiation and activation. *Cell* 93(2):165-176.
5. Anastassova-Kristeva M (2003) The origin and development of the immune system with a view to stem cell therapy. *Journal of hematotherapy & stem cell research* 12(2):137-154.
6. Delsol G, *et al.* (1982) Warthin-Finkeldey-like cells in benign and malignant lymphoid proliferations. *Histopathology* 6(4):451-465.
7. Kamel OW, LeBrun DP, Berry GJ, Dorfman RF, & Warnke RA (1992) Warthin-Finkeldey polykaryocytes demonstrate a T-cell immunophenotype. *American journal of clinical pathology* 97(2):179-183.
8. Kubota K, *et al.* (1988) Warthin-Finkeldey-like giant cells in a patient with systemic lupus erythematosus. *Human pathology* 19(11):1358-1359.
9. da Costa CE, *et al.* (2005) Presence of osteoclast-like multinucleated giant cells in the bone and nonostotic lesions of Langerhans cell histiocytosis. *The Journal of experimental medicine* 201(5):687-693.
10. Abuel-Haija M & Hurford MT (2007) Kimura disease. *Archives of pathology & laboratory medicine* 131(4):650-651.
11. Tambuyzer BR, Ponsaerts P, & Nouwen EJ (2009) Microglia: gatekeepers of central nervous system immunology. *Journal of leukocyte biology* 85(3):352-370.
12. Einarsson HB, Jensen S, & Rasmussen LB (2002) [Pseudomembranous upper respiratory tract infection caused by herpes simplex virus in an adult]. *Ugeskrift for laeger* 164(50):5954-5955.
13. Procop GW & Wilson M (2001) Infectious disease pathology. *Clinical infectious diseases : an official publication of the Infectious Diseases Society of America* 32(11):1589-1601.
14. Sakai H, *et al.* (2012) The CD40-CD40L axis and IFN-gamma play critical roles in Langhans giant cell formation. *International immunology* 24(1):5-15.
15. Kukita T, *et al.* (2004) RANKL-induced DC-STAMP is essential for osteoclastogenesis. *The Journal of experimental medicine* 200(7):941-946.
16. Yagi M, *et al.* (2005) DC-STAMP is essential for cell-cell fusion in osteoclasts and foreign body giant cells. *The Journal of experimental medicine* 202(3):345-351.
17. Chacko G, Rajshekhar V, Chandy MJ, & Chandi SM (2000) The calcified intracorporeal vacuole: an aid to the pathological diagnosis of solitary cerebral cysticercus granulomas. *Journal of neurology, neurosurgery, and psychiatry* 69(4):525-527.
18. Wong CW & Ho YS (1994) Intraventricular haemorrhage and hydrocephalus caused by intraventricular parasitic granuloma suggesting cerebral sparganosis. *Acta neurochirurgica* 129(3-4):205-208.
19. Gazzoni AF, Severo CB, Salles EF, & Severo LC (2009) Histopathology, serology and cultures in the diagnosis of cryptococcosis. *Revista do Instituto de Medicina Tropical de Sao Paulo* 51(5):255-259.
20. Mukhopadhyay S & Katzenstein AL (2010) Biopsy findings in acute pulmonary histoplasmosis: unusual histologic features in 4 cases mimicking lymphomatoid granulomatosis. *The American journal of surgical pathology* 34(4):541-546.

21. Bagnasco SM, Subramanian AK, & Desai NM (2012) Fungal infection presenting as giant cell tubulointerstitial nephritis in kidney allograft. *Transplant infectious disease : an official journal of the Transplantation Society* 14(3):288-291.
22. el-Shoura S (1993) Ultrastructural interaction between multinucleate giant cells and the fungus in aspergillomas of human paranasal sinuses. *Virchows Archiv. B, Cell pathology including molecular pathology* 64(6):395-400.
23. Hill JO (1992) CD4+ T cells cause multinucleated giant cells to form around Cryptococcus neoformans and confine the yeast within the primary site of infection in the respiratory tract. *The Journal of experimental medicine* 175(6):1685-1695.
24. Begin R, Filion R, & Ostiguy G (1995) Emphysema in silica- and asbestos-exposed workers seeking compensation. A CT scan study. *Chest* 108(3):647-655.
25. McCormick LM, Goddard M, & Mahadeva R (2008) Pulmonary fibrosis secondary to siderosis causing symptomatic respiratory disease: a case report. *Journal of medical case reports* 2:257.
26. Petsonk EL, Rose C, & Cohen R (2013) Coal mine dust lung disease. New lessons from old exposure. *American journal of respiratory and critical care medicine* 187(11):1178-1185.
27. Balmes JR (2013) Asbestos and lung cancer: what we know. *American journal of respiratory and critical care medicine* 188(1):8-9.
28. Lenters V, *et al.* (2011) A meta-analysis of asbestos and lung cancer: is better quality exposure assessment associated with steeper slopes of the exposure-response relationships? *Environmental health perspectives* 119(11):1547-1555.
29. Raffn E, Lynge E, Juel K, & Korsgaard B (1989) Incidence of cancer and mortality among employees in the asbestos cement industry in Denmark. *British journal of industrial medicine* 46(2):90-96.
30. Ribak J, Lilis R, Suzuki Y, Penner L, & Selikoff IJ (1988) Malignant mesothelioma in a cohort of asbestos insulation workers: clinical presentation, diagnosis, and causes of death. *British journal of industrial medicine* 45(3):182-187.
31. Rosenthal GJ, *et al.* (1994) Asbestos stimulates IL-8 production from human lung epithelial cells. *Journal of immunology* 153(7):3237-3244.
32. Prieditis H & Adamson IY (1996) Alveolar macrophage kinetics and multinucleated giant cell formation after lung injury. *Journal of leukocyte biology* 59(4):534-538.
33. Ectors NL, *et al.* (1993) Granulomatous gastritis: a morphological and diagnostic approach. *Histopathology* 23(1):55-61.
34. Soriano A, *et al.* (2012) Giant cell arteritis and polymyalgia rheumatica after influenza vaccination: report of 10 cases and review of the literature. *Lupus* 21(2):153-157.
35. Lemperle G, Knapp TR, Sadick NS, & Lemperle SM (2010) ArteFill permanent injectable for soft tissue augmentation: I. Mechanism of action and injection techniques. *Aesthetic plastic surgery* 34(3):264-272.
36. Lemperle G, Romano JJ, & Busso M (2003) Soft tissue augmentation with artecoll: 10-year history, indications, techniques, and complications. *Dermatologic surgery : official publication for American Society for Dermatologic Surgery [et al.]* 29(6):573-587; discussion 587.
37. Wolfram D, Tzankov A, & Piza-Katzer H (2006) Surgery for foreign body reactions due to injectable fillers. *Dermatology* 213(4):300-304.
38. Reisberger EM, Landthaler M, Wiest L, Schroder J, & Stolz W (2003) Foreign body granulomas caused by polymethylmethacrylate microspheres: successful treatment with allopurinol. *Archives of dermatology* 139(1):17-20.
39. Ando A, Hatori M, Hagiwara Y, Isefuku S, & Itoi E (2009) Imaging features of foreign body granuloma in the lower extremities mimicking a soft tissue neoplasm. *Upsala journal of medical sciences* 114(1):46-51.

40. Leek MD & Barlow YM (1992) Tissue reactions induced by hydrocolloid wound dressings. *Journal of anatomy* 180 (Pt 3):545-551.
41. Sayegh S, *et al.* (2003) Suture granuloma mimicking infection following total hip arthroplasty. A report of three cases. *The Journal of bone and joint surgery. American volume* 85-A(10):2006-2009.
42. Conn J, Jr., Oyasu R, Welsh M, & Beal JM (1974) Vicryl (polyglactin 910) synthetic absorbable sutures. *American journal of surgery* 128(1):19-23.
43. Inoue G, *et al.* (2012) Postoperative lumbar spinal stenosis after intertransverse fusion with granules of hydroxyapatite: a case report. *Diagnostic pathology* 7:153.
44. Klinge U, Klosterhalfen B, Muller M, & Schumpelick V (1999) Foreign body reaction to meshes used for the repair of abdominal wall hernias. *The European journal of surgery = Acta chirurgica* 165(7):665-673.
45. Adams TS, Crook T, & Cadier MA (2007) A late complication following the insertion of hydrogel breast implants. *Journal of plastic, reconstructive & aesthetic surgery : JPRAS* 60(2):210-212.
46. Dvorak P, *et al.* (2012) Histological findings around electrodes in pacemaker and implantable cardioverter-defibrillator patients: comparison of steroid-eluting and non-steroid-eluting electrodes. *Europace : European pacing, arrhythmias, and cardiac electrophysiology : journal of the working groups on cardiac pacing, arrhythmias, and cardiac cellular electrophysiology of the European Society of Cardiology* 14(1):117-123.
47. Koh A, Nichols SP, & Schoenfisch MH (2011) Glucose sensor membranes for mitigating the foreign body response. *Journal of diabetes science and technology* 5(5):1052-1059.
48. Ruoslahti E & Pierschbacher MD (1987) New perspectives in cell adhesion: RGD and integrins. *Science* 238(4826):491-497.
49. Ruoslahti E (1996) Integrin signaling and matrix assembly. *Tumour biology : the journal of the International Society for Oncodevelopmental Biology and Medicine* 17(2):117-124.
50. Nesbitt S, Nesbit A, Helfrich M, & Horton M (1993) Biochemical characterization of human osteoclast integrins. Osteoclasts express alpha v beta 3, alpha 2 beta 1, and alpha v beta 1 integrins. *The Journal of biological chemistry* 268(22):16737-16745.
51. Oldberg A, Franzen A, & Heinegard D (1986) Cloning and sequence analysis of rat bone sialoprotein (osteopontin) cDNA reveals an Arg-Gly-Asp cell-binding sequence. *Proceedings of the National Academy of Sciences of the United States of America* 83(23):8819-8823.
52. McNally AK & Anderson JM (2002) Beta1 and beta2 integrins mediate adhesion during macrophage fusion and multinucleated foreign body giant cell formation. *The American journal of pathology* 160(2):621-630.
53. Hynes RO (2002) Integrins: bidirectional, allosteric signaling machines. *Cell* 110(6):673-687.
54. Haahr-Pedersen S, *et al.* (2009) Level of complement activity predicts cardiac dysfunction after acute myocardial infarction treated with primary percutaneous coronary intervention. *The Journal of invasive cardiology* 21(1):13-19.
55. Bjerre M, *et al.* (2010) Soluble membrane attack complex in ascites in patients with liver cirrhosis without infections. *World journal of hepatology* 2(6):221-225.
56. Arrington ED, Smith WJ, Chambers HG, Bucknell AL, & Davino NA (1996) Complications of iliac crest bone graft harvesting. *Clinical orthopaedics and related research* (329):300-309.
57. Banwart JC, Asher MA, & Hassanein RS (1995) Iliac crest bone graft harvest donor site morbidity. A statistical evaluation. *Spine* 20(9):1055-1060.
58. Goulet JA, Senunas LE, DeSilva GL, & Greenfield ML (1997) Autogenous iliac crest bone graft. Complications and functional assessment. *Clinical orthopaedics and related research* (339):76-81.
59. Laurie SW, Kaban LB, Mulliken JB, & Murray JE (1984) Donor-site morbidity after harvesting rib and iliac bone. *Plastic and reconstructive surgery* 73(6):933-938.

60. Seiler JG, 3rd & Johnson J (2000) Iliac crest autogenous bone grafting: donor site complications. *Journal of the Southern Orthopaedic Association* 9(2):91-97.
61. Simonds RJ, *et al.* (1992) Transmission of human immunodeficiency virus type 1 from a seronegative organ and tissue donor. *The New England journal of medicine* 326(11):726-732.
62. Mroz TE, *et al.* (2009) The use of allograft bone in spine surgery: is it safe? *The spine journal : official journal of the North American Spine Society* 9(4):303-308.
63. Nielsen HT, Larsen S, Andersen M, & Ovesen O (2001) Bone bank service in Odense, Denmark. Audit of the first ten years with bone banking at the Department of Orthopaedics, Odense University Hospital. *Cell and tissue banking* 2(3):179-183.
64. Fideler BM, Vangsness CT, Jr., Moore T, Li Z, & Rasheed S (1994) Effects of gamma irradiation on the human immunodeficiency virus. A study in frozen human bone-patellar ligament-bone grafts obtained from infected cadavera. *The Journal of bone and joint surgery. American volume* 76(7):1032-1035.
65. Zhang Q, Cornu O, & Delloye C (1997) Ethylene oxide does not extinguish the osteoinductive capacity of demineralized bone. A reappraisal in rats. *Acta orthopaedica Scandinavica* 68(2):104-108.
66. Kaku N, Tsumura H, Kataoka M, Taira H, & Torisu T (2002) Influence of aeration, storage, and rinsing conditions on residual ethylene oxide in freeze-dried bone allograft. *Journal of orthopaedic science : official journal of the Japanese Orthopaedic Association* 7(2):238-242.
67. Hofmann A, *et al.* (2005) The influence of bone allograft processing on osteoblast attachment and function. *Journal of orthopaedic research : official publication of the Orthopaedic Research Society* 23(4):846-854.
68. Hirn MY, Salmela PM, & Vuento RE (2001) High-pressure saline washing of allografts reduces bacterial contamination. *Acta orthopaedica Scandinavica* 72(1):83-85.
69. Pruss A, Kao M, Kiesewetter H, von Versen R, & Pauli G (1999) Virus safety of avital bone tissue transplants: evaluation of sterilization steps of spongiosa cuboids using a peracetic acid-methanol mixture. *Biologicals : journal of the International Association of Biological Standardization* 27(3):195-201.
70. Aspenberg P & Lindqvist SB (1998) Ethene oxide and bone induction. Controversy remains. *Acta orthopaedica Scandinavica* 69(2):173-176.
71. Thoren K & Aspenberg P (1995) Ethylene oxide sterilization impairs allograft incorporation in a conduction chamber. *Clinical orthopaedics and related research* (318):259-264.
72. Fideler BM, Vangsness CT, Jr., Lu B, Orlando C, & Moore T (1995) Gamma irradiation: effects on biomechanical properties of human bone-patellar tendon-bone allografts. *The American journal of sports medicine* 23(5):643-646.
73. Currey JD, *et al.* (1997) Effects of ionizing radiation on the mechanical properties of human bone. *Journal of orthopaedic research : official publication of the Orthopaedic Research Society* 15(1):111-117.
74. Boyce T, Edwards J, & Scarborough N (1999) Allograft bone. The influence of processing on safety and performance. *The Orthopedic clinics of North America* 30(4):571-581.
75. Sorger JI, *et al.* (2001) Allograft fractures revisited. *Clinical orthopaedics and related research* (382):66-74.
76. Mankin HJ, Hornicek FJ, & Raskin KA (2005) Infection in massive bone allografts. *Clinical orthopaedics and related research* (432):210-216.
77. Jansen J, Ooms E, Verdonschot N, & Wolke J (2005) Injectable calcium phosphate cement for bone repair and implant fixation. *The Orthopedic clinics of North America* 36(1):89-95, vii.
78. Li YW, *et al.* (2000) A novel injectable bioactive bone cement for spinal surgery: a developmental and preclinical study. *Journal of biomedical materials research* 52(1):164-170.
79. Mankin HJ, Hornicek FJ, & Harris M (2005) Total femur replacement procedures in tumor treatment. *Clinical orthopaedics and related research* 438:60-64.

80. Lewis G (1997) Properties of acrylic bone cement: state of the art review. *Journal of biomedical materials research* 38(2):155-182.
81. Huiskes R, Weinans H, & van Rietbergen B (1992) The relationship between stress shielding and bone resorption around total hip stems and the effects of flexible materials. *Clinical orthopaedics and related research* (274):124-134.
82. Kanayama M, *et al.* (2000) In vitro biomechanical investigation of the stability and stress-shielding effect of lumbar interbody fusion devices. *Journal of neurosurgery* 93(2 Suppl):259-265.
83. Augustin G, *et al.* (2008) Thermal osteonecrosis and bone drilling parameters revisited. *Archives of orthopaedic and trauma surgery* 128(1):71-77.
84. van den Dolder J, Spauwen PH, & Jansen JA (2003) Evaluation of various seeding techniques for culturing osteogenic cells on titanium fiber mesh. *Tissue engineering* 9(2):315-325.
85. Zou X, Li H, Baatrup A, Lind M, & Bunger C (2003) Engineering of bone tissue with porcine bone marrow stem cells in three-dimensional trabecular metal: in vitro and in vivo studies. *APMIS. Supplementum* (109):127-132.
86. El-Ghannam A (2005) Bone reconstruction: from bioceramics to tissue engineering. *Expert review of medical devices* 2(1):87-101.
87. Thomas MV, Puleo DA, & Al-Sabbagh M (2005) Bioactive glass three decades on. *Journal of long-term effects of medical implants* 15(6):585-597.
88. Louis-Ugbo J, Murakami H, Kim HS, Minamide A, & Boden SD (2004) Evidence of osteoinduction by Grafton demineralized bone matrix in nonhuman primate spinal fusion. *Spine* 29(4):360-366; discussion Z361.
89. Mauney JR, *et al.* (2005) In vitro and in vivo evaluation of differentially demineralized cancellous bone scaffolds combined with human bone marrow stromal cells for tissue engineering. *Biomaterials* 26(16):3173-3185.
90. Behravesh E, Yasko AW, Engel PS, & Mikos AG (1999) Synthetic biodegradable polymers for orthopaedic applications. *Clinical orthopaedics and related research* (367 Suppl):S118-129.
91. Hollinger JO, Brekke J, Gruskin E, & Lee D (1996) Role of bone substitutes. *Clinical orthopaedics and related research* (324):55-65.
92. Goldstein AS, Zhu G, Morris GE, Meszlenyi RK, & Mikos AG (1999) Effect of osteoblastic culture conditions on the structure of poly(DL-lactic-co-glycolic acid) foam scaffolds. *Tissue engineering* 5(5):421-434.
93. Meinel L, *et al.* (2004) Bone tissue engineering using human mesenchymal stem cells: effects of scaffold material and medium flow. *Annals of biomedical engineering* 32(1):112-122.
94. Roether JA, *et al.* (2002) Novel bioresorbable and bioactive composites based on bioactive glass and polylactide foams for bone tissue engineering. *Journal of materials science. Materials in medicine* 13(12):1207-1214.
95. Mygind T, *et al.* (2007) Mesenchymal stem cell ingrowth and differentiation on coralline hydroxyapatite scaffolds. *Biomaterials* 28(6):1036-1047.
96. Stiehler M, *et al.* (2009) Effect of dynamic 3-D culture on proliferation, distribution, and osteogenic differentiation of human mesenchymal stem cells. *Journal of biomedical materials research. Part A* 89(1):96-107.
97. Bjerre L, Bunger CE, Kassem M, & Mygind T (2008) Flow perfusion culture of human mesenchymal stem cells on silicate-substituted tricalcium phosphate scaffolds. *Biomaterials* 29(17):2616-2627.
98. Goldberg VM & Stevenson S (1987) Natural history of autografts and allografts. *Clinical orthopaedics and related research* (225):7-16.
99. Mulliken JB, Kaban LB, & Glowacki J (1984) Induced osteogenesis--the biological principle and clinical applications. *The Journal of surgical research* 37(6):487-496.

100. Buckwalter JA & Cooper RR (1987) Bone structure and function. *Instructional course lectures* 36:27-48.
101. Williams JM, *et al.* (2005) Bone tissue engineering using polycaprolactone scaffolds fabricated via selective laser sintering. *Biomaterials* 26(23):4817-4827.
102. Ray SS & Bousmina M (2005) Biodegradable polymers and their layered silicate nano composites: In greening the 21st century materials world. *Prog Mater Sci* 50(8):962-1079.
103. Nair LS & Laurencin CT (2007) Biodegradable polymers as biomaterials. *Prog Polym Sci* 32(8-9):762-798.
104. Agbay A, Mohtaram NK, & Willerth SM (2014) Controlled release of glial cell line-derived neurotrophic factor from poly(epsilon-caprolactone) microspheres. *Drug delivery and translational research* 4(2):159-170.
105. Sun M, *et al.* (2015) A tissue-engineered therapeutic device inhibits tumor growth in vitro and in vivo. *Acta biomaterialia*.
106. Jensen J, *et al.* (2014) Surface-modified functionalized polycaprolactone scaffolds for bone repair: in vitro and in vivo experiments. *Journal of biomedical materials research. Part A* 102(9):2993-3003.
107. Susa M, Luong-Nguyen NH, Cappellen D, Zamurovic N, & Gamse R (2004) Human primary osteoclasts: in vitro generation and applications as pharmacological and clinical assay. *Journal of translational medicine* 2(1):6.
108. Wang W, Ferguson DJ, Quinn JM, Simpson AH, & Athanasou NA (1997) Biomaterial particle phagocytosis by bone-resorbing osteoclasts. *The Journal of bone and joint surgery. British volume* 79(5):849-856.
109. Wang W, Ferguson DJ, Quinn JM, Simpson AH, & Athanasou NA (1997) Osteoclasts are capable of particle phagocytosis and bone resorption. *The Journal of pathology* 182(1):92-98.
110. Gjelstrup LC, *et al.* (2010) Shedding of large functionally active CD11/CD18 Integrin complexes from leukocyte membranes during synovial inflammation distinguishes three types of arthritis through differential epitope exposure. *Journal of immunology* 185(7):4154-4168.
111. Prochaska HJ & Santamaria AB (1988) Direct measurement of NAD(P)H:quinone reductase from cells cultured in microtiter wells: a screening assay for anticarcinogenic enzyme inducers. *Analytical biochemistry* 169(2):328-336.
112. Haugland RP (1995) Detecting enzymatic activity in cells using fluorogenic substrates. *Biotechnic & histochemistry : official publication of the Biological Stain Commission* 70(5):243-251.
113. Udagawa N, *et al.* (1990) Origin of osteoclasts: mature monocytes and macrophages are capable of differentiating into osteoclasts under a suitable microenvironment prepared by bone marrow-derived stromal cells. *Proceedings of the National Academy of Sciences of the United States of America* 87(18):7260-7264.
114. Connor JR, Dodds RA, James IE, & Gowen M (1995) Human osteoclast and giant cell differentiation: the apparent switch from nonspecific esterase to tartrate resistant acid phosphatase activity coincides with the in situ expression of osteopontin mRNA. *The journal of histochemistry and cytochemistry : official journal of the Histochemistry Society* 43(12):1193-1201.
115. Siparsky GL, Voorhees KJ, & Miao FD (1998) Hydrolysis of polylactic acid (PLA) and polycaprolactone (PCL) in aqueous acetonitrile solutions: Autocatalysis. *J Environ Polym Degr* 6(1):31-41.
116. Fukushima K, *et al.* (2010) Biodegradation trend of poly(epsilon-caprolactone) and nanocomposites. *Mat Sci Eng C-Mater* 30(4):566-574.
117. Li F, *et al.* (2012) Biodegradation of poly(epsilon-caprolactone) (PCL) by a new Penicillium oxalicum strain DSYD05-1. *World journal of microbiology & biotechnology* 28(10):2929-2935.
118. Woodward SC, Brewer PS, Moatamed F, Schindler A, & Pitt CG (1985) The intracellular degradation of poly(epsilon-caprolactone). *Journal of biomedical materials research* 19(4):437-444.

119. Pitt CG, Gratzl MM, Kimmel GL, Surles J, & Schindler A (1981) Aliphatic Polyesters .2. The Degradation of Poly(Dl-Lactide), Poly(Epsilon-Caprolactone), and Their Copolymers Invivo. *Biomaterials* 2(4):215-220.
120. Postlethwaite AE, Jackson BK, Beachey EH, & Kang AH (1982) Formation of multinucleated giant cells from human monocyte precursors. Mediation by a soluble protein from antigen-and mitogen-stimulated lymphocytes. *The Journal of experimental medicine* 155(1):168-178.
121. Kong YY, *et al.* (1999) Activated T cells regulate bone loss and joint destruction in adjuvant arthritis through osteoprotegerin ligand. *Nature* 402(6759):304-309.
122. Takayanagi H, *et al.* (2000) T-cell-mediated regulation of osteoclastogenesis by signalling cross-talk between RANKL and IFN-gamma. *Nature* 408(6812):600-605.
123. Arron JR & Choi Y (2000) Bone versus immune system. *Nature* 408(6812):535-536.

Appendix

Supplementary work

Paper 1

Paper 2

Paper 3

Paper 4

PhD at a glance

CD200 and its receptor, CD200R, modulate bone mass via the differentiation of osteoclasts

Weiguo Cui*†, Esteban Cuartas*, Juan Ke*‡, Qing Zhang*, Halldor B. Einarsson*, Jonathon D. Sedgwick§¶, Jun Li‖, and Agnès Vignery*,**

*Department of Orthopedics and Rehabilitation, Yale School of Medicine, 310 Cedar Street, New Haven, CT 06510; §Schering–Plough Biopharma (DNAX), Palo Alto, CA 94304; and ‖Department of Immunology and Inflammation, Boehringer Ingelheim Pharmaceuticals, Inc., Ridgefield, CT 06877

Edited by Richard A. Flavell, Yale University School of Medicine, New Haven, CT, and approved July 25, 2007 (received for review April 11, 2007)

Fusion of macrophages is an essential step in the differentiation of osteoclasts, which play a central role in the development and remodeling of bone. Osteoclasts are important mediators of bone loss, which leads, for example, to osteoporosis. Macrophage fusion receptor/signal regulatory protein α (MFR/SIRPα) and its ligand CD47, which are members of the Ig superfamily (IgSF), have been implicated in the fusion of macrophages. We show that CD200, which is not expressed in cells that belong to the myeloid lineage, is strongly expressed in macrophages at the onset of fusion. By contrast, the CD200 receptor (CD200R), which, like CD200, belongs to the IgSF, is expressed only in cells that belong to the myeloid lineage, including osteoclasts, and in CD4$^+$ T cells. Osteoclasts from CD200$^{-/-}$ mice differentiated at a reduced rate. Activation of the NF-κB and MAP kinase signaling pathways downstream of RANK, a receptor that plays a central role in the differentiation of osteoclasts, was depressed in these cells. A soluble recombinant protein that included the extracellular domain of CD200 rescued the fusion of CD200$^{-/-}$ macrophages and their activation downstream of RANK. Conversely, addition of a soluble recombinant protein that included the extracellular domain of CD200R or short-hairpin RNA-mediated silencing of the expression of CD200R prevented fusion. Thus CD200 engagement of the CD200R at the initiation of macrophage fusion regulated further differentiation to osteoclasts. Consistent with *in vitro* observations, CD200$^{-/-}$ mice contained fewer osteoclasts and accumulated more bone than CD200$^{+/+}$ mice. The CD200-CD200R axis is therefore a putative regulator of bone mass, via the formation of osteoclasts.

fusion | macrophage | RANK | MAPK

Multinucleate osteoclasts originate from the fusion of macrophages and play a major role in the resorption of bone (1–4). Osteoclasts are essential for both the development and remodeling of bone, and increases in the number and/or activity of osteoclasts lead to diseases associated with generalized bone loss, such as osteoporosis, and others associated with localized bone loss, such as rheumatoid arthritis and periodontal disease. Because fusion is a key step in the differentiation of osteoclasts, a detailed understanding of the molecular mechanism of macrophage fusion should help develop strategies to prevent bone loss.

The adhesion of cells to one another that precedes fusion appears to involve a set of proteins similar to those exploited by viruses for fusion with host cells (5). It has been postulated, moreover, that viruses usurped the fusion-protein machinery from their target cells (1). It is now generally accepted that virus-cell fusion requires both an attachment mechanism and a fusion peptide. An example of such fusion involves gp120 of the HIV, which binds to CD4 on T lymphocytes and macrophages (6, 7), whereas the fusion molecule gp40, which is derived from the same precursor (gp160) as gp120, is thought to trigger the actual fusion event. We postulated (8) that the fusion machinery used by macrophages is similar to that used by viruses to infect cells. In 1998, we reported that the expression of macrophage fusion receptor/signal regulatory protein α (MFR/SIRPα) is induced transiently in macrophages at the onset of fusion (9). MFR/SIRPα and its receptor, CD47, belong to the superfamily of immunoglobulins (IgSF), as does CD4, and their interaction plays a role in the recognition of self and in the fusion of macrophages (10). To gain further insight into the mechanism of macrophage fusion, we subjected fusing alveolar macrophages from rats to genome-wide oligonucleotide microarray analysis, and we discovered the expression of CD200 *de novo* at the onset of fusion.

CD200 also belongs to the IgSF and has a short cytoplasmic tail. It is expressed on various types of mouse and human cells (see ref. 11 for a review) and on mouse osteoblasts (12), but not on macrophages. By contrast, the receptor for CD200 (CD200R), which, resembling CD200, contains two IgSF domains, is expressed predominantly in myeloid cells and includes an intracellular domain that mediates downstream signaling, typically delivering an inhibitory signal. Although five mouse CD200R-related genes, termed mCD200RLa-e, were identified, only one human homolog, called hCD200RLa, is known, yet apparently not expressed (see ref. 11 for a review). Both mCD200RLa and -Lb isoforms were characterized further and show close homology to CD200R in the extracellular region, with short cytoplasmic regions that contain a positively charged lysine residue in the transmembrane domain, possibly interacting with DAP12 to deliver an activating signal. It appears, however, that only CD200R and possibly the strain-specific CD200RLe bind CD200 (11, 13).

CD200-CD200R has a pattern of expression similar to that of MFR/SIRPα-CD47 in that CD200, like CD47, is widely expressed, whereas CD200R, like MFR/SIRPα, is expressed predominantly in cells that belong to the myeloid lineage. Therefore, we postulated that the CD200-CD200R axis might play a role in the fusion of macrophages based on the clearly defined role for the CD200-CD200R interaction to regulate macrophage function (14), and that mice that lack CD200 would have a defect in macrophage fusion and, as a result, in both osteoclast differentiation and bone remodeling.

We found that the expression of CD200 was potently induced *de novo* in macrophages at the onset of fusion, and that osteoclasts deficient in CD200 had a defect in multinucleation and in signaling downstream of receptor activator of NF-κB (RANK), which are essential for osteoclastogenesis. We also found that CD200-

Author contributions: A.V. designed research; W.C., E.C., J.K., Q.Z., H.B.E., and J.L. performed research; J.D.S. contributed new reagents/analytic tools; and A.V. wrote the paper.

The authors declare no conflict of interest.

This article is a PNAS Direct Submission.

Freely available online through the PNAS open access option.

Abbreviations: IgSF, Ig superfamily; CD200R, CD200 receptor; ALP, alkaline phosphatase; MFR/SIRPα, macrophage fusion receptor/signal regulatory protein α; MEM, minimum essential medium; RANK, receptor activator of NF-κB; RANKL, RANK ligand; M-CSF, macrophage colony-stimulating factor.

†Present address: Department of Immunobiology, Yale School of Medicine, 300 Cedar Street, New Haven, CT 06510.

‡Present address: Amgen Inc., One Amgen Center Drive, Thousand Oaks, CA 91320.

¶Present address: Eli Lilly and Company, Indianapolis, IN 46285.

**To whom correspondence should be addressed. E-mail: agnes.vignery@yale.edu.

This article contains supporting information online at www.pnas.org/cgi/content/full/0702811104/DC1.

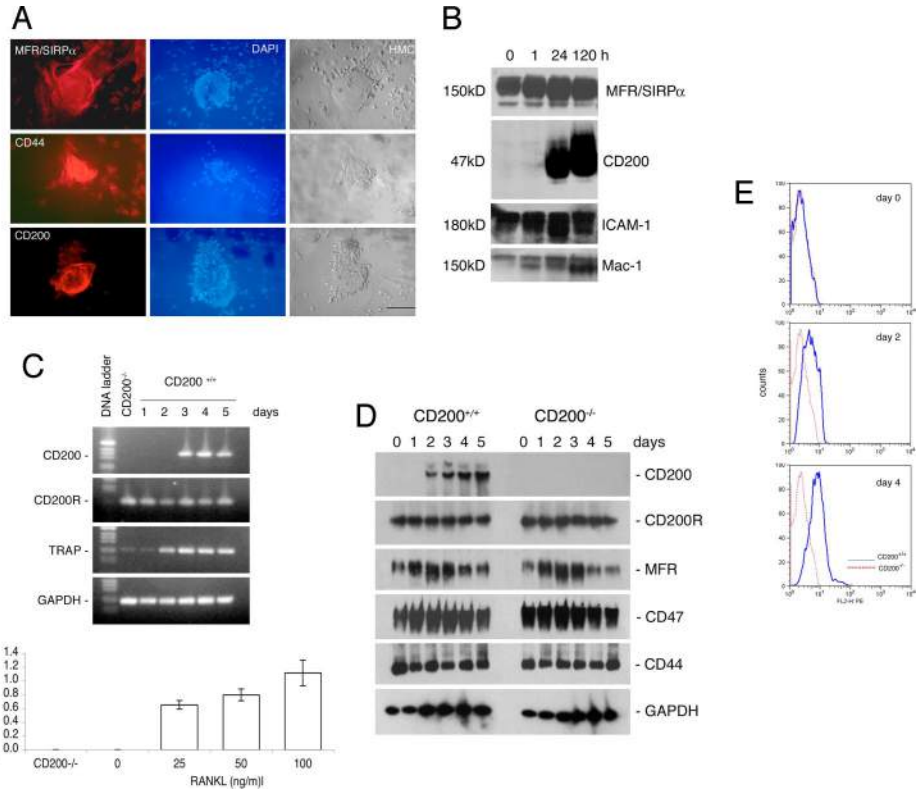

Fig. 1. Rat alveolar macrophages and mouse bone marrow-derived macrophages express CD200 upon multinucleation. (*A*) Freshly isolated rat alveolar macrophages were plated at confluency over 50% of the surface of each well to promote fusion and multinucleation. After 5 days, they were subjected to immunohistochemical analysis. Note that mononucleated macrophages were positive for MFR/SIRPα and CD44 but not for CD200. (Scale bar, 1 mm.) Also note that multinucleate rat alveolar macrophages contained hundreds of nuclei that were stained with DAPI (blue). (*B*) Freshly isolated rat alveolar macrophages were plated as in *A* and subjected to Western blot analysis at the indicated times. Note that CD200 was not detected in macrophages for the first 24 h. (*C*) Mouse bone marrow-derived macrophages were cultured in the presence of M-CSF (30 ng/ml) and RANKL (50 ng/ml) for the indicated times to induce the differentiation of multinucleate osteoclasts. Cells were analyzed by RT-PCR. Note that mouse bone marrow-derived macrophages expressed transcripts for CD200 receptor (CD200R) but not for CD200. The abundance of CD200 mRNA relative to that of GAPDH, in response to M-CSF (30 ng/ml) and increasing doses of RANKL, was determined. (Scale bars represent standard deviations; $n = 3$.) (*D*) Mouse bone marrow-derived macrophages were cultured in the presence of M-CSF (30 ng/ml) and RANKL (50 ng/ml) for the indicated times to induce the differentiation of multinucleate osteoclasts. Cells were subjected to Western blot analysis by using antibodies directed against the indicated antigens. (*E*) Flow-cytometric analysis (in a FACS) of the expression of CD200. Mouse bone marrow-derived macrophages were isolated from CD200$^{+/+}$ and CD200$^{-/-}$ mice, cultured in the presence of M-CSF (30 ng/ml) and RANKL (50 ng/ml) and subjected to flow-cytometric analysis at the indicated times with an antibody directed against CD200 and a control isotype antibody. Bone marrow-derived macrophages expressed increasing amounts of CD200 with time in the presence of M-CSF and RANKL, which promote fusion, multinucleation and osteoclastogenesis.

deficient mice had a lower number of osteoclasts and a higher bone density than wild-type mice. Together, our observations indicate that the CD200-CD200R axis plays a central role in the fusion of macrophages and the formation of osteoclasts.

Results

Expression of CD200 *de Novo* in Macrophages at the Onset of Fusion. To identify previously undescribed components of the machinery of macrophage fusion, we submitted fusing alveolar macrophages from rats to genome-wide microarray analysis. Such macrophages provide an efficient and homogeneous model system for studies of macrophage fusion (refs. 8–10, 15; see ref. 2 for a review), because they are "naïve" and fuse spontaneously *in vitro* when plated confluently, without the addition of cytokines. Barely any transcripts encoding CD200 (GenBank accession no. X01785) were detected in freshly isolated macrophages, but the levels of transcripts in fusing macrophages were 0.6 ± 1.4, 34.9 ± 7.2, and 61.6 ± 23.4 times higher than those in freshly isolated cells 1, 24, and 120 h after plating, respectively (mean $\pm$ SD; $n = 3$). To confirm the cell-surface expression of CD200, we reacted multinucleated alveolar macrophages with a monoclonal antibody raised against the extracellular domain of CD200. In parallel, we subjected fusing alveolar macrophages to Western blot analysis at different times. We used antibodies directed against MFR/SIRPα as a control, because the expression of this protein is induced at the onset of macrophage fusion (8). Our results confirmed the strong and *de novo* expression of CD200 as early as 24 h after plating (Figs. 1 *A* and *B*). However, unlike MFR/SIRPα, CD200 was not expressed in mononucleate macrophages (Fig. 1*A*).

To investigate whether CD200 was also expressed in osteoclasts, we cultured mouse bone marrow-derived macrophages in the presence of macrophage colony-stimulating factor (M-CSF) (30 ng/ml) and RANK ligand (RANKL) (50 ng/ml) for 5 days to generate osteoclasts (16). Unlike MFR/SIRPα and CD44, neither transcripts encoding CD200 nor CD200 protein were detected in macrophages, but strong expression of such transcripts and of CD200 was induced by RANKL as early as day 2. Moreover, the induction of expression of CD200 transcripts depended on the dose of RANKL (Fig. 1*C*). By contrast, the expression of CD200R was clearly constitutive (Fig. 1 *C* and *D*). Of note, MFR/SIRPα, CD47, and CD44 were expressed in mouse osteoclasts during their differentiation, and the levels of these proteins were unaffected by disruption of the expression of CD200, because osteoclasts from mice deficient in CD200 expressed similar levels of these proteins. This observation suggests that the expression of these fusion molecules is regulated by a mechanism that is independent of and different from CD200.

To confirm that CD200 was expressed on the surface of osteoclasts, we cultured bone macrophages as described (16), reacted them at different times with a monoclonal antibody that recognized the extracellular domain of CD200, and subjected them to flow-cytometric analysis. The results, shown in Fig. 1*E*, confirm the strong and *de novo* cell-surface expression of CD200 at the onset of osteoclast fusion/multinucleation.

Together, our results indicate that CD200 might be a previously unrecognized component of the macrophage fusion machinery. Therefore, we postulated that the deletion of CD200 could affect the differentiation of osteoclasts.

The Absence of CD200 Impaired the Differentiation of Osteoclasts. To examine first whether CD200 affects the number of osteoclast

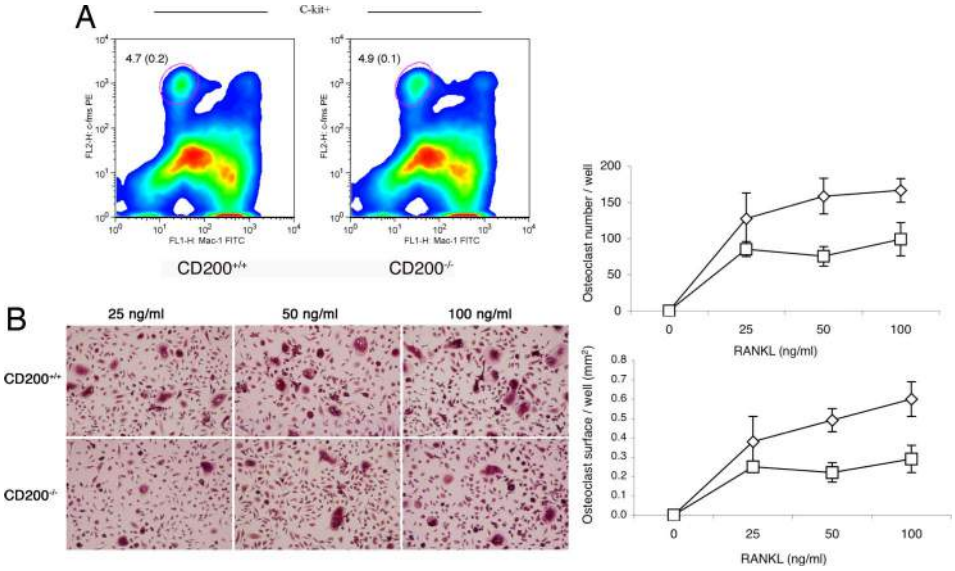

Fig. 2. Osteoclasts and their precursors are affected by the absence of CD200. (*A*) Bone marrow cells from 6-week-old CD200-deficient and wild-type mice were subjected to flow-cytometric analysis with antibodies directed against c-fms, Mac-1, and C-*kit*, as surface markers. Note that the absence of CD200 did not affect the number of osteoclast precursor cells (*Left*). (Scale bars, SD; $n = 5$.) (*B*) Bone-marrow-derived macrophages from 6-week-old CD200-deficient mice were cultured in the presence of M-CSF (30 ng/ml) and increasing concentrations of RANKL for 5 days to induce the differentiation of osteoclasts (*Left*). Bone marrow macrophages that lacked CD200 formed fewer osteoclasts than wild-type cells (*Right*). (Scale bars, SD; $n = 5$.)

precursors, we subjected freshly isolated bone marrow cells to flow-cytometric analysis using surface markers expressed by preosteoclasts (17, 18). The percentage of precursor cells relative to the total number of bone marrow cells was similar in $CD200^{+/+}$ and $CD200^{-/-}$ mice (Fig. 2*A*). We then compared the rates of osteoclastogenesis *in vitro* in $CD200^{+/+}$ and $CD200^{-/-}$ mice. We cultured mouse bone marrow macrophages in the presence of M-CSF (30 ng/ml) and increasing concentrations of RANKL for 5 days to generate osteoclasts. The absence of CD200 resulted in a dose-dependent decrease in the number of osteoclasts and in the surface area covered by osteoclasts (Fig. 2*B*). These data strongly supported our hypothesis that CD200 plays a role in the formation of osteoclasts. Although fewer and smaller, bone-marrow-derived $CD200^{-/-}$ macrophages differentiated into osteoclasts that formed an actin ring and resorbed dentin; hence, they appeared morphologically and functionally mature [supporting information (SI) Fig. 6]. In addition, $CD200^{-/-}$ osteoclasts, like wild types, expressed mature osteoclast markers, such as calcitonin receptors, and osteoclast-associated receptor (OSCAR) and to a lesser level cathepsin K (SI Table 1). Together, our data suggest that CD200 plays a role in the multinucleation of osteoclasts but not in their ability to differentiate into active osteoclasts (SI Fig. 6).

Because RANKL, which activates the NF-κB and MAP kinase signaling pathways that operate downstream of RANK, is essential for osteoclastogenesis, we next asked whether a deficiency in CD200 might affect signaling downstream of RANK. We cultured bone marrow cells from CD200-deficient and wild-type mice in the presence of M-CSF (30 ng/ml) for 2 days, then, after starving them for 2 h, we treated them with RANKL (50 ng/ml) up to 2 h and, finally, we subjected them to Western blot analysis with phosphorylated form-specific and control antibodies directed against IkBα, p38, ERK1/2, and JNK. Although activation of IkBα was slightly decreased, activation of JNK was almost completely abolished in cells that lacked CD200 (Fig. 3). These results revealed that the absence of CD200 attenuated the transduction of signals downstream of RANK and suggested that the CD200-CD200R interaction might play a role in this signaling pathway and in the formation of osteoclasts.

The CD200-CD200R Axis Is a Component of the Fusion Machinery. To address the putative role of the CD200-CD200R axis in the fusion of macrophages, we used several complementary strategies. First, we asked whether exogenous CD200 could rescue the differentiation of osteoclasts *in vitro* in cells that lack CD200. We generated a histidine-tagged soluble recombinant protein that included the extracellular domain of mouse CD200 (sCD200). We cultured bone marrow cells isolated from CD200-deficient and wild-type mice in the presence of M-CSF (30 ng/ml), RANKL (50 ng/ml), and sCD200 (0.5 μg/ml). The addition of sCD200 rescued multinucleation of CD200-deficient macrophages (Fig. 4*A*), whereas soluble histidine-tagged recombinant prostate-specific antigen, used as a control, did not (data not shown). We next asked whether sCD200-induced fusion resulted from the activation of JNK and IκB activation, which is suppressed in the absence of CD200. We cultured bone marrow cells from CD200-deficient and wild-type mice in the presence of M-CSF (5 ng/ml) for 2 days. After starving them for 2 h, we treated them for 30 min with RANKL (50 ng/ml), in the presence and absence of sCD200 (0.5 μg/ml) and, finally, we subjected them to Western blot, as described above. The addition of sCD200 restored the activation of JNK, but not of IκB, support-

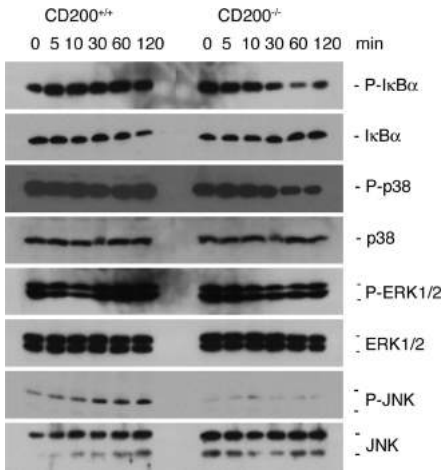

Fig. 3. In osteoclasts deficient in CD200, the activation of signaling molecules downstream of RANK is suppressed. Bone marrow macrophages isolated from CD200-deficient, and wild-type mice were cultured in the presence of M-CSF (5 ng/ml) for 12–18 h. Nonadherent cells were further cultured for 2 days in 24-well dishes, starved for 2 h, and then stimulated with 50 ng/ml RANKL for the indicated times. Cells were subjected to Western blot analysis with antibodies directed against the indicated antigens. The activation, by phosphorylation, of IκB and JNK was less extensive in cells that lacked CD200 than in wild-type cells. This experiment was repeated three times with similar results.

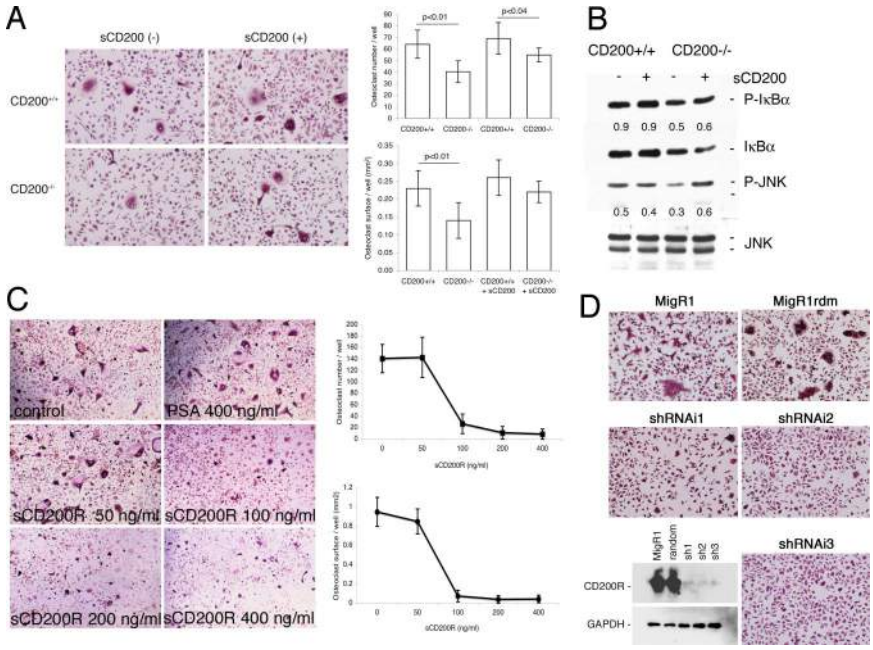

Fig. 4. The CD200-CD200R axis is required for osteoclast fusion/multinucleation. (*A*) Bone-marrow-derived macrophages from 6-week-old wild-type mice were cultured in the presence of M-CSF (30 ng/ml) and RANKL (50 ng/ml) with or without the recombinant extracellular domain of CD200 (sCD200; 0.5 μg/ml) or recombinant prostate-specific antigen as a control. sCD200 allowed the differentiation of osteoclasts in macrophages that lacked CD200 (SD; $n = 3$). (*B*) Bone marrow macrophages isolated from CD200-deficient and wild-type mice were cultured in the presence of M-CSF (5 ng/ml) for 12–18 h. Nonadherent cells were cultured for a further 2 days in the presence of M-CSF (30 ng/ml), starved for 2 h, and then treated with RANKL (50 ng/ml) with or without sCD200 (0.5 μg/ml) for 30 min. The cells were then subjected to Western blot analysis with the indicated antibodies against IkBα and JNK and their phosphorylated forms. Numbers represent relative expression of P-IκB and P-JNK over JNK. The addition of sCD200 restored the activation of JNK but not of IκBα. (*C*) Bone-marrow-derived macrophages from 6-week-old wild-type mice were cultured in the presence of M-CSF (30 ng/ml) and RANKL (50 ng/ml) with or without the recombinant extracellular domain of the CD200 receptor (sCD200R). sCD200R blocked the fusion of macrophages (SD; $n = 5$), whereas recombinant prostate-specific antigen had no effect (osteoclast surface, 0.38 $\pm$ 0.1; osteoclast number, 170.0 $\pm$ 23.3). (*D*) Bone-marrow-derived macrophages from 6-week-old wild-type mice were cultured in the presence of M-CSF (30 ng/ml) for 2 days before being transduced with the retroviral vector MigR1, which encoded, or not, shRNAs designed after the CD200R1 cDNA. A construct encoding random (rdm) oligonucleotides was used as a control. Each of the three targeting retroviral constructs, namely shRNAi1, shRNAi2, and shRNAi3, abolished the expression of CD200R1 (see Western blot, *Bottom Left*) and prevented the formation of multinucleate osteoclasts (*Top* and *Right*). These experiments were reproduced several times with similar results.

ing a role for CD200 in the differentiation of osteoclasts via CD200R-mediated downstream signaling (Fig. 4*B*).

We postulated next that, if the CD200-CD200R interaction plays a role in fusion, interference with this interaction should block fusion. We engineered a histidine-tagged soluble recombinant protein that included the extracellular domain of mouse CD200R (sCD200R). We cultured bone marrow cells from wild-type mice in the presence of M-CSF (30 ng/ml) and RANKL (50 ng/ml) in the absence and presence of sCD200R (50–400 ng/ml) and soluble histidine-tagged recombinant prostate-specific antigen (400 ng/ml). As anticipated, osteoclastogenesis was blocked in the presence of sCD200R in a dose-dependent manner (Fig. 4*C*).

We next asked whether osteoclasts express other CD200R-like molecules (19). We found that mouse osteoclasts expressed transcripts that encoded CD200R and also CD200RLc (data not shown). To date, the function of this additional receptor remains unclear. Because CD200 could activate alternative receptors, such as CD200Lc, and because sCD200R could block the interaction of CD200 with alternative receptors, we questioned whether CD200 signals specifically through CD200R to modulate fusion. To do so, we attempted to silence the expression of CD200R in fusing macrophages by RNAi with short-hairpin RNA (shRNA). We generated three retrovirus-based shRNA constructs that targeted mouse CD200R (shRNAi1, shRNAi2, and shRNAi3), as well as a construct that encoded random sequences (MigR1rdm). We transduced bone marrow macrophages isolated from wild-type mice with these constructs, as well as the empty vector (MigR1). Each one of the shRNA constructs (shRNAi1, shRNAi2, and shRNAi3) interfered with the expression of CD200R and prevented the fusion of osteoclasts (Fig. 4*D*). By contrast, neither MigR1 nor MigR1rdm affected the expression of CD200R and the differentiation of osteoclasts. Together, these results confirmed the proposed central role for the CD200-CD200R axis in the fusion of macrophages and in osteoclastogenesis.

The Absence of CD200 Does Not Impair the Differentiation of Osteoblasts. To determine whether osteoblasts express CD200 and its receptor, CD200R, we cultured bone marrow cells for 9 days in the presence of ascorbic acid (50 μg/ml) and β-glycerophosphate (10 mM). We then subjected these bone marrow-derived osteoblasts to Western blot analysis. Such an approach confirmed the relatively low-level expression of CD200 (12) and the absence of CD200R in osteoblasts (Fig. 5*A*). To determine whether the absence of CD200 affects the differentiation of osteoblasts, we compared the alkaline phosphatase (ALP) activity and the ability to form bone-like nodules of bone marrow-derived osteoblasts from CD200-deficient and wild-type mice. The absence of CD200 had no effect on ALP activity and on the formation of nodules by osteoblasts (Fig. 5*B*).

CD200-Deficient Mice Had Higher Bone Density and Fewer Osteoclasts than Wild-Type Mice. Our *in vitro* data clearly indicate that CD200 and its receptor CD200R play a positive role in the differentiation of osteoclasts but not of osteoblasts. If this is true, then mice that lack CD200 should have a lower number of osteoclasts and a higher bone mass.

To address this question, we first subjected 2-month-old male and female CD200$^{-/-}$ and wild-type mice to DEXA analysis (see *Material and Methods*). Consistent with our hypothesis, both male and female CD200$^{-/-}$ mice had higher spinal bone densities than corresponding wild-type mice (SI Fig. 7*A*). Peripheral quantitative tomography analysis of the femurs from these mice revealed that CD200 deficiency was associated with an increase in the total density of the shaft in both males and females and of the distal femur in females, as compared with age- and sex-matched wild-type mice (SI Fig. 7*B*). In CD200-deficient female mice, there was a decrease in the trabecular area of the shaft and the distal part of the femur, whereas in CD200-deficient male mice, there was an increase in the trabecular area of the distal femur only, as compared with the respective wild-type mice. In CD200-deficient male mice, there was an increase and in CD200-deficient female mice a decrease in periosteal circumference, in both the shaft and the distal femur, as compared with corresponding wild-type mice. It appeared, therefore, that CD200 deficiency has led to the enhanced accumulation of bone.

To confirm that the increase in total bone density was the result

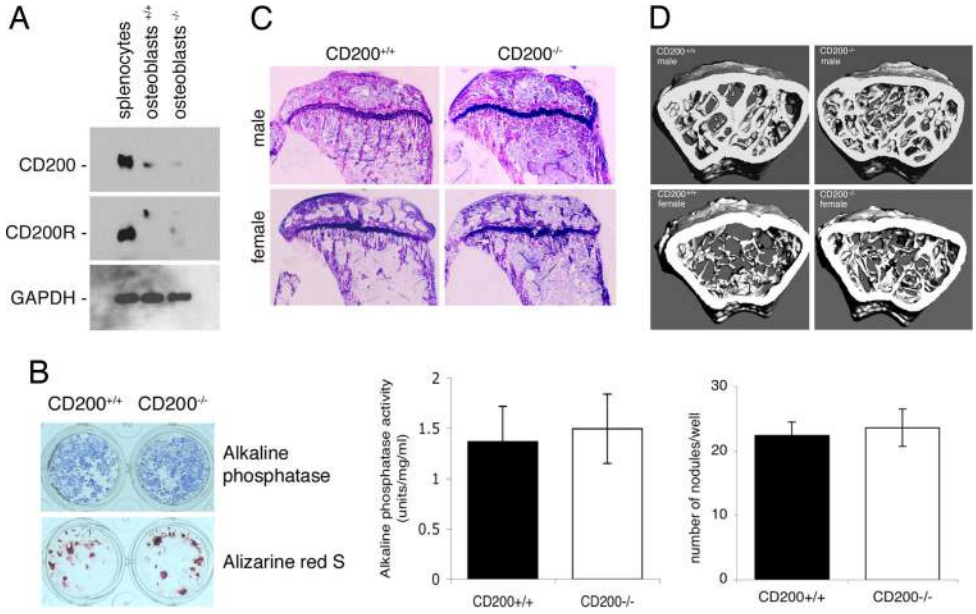

Fig. 5. The absence of CD200 increases bone density. (*A*) Bone marrow cells from 6- to 8-week-old CD200-deficient and wild-type mice were plated in 24-well plates (5×10^6 cells/well) and cultured for 9–11 days in α-MEM supplemented with ascorbic acid (50 μg/ml) and β-glycerophosphate (10 mM) to acquire the osteoblast phenotype. Osteoblast lysates were analyzed for protein concentration and subjected to Western blot analysis with antibodies directed against mouse CD200, CD200R, and GAPDH. (*B*) Bone-marrow-derived osteoblasts were examined for ALP activity and stained for calcium with alizarin red S to allow quantitation of the number of nodules per well (SD; $n = 6$). Cell lysates were analyzed for ALP activity (*Left*; SD; $n = 6$). These experiments were repeated three times with similar results. (*C*) Toluidine blue-stained sections of proximal tibiae from 2-month-old CD200-deficient male and female mice and wild-type mice. (Scale bar, 1 mm.) (*D*) Microcomputed tomography analysis of distal femurs from 6-month-old male and female CD200-deficient mice. Note the increased density of trabeculae inside the distal femur of CD200-deficient male and female mice as compared with wild types. The widest diameter of the bone sections correspond ≈3 mm.

of a decrease in the number of osteoclasts, we subjected the distal femurs from CD200-deficient and age- and sex-matched wild-type mice to histomorphometric analysis. Our results confirmed that CD200-deficient mice, both males and females, had an increase in trabecular bone volume when compared with wild types (Fig. 5*C* and SI Fig. 7*C*). We also found a decrease in the relative bone surface area that was occupied by osteoclasts in both male and female CD200-deficient mice. To our surprise, despite the increase in bone density in CD200-deficient female mice, we found a decrease in the relative surface area of bone that was covered by osteoblasts (SI Fig. 7*C*). This result further suggested that it was, indeed, the osteoclasts that were responsible for the higher bone volume in CD200-deficient mice.

To determine whether the increase in bone volume persisted with aging, we subjected the distal femurs from both CD200-deficient and wild-type 6-month-old mice to high-resolution microcomputed tomography analysis. Both male and female CD200-deficient mice had accumulated more trabecular bone than the corresponding wild types (Fig. 5*D* and SI Table 2). This observation was supported by peripheral quantitative tomography analysis of the same bones, which showed that trabecular density was higher in the CD200-deficient mice than in the corresponding wild types (SI Fig. 7*D*).

Discussion

The CD200-CD200R axis appears to be a central player in the fusion and/or multinucleation of macrophages, which is required for the differentiation of osteoclasts, and the regulation of bone mass. Although our results confirm that mononucleate macrophages do not express CD200 (14), they reveal that their fusion is accompanied by strong and *de novo* expression of CD200. Not only is the expression of CD200 abruptly induced in fusing osteoclasts, but absence of CD200 impairs osteoclastogenesis, with a subsequent increase in bone volume and, hence, a form of osteosclerosis.

Our analysis of the number of bone marrow macrophages/osteoclast precursor cells as a percentage of the total number of bone marrow cells, which was similar in CD200-deficient and wild-type mice, suggests the CD200-CD200R axis does not control the differentiation of premonocytes (17, 18). This is in contrast with the numbers of splenic and mesenteric lymph node macrophages, which are elevated in mice that lack CD200 (14). It is possible that monocytes from bone marrow are less differentiated than those from lymphoid organs, which might express low levels of CD200. Nevertheless, the decreases in the numbers of osteoclasts in CD200-deficient mice cannot be attributed to decreases in numbers of precursor cells.

Of possible relevance to fusion, genes for CD200-like proteins have been identified in the genomes of some, but not all, members of families of double-stranded DNA viruses, such as poxviruses, herpesviruses, and adenoviruses (20, 21). Moreover, the product of the K14 gene of Kaposi's sarcoma-associated herpesvirus is a ligand for CD200R (20, 21). Similarly, M141R is a cell-surface protein encoded by myxoma virus with significant homology at the amino acid level to CD200, required for the full pathogenesis of myxoma virus in the European rabbit (22). Most importantly, both CD200 and its viral homologs activate the CD200R to down-regulate basophil (HHV-8; ref. 23) and macrophage (HHV-8 and M141R; refs. 21 and 22) function. Hence, as might be the case for CD47, which is homologous to proteins encoded by vaccinia and myxoma virus (24, 25), viruses might have "stolen" CD200 to allow them to evade the immune response and to fuse with and infect cells. Of note, in both *Drosophila* myoblast fusion and mammalian macrophage fusion, members of the IgSF mediate adhesion and also initiate intracellular signaling events (4), suggesting a supporting role for the CD200-CD200R axis in fusion; however, this is highly hypothetical.

Although the CD200-CD200R axis plays an inhibitory role in the immune system (see ref. 11 for a review), it appears to play a supporting role in macrophage fusion via RANK signaling, because the absence of CD200 or the silencing of CD200R slow down the differentiation of osteoclasts. Because it has been proposed that the MFR/SIRPα also transmits an inhibitory signal to myeloid cells via its ITIM domain and facilitates macrophage fusion (1, 2), it is possible that these two axes, namely MFR/SIRPα-CD47 and CD200-CD200R, work in tandem to secure the fusion of osteoclasts while preventing their activation in response to CD200R and MFR/SIRPα ligation. Indeed, macrophages might require "deactivation" or "suppression" to proceed with fusion. This is a concept that necessitates further investigation. In that respect, mice that lack both CD47 and CD200 might provide a model to answer this question. In addition, we cannot exclude the possibility that CD200 and its receptor associate both in cis and in trans via their N-terminal domains, because the fusing partners are both macro-

phages. Indeed, it will be of interest to determine whether downstream signaling is differentially activated in cis or in trans in future studies.

That a defect in osteoclastogenesis in CD200-deficient mice results from a defect in activation downstream of RANK suggests possible cross-talk between CD200R and RANK. We should note, however, that, although the absence of CD200 slows down osteoclastogenesis, it does not prevent the expression of MFR/SIRPα and CD44, which are candidate members of the fusion machinery in macrophages. It remains to be determined whether the absence of CD200 affects the expression of DC-STAMP, the most recently identified component of the macrophage fusion machinery (2, 26). Together, our results suggest that the machinery for macrophage fusion involves multiple and, possibly, redundant molecules.

The absence of CD200 increased bone mass, and the soluble recombinant extracellular domain of CD200R blocked macrophage fusion *in vitro*. Thus, CD200 and its receptor might be recently discovered targets in efforts to prevent bone loss. However, even though osteoblasts in culture express low levels of CD200, and the absence of CD200 does not affect their differentiation *in vitro*, we cannot exclude a possible role for CD200 in these cells *in vivo*. Further studies involving the treatment of animal models with the soluble recombinant extracellular domain of CD200R will help clarify this issue.

Materials and Methods

Animals and Cells. $CD200^{-/-}$ mice were produced by homologous recombination, as described (14). Mice whose bones were subjected to histomorphometric analysis received two i.p. injections of calcein (3 μg/g body weight; Merck, Darmstadt, Germany) on days 1 and 6 before death. The Yale Animal Care and Use Committee approved all experiments.

Bone-marrow-derived macrophages and osteoclasts were generated from 6- to 12-week old $CD200^{-/-}$, and $CD200^{+/+}$ mice were prepared as before (16). Osteoblast ALP and mineralized nodule formation assays were performed according to ref. 27.

Reagents. Recombinant mouse RANKL and M-CSF were obtained from R&D Systems (Minneapolis, MN). A mouse monoclonal antibody directed against rat CD200 and rat monoclonal antibodies directed against mouse CD200 and its receptor CD200R were purchased from Serotec (Raleigh, NC). Mouse anti-rat CD200R antibody was kindly provided by A. N. Barclay (Oxford University, Oxford, U.K.). A polyclonal antibody directed against the intracellular domain of MFR has been published (10). Rabbit polyclonal antibodies directed against p38, phosphorylated-p38 (P-p38), ERK1/2, P-ERK1/2, JNK, and mouse monoclonal antibodies directed against IκB, P-IκB, and P-JNK were obtained from Cell Signaling Technology (Beverly, MA). A monoclonal antibody directed against mouse CD44 was obtained from BD Bioscience (Franklin Lakes, NJ). A mouse monoclonal antibody directed against GAPDH was purchased from Novus Biologicals (Littleton, CO). Horseradish peroxidase-conjugated $F(ab')_2$ directed against rabbit and mouse IgG were purchased from Jackson ImmunoResearch (West Grove, PA). Rat anti-mouse monoclonal antibodies used for flow cytometry included anti-Mac1 (CD11b) conjugated to fluorescein (Mac1-FITC; M1/70) and rat FITC-IgG2b (PharMingen, San Diego, CA); anti-c-fms conjugated to phycoerythrin (c-fms-PE; IgG2b) and anti-c-*Kit* conjugated to allophycocyanin (c-*kit*-APC; IgG2b); and isotype matching antibodies (eBioscience, San Diego, CA). Secondary antibody anti-rat IgG2a conjugated to FITC was purchased from PharMingen. Phalloidin-Alexa fluor 568 was purchased from Invitrogen (Carlsbad, CA) and dentin discs from IDS (Bolton, U.K.). All supplies and reagents for tissue culture were endotoxin-free. Some bone marrow cells were treated with polymyxin B sulfate for 24 h to avoid the effects of the endotoxin before treatment. Dentin discs were obtained from IDS and osteologic slides from BD Bioscience.

Flow Cytometry. Cells were stained with the primary antibody, incubated for 30 min on ice, and washed twice with washing buffer (5% FCS/PBS). The secondary antibody was added, and the cells were incubated for 30 min on ice. After incubation, cells were washed twice with washing buffer and suspended in washing buffer for FACS analysis, which was performed by using a FACScalibur (BD Bioscience).

RT-PCR. See *SI Text*.

Real-Time PCR. See *SI Text*.

Generation of the Soluble Extracellular Domain of Mouse CD200 (sCD200) and CD200R (sCD200R). See *SI Text*.

Retrovirus-Mediated shRNAi. See *SI Text*.

Bone Radiography, Microcomputed Tomography, Bone Densitometry, and Histomorphometry. See *SI Text*.

Statistical Analysis. Statistically significant differences among experimental groups were evaluated by the analysis of variances (28). The significance of mean changes was determined by an unpaired Student's two-tailed t test, and significance was recognized when $P < 0.05$.

We thank Dr. N. A. Barclay for his generous gift of the anti-rat CD200R antibody and Dr. Hua Zhu Ke for his help with pQCT and microCT analyses. We thank Dr. Ann Altman for careful editing of this manuscript. J.K. was the recipient of a Boehringer Ingelheim Fellowship. This work was supported by funds from the National Institutes of Health (Grant DE12110, to A.V.).

1. Vignery A (2000) *Int J Exp Pathol* 81:291–304.
2. Vignery A (2005) *Trends Cell Biol* 15:188–193.
3. Vignery A (2005) *J Exp Med* 202:337–340.
4. Chen EH, Grote E, Mohler W, Vignery A (2007) *FEBS Lett* 581:2181–2193.
5. Hernandez LD, Hoffman LR, Wolfsberg TG, White JM (1996) *Annu Rev Cell Dev Biol* 12:627–661.
6. Dalgleish AG, Beverly, P. Clapham P, Crawford D, Greaves M, Weiss R (1984) *Nature* 312:763–767.
7. Klatzmann D, Champagne E, Chamaret S, Grust J, Guetard D, Hercent T, Gluckmann JC, Montagnier L (1984) *Nature* 312:767–768.
8. Saginario C, Qian H-Y, Vignery A (1995) *Proc Natl Acad Sci USA* 92:12210–12214.
9. Saginario C, Sterling H, Beckers C, Kobayashi R, Solimena M, Ullu E, Vignery A (1998) *Mol Cell Biol* 18:6213–6223.
10. Han X, Sterling H, Chen Y, Saginario C, Brown EJ, Frazier WA, Lindberg FP, Vignery A (2000) *J Biol Chem* 275:37984–37992.
11. Minas K, Liversidge J (2006) *Crit Rev Immunol* 26:213–230.
12. Lee L, Liu J, Manuel J, Gorczynski RM (2006) *Immunol Lett* 105:150–158.
13. Hatherley D, Cherwinski HM, Moshref M, Barclay AN (2005) *J Immunol* 175:2469–2474.
14. Hoek RM, Ruuls SR, Murphy CA, Wright GJ, Goddard R, Zurawski SM, Blom B, Homola ME, Streit WJ, Brown MH, *et al.* (2000) *Science* 290:1768–1771.
15. Sterling H, Saginario C, Vignery A (1998) *J Cell Biol* 143:837–847.
16. Li H, Cuartas C, Cui W, Choi Y, Crawford DT, Ke, H.-Z., Kobayashi KS, Flavell RA, Vignery A (2005) *J Exp Med* 201:1169–1177.
17. Arai F, Miyamoto T, Ohneda O, Inada T, Sudo T, Brasel K, Miyata T, Anderson DM, Suda T (1999) *J Exp Med* 190:1741–1754.
18. Jimi E, Aoki K, Saito H, D'Acquisto F, May MJ, Nakamura I, Sudo T, Kojima T, Okamoto F, Fukushima H, *et al.* (2004) *Nat Med* 10:617–624.
19. Wright GJ, Puklavec MJ, Willis AC, Hoek RM, Sedgwick JD, Brown MH, Barclay AN (2000) *Immunity* 13:233–242.
20. Chung YH, Means RE, Choi JK, Lee BS, Jung JU (2002) *J Virol* 76:4688–4698.
21. Foster-Cuevas M, Wright GJ, Puklavec MJ, Brown MH, Barclay AN (2004) *J Virol* 78:7667–7676.
22. Cameron CM, Barrett JW, Liu L, Lucas AR, McFadden G (2005) *J Virol* 79:6052–6067.
23. Shiratori I, Yamaguchi M, Suzukawa M, Yamamoto K, Lanier LL, Saito T, Arase H (2005) *J Immunol* 175:4441–4449.
24. Parkinson JE, Sanderson CM, Smith GL (1995) *Virology* 214:177–188.
25. Cameron CM, Barrett JW, Mann M, Lucas A, McFadden G (2005) *Virology* 337:55–67.
26. Yagi M, Miyamoto T, Sawatani Y, Iwamoto K, Hosogane N, Fujita N, Morita K, Ninomiya K, Suzuki T, Miyamoto K, *et al.* (2005) *J Exp Med* 202:345–351.
27. Morinobu M, Nakamoto T, Hino K, Tsuji K, Shen ZJ, Nakashima K, Nifuji A, Yamamoto H, Hirai H, Noda M (2005) *J Exp Med* 201:961–970.
28. Zar JH (1984) *Biostatistical Analysis* (Prentice-Hall, Englewood Cliffs, NJ).

Spontaneous generation of functional osteoclasts from synovial fluid mononuclear cells as a model of inflammatory osteoclastogenesis

Stinne Ravn Greisen[1,2], Halldór Bjarki Einarsson[1], Malene Hvid[1], Ellen-Margrethe Hauge[2,3], Bent Deleuran[1,2] , Tue Wenzel Kragstrup[1,2]

[1]Department of Biomedicine, Aarhus University, Wilhelm Meyers Allé 4, 8000 Aarhus C, Denmark. Phone: +4587150000. Mail: biomed@au.dk. Fax: +4586196128

[2]Department of Rheumatology, Aarhus University Hospital, Nørrebrogade 44, 8000 Aarhus C Denmark

[3]Department of Anatomy, Aarhus University, Wilhelm Meyers Allé 3, 8000 Aarhus C, Denmark

Running title: Osteoclastogenesis from synovial cells.

Summary

Authors:
(SRG) Stinne R. Greisen, MD, PhD student. srg@biomed.au.dk
(HBE) Halldór Bjarki Einarsson, MD, PhD student. hbe@mikrobilogi.au.dk
(MH) Malene Hvid, PhD, associate professor. malene.hvid@biomed.au.dk
(EH) Ellen-Margretehe Hauge, MD, PhD, associate professor. ellen.hauge@clin.au.dk
(BD) Bent Deleuran, MD, DMSc, professor. bd@biomed.au.dk
(TWK) Tue Wenzel Kragstrup, MD, PhD student. kragstrup@biomed.au.dk

Title: Spontaneous generation of functional osteoclasts from synovial fluid mononuclear cells as a model of inflammatory osteoclastogenesis

Abstract
(max 200 words)
In osteoimmunology, osteoclastogenesis is understood in the context of the immune system. Today, the in vitro model for osteoclastogenesis necessitates the addition of recombinant human receptor activator of nuclear factor kappa-B ligand (RANKL) and macrophage colony stimulating factor (M-CSF). The peripheral joints of patients with rheumatoid arthritis (RA) and spondyloarthritis (SpA) are characterized by an immune mediated inflammation that can lead to bone destruction. Here, we evaluate spontaneous in vitro osteoclastogenesis in cultures of synovial fluid mononuclear cells (SFMCs) activated only in vivo. SFMCs were isolated and cultured for 21 days at 0.5-1.0x10^6 cells/ml in culture medium. SFMCs and healthy control peripheral blood monocytes were cultured with RANKL and M-CSF as controls. Tartrate resistant acid phosphatase (TRAP) positive multinucleated cells were found in the SFMC cultures after 21 days. These cells expressed the osteoclast genes calcitonin receptor, cathepsin K and integrin β3, formed lacunae on dentin plates and secreted matrix metalloproteinase 9 (MMP9) and TRAP. Adding RANKL and M-CSF potentiated this secretion. In conclusion, we show that SFMCs from inflamed peripheral joints can spontaneously develop into functionally active osteoclasts ex vivo. Our study provides a simple in vitro model for studying inflammatory osteoclastogenesis.

Keywords: Arthritis, osteoclast, inflammation, osteoimmunology

Correspondence and reprint requests to:
Stinne Greisen, Department of Biomedicine, Aarhus University, Building 1240, Wilhelm Meyers Allé 4, 8000 Aarhus C, Denmark.
Email: srg@biomed.au.dk

Introduction

(max 10 pages incl figs and tables)

A balance between osteoclast and osteoblast activity ensures that bones are renewed and maintained. If the balance is disrupted, bone structure is affected. Inflammation can cause such a disruption and is believed to increase osteoclast activity (1-3). This interplay between the immune system and bone homeostasis is termed osteoimmunology (4).

Osteoclasts are defined as tartrate-resistant acid phosphatase (TRAP) positive multinucleated cells (three or more nuclei) capable of digesting bone. Other markers of osteoclasts include cathepsin K, calcitonin receptor, integrin β_3 and matrix metalloproteinase 9 (MMP9) (5-7). Pre-osteoclasts are also TRAP positive cells, but with only one or two nuclei (8). *In vivo* osteoclastogenesis induced by receptor activator of nuclear factor kappa-B ligand (RANKL) produced by osteoblasts, B cells, T cells and fibroblasts is well described (9-11). Therefore, generation of osteoclasts by stimulating monocytes with macrophage colony stimulating factor (M-CSF) and RANKL has become an established *in vitro* method for studying osteoclastogenesis (7,12,13). However, the many other factors also involved in inflammatory osteoclastogenesis are not taken into account in this model (14).

Rheumatoid arthritis (RA) and spondyloarthritis (SpA) are immune mediated inflammatory diseases. The peripheral joints of both diseases are characterized by inflammation that can lead to bone destruction (2,15,16). Importantly, immune cells present in the inflamed joints of both RA and SpA patients, are under continuous activation leading to ongoing inflammation and cytokine production (17). Tumor necrosis factor alpha (TNFα) is one established promoter of inflammation, and anti-TNFα treatment attenuate radiographic progression in RA (18).

Inflammatory osteoclastogenesis has previously been observed using synovial tissue derived inflammatory cells from RA patients (19,20). Here, we investigated the osteoclastogenic potential of density gradient separated and cryopreserved synovial fluid mononuclear cells (SFMCs) from the peripheral joints of a heterogeneous group of RA and SpA patients. We report that *in vivo* activated SFMCs from all patients possessed the ability to spontaneously develop into functional osteoclasts *ex vivo*. Because SFMCs are easily accessible from the synovial fluid, this could provide a simple model for investigating factors inhibiting or promoting inflammatory osteoclastogenesis.

Methods

Preparation of synovial fluid mononuclear cells

Synovial fluid was collected from chronic RA (n=6) and SpA (n=6) patients at the out clinic at Aarhus University Hospital in association with therapeutic arthrocenthesis. RA patients fulfilled the ACR 1987 revised criteria, and SpA patients fulfilled the ESSG criteria (21,22). At the time of synovial fluid collection, patients presented with disease flare, typically with a swollen knee or ankle joint. All patients gave written consent to participate in the study and the protocol was conducted in accordance with the Helsinki Declaration and approved by the local ethics committee (20121329) and the Danish data protection agency.

Synovial fluid was centrifuged at 300 g. Then, the supernatant was collected and SFMCs were isolated using Ficoll-Paque PLUS (GE Healthcare, USA). Cells were cryopreserved at -135°C until later use.

Culture of synovial fluid mononuclear cells

Synovial fluid mononuclear cells were grown (at 37°C, 5% CO_2 in a humidified incubator) in Dulbecco's Modified Eagle's medium (DMEM) (Gibco, Life Technologies, USA) with 10% fetal calf serum (FCS), 2% penicillin/steptamycin, and 1% glutamin. Medium was changed every three to four days. For TRAP staining, SFMCs were seeded at a density of $0.5x10^6$ cells/ml. For other assays the concentration used was $1x10^6$ cells/ml. All cultures were evaluated after 21 days if not stated otherwise. To test whether the spontaneous osteoclastogenesis could be potentiated, RANKL (50 ng/ml) and M-CSF (25 ng/ml) were added to the cultures.

Generation of conventional osteoclasts from peripheral blood mononuclear cells

Healthy control (HC) peripheral blood mononuclear cells (PBMCs) were isolated from buffy coats obtained from the blood bank at Aarhus University Hospital using the same protocol as for the SFMCs. Cells were seeded at a density of $8x10^6$ cells/ml, cultured (at 37°C, 5% CO_2 in a humidified incubator) for 24 h for allowing plastic adherence and then washed with phosphate buffered saline (PBS) pH 7.4. Adherent cells were then cultured in DMEM with M-CSF (100ng/ml) for 24 h followed by stimulation with M-CSF (25ng/ml) and RANKL (50ng/ml). Medium was then changed and cells restimulated every three days.

Tartrate-resistant acid phosphatase staining

Autoclaved cover slides (1 cm diameter) were placed in the bottom of 24-well culture plates. Following 21 days of SFMC culture slides were washed twice in tris-buffered saline (TBS, pH7.6) and fixed in 70% alcohol. Slides were then washed for 3x5 min in distilled water and kept in the dark for 1 h before staining with Mayers Hematoxylin for 5 sec. Following another wash of 3x5 min in distilled water slides were mounted with glycerol. Tartrate-resistant acid phosphatase (TRAP) enzymatic staining was performed by adding a mix of 2 ml of solution A (Naphtol-as-bi-phosphat 20 mg (cat: N2125, Sigma-Aldrich, USA) and N,N-dimethylformamid (cat: 3034, Merck, USA)) in addition to 100 µl of solution B (4% pararosanilin,/ 2M HCl, 100µl and 4% natriumnitrit (cat: 1.06549, Merck, USA)) mixed with wine acid and Michaelis buffer (cat: 1.00804, Merck, USA) and adjusted to pH 5.0-5.1 using 2M NaOH. Slides were dark-incubated within solution A and B for 30 min and subsequently washed in distilled water.

Cells were counted using a light microscope (Nikon Eclipse 80i, Japan) equipped with a motorized Proscan 11 stage (Prio, USA), a MT1201 microrater (Heidenhain, Germany), a DP72 camcorder (Olympus, Denmark) and a computer with newCAST software version 3.4.1.0 (Visiopharm, Denmark), displaying an unbiased counting frame and sampling the culture slides systematic randomly (23). Osteoclasts were defined as TRAP positive cells with three or more nuclei. TRAP positive cells with one or two nuclei were defined as pre-osteoclasts and counted separately (8). The presence of osteoclasts was expressed as a percentage of the total number of cells counted.

Polymerase chain reaction for calcitonin receptor, cathepsin K and integrin β3

SFMCs and HC PBMCs were grown in a 48-bottum plate without cover slides. After culture the cells were washed twice with PBS and lysed in a lysis buffer for total RNA extraction (cat:

L8285; Sigma Aldrich, USA) with the addition of 1% betamecarptoethanol (cat: M3148; Sigma Aldrich, USA). Cell lysates were kept at -80˚C until polymerase chain reaction (PCR). RNA was thawed and kept on ice and the concentration of RNA was measured using NanoDrop 2000 Spectrophotometer (Thermo Scientific, USA) and adjusted to 50ng/ml. PCR was performed according to manufacturers instructions. The PCR reactions were normalised against the best keeper (BK) index for the household genes RPII (assay ID: Hs00172187_m1) and HPRT1 (assay ID: Hs02800695_m1). Appropriate cDNA dilutions were used subsequently for the RT-PCR reactions using specific primers for calcitonin receptor (assay ID: Hs01016882_m1), cathepsin K (assay ID: Hs00166156_m1) and integrin β3 (assay ID: Hs01001469_m1). All from Applied Biosystems, Life Technologies (Thermo Fisher Scientific, USA). RNA was added in duplicates. The qPCR protocol was set up on a Stratagene Mx3005P (Agilent Technologies, USA) with the thermal profile Pre-melt: 48°C for 15 min and 95°C for 10 min. Amplification x 40: 95°C for 15 sec and 60°C for 1 min.

Dentin plate assay

Human caries-free third molars were obtained and stored in Minimum Essential Media (Gibco, Life Technologies, USA) for less than 2 weeks before sectioning. The teeth were mounted onto Plexiglas slides with Technovit 4000 (Exakt, Germany) and hereafter cut perpendicular to the long axis of the root into 150 µm thick discs using a Exakt 3031 precision saw (Exakt, Germany). Discs were hereafter rinsed in PBS and sterilized by gamma radiation (173 krad per tooth) using Gammacelle 2000 (RH, AEK, Denmark) (24). Dose at center of the chamber equaled to 1.65 Gy and exposure time per 150 µm dentine plate hence 162 sec. Prior to cell culture discs were furthermore placed in 70% ethanol for 3 hours and washed x 4 in PBS.

To study lacuna formation after cell culture, dentin plates were washed x 2 in PBS and treated with 1 molar (N) sodium hypochlorite solution for 10 min. followed by sonication (Diagenode, Bioruptor, USA) in 1 N hypochlorite for 10 min. and distilled water for another 10 min. Discs were then washed thoroughly x 4 in distilled water, air dried and stained by using Coomassie brilliant blue (1X) for 30 sec, rinsed in distilled water for 1 hour and air dried prior to light microscopy and evaluation using the above noted newCast software (Visiopharm, Denmark).

Quantifying the secretion of TRAP and MMP-9

SFMCs were grown in 96 bottom plates. The supernatant was kept at -20°C after changing media. The produced and secreted TRAP ultimately dissolved in the supernatant was evaluated by a commercially available enzymatic assay (Cat. AK104, B-bridge international, USA). The supernatants were thawed, and the manufacturers protocol was followed. The OD from wells only containing DMEM was subtracted as the blank value. Data are expressed as OD subtracted the blank value.

MMP-9 production was evaluated in a similar manner, as the protocol from a commercially available ELISA kit (DY911, R&D systems, USA) was followed. The blank value was subtracted and concentrations were calculated from the standard curve.

Statistics

Data were analyzed using GraphPad Prism 5 (GraphPad SoftWare Inc, USA). Data were expressed as median (interquartile range) when not stated otherwise. Applied statistics were

done with log-transformed data. Differences were evaluated using one-way or two-way repeated measures ANOVA. Results were considered statistically significant when $p < 0.05$.

Results

Light microscopy and TRAP staining

To study the SFMC cultures we first studied the cultures by light microscopy whenever medium was changed. All cultures assessed contained cells with three or more nuclei after 21 days of culture (Fig. 1). At this time point, cells were TRAP stained. The SFMC cultures contained a large number of TRAP positive cells, with either three or more nuclei (10.2% (3.3%-10.5%)) or two or less nuclei (42.8% (30.2%-43.5%)) (Fig. 1). Monocytes from HCs were stimulated with RANKL and M-CSF, assessed equivalently for comparison and used as positive controls (Fig. 1).

Expression of the calcitonin receptor, cathepsin K and integrin β3 genes

We performed qPCR on established osteoclast genes in the SFMC cultures, to further determine the nature of the cells present in the cultures. The mRNA of the calcitonin receptor, cathepsin K and the β_3 chain of the $\alpha_v\beta_3$ integrin complex were all present in the SFMC lysates (Fig. 2). As a positive control, monocytes from HCs were stimulated with RANKL and M-CSF and assessed similarly. The calcitonin receptor mRNA levels were slightly lower in the SFMC cultures compared with the levels in conventionally RANKL and M-CSF stimulated HC osteoclasts (Fig. 2). As a negative control, non-stimulated HC PBMCs were also analyzed for the expression of the calcitonin receptor. No calcitonin receptor expression was observed in these cells (Fig. 2).

Lacunae formation on dentin plates

We tested whether the spontaneously formed multinuclear, TRAP positive cells in the SFMC cultures showed functional osteoclast characteristics. SFMCs were seeded on 150 µm thick dentin plates and the lacunae formation evaluated. Again, conventionally generated osteoclasts from HC monocytes were used as a positive control. We observed that dentin was absorbed and lacunae were formed in both SFMC cultures and conventionally RANKL and M-CSF stimulated HC osteoclasts (Fig. 2). Taken together, multinucleated, TRAP positive cells were found in the SFMC cultures after 21 days. These cells expressed cathepsin K, calcitonin receptor, and integrin β_3, and formed lacunae on dentin plates. These are all characteristics consistent with cells fully differentiated into osteoclasts.

Stimulation of SFMC cultures with RANKL and M-CSF

We then studied whether the conventional osteoclast stimulators RANKL and M-CSF could increase the generation of osteoclasts from SFMCs. Adding M-CSF and RANKL to the SFMC cultures potentiated the spontaneous formation of multinucleated TRAP positive osteoclasts from 10.2% (3.3%-10.5%) to 14.2% (13.3%-16.3%) (Fig. 3). The percentage of TRAP positive cells with two or less nuclei was not affected (Fig. 3). To further evaluate osteoclast activity and differentiation we measured TRAP and MMP-9 secretion in the SFMC cultures at different time points. Both TRAP and MMP-9 secretion increased significantly (all $p < 0.05$) during 19 days of culture (Fig. 4). Adding RANKL and M-CSF to the SFMC cultures significantly

potentiated TRAP secretion ($p = 0.028$) that moreover was the tendency for MMP-9 secretion (Fig. 4).

Discussion

In osteoimmunology, osteoclastogenesis is understood in the context of the immune system (4). Here, SFMCs isolated from inflamed peripheral joints of patients with RA and SpA possessed the ability to spontaneously develop into functional osteoclasts *ex vivo*. We therefore suggest that our findings provide a simple model for investigating inflammatory osteoclastogenesis.

Osteoimmunology is receiving increased attention as most disease conditions with even low-grade inflammation can result in osteoporosis (25). Thus, understanding osteoclastogenesis and osteoclast function in relation to immune mediators in chronic inflammatory disorders is important. The peripheral joints of both RA and SpA are characterized by inflammation that can lead to bone destruction (2,15). In line with this, RANKL is expressed in equal amounts in RA and SpA peripheral joints (26). Immune factors known to increase osteoclast activity are however present in both the synovium and plasma (11,27). This means that osteoporosis is also seen in both diseases because of the inflammatory activation of bone degradation outside the synovial joint (28). RANKL, TNFα, IL-17A, M-CSF, IL-34 and IL-23 are some of the cytokines suggested to induce osteoclast formation and activation (27,29,30).

Understanding osteoclastogenesis through *in vitro* studies is an appreciated method. Today, *in vitro* studies on osteoclastogenesis using high concentrations of RANKL and M-CSF or 1,25 dihydroxyvitamin D3 do not take into account the many factors regulating osteoclast differentiation and activity in chronic inflammation (14,31). Spontaneous osteoclast development *in vitro* has been documented in cultures of synovial tissue cells from RA patients and non-adherent SFMCs and PBMCs from psoriatic arthritis patients (19,20,32). Here, we determine the potential of gradient separated and cryopreserved SFMCs from both RA and SpA patients to differentiate into functionally active osteoclasts *in vitro* without any additional preparation or stimulation. In these cultures, we found multinucleated TRAP positive cells expressing osteoclast genes and the ability to form lacunae on dentin plates. In addition, we observed high numbers of TRAP positive cells with two or less nuclei. The presence of such pre-osteoclasts is acknowledged *in vivo* and the SFMC cultures seems to reflect this (1,33,34).

The SFMC model described in this study takes into account the many different factors secreted by both lymphocytes, fibroblasts and macrophages regulating osteoclast differentiation and activity (14). Because the generation of osteoclasts in this model is spontaneous, it is an intriguing model for studying the prevention of inflammatory osteoclastogenesis with potential inhibitors. Adding RANKL and M-CSF further augmented the spontaneous development of osteoclasts. This we consider of great importance as it additionally makes the model suitable for studying factors that potentially increase the genesis of osteoclasts. Finally, measuring the secretion of MMP9 and TRAP in the supernatants seems to be a simple outcome measure for such studies.

In conclusion, we hereby provide a simple and easy method for studying inflammatory osteoclastogenesis. Furthermore, we view and appreciate the presented

method as a suitable *ex vivo* model for testing treatments regulating or mediators potentiating osteoclast formation and activity.

Acknowledgments

The authors thank associate professor David Chr. Kraft and laboratory technician Sussi Madsen at Department of Orthodontics, School of Dentistry, Aarhus University, for their technical help and for providing us with dentin plates. The authors also thank laboratory technician Jette Barlach for providing technical help with the enzymatic TRAP staining. Finally the authors thank The Danish Rheumatism Association (unrestricted grant).

Figures and legends

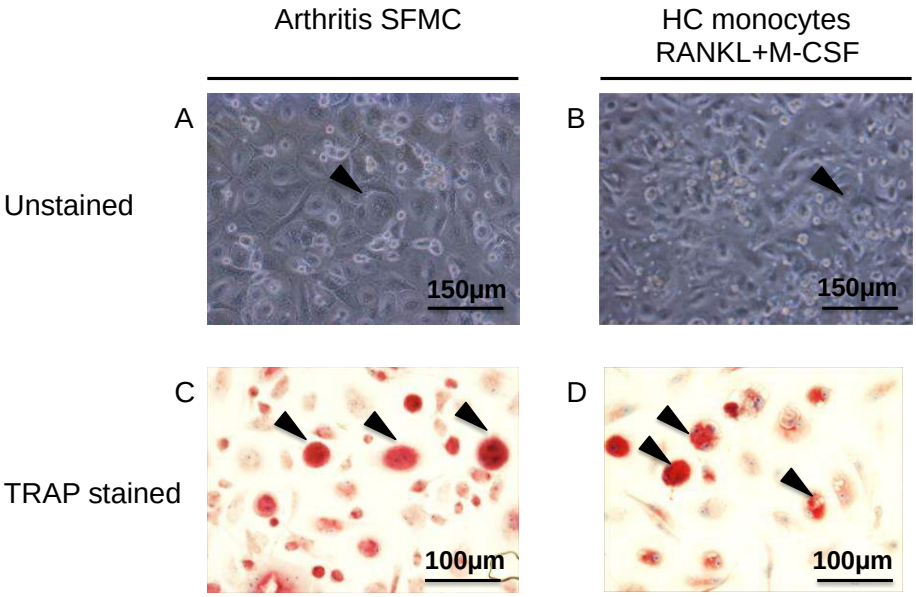

Fig. 1. Light microscopy imaging and TRAP staining of SFMCs and stimulated HC monocyte cultures. (A and B) Light microscopy images of a representative SFMC culture on day 21 (n=12) and a representative HC monocyte culture stimulated with RANKL and M-CSF (n=6). Arrows indicate multinucleated cells. (C and D) TRAP stained samples of a representative SFMC culture on day 21 (n=8) and from a representative HC monocyte culture stimulated with RANKL and M-CSF (n=6). Arrows indicate TRAP positive multinucleated giant cells. Objective x20 and scale bars as indicated 150 and 100 µm respectively.

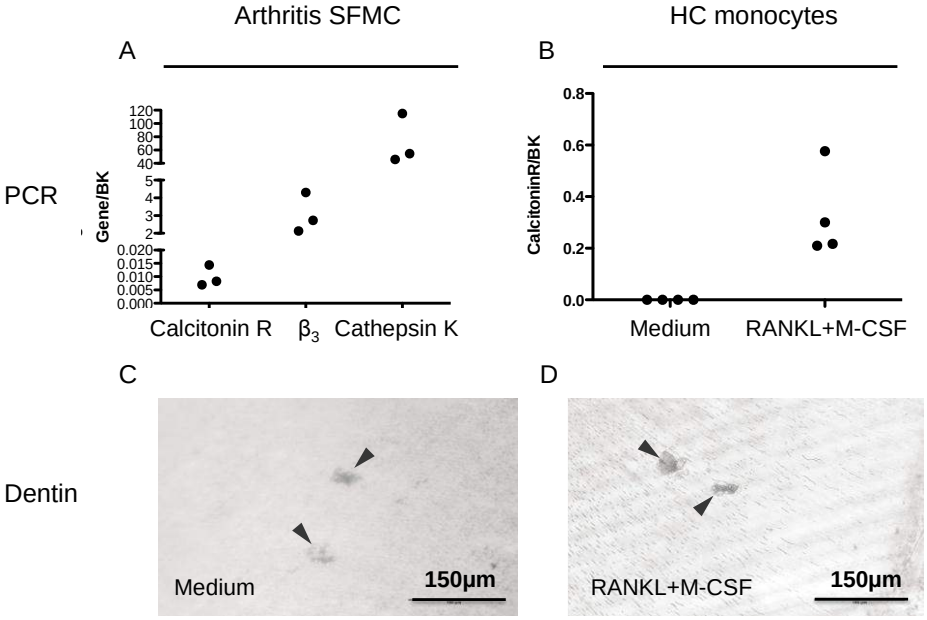

Fig. 2. Expression of osteoclast genes and lacunae formation in SFMC and stimulated HC monocyte culture. (A and B) PCR data for SFMC cultures on day 21 (n=3) and stimulated HC monocyte cultures (n=4). Genes were normalized to BK household gene. Arthritis SFMC cultures expressed the established osteoclast genes calcitonin receptor, integrin beta3 and cathepsin K. In addition HC monocyte cultures expressed calcitoninR, whereas no expression was found in unstimulated HC PBMCs. (C and D) Arthritis SFMCs (n=3) and stimulated HC monocytes (n=4) were grown on dentin plates to evaluate the resorptive capacity of the cells. Both arthritis SFMCs after 21 days and osteoclasts grown from stimulated HC monocytes were able to create lacunae in the dentin plates. Objective x20 and scale bars as indicated 150 µm.

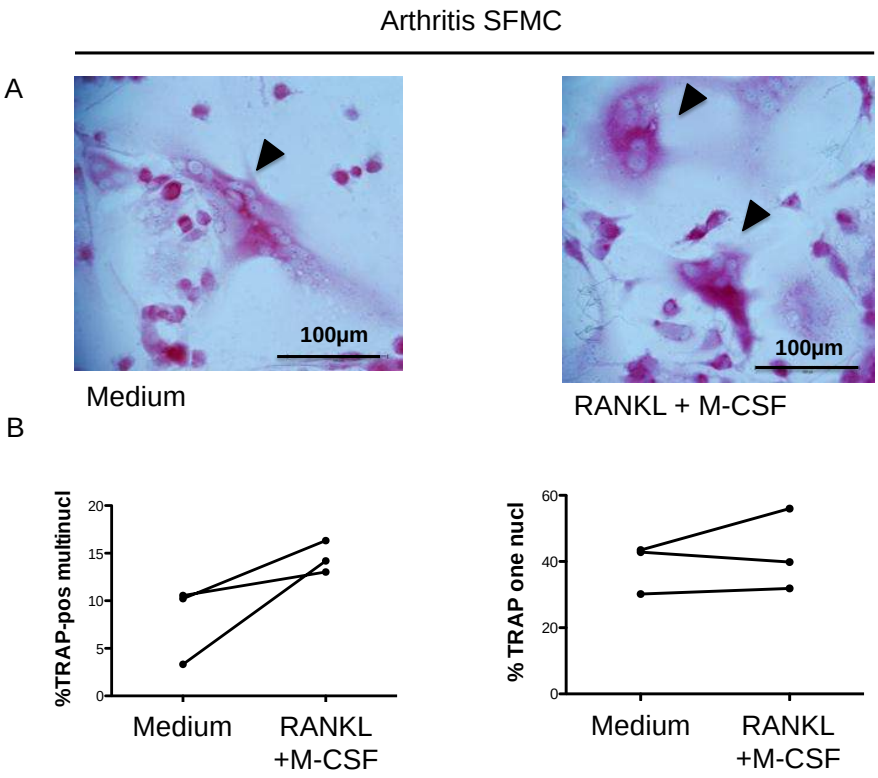

Fig. 3. TRAP staining of SFMC cultures with and without RANKL and M-CSF stimulation. (A) Microscopy images showing TRAP stained multinucleated osteoclasts in the SFMC culture with and without RANKL and M-CSF (n=3). Objective x40 and scale bars 100 µm. (B) Arthritis SFMCs grown in medium alone or in medium with RANKL (50ng/ml) and M-CSF (25 ng/ml) (n=3). The cells were counted on day 21. By adding RANKL and M-CSF to the culture medium increased the percentage of TRAP positive multinucleated osteoclasts.

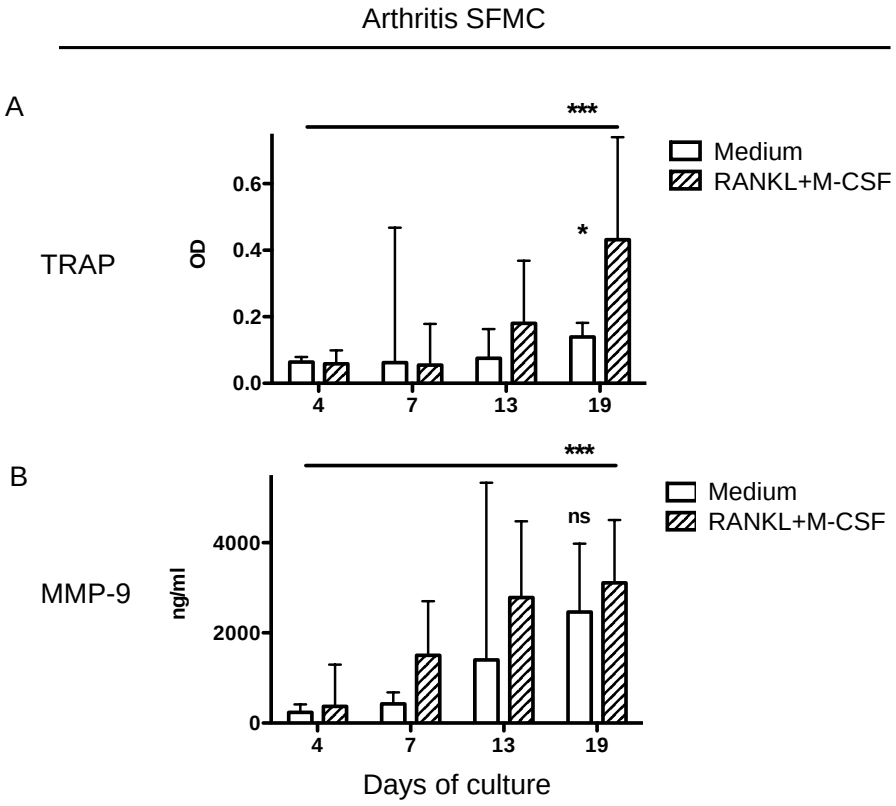

Fig. 4. TRAP and MMP-9 secretion in SFMC cultures with and without RANKL and M-CSF stimulation. (A) TRAP secretion in SFMC cultures without additional stimulation (clear bars) and stimulated with RANKL (50 ng/ml) and M-CSF (25 ng/ml) (filled bars). Data are expressed as the OD of wells with the supernatant subtracted the OD of the blank. (B) MMP-9 secretion in SFMC cultures without additional stimulation (clear bars) and stimulated with RANKL (50 ng/ml) and M-CSF (25 ng/ml) (filled bars). Data are expressed as concentration of MMP-9 in ng/ml. All n=4. Bars indicate median with range. All data were log transformed in order to fit the normal distribution. The increase in TRAP and MMP-9 during 19 days of culture was analyzed with the one-way repeated measures ANOVA. The difference between stimulated and non-stimulated cultures was evaluated with the two-way repeated measures ANOVA. * indicates $p < 0.05$ and *** indicates $p < 0.001$, ns indicates non significant.

List of abbreviations:

Best Keeper index to household genes (BK)
Dulbecco's Modified Eagle's medium (DMEM)
Fetal calf serum (FCS)
Healthy control (HC)
Interleukin (IL)
Macrophage colony stimulating factor (M-CSF)
Messenger Ribonucleic acid (mRNA)
Receptor activator of nuclear factor kappa-B ligand (RANKL)
Rheumatoid Arthritis (RA)
Spondyloarthritis (SpA)

Synovial fluid mononuclear cell (SFMC)

Tartrate resistant acid phosphatase (TRAP)

Tumor necrosis factor (TNF)

References

1. Nose M, Yamazaki H, Hagino H, Morio Y, Hayashi S-I, Teshima R. Comparison of osteoclast precursors in peripheral blood mononuclear cells from rheumatoid arthritis and osteoporosis patients. *J Bone Miner Metab* 2009.

2. Goldring SR, Gravallese EM. Pathogenesis of bone erosions in rheumatoid arthritis. *Curr Opin Rheumatol* 2000;12:195.

3. Nakashima T, Takayanagi H. Osteoclasts and the immune system. *J Bone Miner Metab* 2009.

4. Arron JR, Choi Y. Osteoimmunology: Bone versus immune system. *Nature* 2000;408:535–536.

5. Kaye M. When is it an osteoclast? *J Clin Pathol* 1984;37:398–400.

6. Pierce AM, Lindskog S, Hammarström L. Osteoclasts: structure and function. Electron Microsc Rev. 1990 Dec 31;4(1):1–45.

7. Sørensen MG, Henriksen K, Schaller S, Henriksen DB, Nielsen FC, Dziegiel MH, et al. Characterization of osteoclasts derived from CD14+ monocytes isolated from peripheral blood. *J Bone Miner Metab* 2007;25:36–45.

8. Andersen TL, Sondergaard TE, Skorzynska KE, Dagnæs-Hansen F, Plesner TL, Hauge E-M, et al. A physical mechanism for coupling bone resorption and formation in adult human bone. *Am J Pathol* 2009;174:239–247.

9. Troen BR. Molecular mechanisms underlying osteoclast formation and activation. *Exp Gerontol* 2003;38:605–614.

10. Yeo L, Toellner K-M, Salmon M, Filer A, Buckley CD, Raza K, et al. Cytokine mRNA profiling identifies B cells as a major source of RANKL in rheumatoid arthritis. *Ann Rheum Dis* 2011;70:2022–2028.

11. Takayanagi H. New developments in osteoimmunology. *Nat Rev Rheumatol* 2012;8:684–689.

12. Susa M, Luong-Nguyen N-H, Cappellen D, Zamurovic N, Gamse R. Human primary osteoclasts: in vitro generation and applications as pharmacological and clinical assay. *J Transl Med* 2004;2:6.

13. Lacey DL, Timms E, Tan HL, Kelley MJ, Dunstan CR, Burgess T, et al. Osteoprotegerin ligand is a cytokine that regulates osteoclast differentiation and activation. *Cell* 1998;93:165–176.

14. Takayanagi H. Osteoimmunology and the effects of the immune system on bone. *Nat Rev Rheumatol* 2009;5:667–676.

15. Goldring SR. Osteoimmunology and Bone Homeostasis: Relevance to Spondyloarthritis. *Curr Rheumatol Rep* 2013;15:1–6.

16. Schett G, Gravallese E. Bone erosion in rheumatoid arthritis: mechanisms, diagnosis and treatment. *Nat Rev Rheumatol* 2012;8:656–664.

17. Fox DA, Gizinski A, Morgan R, Lundy SK. Cell-cell interactions in rheumatoid arthritis synovium. *Rheum Dis Clin North Am* 2010;36:311–323.

18. Binder NB, Puchner A, Niederreiter B, Hayer S, Leiss H, Blüml S, et al. Tumor necrosis factor-inhibiting therapy preferentially targets bone destruction but not synovial inflammation in a tumor necrosis factor-driven model of rheumatoid arthritis. *Arthritis Rheum* 2013;65:608–617.

19. Nozaki T, Takahashi K, Ishii O, Endo S, Hioki K, Mori T, et al. Development of an ex vivo

cellular model of rheumatoid arthritis: critical role of CD14-positive monocyte/macrophages in the development of pannus tissue. *Arthritis Rheum* 2007;56:2875–2885.

20. Suzuki Y, Tsutsumi Y, Nakagawa M, Suzuki H, Matsushita K, Beppu M, et al. Osteoclast-like cells in an in vitro model of bone destruction by rheumatoid synovium. *Rheumatology (Oxford)* 2001;40:673–682.

21. Arnett FC, Edworthy SM, Bloch DA, Mcshane DJ, Fries JF, Cooper NS, et al. The american rheumatism association 1987 revised criteria for the classification of rheumatoid arthritis. *Arthritis Rheum* 1988;31:315–324.

22. Dougados M, van der Linden S, Juhlin R, Huitfeldt B, Amor B, Calin A, et al. The European Spondylarthropathy Study Group preliminary criteria for the classification of spondylarthropathy. *Arthritis Rheum* 1991;34:1218–1227.

23. Gundersen HJ. Estimators of the number of objects per area unbiased by edge effects. *Microsc Acta* 1978;81:107–117.

24. White JM, Goodis HE, Marshall SJ, Marshall GW. Sterilization of teeth by gamma radiation. *J DENT RES* 1994;73:1560–1567.

25. Hardy R, Cooper MS. Bone loss in inflammatory disorders. *Journal of Endocrinology* 2009;201:309–320.

26. Vandooren B, Cantaert T, Noordenbos T, Tak PP, Baeten D. The abundant synovial expression of the RANK/RANKL/Osteoprotegerin system in peripheral spondylarthritis is partially disconnected from inflammation. *Arthritis Rheum* 2008;58:718–729.

27. Braun T, Schett G. Pathways for Bone Loss in Inflammatory Disease. *Curr Osteoporos Rep* 2012;10:101–108.

28. Will R, Palmer R, Bhalla AK, Ring F, Calin A. Osteoporosis in early ankylosing spondylitis: a primary pathological event? *Lancet* 1989;2:1483–1485.

29. Moon Y-M, Yoon B-Y, Her Y-M, Oh H-J, Lee J-S, Kim K-W, et al. IL-32 and IL-17 interact and have the potential to aggravate osteoclastogenesis in rheumatoid arthritis. *Arthritis Res Ther* 2012;14:R246.

30. Goldring SR. Osteoimmunology and bone homeostasis: relevance to spondyloarthritis. *Curr Rheumatol Rep* 2013;15:342–6.

31. Kassem M, Mosekilde L, Rungby J, Melsen F, Eriksen EF. Formation of osteoclasts and osteoblast-like cells in long-term human bone marrow cultures. *APMIS* 1991;99:262–268.

32. Colucci S, Brunetti G, Cantatore FP, Oranger A, Mori G, Quarta L, et al. Lymphocytes and synovial fluid fibroblasts support osteoclastogenesis through RANKL, TNFalpha, and IL-7 in an in vitro model derived from human psoriatic arthritis. *J Pathol* 2007;212:47–55.

33. Keller KK, Stengaard-Pedersen K, Dagnaes-Hansen F, Nyengaard JR, Sakaguchi S, Hauge E-M. Histological changes in chronic autoimmune SKG-arthritis evaluated by quantitative three-dimensional stereological estimators. *Clin Exp Rheumatol* 2011;29:536–543.

34. Gravallese EM, Harada Y, Wang JT, Gorn AH, Thornhill TS, Goldring SR. Identification of cell types responsible for bone resorption in rheumatoid arthritis and juvenile rheumatoid arthritis. *Am J Pathol* 1998;152:943–951.

Int. J. Mol. Sci. **2012**, *13*, 14579-14605; doi:10.3390/ijms131114579

OPEN ACCESS
International Journal of
Molecular Sciences
ISSN 1422-0067
www.mdpi.com/journal/ijms

Review

Glatiramer Acetate in Treatment of Multiple Sclerosis: A Toolbox of Random Co-Polymers for Targeting Inflammatory Mechanisms of both the Innate and Adaptive Immune System?

Babak Jalilian, Halldór Bjarki Einarsson and Thomas Vorup-Jensen *

Department of Biomedicine, Aarhus University, Wilhelm Meyers Allé 4, Building 1242, DK-8000, Aarhus C, Denmark; E-Mails: babak.jalilian@microbiology.au.dk (B.J.); hbe@ki.au.dk (H.B.E.)

***** Author to whom correspondence should be addressed; E-Mail: vorup-jensen@microbiology.au.dk; Tel.: +45-8716-7853; Fax: +45-8619-6128.

Received: 29 September 2012; in revised form: 23 October 2012 / Accepted: 5 November 2012 / Published: 9 November 2012

Abstract: Multiple sclerosis is a disease of the central nervous system, resulting in the demyelination of neurons, causing mild to severe symptoms. Several anti-inflammatory treatments now play a significant role in ameliorating the disease. Glatiramer acetate (GA) is a formulation of random polypeptide copolymers for the treatment of relapsing-remitting MS by limiting the frequency of attacks. While evidence suggests the influence of GA on inflammatory responses, the targeted molecular mechanisms remain poorly understood. Here, we review the multiple pharmacological modes-of-actions of glatiramer acetate in treatment of multiple sclerosis. We discuss in particular a newly discovered interaction between the leukocyte-expressed integrin $\alpha_M\beta_2$ (also called Mac-1, complement receptor 3, or CD11b/CD18) and perspectives on the GA co-polymers as an influence on the function of the innate immune system.

Keywords: glatiramer acetate; copaxone; biosimilar; integrin; immunotherapy

---

1. A Brief Introduction to the Etiology and Symptoms of Multiple Sclerosis

Multiple sclerosis or MS was first described by Jean-Martin Charcot in 1868 [1]. MS is a disease of the central nervous system (CNS) causing non-traumatic chronic neurological disability, mostly in young and middle-aged adults, affecting over 2 million people worldwide [2]. The prevalence of MS may vary between different populations with incidences from 2 to 150 per 100,000. It is more common among Caucasian races in temperate regions [2,3] where MS affects 1 out of 1000 people [4]. The debut is typically occurring at the age 20–45 and women are almost twice as often affected as men [5]. There is a North-to-South gradient distribution in the MS frequency, however, with many exceptions [6].

The pathophysiology of MS has not been entirely mapped out and appears to involve multiple factors [7]. The most significant pathohistological characteristics are localized areas of demyelination in the CNS and relative preservation of axons. There are periods of focal demyelination followed by complete or partial re-myelination [8]. There is evidence that protein components of the myelin sheath stimulate the inflammatory response, which contributes to the demyelination of nerves. The process is, however, complicated and involves both lymphocytes and myeloid cells of the immune system. Experimental evidence suggests that proteins, such as myelin basic protein (MBP), act as so-called autoantigens [9], which triggers an inflammatory response towards the host tissue. The role of the immune system in MS is strongly supported by the observation that immune suppressive treatment, discussed further below, seems at least partially to be able to slow down neural decay and ameliorate symptoms. Demyelination leads to decreased conductivity or conduction block that results in neurological symptoms of MS disease. Periventricular infiltrations of lymphocytes and macrophages manifest as Dawson fingers representing demyelinating plaques through *corpus callosum* as observed by magnetic resonance imaging (MRI) modality. In addition to white substance affection, the grey matter of the CNS can also be affected [10].

There is strong evidence that a combination of genetic predisposition and exposure to one or more environmental factors are linked to the etiology of MS [11–13]. The vitamin-D status, particularly in geographical regions with a limited sun light exposure, and cigarette smoking [14], have been suggested as the most consistent risk factors. Furthermore, exacerbation of MS is often associated with stress [15]. Links to infectious diseases have been suggested, both from experimental studies as well as from clinical investigations. These studies included work on bacterial antigens inducing an autoimmune response [16] as well as several studies on the role of Epstein-Barr virus (EBV) infection [17–19] and endogenous retroviruses [20]. These are potential sources of microbial manipulation of the immune system leading to excessive or uncontrolled immune responses. For the discussion in Section 5, it is of considerable interest that viral infections may alter the level of post-translational modifications of proteins expressed by infected cells, both affecting cellular gene transcription [21] and protein structure. Specifically, MBP in the human body is not a homogeneous species of molecules and present itself as a group of charge isomers [22]. This diversity in charge, results from the deimination of arginine side chains, producing a citrulline residue (Figure 1).

Figure 1. Schematic representation of the citrullination (or deimination) of the free arginine amino acid. In proteins, arginine restudies are converted into citrulline by Ca^{2+}-dependent enzymes *i.e.*, peptidylarginine deiminases, of which at least six forms are known [22,23].

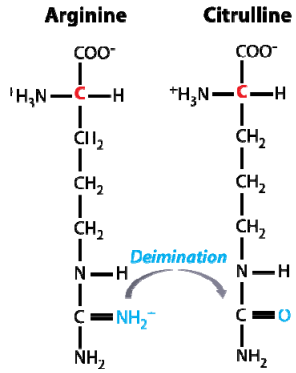

Since the positively-charged side chains are important in forming contact with the negatively-charged membrane lipids, as well as in certain structural properties of MBP, changes in the content of citrulline may both affect the membrane-association of MBP, inducing structural changes that expose epitopes of importance for the autoimmune recognition, and generate novel epitopes that are recognized by the immune system [24,25]. Finally, hereditary factors may play an important role in the development of MS [26] considering the statistics that approximately 15% of MS patients have a relative with MS and children of parents suffering from MS have 1–2% higher risk of developing MS compared to the MS risk factor in the same population. It is classic observation that certain major histocompatibility complex (MHC) alleles increase the risk of MS [27,28] by a factor of three as reported for the haplotype DRB1*1501 [29]. Experiments in animals also suggest MHC molecules to be a determinant in developing MS-like symptoms [30,31].

The pathogenesis of MS leads to four standardized clinical categories, namely relapsing remitting MS (RRMS), primary progressive, secondary progressive, and progressive relapsing MS [32]. Moreover, a significant portion of patients with clinically isolated syndrome (CIS) will develop a clinical definite MS [33]. The RRMS is observed in approximately 80–85% of the MS cases. This condition is clinically represented as repeated outbreaks of disease (attacks or relapsing form) with more or less complete recovery after each attack. The neurological dysfunction is seen usually to increase for each relapse with potential development of secondary progressive MS after some years. In some patients, MS is represented clinically by mild neurological symptoms with very few attacks and little or no impairment. However, on average, MS patients relapse 0.8 times per year and 15% of them enter the chronic progressive MS category (secondary progressive MS) [34,35]. The clinical findings are typically a combination of neurological deficits involving paresis, hyperreflexia, clonus, Babinski's sign and increased tone, sensory dysfunction, ataxic eye movements, and loss of abdominal reflexes. In the case of MS, optic neuritis visual reduction, and color blindness has been reported [36,37]. Lesions in the brainstem and the cerebellum can cause manifestations such as nystagmus, dysarthria and ataxia or balance disorders as well as Lhermitte's sign suggesting spinal involvement at a cervical level.

The consequences of having MS are often profound. It has been noted that MS disability progression follows a two-stage process [38] with approximately 10 years reduction in life

expectancy [39]. The best prognosis is within the RRMS group and favorable prognostic factors are young age, sensory and visual symptoms and long intervals between acute exacerbations in the first two years after diagnosis [40]. Disease progression can stop at any given time. MS can cause diverse neurological deficits depending on the degree of dissemination and location of inflammation. The symptoms develop over minutes to days and possibly even longer, however, with the sub-acute development of symptoms being the most common. In rare cases, MS begins with acute and significant neurological deficits. Common onsets of symptoms are diplopia, unilateral optic nerve affection, paralysis, incoordination or imbalance, sensory disturbances and impaired bladder and/or bowel control. In early-stage MS the first symptoms are often weak and fast transient. The symptomatology in late stage MS varies but frequent problems are painful spasms, ataxia and dysarthria and paroxysmal symptoms like trigeminal neuralgia. More than 60% of the patients experience MS-related pain [41] and up to 50% are considerably affected by depression [42].

2. Differential Diagnosis of Multiple Sclerosis

The diagnosis can solely be made on the basis of medical history and clinical findings from a neurological examination when other causes are excluded. This requires medical history of neurological deficits in at least two distinct phases and the clinical findings from at least two discrete lesions in the CNS. In most cases however, the diagnosis is based on anamnesis, physical examination, results from MRI and lumbar puncture *via* detection of oligoclonal bands of immunoglobulins in the cerebrospinal fluid (CSF) [43] and/or on visually-evoked electrical potentials (VEP) recorded from the nervous system [44,45].

MRI, CSF analysis, VEP, somatosensory and motor evoked potentials can all provide important information and can be of great importance when the clinical presentation alone does not provide certainty for the diagnosis and to exclude differential diagnosis. MRI scanning of the CNS shows in typical cases multiple high signal areas in the white matter on a T2 sequence. MRI is the most sensitive method, although it does not have optimal sensitivity and specificity causing both risk of over-diagnosis and over-treatment of MS [46]. In exceptional cases, MRI findings can be negative even in clinically established MS and there are not always correlations between the imaging outcome and the clinical picture itself.

3. Anti-Inflammatory Treatments of MS

At present, there is no curative treatment of MS. The goal of treatment is to improve the quality of life, reducing the duration and frequency of attacks and thus potentially reduce progressive development of malfunctioning. Rehabilitory treatments are often needed due to bladder dysfunction, constipation, neurogenic pain, spasticity and psychosocial problems. However, it is arguably the case that anti-inflammatory treatments are leading in relieving the symptoms of MS. Their effectiveness also shows the importance of the immune system in developing MS.

A number of relatively simple chemical compounds exert a beneficial effect on MS, probably at least in part as a consequence of an immunosuppressive influence through inhibition of cell division. A temporary improvement is often obtained by using glucocorticoids monotherapy when other treatments are not effective or are not feasible. Typically, 3–5 days of administration of methylprednisolone

intravenously, aiming to reduce the duration and number of individual relapses [47]. RRMS treatment with glucocorticoids may alternatively be given orally. Mitoxantrone is an antineoplastic drug which inhibits topoisomerase enzymes thus inhibiting RNA and DNA synthesis, and as a result is confined in highly active RRMS or secondary progressive MS with superimposed attacks [48]. Drugs like azathioprine (6-mercaptopurine) and methotrexate may reduce the relapse rate in MS patients, but are used infrequently due to sparse evidence of improvement [49–52]. A perhaps surprising source of anti-inflammatory treatment is derived from the use of statins. The best-described pharmacological effect of treatment with statins relates to their function as plasma cholesterol-lowering agents through the activity as a 3-hydroxy-3-methyl-glutaryl-CoA reductase. However, statins such as simvastatin and lovastatin also acts as allosteric inhibitors of integrin $\alpha_L\beta_2$ (also named lymphocyte function-associated antigen-1 or CD11a/CD18) ligand binding [53,54]. This has been documented through studies on the function of leukocytes *in vitro*, structural studies on the α_L ligand binding domain in complex with lovastatin, and the observation that statins apparently exert an immunosuppressive effect in treated patients [53–55]. Several studies have investigated simvastatin and atorvastatin for effects on MS. The findings have so far remained negative, signifying no improvement in condition of treated MS patients [26,56]. It is interesting however, that lovastatin to our knowledge has not been tested in these trials. Furthermore, according to experiments *in vitro*, statins such as simvastatin and lovastatin may not inhibit the function of $\alpha_M\beta_2$ suggesting that therapy with, e.g., simvastatin, would not block the function of all relevant cell adhesion molecules possibly explaining the lack of efficacy.

Direct interference with the cellular constituents of the immune system in patients can be obtained by plasmapheresis as adjunctive therapy, which is used in some cases of primary progressive MS and often considered as adjunctive therapy of exacerbations in relapsing forms of MS [57].

The pharmacological agents mentioned above are broad-acting drugs with several influences that potentially are important for reducing MS disease progression or severity. However, there are several significant side effects of these treatments. Biological therapy—typically with purified or recombinant human proteins, monoclonal antibodies, or receptor analogues—far more specifically targets certain functions of the immune response. Human immunoglobulin may be an alternative for patients with RRMS and when other treatments are not feasible or effective. The documentation is limited, but one study has recently shown some effect at one year of observation [58]. While the pharmacological mode of action is not clear, evidence from other inflammatory diseases of the CNS, seems to suggest that at least partial saturation of cellularly-expressed Fc receptors may play a role [59]. Interferon beta is indicated in RRMS and it appears to slow disease progression in selected patients [60]. Early treatment with Interferon beta, *i.e.*, after the first attack, may extend the time of conversion to clinically definite MS [61,62]. Monoclonal antibodies to cell adhesion molecules have proven remarkably effective in treating disorders involving excessive inflammation. Yednock *et al.* showed [63] that a function-blocking antibody to the α_4 chain of the integrin $\alpha_4\beta_1$ (also named very-late antigen-4 or CD49d/CD29) and $\alpha_4\beta_7$ in rats, prevented experimental autoimmune encephalomyelitis (EAE), which is a well-established albeit not unproblematic animal model of MS [64]. A fully humanized antibody (natalizumab or Tysabri®) is indicated as a monotherapy in very active RRMS stage, despite treatment with interferon beta. It has been shown that the treatment reduces relapsing rate at 1 year from 0.75 to 0.25 (68% reduction) and the number of new or enlarged brain lesions on MRI reduces by 83% [65,66]. Development of neutralizing antibodies to Natalizumab may however lead to a reduced

treatment effect and should be controlled during treatment [67,68]. In addition, it should be noted that progressive multifocal leukoencephalopathy is associated with Natalizumab treatment [69]. These side effects were also observed for function blocking antibodies to other cell adhesion molecules such as integrin $\alpha_L\beta_2$ [70]. As reviewed elsewhere [71], a future perspective may involve the use of various nanomedicine formulations of integrin ligand binding competitors as a safer alternative to function-blocking monoclonal antibodies. However, the presence of soluble adhesion molecules in human plasma, generated by proteolytic shedding, adds complexity to regulating the outcome of blocking receptor function with either monoclonal antibodies or other means [71]. Several strategies now also target B-lymphocytes. The CNS of MS patients is both the target of the immunopathological process as well as a site of local antibody production. B cells can increase or dampen CNS inflammation. Since B-cell depletion is a promising therapeutic strategy their proinflammatory effects seem to be more prominent in most patients [72].

Copaxone® is an immunomodulator with glatiramer acetate as active ingredient. In 1987, Bronstein *et al.*, studied and compared a group of MS patients receiving GA against a placebo group in which, the group receiving GA, showed 30% more improvement in their disability score [73]. Since the approval of Copaxone® for MS treatment in the US in 1996, it has remained popular for treatment of MS considering the life-threatening side effects of other competitors such as Tysabri and Mitoxantrone [74]. In two different projects Miller *et al.* studied the long term (up to 22 years) effects of Copaxone® as the sole therapy for relapsing-remitting MS (RR-MS) patients. In these studies, the long term use of Copaxone® did not influence the efficacy and safety showing its important features as a safe and reliable treatment for MS considering the chronic nature of the disease [74–76]. The superiority of GA treatment over placebo has been indicated by a double-blind, randomized, placebo-controlled study of the effects of GA on MRI. This study shows, by its highly statistical significance, that the total number of CNS lesions on T1- and T2 weighted MRI, involving 239 patients with RRMS, was reduced ($p = 0.003$), showing in addition a significant reduction by 33% in relapse rate [77]. A multicenter double-blind placebo-controlled study from 1995 then demonstrated GA to reduce the number of new relapses by approximately 30% without significant side effects [78] leading to regulatory authorization of MS treatment from 1996 in the US and 2000 in Europe. In addition, a meta-analysis from Boneschi *et al.* supported these findings by bringing to light a highly statistical significant difference between the intervention groups receiving GA and the placebo group as to the following endpoints; adjusted annualized relapse rate, adjusted risk ratio for the on-trial total number of relapses and time to first relapse [79]. The research group stated that the meta-analysis reaffirms the effectiveness of GA in reducing relapse rate and disability accumulation in RRMS, at a magnitude comparable to that of other available immune modulating treatments. They also suggested that the efficacy of GA is not significantly influenced by the patients' clinical characteristics at the time of treatment initiation. However, a recent meta-analysis by La Mantia *et al.* states otherwise [80]. All randomized controlled trials comparing GA and placebo in patients with definite MS, whatever the administration schedule and disease course, were eligible for their review. The objectives, in their study, were to verify the clinical efficiency of GA in the treatment of MS patients with RRMS and progressive-course MS (PMS). Five hundred and forty RRMS patients and 1049 PMS were selected for the analysis and they concluded that GA has a partial efficiency in RRMS, *i.e.*, in terms of relapse-related clinical outcomes, without any significant effect on clinical progression of disease

measured as sustained disability. The drug showed no effect in progressive MS patients and, therefore, continuing the treatment with GA seems to have few beneficial effects in RRMS, and no significant impact in PMS patients [80]. In other words, the study showed no beneficial effects on disease progression in two MS forms. However, they found a slight reduction in the frequency of relapses in RRMS patients and as mentioned no positive improvements in the conditions of the PMS group were observed. Side effects as flushing, chest tightness, sweating, palpitations, anxiety and local injection-site reactions occurred quiet frequently, but no major side effects were observed. Currently it is recommended that the treatment is terminated or switched to another approved treatment, if the frequency or severity of clinical relapses become worse during the GA-treatment or that the progression of disease is to such an extent that the patient no longer is thought to benefit from the treatment (*i.e.*, GA is not indicated for use in a progressive state of the disease). Patients receiving treatment with GA should be informed on side effects according to *lege artis*, health and medicines authorities, and that a reaction with one or more of the following symptoms may occur within minutes after injection: mild injection-site reaction, manifested by erythema, inflammation, and induration. The most remarkable side effect has been reported to be systemic post-injection reaction that occurred in 10% of patients manifested by flushing, chest tightness, palpitations, dyspnea, and anxiety [81]. Most of these symptoms are transient and disappear spontaneously and without sequelae. There is no risk that special populations are at a particular risk for these reactions. Nevertheless, caution should be applied when GA is administrated to patients with cardiac disease and plasma for its content of GA, should be monitored during and after treatment. Serious hypersensitivity reactions (e.g., bronchospasm, anaphylaxis or urticaria) may rarely occur [82]. There are no adequate data for treatment during pregnancy and breastfeeding (*i.e.*, no information can be found on GA excretion, GAs' metabolites or its antibodies in breast milk). Animal studies are insufficient with respect to pregnancy, on embryonic development, delivery and postnatal health. Therefore treatment with GA is not recommended during pregnancy [82]. Renal function should be monitored regularly in patients with renal impairment, but there is no evidence of glomerular deposition of immune complexes in humans. However, the possibility cannot be excluded as GA-reactive antibodies have been found in patient receiving GA treatment [83,84]. The peak in antibody titers to GA was here reached on average after 3–4 months of treatment, followed by a reduction in the titers. In conclusion, the current scheme of GA-treatment with 20 mg injection subcutaneously per 24 h is considered a good option for RRMS patients when walking mobility is persevered and there are clinical signs of disease activity, *i.e.*, evidence of relapses during previous two years. In addition, GA-treatment is indicated in clinically well-defined first demyelinating episode and when alternative or differential diagnosis has been excluded. This is not trivial and it must be noted that GA prescription and administration should only be done by a physicians experienced in neurology and in treating MS patients. Furthermore, the treatment should be followed up with clinical examination three and six months after treatment and followed up every six months, with registration of number of attacks, side effects and objective neurological examination. Currently, it is not known how long patients should be treated.

While the clinical data supports a beneficial effect of GA in the treatment of MS, there is considerable uncertainty as to what are the major pharmacological modes of action (PMA). As presented in the following sections the chemical nature of the compound is complex and for this reason sometimes misrepresented unintentionally in the scientific literature.

4. What Is Glatiramer Acetate?

As a starting point, it is beneficial to recapitulate briefly the historical development of GA, as it can be extracted from the original reports and a few reviews detailing the chemistry [85–87]. In the mid-1900, the science of amino acid polymerization had moved to a level where it seemed possible to make synthetic high-molecular weight compounds as models of biopolymers, here, of course, most notably proteins. Through the work of Katchalski-Katzir *et al.*, it became possible to make poly amino acids from their *N*-carboxy-α-amino acid anhydrides (NCA), in some cases modified with appropriate protecting groups, which were removed to generate the final product in processes also introduced from this work [88,89]. Initially, homopolymers such as poly-L-lysine and poly-L-glutamate were made [90]. Even in some of the first experiments average lengths of the polypeptides reached more than 30 units and procedures for making polymers with a degree-of-polymerization (DP) at approximately 200 was soon reached [91]. The DP is influenced by temperature, with low temperatures favoring the formation of polymers with high DP when the reaction takes place in solution. In inert media the reaction requires initiation by addition of amines or strong bases such as NaOH. Interestingly, the choice of initiator, e.g., primary, secondary or tertiary amines, and molar fraction of the initiator may also influence DP of the polymers. With such control over the chemistry of polymers made according to this scheme, the polypeptides turned out to be instrumental in forming a solid basis for our current understanding of protein structure. Among many significant achievements, the alpha helical structure in proteins predicted by Pauling and Corey [92] was found by Perutz using poly-γ-benzyl-L-glutamate [93]. Also, the ability to make polymers as model of collagens, using block polymers of poly (Pro-Gly-Pro), identified the critical chemistry behind the triple helical structure attributed to collagen fibers by Rich and Crick [94] and was the first example of synthetic polymers forming a trimer. This principle was used subsequently in numerous investigations on the properties of collagen [95]. In addition to X-ray diffraction on the fibrous material, the use of ultraviolet rotatory dispersion spectroscopy was quickly introduced to confirm the formation of secondary structure in the polymers in various aqueous environments [91].

The chemistry of GA is tightly linked with the observation that the polypeptide polymers have various biological activities, including the ability to act as a substrate for enzymes [96] as well as being antigenic, *i.e.*, able to stimulate an immune response as shown in several reports by Sela and Arnon [97–100]. A classic experimental animal model for the development of MS in humans involves injection of MBP and adjuvant (typically “Complete Freund’s adjuvant”, which contains strongly immunostimulatory components) into animals, mostly rodents but also primates [64]. As suggested by the name, this protein is a highly positively charged constituent of the myelin sheath surrounding the nerve axon [22]. In consequence of MBP’s antigenic properties, this injection directs an immune response to nerve tissue causing encephalitis with some similarities to the pathology of human MS. Since MBP obviously is a host protein, this model has greatly served to strengthen the idea that MS is an autoimmune disease and the model is usually referred to as EAE. Previously it had been observed, however, that MBP can suppress EAE when injected in the absence of adjuvant [87,101]. These capacities prompted Teitelbaum *et al.* to synthesize a polypeptide from the acid anhydrides of γ-benzyl-L-glutamate, ε,*N*-trifluoroacetyl-L-lysine, L-alanine, and L-tyrosine with molar ratios of 1.9:4.6:6.0:1.0 in the formed polymers [102]. This formulation was named Copolymer-1 or Cop-1. In

this way, the four cardinal biochemical properties of amino acid side chains, *i.e.*, side chains with negative or positive charge or polar or hydrophobic groups, were represented when the protecting groups were removed from the glutamate and lysine residues. Compared with the scientific publication [102] further detail on the synthesis methodology can be found in patent filed in 1971, which identified diethylamine as initiator of the polymerization carried out at ambient temperature in anhydrous dioxane [103]. This removal was carried out by de-blocking of the γ-benzyl-L-glutamate affected with hydrogen bromide in glacial acid, followed by removal of the ε,*N*-trifluoroacetyl from lysine residues by 1 M piperidine [103] (Figure 2).

Figure 2. Schematic representation of some of the reactions forming Cop-1 co-polymers [91,104]. The co-polymers are made from the NCA of L-alanine (4-methyl-2,5-oxazolidinedione), and L-tyrosine (2,5-oxazolidinedione,4-(p-hydroxybenzyl)). L-glutamate is included with a protecting group (X': γ-benzyl ester) as 4-oxazolidinepropionic acid, 2,5-dioxo-, benzyl ester. L-lysine is included with a protecting group (X": ε,*N*-trifluoroacetamide) as *N*-(4-(2,5-dioxo-4-oxazolidinyl) butyl)-2,2,2-trifluoroacetamide. As examples, the C-termini of two co-polymers are shown in the panel. Following the polymerization, which may take place at room temperature [103], X' was removed by treatment with hydrogen bromide in glacial acid and X" was removed by treatment with 1 M piperidine, which produces the final acetate salt of co-polymers of the four amino acids.

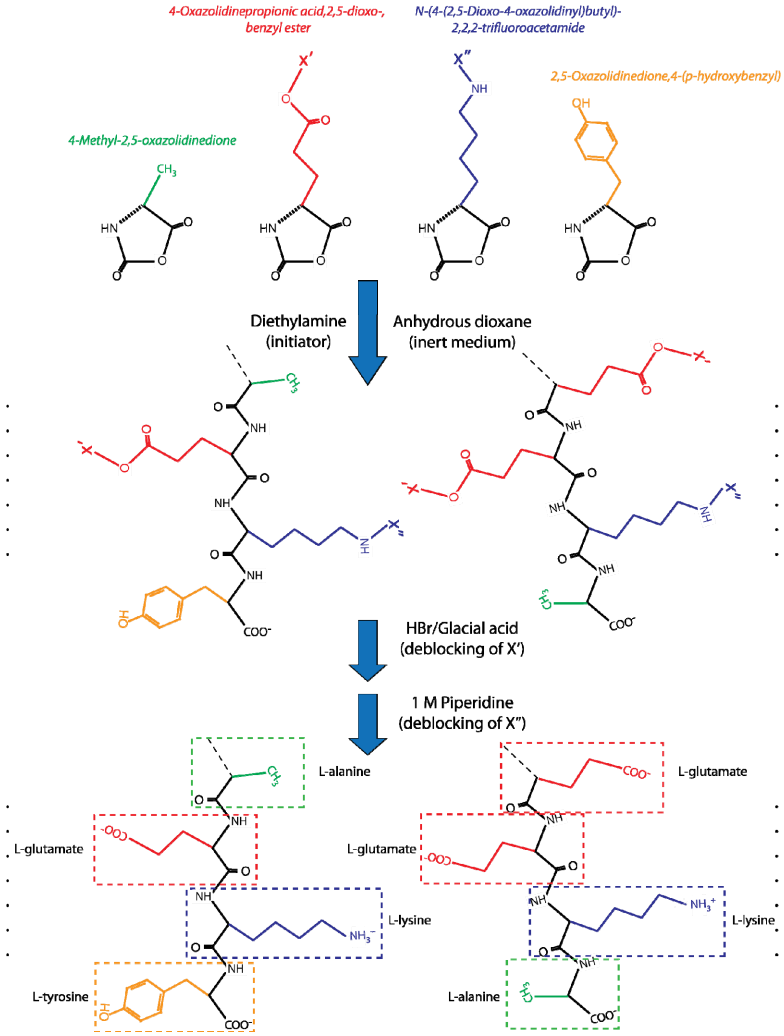

In the case of Copolymer-1, the ratios of NCA were chosen to mimic the stoichiometry of side chains in MBP with negative or positive charge or polar or hydrophobic groups, which at the time was essentially the only known property of MBP's structure. By making random co-polymers with this stoichiometric composition at the very least some of the immunoregulatory properties of MBP would be presented by synthetic polymers. Indeed, it was found that Cop-1 worked to block the encephalitis [102]. By contrast, other polymers, including one similar to Cop-1 except not containing lysine, could not suppress EAE [102]. It should be noted that the co-polymers forming a part of the currently used GA formulation apparently are synthesized in a way which results in ratios of alanine, lysine, glutamate, and tyrosine in the GA polymers of 1.4:3.4:4.2:1, which is different from the original report on Copolymer-1. To our knowledge, no explanation for this difference has been indicated in the scientific literature. For the discussion below, it is also of interest, that the patent mentioned two other polymers consisting of tyrosine, aspartate, alanine, and lysine or glutamate, alanine, and lysine, respectively, leading to similar results as the Cop-1 formulation for treatment of EAE [103]. These polymers all had a relatively high content of lysine and hence a net positive charge, which, as noted by Teitelbaum *et al.*, pointed out the importance of this amino acid and the positive charge to trigger suppression of EAE by the polymers [102]. However, the chemistry of these co-polymers was different from Cop-1 and hence not matching MBP in the way the Cop-1 does. Indeed, co-polymers chemically different from Cop-1 may exert a stronger suppressive influence on EAE than Cop-1 [105].

By definition, co-polymers such as those found in GA are derived from two or more monomers, *i.e.*, in the case of GA the four acid anhydrides mentioned above, unlike homopolymers which are derived from only one type of monomeric species. In the medical literature GA is, however, rarely indicated as containing co-polymers, probably, one may speculate, because pharmacological treatment with even simpler polymeric substances is still rather limited. Indeed, GA was the first synthetic polymeric pharmacological agent to be used in internal medicine. In this situation references to GA as belonging to the class of co-polymers are rarely added in databases indexing drugs, although an expert probably would be able to infer from the provided information that GA is likely to be a co-polymer. The exact nomenclature may seem only of semantic interest, however. By contrast, a more important challenge in understanding the nature of the drug resides in the extraordinary structural variation found amongst the synthesized co-polymers. As a typical result of polymer synthesis, the copolymers are not size uniform. Indeed, the clinically-used formulation of GA contains copolymers with a range of M_rs ranging from 5000 to approximately 9000 corresponding to DPs of 45–80 residues. As noted by Arnon and Sela [87], this is nevertheless a narrow distribution in size compared to most products of polymer synthesis, which is a result of the chemistry of the polymerization process, where the polymers grow only from coupling with the acid anhydride monomers and not through coupling with polymerized species [87,91]. Another limitation on the size heterogeneity comes from the observation that termination of the polymerization occurs mainly through an intermolecular reaction with acid anhydrides creating a terminal carboxyl group [87,91]. A striking contribution to the heterogeneity among copolymers comes from the randomness of the sequences. If the co-polymers contain approximately 50 residues, the number of possible combinations with four polymerizing amino acids equals $\sim 4^{50}$ (*i.e.*, equal to $\sim 10^{30}$) possible peptides. Since patients receive in the order of $\sim 10^{17}$ such polymers per injection, a patient will never in his or her lifetime receive chemically identical co-polymers.

Furthermore, this variation among the co-polymers also affects the composition of the purified material where a batch-to-batch variation make the molar fraction of L-glutamate, L-alanin, L-tyrosine, and L-lysine vary in intervals of 0.129–0.153, 0.392–0.462, 0.086–0.100 and 0.300–0.374, respectively.

The chemical heterogeneity makes GA hard to characterize by available methodologies. Interestingly, this situation is remarkably similar to another polymeric substance, which is used in the clinic, namely heparin. Heparin is a random co-polymer with an average DP of 20, polymerized from a choice of 32 disaccharide units [106]. This produces a theoretical diversity of ~10^{14} distinct co-polymers—if not as many as for GA, then still a considerable heterogeneity for a compound. An important market regulator of the costs of pharmacological treatment, and hence overall cost of health care systems, is the availability of generic drugs. Usually, a generic drug would be pharmaceutically equivalent to the original formulation, meaning that it contains the same active ingredient. However, in the case of enoxaparin sodium injection (Lovenox®), an anticoagulant with biologically-derived heparin as the active ingredient, the manufacture of a generic product caused significant challenges in the absence of precise chemical insight on the structure of the heparin co-polymers. However, as judged from available accounts in the literature and on the internet the company Momenta Pharmaceuticals (Cambridge, MA, USA) applied advanced methodologies to sequence heparin co-polymers originally developed at the Massachusetts Institute of Technology, by use of matrix-assisted laser desorption ionization mass spectrometry, hereby obtaining information sufficient for bringing generic Lovenox on the market for prevention of deep vein thrombosis [107]. Such a product is now referred to as a "biosimilar", or "follow-on biologic", indicating that the pharmacological innovative aspect was made with the prior manufacture of another drug [108]. Apparently, Momenta Pharmaceuticals is currently in the pursuit of making generic Copaxone®, here named M356, which is likely also to involve technologies capable of characterizing complex protein drugs albeit the specifics are not clear. A second company, Synthon (Nijmegen, The Netherlands) is also pursuing the manufacture of generic Copaxone according to their web site, but details on the process of characterization or manufacture is also in this case not available to our knowledge. Finally, both in the case of heparin-based anticoagulants and GA, products with a more well-defined chemical nature were made. Following the "heparin crisis" where naturally-derived heparin contaminated with chondroitin sulfate caused adverse clinical events [109,110] considerable efforts have been invested in making synthetic heparin [109,111]. Similarly, efforts have been invested in making peptidic substances with a considerable less heterogeneous composition than Cop-1 [112]. While it is unclear if such a strategy is currently being commercially explored in the case of GA, at least in principle it suggests one route of making competing drugs.

5. The Pharmacological Modes-of-Action of GA

As pointed out above, the extraordinary diversity of the GA co-polymers raises an important question as to how the effects in the EAE model and the human MS disease are obtained. As identified below, the suggested mechanisms can largely be divided into three groups, two of which relate to an influence on the inflammatory response. Here, focus is placed on the possible influences of GA on the adaptive and innate immune system. Finally, a brief mentioning is made of a neuroprotective effects, that, however, also appears to involve cells of the immune system.

The adaptive immune response critically relies on the interconnected function of T and B lymphocytes with the T cells being an important source of regulatory cytokines and B lymphocytes a precursor state of the antibody-producing plasma cells. A considerable body of studies has addressed the influence of Cop-1 or GA on these cells, mainly through the use of the EAE model as well as from observations made on clinical samples. Some of these studies are reviewed below. A hallmark of adaptive immunity is sequence-specific recognition of peptidic motifs by the T and B cell receptors, which are formed through somatic recombination and mutation of germ line genes and makes a large diversity of receptors permitting the recognition of large number of antigens. Clonal selection in lymphoid organs both removes autoreactive clones and selects those clones with receptors strongly recognizing antigens.

Following the initial study on Cop-1 suppressing EAE [102], it was demonstrated that Cop-1 induced the formation of specific antibodies to the co-polymers, which cross-reacted with MBP [113]. A correlation between this immunological cross-reactivity and the suppression of EAE clearly pointed that injection of the co-polymers manipulated the immune response. As noted above, another important observation was that Cop-1 may compete with MBP for binding to MHC class II molecules [114,115]. EAE may be induced by other agents than MBP, such as peptides from proteolipid protein (PLP) or myelin oligodendrocyte glycoprotein (MOG). Both of these proteins are not structurally related to MBP but carry a net positive charge (*i.e.*, with isoelectric points of ~8) at a more moderate level than MBP (with an isolectric point of ~10). Interestingly, Cop-1 also suppressed EAE induced by these agents [116,117]. It is unclear if any critical similarity exists between PLP, MOG, and MBP, but it is, of course, striking that the positive charge of these proteins and Cop-1 may be an important shared characteristic also adding to findings mentioned above that co-polymers with lysine—but otherwise no obvious mimicry of MBP—were suppressing EAE. Taken together, it is debatable if the antigenetic similarities between Cop-1 and MBP are critical for the EAE suppression. Rather, it would seem likely that Cop-1 and GA works through a more general mechanism with regard to influencing the adaptive immune system. Support for the latter point may be derived from the observation that Cop-1 also works to block the inflammatory response in animal models of cerebral stroke [118] and graft-versus-host disease [119]. In particular the study on graft-versus-host disease [119] suggests that Cop-1, and hence GA, may act as a general immunomodulatory compound not requiring a role of MBP in the inflammatory response. This is supported by an important study on GA co-polymers, *i.e.*, the clinically-used formulation, as antigen, carried out by Duda *et al.* [120]. This paper showed that the co-polymers induced $CD4^+$ T cell proliferation of both naïve and memory T cells. In this sense, the GA co-polymers may act as universal antigens, which could be thought to alter T cell receptor repertoire in treated patients. However, a recent analysis failed to find such alterations in MS patients treated with GA compared to patients not receiving this treatment albeit the numbers of analyzed patients were low [121]. Another important influence of GA on T cell function was reported by Aharoni *et al.* reporting that GA generate bystander suppressor T cells and, more recently, a similar suggestion was made by Kala *et al.* pointing to GA modulation of regulatory B cells [122,123]. These cellular effects induce the synthesis of a plethora of cytokines, presumably mostly anti-inflammatory, supporting the view that several independent mechanisms contribute to the therapeutic effect of GA [124]. GA-reacting T helper cells are found in all patients with MS. During treatment with GA, these cells will differentiate in the direction of Th2 regulatory T cells, which have anti-inflammatory properties

through their secretion of cytokines [120]. In the case of human MS it has been hypothesized that these cells pass the blood-brain barrier (BBB) (Figure 3) [125]. In the case of EAE Th2 cells were demonstrated to localize in the CNS [122] where myelin antigens are presented [126]. Here, they then reactivate, resulting in secretion of anti-inflammatory cytokines. These cytokines (e.g., IL4, IL-6, IL-10) inhibit the activity of potential surrounding autoaggressive T cells. This action is called bystander suppression (Figure 3) [122,127]. Despite these findings, experiments with IL-4- and IL-10-deficient mice show that GA still had beneficial effects in suppressing EAE in the absence of these two prominent Th2 cytokines. Thus, Jee *et al.* suggested that alternative modes-of-action to bystander suppression may be responsible for these effects of GA [128].

Figure 3. Some of the pharmacological modes-of-action (PMA) of GA-treatment of MS patients. Three selected mechanisms are indicated, representing neuroprotective effects through (1) IL-4 mediated suppression of microgial free radical release [128,129] or modulation of the adaptive immune response through (2) by-stander suppression of autoreactive T cell proliferation [122,127]. Based on experiments *in vitro*, Stapulionis *et al.* suggested an influence of GA on the innate immune system through (3) inhibition of phagocytic damage to the myelin sheath by inhibition of integrin $\alpha_M\beta_2$ binding to the exposed MBP [130].

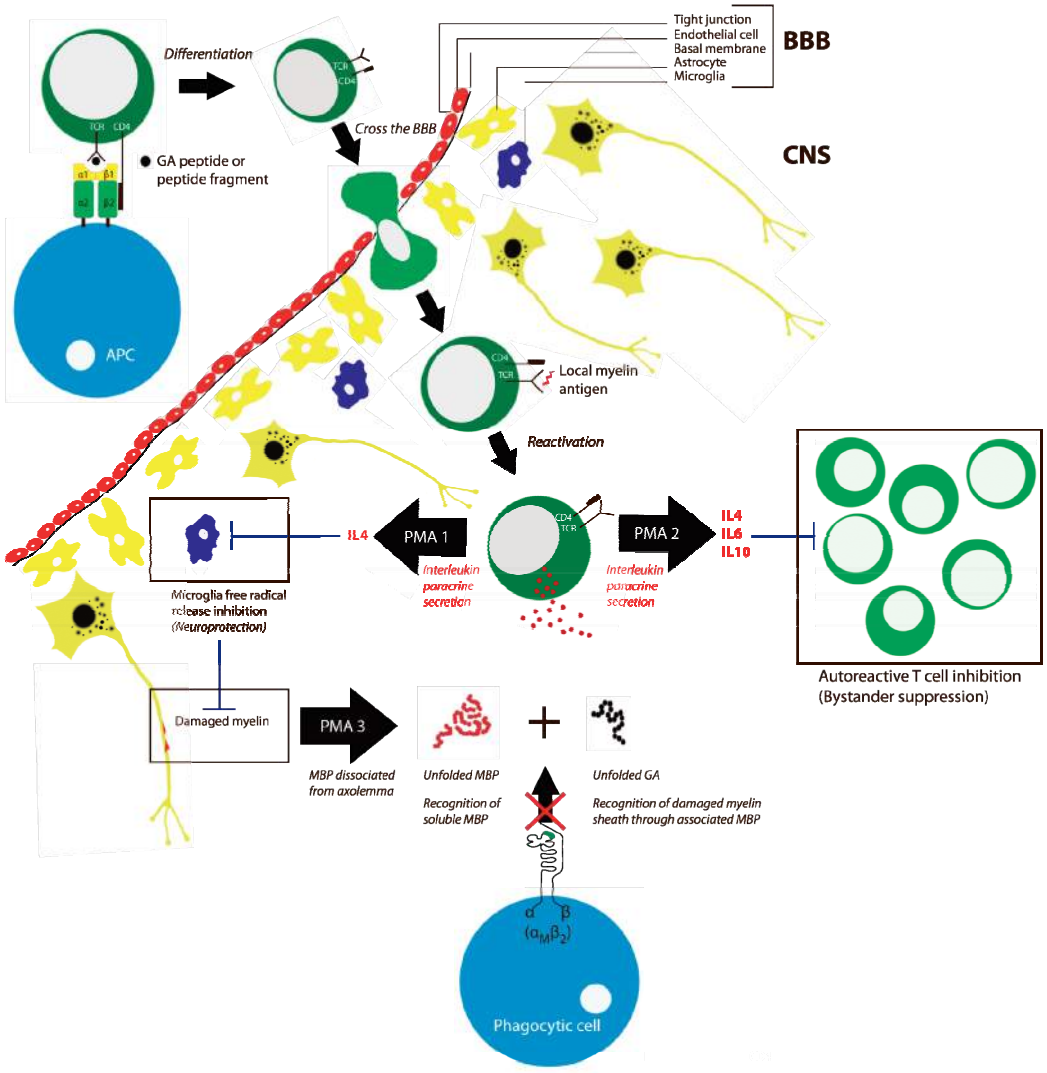

The innate immune system functions, in part, through receptors and soluble molecules encoded by germ line genes. These are evolutionary selected to encode proteins that permit the recognition of certain microbes, usually through the exposure of pathogen-associated molecular patterns that distinguishes these microbes from host cells. However, an increasing body of literature now shows that the innate immune system also plays a role in recognizing damaged tissue or molecular species of the host [131]. Such functions are at least partially mediated by cell membrane-expressed receptors that recognize structurally or decayed molecules [132].

The β_2 integrins are exclusively expressed on leukocytes where they support cellular adhesion to ICAMs, fragments of complement component C3 deposited on target surfaces through the activation of the complement system, or protein components of the extracellular matrix such as fibrin [133,134]. The receptors are linked with the cytoskeleton through transmembrane domains and this contact, in turn, permits allosteric regulation of ligand binding through conformational changes in the receptor ecto-domain [135]. Recently, it has become clear that the full functionality of these receptors in supporting cellular migration probably requires several proteases that shed the ecto domain of β_2 enabling the de-adhesion of migrating cells [71,136,137]. Inspired by the many findings suggesting that adhesion molecules are important drug targets in anti-inflammatory therapy, Stapulionis *et al.* investigated if GA influences the function of β_2 integrins [130]. $\alpha_M\beta_2$ (also known as Mac-1, complement receptor 3, or CD11b/CD18) and $\alpha_X\beta_2$ (p150,95, complement receptor 4, or CD11c/CD18) are mainly expressed on NK cells and myeloid-derived leukocytes, such as neutrophil granulocytes and monocytes/macrophages, which are usually thought to constitute the cellular arm of the innate immune system. However, these receptors are also expressed on dendritic cells, which play a significant role in establishing an antigen-specific response by T lymphocytes. While integrin $\alpha_L\beta_2$ is relatively specific in its interaction with the ICAMs, integrins $\alpha_M\beta_2$ and $\alpha_X\beta_2$ are far more promiscuous in their interactions with ligands. Consequently, a large number of biomacromolecules, not only including proteins and several peptides but also carbohydrates and components of the microbial cell wall were reported as ligands [71]. A chemical rationale for the underlying principles in ligand recognition by these integrins was proposed by Vorup-Jensen *et al.* [138]. According to these studies, central properties of ligands are the presence of acidic groups to coordinate a Mg^{2+} ion in the ligand binding domain and a low abundance of secondary structure. Such a system would enable phagocytes expressing these integrins to clear decayed molecular species, which are produced through the activity of, in particular, proteases, which destroys the structure of proteins. In the context of the discussion below on the binding between integrin $\alpha_M\beta_2$ and GA, it should be noted that another polymer reported to bind strongly to integrin $\alpha_X\beta_2$, and less strongly by integrin $\alpha_M\beta_2$, is heparin [139]. As discussed in Section 4, heparin is a random co-polymer with little, if any, secondary structure in solution [106]. In this way, the observation that heparin binds $\alpha_X\beta_2$ and $\alpha_M\beta_2$ supports the idea that random co-polymers can be ligands for these integrins albeit the structural biology of these interactions is unclear. The ability of integrin $\alpha_X\beta_2$ to preferentially bind certain unfolded proteins is shared by integrin $\alpha_M\beta_2$, however, the binding by this integrin is not strengthened by a polyanionic character of the ligand as was found for $\alpha_X\beta_2$ [71,138,140]. Indeed, the observation that MBP is a ligand for this integrin [130] may suggest that positively-charged species bind well to the integrin $\alpha_M\beta_2$. Likewise, studies using synchrotron radiation circular dichroism spectroscopy revealed that the GA co-polymers present little secondary structure, probably in consequence of the high content of lysine, which contributes a

hydrophilic and positively charged character to the peptide [130]. In this sense, the GA co-polymers and MBP share biophysical characteristics since MBP in aqueous environment are a classic and well-studied examples of an intrinsically unordered protein [22]. In experiments carried out *in vitro* Stapulionis *et al.* reported that the GA co-polymers bind integrin $\alpha_M\beta_2$ to a level where they may act as competitive ligand binding antagonist, blocking the binding of this integrin to MBP [130].

These *in vitro* findings inspired a suggestion on the PMA of GA. Following injury to myelin sheath of the nerve, MBP is brought into contact with the aqueous environments of the CSF, which unfolds the protein making it a ligand for integrin $\alpha_M\beta_2$. It has been shown that MBP can be detected in CSF of MS patients, presumably as a consequence of demyelination in the white matter of the brain [141,142]. The interaction with integrin $\alpha_M\beta_2$ promotes the phagocytic uptake of MBP, possibly in a format where MBP is part of myelin sheath fragments, which was shown earlier to be internalized by phagocytes [143,144]. Such internalization may lead to cytokine production by the phagocytes as well as a direct attack by these cells on the myelin sheath, which could affect both myelination and remyelinination processes. Studies in mice clearly suggest that there is complex interplay between leukocyte subsets in the process of healing CNS lesions [145]. Both under normophysiological conditions as well as in the pathophysiology of MS, several types of integrin $\alpha_M\beta_2$-expressing cells can be found in the CNS. In particular, these include microglial cells as well as other cells of myeloid origin invading the CNS from the blood, most notably monocytes and neutrophil granulocytes under extreme circumstances [146].

For GA to be efficient in blocking the binding between $\alpha_M\beta_2$ and MBP in the CNS, an obvious prerequisite is the ability of GA to pass the BBB. As a first step on the route to reach the CNS, the survival following the injection would seem particularly important. *In vitro* data and data from clinical trials in healthy volunteers indicate that after subcutaneous administration, GA is rapidly absorbed. The pharmacokinetics of GA have indeed been evaluated in mice, rats and monkeys by radiolabeling technique [147]. Maximum serum radioactivity is observed after 2 to 4 hours in monkeys. The active substance is rapidly absorbed after subcutaneous injection (20 mg daily) with 10% remaining at the injection site after 1 h [148]. There is a rapid hydrolysis to amino acids and shorter peptides and a large part of the degradation already occur in the subcutaneous tissue. Furthermore, no systemic plasma, urinary or fecal excretion of GA is indicated [148]. However, this may not impair the influence on integrin $\alpha_M\beta_2$ since it is well established that even small peptides may act as binding antagonists *in vivo*. With regard to the actual site of action for the MBP binding-antagonistic effects of GA, both the report by Stapulionis *et al.* [130] as well in Figure 3, it is suggested that this would be relevant in the immediate contact between the damaged myelin sheath and an integrin $\alpha_M\beta_2$-expressing phagocyte such as microglial cells or monocytes having crossed the BBB [149,150]. An important caveat to this suggestion concerns the biodistribution of GA, or more specifically, if the GA polymers are able to cross the BBB. We are not aware of any studies addressing if GA may actually reach the CNS, but an important reason to suggest such a possibility may be the dysfunction, or breakdown, of the BBB, which is thought to occur in MS. It is a classic finding that the concentration of high-molecular weight proteins such as fibrinogen increases in the CSF in the event of a break-down of the BBB and even in healthy individuals there appears to be an exchange of substances with a M_r of less than 160,000 [151]. Any proteolytic break-down products of the GA polymers, and maybe even the intact co-polymers themselves, would seem ideally suited for crossing the BBB. Furthermore, in addition to the

co-polymers the GA formulation contains 40 mg/mL mannitol. The addition of mannitol is a method to bring drugs across the BBB [152]. It should be noted, however, that this addition was apparently not part of the Cop-1 formulations used in the many studies on EAE mentioned above.

It is also possible, however, that the $\alpha_M\beta_2$ ligand binding antagonistic properties of GA may influence the immune response to myelin sheath by acting on leukocytes outside the CNS, *i.e.*, in plasma or secondary lymphoid tissues. A recent study by Toker *et al.* pointed that fluorescently tagged GA co-polymers are selectively bound by $CD11b^+$ (*i.e.*, integrin $\alpha_M\beta_2$-expressing) peripheral monocytes in an MHC class II independent mechanism [153]. This finding indicates that GA may form stable ligation to receptors on monocyte cell surface over a significant time span. Monocytes are usually considered a part of the innate immune system, but their potential to differentiate into macrophages and possibly myeloid-derived dendritic cells also enables functions in the acquired immune system, most notably with regard to regulating T cell functions. This is important to note since the many reported influences on the adaptive immunity by GA treatment mentioned above at the very least could come about through an indirect route targeting myeloid cells of the innate immune system. Any interaction between integrin $\alpha_M\beta_2$ and MBP, or fragments hereof, in blood is purely speculative. In principle, the MBP found in the cerebrospinal fluid [141] could leak through a damaged BBB into plasma as it has been reported for both acute brain damage as well as chronic progressive neurological disorders [154]. However, yet other roles of the influence of GA on the function of $\alpha_M\beta_2$ may be suggested. In a clinical setting, Sellebjerg *et al.* reported that GA treatment increased the number of circulating monocytes with approximately 20% [84]. Obviously, these effects of GA treatment are taking place outside the CNS. While the mechanistic explanation for this finding remains to be explored, one possibility is that GA releases the otherwise adherent monocytes through GA's ligand binding-antagonistic properties towards the integrin $\alpha_M\beta_2$. The GA-activity on monocyte function is of considerable interest since recent findings have indicated this leukocyte subset to play a major role in processes affected by MS [149,150] apparently through the ability of monocytes to modulate the function of T lymphocytes. The findings by Toker *et al.* [153] are strong evidence that the GA co-polymers may target integrin $\alpha_M\beta_2$ under physiological conditions affecting this leukocyte subset of the innate immune system.

Alternative modes of action of GA may include a neuro-protective activity [129], apparently in a way connected to the ability of the drug to skew the inflammation towards a Th2 type humoral immune response. In a mouse model, accumulated GA-specific cells have been reported to express brain-derived neurotrophic factor (BDNF) *in situ* as detected by BDNF-immunostaining and confocal microscopy [155]. Interestingly, BDNF production may also be induced in dendritic cells following Cop-1 treatment. With regard to the humoral response, GA-reactive antibodies do not reduce the clinical efficiency of GA [83]. Indeed, Ure *et al.* showed that GA-reactive antibodies mediate positive effect on re-myelination [156]. This effect is not limited to EAE and can be observed in other models of encephalitis, one example being neuroprotecting effects in a murine model HIV-induced encephalitis.

6. Conclusions

As yet, no curative treatment exists for MS. However, it is clear that biological therapy targeting functions of the immune system presents several benefits, although strong suppression of the immune

system is associated with severe opportunistic infections as a side effect. Particularly from this perspective, the efficacy of GA treatment is of interest. This review of the current knowledge on the PMA of GA, points to several routes targeting the immune system. Remarkably, in addition to the effects on the adaptive immune system, more recent findings now suggest that cellular components of the innate immune system are targeted, at least partially, through cell adhesion molecules such as integrin $\alpha_M\beta_2$. From a biochemical point of view, it is perhaps not surprising that several PMA are at play when treating patients with random co-polymers of such diversity as in the case of GA. A more detailed understanding of these PMA is likely to support the development of a more potent drug. Furthermore, an important aspect is the development of new types of random copolymers for anti-inflammatory treatment. The case of GA suggests that such strategies may hold particular promise when several inflammatory responses are part of the pathogenic processes, which is likely to expand the use of GA or similar drugs to aid additional inflammatory disorders.

Acknowledgments

Our studies on GA were generously supported by The Danish Multiple Sclerosis Association, The Naomi Bramson Foundation, UK, and The Lundbeck Foundation through support of the "The Lundbeck Foundation Nanomedicine Centre for Individualized Management of Tissue Damage and Regeneration".

Conflicts of Interest

The authors declare no conflict of interest.

References

1. Charcot, J. Histologie de la sclerose en plaques. *Gaz. Hop.* **1868**, *41*, 554–555.
2. Kachuck, N.J. Sustained release oral fampridine in the treatment of multiple sclerosis. *Expert Opin. Pharmacother.* **2009**, *10*, 2025–2035.
3. Compston, A.; Coles, A. Multiple sclerosis. *Lancet* **2008**, *372*, 1502–1517.
4. Sadovnick, A.D.; Ebers, G.C. Epidemiology of multiple sclerosis: A critical overview. *Can. J. Neurol. Sci.* **1993**, *20*, 17–29.
5. Calabresi, P.A. Diagnosis and management of multiple sclerosis. *Am. Family Phys.* **2004**, *70*, 1935–1944.
6. Rosati, G. The prevalence of multiple sclerosis in the world: An update. *Neurol. Sci.: Off. J. Ital. Neurol. Soc. Ital. Soc. Clin. Neurophysiol.* **2001**, *22*, 117–139.
7. Stys, P.K.; Zamponi, G.W.; van Minnen, J.; Geurts, J.J. Will the real multiple sclerosis please stand up? *Nat. Rev. Neurosci.* **2012**, *13*, 507–514.
8. Compston, A. Genetic epidemiology of multiple sclerosis. *J. Neurol. Neurosurg. Psychiatry* **1997**, *62*, 553–561.
9. Ota, K.; Matsui, M.; Milford, E.L.; Mackin, G.A.; Weiner, H.L.; Hafler, D.A. T-cell recognition of an immunodominant myelin basic protein epitope in multiple sclerosis. *Nature* **1990**, *346*, 183–187.

10. Frohman, E.M.; Racke, M.K.; Raine, C.S. Multiple sclerosis—the plaque and its pathogenesis. *N. Engl. J. Med.* **2006**, *354*, 942–955.
11. Ascherio, A.; Munger, K.L. Environmental risk factors for multiple sclerosis. Part I: The role of infection. *Ann. Neurol.* **2007**, *61*, 288–299.
12. Ascherio, A.; Munger, K.L. Environmental risk factors for multiple sclerosis. Part II: Noninfectious factors. *Ann. Neurol.* **2007**, *61*, 504–513.
13. Ebers, G.C. Environmental factors and multiple sclerosis. *Lancet Neurol.* **2008**, *7*, 268–277.
14. Palacios, N.; Alonso, A.; Bronnum-Hansen, H.; Ascherio, A. Smoking and increased risk of multiple sclerosis: Parallel trends in the sex ratio reinforce the evidence. *Ann. Epidemiol.* **2011**, *21*, 536–542.
15. Mohr, D.C.; Hart, S.L.; Julian, L.; Cox, D.; Pelletier, D. Association between stressful life events and exacerbation in multiple sclerosis: A meta-analysis. *BMJ* **2004**, *328*, doi:10.1136/bmj.38041.724421.55.
16. Harkiolaki, M.; Holmes, S.L.; Svendsen, P.; Gregersen, J.W.; Jensen, L.T.; McMahon, R.; Friese, M.A.; van Boxel, G.; Etzensperger, R.; Tzartos, J.S.; *et al.* T cell-mediated autoimmune disease due to low-affinity crossreactivity to common microbial peptides. *Immunity* **2009**, *30*, 348–357.
17. Levin, L.I.; Munger, K.L.; Rubertone, M.V.; Peck, C.A.; Lennette, E.T.; Spiegelman, D.; Ascherio, A. Multiple sclerosis and Epstein-Barr virus. *JAMA* **2003**, *289*, 1533–1536.
18. DeLorenze, G.N.; Munger, K.L.; Lennette, E.T.; Orentreich, N.; Vogelman, J.H.; Ascherio, A. Epstein-Barr virus and multiple sclerosis: Evidence of association from a prospective study with long-term follow-up. *Arch. Neurol.* **2006**, *63*, 839–844.
19. Haahr, S.; Hollsberg, P. Multiple sclerosis is linked to Epstein-Barr virus infection. *Rev. Med. Virol.* **2006**, *16*, 297–310.
20. Christensen, T. HERVs in neuropathogenesis. *J. Neuroimmune Pharmacol.* **2010**, *5*, 326–335.
21. Sharma, P.; Azebi, S.; England, P.; Christensen, T.; Moller-Larsen, A.; Petersen, T.; Batsche, E.; Muchardt, C. Citrullination of Histone H3 Interferes with HP1-Mediated Transcriptional Repression. *PLoS Genet.* **2012**, *8*, e1002934.
22. Harauz, G.; Ishiyama, N.; Hill, C.M.; Bates, I.R.; Libich, D.S.; Fares, C. Myelin basic protein-diverse conformational states of an intrinsically unstructured protein and its roles in myelin assembly and multiple sclerosis. *Micron* **2004**, *35*, 503–542.
23. Harauz, G.; Musse, A.A. A tale of two citrullines—structural and functional aspects of myelin basic protein deimination in health and disease. *Neurochem. Res.* **2007**, *32*, 137–158.
24. Musse, A.A.; Harauz, G. Molecular “negativity” may underlie multiple sclerosis: Role of the myelin basic protein family in the pathogenesis of MS. *Int. Rev. Neurobiol.* **2007**, *79*, 149–172.
25. Carrillo-Vico, A.; Leech, M.D.; Anderton, S.M. Contribution of myelin autoantigen citrullination to T cell autoaggression in the central nervous system. *J. Immunol.* **2010**, *184*, 2839–2846.
26. Sawcer, S.; Hellenthal, G.; Pirinen, M.; Spencer, C.C.; Patsopoulos, N.A.; Moutsianas, L.; Dilthey, A.; Su, Z.; Freeman, C.; Hunt, S.E.; *et al.* Genetic risk and a primary role for cell-mediated immune mechanisms in multiple sclerosis. *Nature* **2011**, *476*, 214–219.
27. Jersild, C.; Svejgaard, A.; Fog, T. HL-A antigens and multiple sclerosis. *Lancet* **1972**, *1*, 1240–1241.

28. Naito, S.; Namerow, N.; Mickey, M.R.; Terasaki, P.I. Multiple sclerosis: Association with HL-A3. *Tissue Antigen.* **1972**, *2*, 1–4.
29. Ramagopalan, S.V.; Maugeri, N.J.; Handunnetthi, L.; Lincoln, M.R.; Orton, S.M.; Dyment, D.A.; Deluca, G.C.; Herrera, B.M.; Chao, M.J.; Sadovnick, A.D.; *et al.* Expression of the multiple sclerosis-associated MHC class II Allele HLA-DRB1*1501 is regulated by vitamin D. *PLoS Genet.* **2009**, *5*, e1000369.
30. Friese, M.A.; Jakobsen, K.B.; Friis, L.; Etzensperger, R.; Craner, M.J.; McMahon, R.M.; Jensen, L.T.; Huygelen, V.; Jones, E.Y.; Bell, J.I.; *et al.* Opposing effects of HLA class I molecules in tuning autoreactive CD8+ T cells in multiple sclerosis. *Nat. Med.* **2008**, *14*, 1227–1235.
31. Madsen, L.S.; Andersson, E.C.; Jansson, L.; krogsgaard, M.; Andersen, C.B.; Engberg, J.; Strominger, J.L.; Svejgaard, A.; Hjorth, J.P.; Holmdahl, R.; *et al.* A humanized model for multiple sclerosis using HLA-DR2 and a human T-cell receptor. *Nat. Genet.* **1999**, *23*, 343–347.
32. Lublin, F.D.; Reingold, S.C. Defining the clinical course of multiple sclerosis: Results of an international survey. National Multiple Sclerosis Society (USA) Advisory Committee on Clinical Trials of New Agents in Multiple Sclerosis. *Neurology* **1996**, *46*, 907–911.
33. Miller, D.; Barkhof, F.; Montalban, X.; Thompson, A.; Filippi, M. Clinically isolated syndromes suggestive of multiple sclerosis, part 2: Non-conventional MRI, recovery processes, and management. *Lancet Neurol.* **2005**, *4*, 341–348.
34. Miller, D.H. Biomarkers and surrogate outcomes in neurodegenerative disease: Lessons from multiple sclerosis. *NeuroRx* **2004**, *1*, 284–294.
35. Flachenecker, P.; Hartung, H.P. Course of illness and prognosis of multiple sclerosis. 1: The natural illness course. *Nervenarzt* **1996**, *67*, 435–443.
36. Moura, A.L.; Teixeira, R.A.; Oiwa, N.N.; Costa, M.F.; Feitosa-Santana, C.; Callegaro, D.; Hamer, R.D.; Ventura, D.F. Chromatic discrimination losses in multiple sclerosis patients with and without optic neuritis using the Cambridge Colour Test. *Vis. Neurosci.* **2008**, *25*, 463–468.
37. Patterson, V.H.; Heron, J.R. Visual field abnormalities in multiple sclerosis. *J. Neurol. Neurosurg. Psychiatry* **1980**, *43*, 205–209.
38. Leray, E.; Yaouanq, J.; le Page, E.; Coustans, M.; Laplaud, D.; Oger, J.; Edan, G. Evidence for a two-stage disability progression in multiple sclerosis. *Brain* **2010**, *133*, 1900–1913.
39. Bronnum-Hansen, H.; Koch-Henriksen, N.; Stenager, E. Trends in survival and cause of death in Danish patients with multiple sclerosis. *Brain* **2004**, *127*, 844–850.
40. Weinshenker, B.G. Natural history of multiple sclerosis. *Ann. Neurol.* **1994**, *36*, S6–S11.
41. Beiske, A.G.; Pedersen, E.D.; Czujko, B.; Myhr, K.M. Pain and sensory complaints in multiple sclerosis. *Eur. J. Neurol.* **2004**, *11*, 479–482.
42. Feinstein, A. Multiple sclerosis and depression. *Mult. Scler.* **2011**, *17*, 1276–1281.
43. Andersson, M.; Alvarez-Cermeno, J.; Bernardi, G.; Cogato, I.; Fredman, P.; Frederiksen, J.; Fredrikson, S.; Gallo, P.; Grimaldi, L.M.; Gronning, M.; *et al.* Cerebrospinal fluid in the diagnosis of multiple sclerosis: A consensus report. *J. Neurol. Neurosurg. Psychiatry* **1994**, *57*, 897–902.
44. Polman, C.H.; Reingold, S.C.; Edan, G.; Filippi, M.; Hartung, H.P.; Kappos, L.; Lublin, F.D.; Metz, L.M.; McFarland, H.F.; O'Connor, P.W.; *et al.* Diagnostic criteria for multiple sclerosis: 2005 revisions to the "McDonald Criteria". *Ann. Neurol.* **2005**, *58*, 840–846.

45. McDonald, W.I.; Compston, A.; Edan, G.; Goodkin, D.; Hartung, H.P.; Lublin, F.D.; McFarland, H.F.; Paty, D.W.; Polman, C.H.; Reingold, S.C.; *et al.* Recommended diagnostic criteria for multiple sclerosis: Guidelines from the International Panel on the diagnosis of multiple sclerosis. *Ann. Neurol.* **2001**, *50*, 121–127.
46. Whiting, P.; Harbord, R.; Main, C.; Deeks, J.J.; Filippini, G.; Egger, M.; Sterne, J.A. Accuracy of magnetic resonance imaging for the diagnosis of multiple sclerosis: systematic review. *BMJ* **2006**, *332*, 875–884.
47. Miller, D.M.; Weinstock-Guttman, B.; Bethoux, F.; Lee, J.C.; Beck, G.; Block, V.; Durelli, L.; LaMantia, L.; Barnes, D.; Sellebjerg, F.; *et al.* A meta-analysis of methylprednisolone in recovery from multiple sclerosis exacerbations. *Mult. Scler.* **2000**, *6*, 267–273.
48. Martinelli Boneschi, F.; Rovaris, M.; Capra, R.; Comi, G. Mitoxantrone for multiple sclerosis. *Cochrane Database Syst. Rev.* **2005**, doi:10.1002/14651858.CD002127.pub2.
49. Swinburn, W.R.; Liversedge, L.A. Long-term treatment of multiple sclerosis with azathioprine. *J. Neurol. Neurosurg. Psychiatry* **1973**, *36*, 124–126.
50. Casetta, I.; Iuliano, G.; Filippini, G. Azathioprine for multiple sclerosis. *J. Neurol. Neurosurg. Psychiatry* **2009**, *80*, 131–132.
51. Lugaresi, A.; Caporale, C.; Farina, D.; Marzoli, F.; Bonanni, L.; Muraro, P.A.; de Luca, G.; Iarlori, C.; Gambi, D. Low-dose oral methotrexate treatment in chronic progressive multiple sclerosis. *Neurol. Sci.* **2001**, *22*, 209–210.
52. Goodkin, D.E.; Rudick, R.A.; VanderBrug Medendorp, S.; Greene, T.; Schwetz, K.M.; Fischer, J.; Daughtry, M.M.; Ross, J.; Van Dyke, C. Low-dose (7.5 mg) oral methotrexate for chronic progressive multiple sclerosis. Design of a randomized, placebo-controlled trial with sample size benefits from a composite outcome variable including preliminary data on toxicity. *Online J. Curr. Clin. Trials* **1992**, *19*, PMID:1343611.
53. Weitz-Schmidt, G.; Welzenbach, K.; Brinkmann, V.; Kamata, T.; Kallen, J.; Bruns, C.; Cottens, S.; Takada, Y.; Hommel, U. Statins selectively inhibit leukocyte function antigen-1 by binding to a novel regulatory integrin site. *Nat. Med.* **2001**, *7*, 687–692.
54. Kallen, J.; Welzenbach, K.; Ramage, P.; Geyl, D.; Kriwacki, R.; Legge, G.; Cottens, S.; Weitz-Schmidt, G.; Hommel, U. Structural basis for LFA-1 inhibition upon lovastatin binding to the CD11a I-domain. *J. Mol. Biol.* **1999**, *292*, 1–9.
55. Katznelson, S.; Kobashigawa, J.A. Dual roles of HMG-CoA reductase inhibitors in solid organ transplantation: lipid lowering and immunosuppression. *Kidney Int. Suppl.* **1995**, *52*, S112–S115.
56. Wang, J.; Xiao, Y.; Luo, M.; Luo, H. Statins for multiple sclerosis. *Cochrane Database Syst. Rev.* **2011**, *12*, CD008386.
57. Cortese, I.; Chaudhry, V.; So, Y.T.; Cantor, F.; Cornblath, D.R.; Rae-Grant, A. Evidence-based guideline update: Plasmapheresis in neurologic disorders: report of the Therapeutics and Technology Assessment Subcommittee of the American Academy of Neurology. *Neurology* **2011**, *76*, 294–300.
58. Achiron, A.; Kishner, I.; Sarova-Pinhas, I.; Raz, H.; Faibel, M.; Stern, Y.; Lavie, M.; Gurevich, M.; Dolev, M.; Magalashvili, D.; *et al.* Intravenous immunoglobulin treatment following the first demyelinating event suggestive of multiple sclerosis: A randomized, double-blind, placebo-controlled trial. *Arch. Neurol.* **2004**, *61*, 1515–1520.

59. Bohn, A.B.; Nederby, L.; Harbo, T.; Skovbo, A.; Vorup-Jensen, T.; Krog, J.; Jakobsen, J.; Hokland, M.E. The effect of IgG levels on the number of natural killer cells and their Fc receptors in chronic inflammatory demyelinating polyradiculoneuropathy. *Eur. J. Neurol.* **2011**, *18*, 919–924.
60. Kappos, L.; European Study Group on interferon beta-1b in secondary progressive MS. Placebo-controlled multicentre randomised trial of interferon beta-1b in treatment of secondary progressive multiple sclerosis. *Lancet* **1998**, *352*, 1491–1497.
61. Jacobs, L.D.; Beck, R.W.; Simon, J.H.; Kinkel, R.P.; Brownscheidle, C.M.; Murray, T.J.; Simonian, N.A.; Slasor, P.J.; Sandrock, A.W.; CHAMPS Study Group.Intramuscular interferon beta-1a therapy initiated during a first demyelinating event in multiple sclerosis. *N. Engl. J. Med.* **2000**, *343*, 898–904.
62. Comi, G.; Filippi, M.; Barkhof, F.; Durelli, L.; Edan, G.; Fernandez, O.; Hartung, H.; Seeldrayers, P.; Sorensen, P.S.; Rovaris, M.; *et al.* Effect of early interferon treatment on conversion to definite multiple sclerosis: A randomised study. *Lancet* **2001**, *357*, 1576–1582.
63. Yednock, T.A.; Cannon, C.; Fritz, L.C.; Sanchez-Madrid, F.; Steinman, L.; Karin, N. Prevention of experimental autoimmune encephalomyelitis by antibodies against alpha 4 beta 1 integrin. *Nature* **1992**, *356*, 63–66.
64. Steinman, L.; Zamvil, S.S. Virtues and pitfalls of EAE for the development of therapies for multiple sclerosis. *Trends Immunol.* **2005**, *26*, 565–571.
65. Polman, C.H.; O'Connor, P.W.; Havrdova, E.; Hutchinson, M.; Kappos, L.; Miller, D.H.; Phillips, J.T.; Lublin, F.D.; Giovannoni, G.; Wajgt, A.; *et al.* A randomized, placebo-controlled trial of natalizumab for relapsing multiple sclerosis. *N. Engl. J. Med.* **2006**, *354*, 899–910.
66. Miller, D.H.; Soon, D.; Fernando, K.T.; MacManus, D.G.; Barker, G.J.; Yousry, T.A.; Fisher, E.; O'Connor, P.W.; Phillips, J.T.; Polman, C.H.; *et al.* MRI outcomes in a placebo-controlled trial of natalizumab in relapsing MS. *Neurology* **2007**, *68*, 1390–1401.
67. Sorensen, P.S.; Ross, C.; Clemmesen, K.M.; Bendtzen, K.; Frederiksen, J.L.; Jensen, K.; Kristensen, O.; Petersen, T.; Rasmussen, S.; Ravnborg, M.; *et al.* Clinical importance of neutralising antibodies against interferon beta in patients with relapsing-remitting multiple sclerosis. *Lancet* **2003**, *362*, 1184–1191.
68. Calabresi, P.A.; Giovannoni, G.; Confavreux, C.; Galetta, S.L.; Havrdova, E.; Hutchinson, M.; Kappos, L.; Miller, D.H.; O'Connor, P.W.; Phillips, J.T.; *et al.* The incidence and significance of anti-natalizumab antibodies: Results from AFFIRM and SENTINEL. *Neurology* **2007**, *69*, 1391–1403.
69. Bloomgren, G.; Richman, S.; Hotermans, C.; Subramanyam, M.; Goelz, S.; Natarajan, A.; Lee, S.; Plavina, T.; Scanlon, J.V.; Sandrock, A.; *et al.* Risk of natalizumab-associated progressive multifocal leukoencephalopathy. *N. Engl. J. Med.* **2012**, *366*, 1870–1880.
70. Tavazzi, E.; Ferrante, P.; Khalili, K. Progressive multifocal leukoencephalopathy: An unexpected complication of modern therapeutic monoclonal antibody therapies. *Clin. Microbiol. Infect.* **2011**, *17*, 1776–1780.
71. Vorup-Jensen, T. On the roles of polyvalent binding in immune recognition: Perspectives in the nanoscience of immunology and the immune response to nanomedicines. *Adv. Drug Deliv. Rev.* **2012**, in press.

72. Krumbholz, M.; Derfuss, T.; Hohlfeld, R.; Meinl, E. B cells and antibodies in multiple sclerosis pathogenesis and therapy. *Nat. Rev. Neurol.* **2012**, doi:10.1038/nrneurol.2012.203.
73. Bornstein, M.B.; Miller, A.; Slagle, S.; Weitzman, M.; Crystal, H.; Drexler, E.; Keilson, M.; Merriam, A.; Wassertheil-Smoller, S.; Spada, V.; *et al.* A pilot trial of Cop 1 in exacerbating-remitting multiple sclerosis. *N. Engl. J. Med.* **1987**, *317*, 408–414.
74. Miller, A.; Spada, V.; Beerkircher, D.; Kreitman, R.R. Long-term (up to 22 years), open-label, compassionate-use study of glatiramer acetate in relapsing-remitting multiple sclerosis. *Mult. Scler.* **2008**, *14*, 494–499.
75. Ford, C.; Goodman, A.D.; Johnson, K.; Kachuck, N.; Lindsey, J.W.; Lisak, R.; Luzzio, C.; Myers, L.; Panitch, H.; Preiningerova, J.; *et al.* Continuous long-term immunomodulatory therapy in relapsing multiple sclerosis: Results from the 15-year analysis of the US prospective open-label study of glatiramer acetate. *Mult. Scler.* **2010**, *16*, 342–350.
76. Ford, C.C.; Johnson, K.P.; Lisak, R.P.; Panitch, H.S.; Shifronis, G.; Wolinsky, J.S. A prospective open-label study of glatiramer acetate: Over a decade of continuous use in multiple sclerosis patients. *Mult. Scler.* **2006**, *12*, 309–320.
77. Comi, G.; Filippi, M.; Wolinsky, J.S. European/Canadian multicenter, double-blind, randomized, placebo-controlled study of the effects of glatiramer acetate on magnetic resonance imaging—measured disease activity and burden in patients with relapsing multiple sclerosis. European/Canadian Glatiramer Acetate Study Group. *Ann. Neurol.* **2001**, *49*, 290–297.
78. Johnson, K.P.; Brooks, B.R.; Cohen, J.A.; Ford, C.C.; Goldstein, J.; Lisak, R.P.; Myers, L.W.; Panitch, H.S.; Rose, J.W.; Schiffer, R.B.; The Copolymer 1 Multiple Sclerosis Study Group. Copolymer 1 reduces relapse rate and improves disability in relapsing-remitting multiple sclerosis: Results of a phase III multicenter, double-blind placebo-controlled trial. *Neurology* **1995**, *45*, 1268–1276.
79. Martinelli Boneschi, F.; Rovaris, M.; Johnson, K.P.; Miller, A.; Wolinsky, J.S.; Ladkani, D.; Shifroni, G.; Comi, G.; Filippi, M. Effects of glatiramer acetate on relapse rate and accumulated disability in multiple sclerosis: Meta-analysis of three double-blind, randomized, placebo-controlled clinical trials. *Mult. Scler.* **2003**, *9*, 349–355.
80. La Mantia, L.; Munari, L.M.; Lovati, R. Glatiramer acetate for multiple sclerosis. *Cochrane Database Syst. Rev.* **2010**, doi:10.1002/14651858.CD004678.pub2.
81. Korczyn, A.D.; Nisipeanu, P. Safety profile of copolymer 1: Analysis of cumulative experience in the United States and Israel. *J. Neurol.* **1996**, *243*, S23–S26.
82. Copaxone 20mg/mL, Solution For Injection, Pre-Filled Syringe. Available online: http://www.medicines.org.uk/emc/medicine/17516/SPC (accessed on 5 November 2012).
83. Johnson, K.P.; Brooks, B.R.; Ford, C.C.; Goodman, A.; Guarnaccia, J.; Lisak, R.P.; Myers, L.W.; Panitch, H.S.; Pruitt, A.; Rose, J.W.; *et al.* Sustained clinical benefits of glatiramer acetate in relapsing multiple sclerosis patients observed for 6 years. Copolymer 1 Multiple Sclerosis Study Group. *Mult. Scler.* **2000**, *6*, 255–266.
84. Sellebjerg, F.; Hedegaard, C.J.; Krakauer, M.; Hesse, D.; Lund, H.; Nielsen, C.H.; Sondergaard, H.B.; Sorensen, P.S. Glatiramer acetate antibodies, gene expression and disease activity in multiple sclerosis. *Mult. Scler.* **2012**, *18*, 305–313.

85. Sela, M. Poly(α-amino acids)—From a better understanding of immune phenomena to a drug against multiple sclerosis. *Acta Polym.* **1998**, *49*, 523–525.
86. Arnon, R.; Sela, M. Immunomodulation by the copolymer glatiramer acetate. *J. Mol. Recognit.* **2003**, *16*, 412–421.
87. Arnon, R.; Sela, M. The chemistry of the Copaxone drug. *Chem. Isr.* **1999**, *1*, 12–17.
88. Katchalski-Katzir, E. My contributions to science and society. *J. Biol. Chem.* **2005**, *280*, 16529–16541.
89. Eisenbach, M. Ephraim Katchalski-Katzir (1916–2009). *Trends Biochem. Sci.* **2009**, *34*, 427–428.
90. Katchalski, E.; Grossfeld, I.; Frankel, M. Poly-lysine. *J. Am. Chem. Soc.* **1947**, *69*, 2564.
91. Katchalski, E.; Sela, M. Synthesis and chemical properties of poly-alpha-amino acids. *Adv. Protein Chem.* **1958**, *13*, 243–492.
92. Pauling, L.; Corey, R.B.; Branson, H.R. The structure of proteins; two hydrogen-bonded helical configurations of the polypeptide chain. *Proc. Natl. Acad. Sci. USA* **1951**, *37*, 205–211.
93. Perutz, M.F. New X-ray evidence on the configuration of polypeptide chains. *Nature* **1951**, *167*, 1053–1054.
94. Rich, A.; Crick, F.H. The structure of collagen. *Nature* **1955**, *176*, 915–916.
95. Engel, J.; Kurtz, J.; Katchalski, E.; Berger, A. Polymers tripeptides as collagen models. II. Conformational changes of poly(L-prolyl-glycyl-L-prolyl) in solution. *J. Mol. Biol.* **1966**, *17*, 255–272.
96. Levin, Y.; Berger, A.; Katchalski, E. Hydrolysis and transpeptidation of lysine peptides by trypsin. *Biochem. J.* **1956**, *63*, 308–316.
97. Arnon, R.; Sela, M. Studies on the chemical basis of the antigenicity of proteins. 2. Antigenic specificity of polytyrosyl gelatins. *Biochem. J.* **1960**, *75*, 103–109.
98. Sela, M.; Arnon, R. Studies on the chemical basis of the antigenicity of proteins. 1. Antigenicity of polypeptidyl gelatins. *Biochem. J.* **1960**, *75*, 91–102.
99. Sela, M.; Arnon, R. Studies on the chemical basis of the antigenicity of proteins. 3. The role of rigidity in the antigenicity of polypeptidyl gelatins. *Biochem. J.* **1960**, *77*, 394–399.
100. Arnon, R.; Maron, E.; Sela, M.; Anfinsen, C.B. Antibodies reactive with native lysozyme elicited by a completely synthetic antigen. *Proc. Natl. Acad. Sci. USA* **1971**, *68*, 1450–1455.
101. Shaw, C.M.; Alvord, E.C., Jr.; Fahlberg, W.J.; Kies, M.W. Specificity of encephalitogen-induced inhibition of experimental "allergic" encephalomyelitis in the guinea pig. *J. Immunol.* **1962**, *89*, 54–61.
102. Teitelbaum, D.; Meshorer, A.; Hirshfeld, T.; Arnon, R.; Sela, M. Suppression of experimental allergic encephalomyelitis by a synthetic polypeptide. *Eur. J. Immunol.* **1971**, *1*, 242–248.
103. Teitelbaum, D.; Gan, R.; Meshorer, A.; Hirsfeld, T.; Arnon, R.; Sela, M. Therapeutic Copolymer. U.S. Patent 3,849,550, March 1971.
104. Katchalski-Katzir, E. Synthesis, physicochemical and biological properties of poly-alpha-amino acids--the simplest of protein models. *Acta Biochim. Polon.* **1996**, *43*, 217–226.
105. Fridkis-Hareli, M.; Santambrogio, L.; Stern, J.N.; Fugger, L.; Brosnan, C.; Strominger, J.L. Novel synthetic amino acid copolymers that inhibit autoantigen-specific T cell responses and suppress experimental autoimmune encephalomyelitis. *J. Clin. Invest.* **2002**, *109*, 1635–1643.

106. Capila, I.; Linhardt, R.J. Heparin-protein interactions. *Angew. Chem. Int. Ed. Engl.* **2002**, *41*, 391–412.
107. Venkataraman, G.; Shriver, Z.; Raman, R.; Sasisekharan, R. Sequencing complex polysaccharides. *Science* **1999**, *286*, 537–542.
108. Berkowitz, S.A.; Engen, J.R.; Mazzeo, J.R.; Jones, G.B. Analytical tools for characterizing biopharmaceuticals and the implications for biosimilars. *Nat. Rev. Drug Discov.* **2012**, *11*, 527–540.
109. Guerrini, M.; Beccati, D.; Shriver, Z.; Naggi, A.; Viswanathan, K.; Bisio, A.; Capila, I.; Lansing, J.C.; Guglieri, S.; Fraser, B.; *et al.* Oversulfated chondroitin sulfate is a contaminant in heparin associated with adverse clinical events. *Nat. Biotechnol.* **2008**, *26*, 669–675.
110. Kishimoto, T.K.; Viswanathan, K.; Ganguly, T.; Elankumaran, S.; Smith, S.; Pelzer, K.; Lansing, J.C.; Sriranganathan, N.; Zhao, G.; Galcheva-Gargova, Z.; *et al.* Contaminated heparin associated with adverse clinical events and activation of the contact system. *N. Engl. J. Med.* **2008**, *358*, 2457–2467.
111. Liu, H.; Zhang, Z.; Linhardt, R.J. Lessons learned from the contamination of heparin. *Nat. Prod. Rep.* **2009**, *26*, 313–321.
112. Fridkis-Hareli, M.; Stern, J.N.; Fugger, L.; Strominger, J.L. Synthetic peptides that inhibit binding of the myelin basic protein 85–99 epitope to multiple sclerosis-associated HLA-DR2 molecules and MBP-specific T-cell responses. *Human Immunol.* **2001**, *62*, 753–763.
113. Teitelbaum, D.; Aharoni, R.; Sela, M.; Arnon, R. Cross-reactions and specificities of monoclonal antibodies against myelin basic protein and against the synthetic copolymer 1. *Proc. Natl. Acad. Sci. USA* **1991**, *88*, 9528–9532.
114. Fridkis-Hareli, M.; Strominger, J.L. Promiscuous binding of synthetic copolymer 1 to purified HLA-DR molecules. *J. Immunol.* **1998**, *160*, 4386–4397.
115. Fridkis-Hareli, M.; Aharoni, R.; Teitelbaum, D.; Arnon, R.; Sela, M.; Strominger, J.L. Binding of random copolymers of three amino acids to class II MHC molecules. *Int. Immunol.* **1999**, *11*, 635–641.
116. Teitelbaum, D.; Fridkis-Hareli, M.; Arnon, R.; Sela, M. Copolymer 1 inhibits chronic relapsing experimental allergic encephalomyelitis induced by proteolipid protein (PLP) peptides in mice and interferes with PLP-specific T cell responses. *J. Neuroimmunol.* **1996**, *64*, 209–217.
117. Ben-Nun, A.; Mendel, I.; Bakimer, R.; Fridkis-Hareli, M.; Teitelbaum, D.; Arnon, R.; Sela, M.; de Rosbo, N.K. The autoimmune reactivity to myelin oligodendrocyte glycoprotein (MOG) in multiple sclerosis is potentially pathogenic: effect of copolymer 1 on MOG-induced disease. *J. Neurol.* **1996**, *243*, S14–S22.
118. Ibarra, A.; Avendano, H.; Cruz, Y. Copolymer-1 (Cop-1) improves neurological recovery after middle cerebral artery occlusion in rats. *Neurosci. Lett.* **2007**, *425*, 110–113.
119. Aharoni, R.; Teitelbaum, D.; Arnon, R.; Sela, M. Copolymer 1 inhibits manifestations of graft rejection. *Transplantation* **2001**, *72*, 598–605.
120. Duda, P.W.; Schmied, M.C.; Cook, S.L.; Krieger, J.I.; Hafler, D.A. Glatiramer acetate (Copaxone) induces degenerate, Th2-polarized immune responses in patients with multiple sclerosis. *J. Clin. Invest.* **2000**, *105*, 967–976.

121. Berthelot, L.; Miqueu, P.; Pettre, S.; Guillet, M.; Moynard, J.; Wiertlewski, S.; Lefrere, F.; Brouard, S.; Soulillou, J.P.; Laplaud, D.A. Failure of glatiramer acetate to modify the peripheral T cell repertoire of relapsing-remitting multiple sclerosis patients. *Clin. Immunol.* **2010**, *135*, 33–42.
122. Aharoni, R.; Teitelbaum, D.; Sela, M.; Arnon, R. Copolymer 1 induces T cells of the T helper type 2 that crossreact with myelin basic protein and suppress experimental autoimmune encephalomyelitis. *Proc. Natl. Acad. Sci. USA* **1997**, *94*, 10821–10826.
123. Kala, M.; Rhodes, S.N.; Piao, W.H.; Shi, F.D.; Campagnolo, D.I.; Vollmer, T.L. B cells from glatiramer acetate-treated mice suppress experimental autoimmune encephalomyelitis. *Exp. Neurol.* **2010**, *221*, 136–145.
124. Racke, M.K.; Lovett-Racke, A.E. Glatiramer acetate treatment of multiple sclerosis: an immunological perspective. *J. Immunol.* **2011**, *186*, 1887–1890.
125. Neuhaus, O.; Farina, C.; Yassouridis, A.; Wiendl, H.; Then Bergh, F.; Dose, T.; Wekerle, H.; Hohlfeld, R. Multiple sclerosis: Comparison of copolymer-1- reactive T cell lines from treated and untreated subjects reveals cytokine shift from T helper 1 to T helper 2 cells. *Proc. Natl. Acad. Sci. USA* **2000**, *97*, 7452–7457.
126. Krogsgaard, M.; Wucherpfennig, K.W.; Cannella, B.; Hansen, B.E.; Svejgaard, A.; Pyrdol, J.; Ditzel, H.; Raine, C.; Engberg, J.; Fugger, L. Visualization of myelin basic protein (MBP) T cell epitopes in multiple sclerosis lesions using a monoclonal antibody specific for the human histocompatibility leukocyte antigen (HLA)-DR2-MBP 85–99 complex. *J. Exp. Med.* **2000**, *191*, 1395–1412.
127. Aharoni, R.; Teitelbaum, D.; Sela, M.; Arnon, R. Bystander suppression of experimental autoimmune encephalomyelitis by T cell lines and clones of the Th2 type induced by copolymer 1. *J. Neuroimmunol.* **1998**, *91*, 135–146.
128. Jee, Y.; Liu, R.; Bai, X.F.; Campagnolo, D.I.; Shi, F.D.; Vollmer, T.L. Do Th2 cells mediate the effects of glatiramer acetate in experimental autoimmune encephalomyelitis? *Int. Immunol.* **2006**, *18*, 537–544.
129. Kipnis, J.; Yoles, E.; Porat, Z.; Cohen, A.; Mor, F.; Sela, M.; Cohen, I.R.; Schwartz, M. T cell immunity to copolymer 1 confers neuroprotection on the damaged optic nerve: possible therapy for optic neuropathies. *Proc. Natl. Acad. Sci. USA* **2000**, *97*, 7446–7451.
130. Stapulionis, R.; Oliveira, C.L.P.; Gjelstrup, M.C.; Pedersen, J.S.; Hokland, M.E.; Hoffmann, S.V.; Poulsen, K.; Jacobsen, C.; Vorup-Jensen, T. Structural insight into the function of myelin basic protein as a ligand for integrin alpha(M)beta(2). *J. Immunol.* **2008**, *180*, 3946–3956.
131. Rathinam, V.A.; Vanaja, S.K.; Fitzgerald, K.A. Regulation of inflammasome signaling. *Nat. Immunol.* **2012**, *13*, doi:10.1038/ni.2237.
132. Gordon, S. Pattern recognition receptors: doubling up for the innate immune response. *Cell* **2002**, *111*, 927–930.
133. Hynes, R.O. Integrins: bidirectional, allosteric signaling machines. *Cell* **2002**, *110*, 673–687.
134. Springer, T.A. Adhesion receptors of the immune system. *Nature* **1990**, *346*, 425–434.
135. Luo, B.H.; Carman, C.V.; Springer, T.A. Structural basis of integrin regulation and signaling. *Annu. Rev. Immunol.* **2007**, *25*, 619–647.

136. Gomez, I.G.; Tang, J.; Wilson, C.L.; Yan, W.; Heinecke, J.W.; Harlan, J.M.; Raines, E.W. Metalloproteinase-mediated Shedding of Integrin beta2 promotes macrophage efflux from inflammatory sites. *J. Biol. Chem.* **2012**, *287*, 4581–4589.
137. Gjelstrup, L.C.; Boesen, T.; Kragstrup, T.W.; Jorgensen, A.; Klein, N.J.; Thiel, S.; Deleuran, B.W.; Vorup-Jensen, T. Shedding of large functionally active CD11/CD18 Integrin complexes from leukocyte membranes during synovial inflammation distinguishes three types of arthritis through differential epitope exposure. *J. Immunol.* **2010**, *185*, 4154–4168.
138. Vorup-Jensen, T.; Carman, C.V.; Shimaoka, M.; Schuck, P.; Svitel, J.; Springer, T.A. Exposure of acidic residues as a danger signal for recognition of fibrinogen and other macromolecules by integrin alphaXbeta2. *Proc. Natl. Acad. Sci. USA* **2005**, *102*, 1614–1619.
139. Vorup-Jensen, T.; Chi, L.; Gjelstrup, L.C.; Jensen, U.B.; Jewett, C.A.; Xie, C.; Shimaoka, M.; Linhardt, R.J.; Springer, T.A. Binding between the integrin alphaXbeta2 (CD11c/CD18) and heparin. *J. Biol. Chem.* **2007**, *282*, 30869–30877.
140. Davis, G.E. The Mac-1 and p150,95 beta 2 integrins bind denatured proteins to mediate leukocyte cell-substrate adhesion. *Exp. Cell. Res.* **1992**, *200*, 242–252.
141. Whitaker, J.N. Myelin basic protein in cerebrospinal fluid and other body fluids. *Mult. Scler.* **1998**, *4*, 16–21.
142. Constantinescu, R.; Zetterberg, H.; Holmberg, B.; Rosengren, L. Levels of brain related proteins in cerebrospinal fluid: an aid in the differential diagnosis of parkinsonian disorders. *Parkinsonism Relat. Disord.* **2009**, *15*, 205–212.
143. Prineas, J.W.; Graham, J.S. Multiple sclerosis: Capping of surface immunoglobulin G on macrophages engaged in myelin breakdown. *Ann. Neurol.* **1981**, *10*, 149–158.
144. Epstein, L.G.; Prineas, J.W.; Raine, C.S. Attachment of myelin to coated pits on macrophages in experimental allergic encephalomyelitis. *J. Neurol. Sci.* **1983**, *61*, 341–348.
145. Nielsen, H.H.; Ladeby, R.; Fenger, C.; Toft-Hansen, H.; Babcock, A.A.; Owens, T.; Finsen, B. Enhanced microglial clearance of myelin debris in T cell-infiltrated central nervous system. *J. Neuropathol. Exp. Neurol.* **2009**, *68*, 845–856.
146. Ransohoff, R.M.; Kivisakk, P.; Kidd, G. Three or more routes for leukocyte migration into the central nervous system. *Nat. Rev. Immunol.* **2003**, *3*, 569–581.
147. Lobel E.; Riven-Kreitman, R.; Amselem, A.; Pinchasi, I. Copolymer 1. *Drug Fut.* **1996**, *21*, 131–134.
148. Ziemssen, T.; Neuhaus, O.; Hohlfeld, R. Risk-benefit assessment of glatiramer acetate in multiple sclerosis. *Drug Saf.* **2001**, *24*, 979–990.
149. Weber, M.S.; Prod'homme, T.; Youssef, S.; Dunn, S.E.; Rundle, C.D.; Lee, L.; Patarroyo, J.C.; Stuve, O.; Sobel, R.A.; Steinman, L.; *et al.* Type II monocytes modulate T cell-mediated central nervous system autoimmune disease. *Nat. Med.* **2007**, *13*, 935–943.
150. Weber, M.S.; Starck, M.; Wagenpfeil, S.; Meinl, E.; Hohlfeld, R.; Farina, C. Multiple sclerosis: glatiramer acetate inhibits monocyte reactivity *in vitro* and *in vivo*. *Brain* **2004**, *127*, 1370–1378.
151. Clausen, J.; Matzke, J.; Gerhardt, W. Agar-Gel Micro-Electrophoresis of Proteins in the Cerebrospinal Fluid Normal and Pathological Findings. *Acta Neurol. Scand. Suppl.* **1964**, *40*, 49–56.

152. Borlongan, C.V.; Glover, L.E.; Sanberg, P.R.; Hess, D.C. Permeating the blood brain barrier and abrogating the inflammation in stroke: Implications for stroke therapy. *Curr. Pharm. Des.* **2012**, *18*, 3670–3676.
153. Toker, A.; Slaney, C.Y.; Backstrom, B.T.; Harper, J.L. Glatiramer acetate treatment directly targets CD11b(+)Ly6G(-) monocytes and enhances the suppression of autoreactive T cells in experimental autoimmune encephalomyelitis. *Scand. J. Immunol.* **2011**, *74*, 235–243.
154. Lamers, K.J.; Vos, P.; Verbeek, M.M.; Rosmalen, F.; van Geel, W.J.; van Engelen, B.G. Protein S-100B, neuron-specific enolase (NSE), myelin basic protein (MBP) and glial fibrillary acidic protein (GFAP) in cerebrospinal fluid (CSF) and blood of neurological patients. *Brain Res. Bull.* **2003**, *61*, 261–264.
155. Aharoni, R.; Kayhan, B.; Eilam, R.; Sela, M.; Arnon, R. Glatiramer acetate-specific T cells in the brain express T helper 2/3 cytokines and brain-derived neurotrophic factor *in situ*. *Proc. Natl. Acad. Sci. USA* **2003**, *100*, 14157–14162.
156. Ure, D.R.; Rodriguez, M. Polyreactive antibodies to glatiramer acetate promote myelin repair in murine model of demyelinating disease. *FASEB J.* **2002**, *16*, 1260–1262.

MCT Molecular and Cellular Therapies

REVIEW Open Access

Properties and prospects of adjuvants in influenza vaccination - messy precipitates or blessed opportunities?

Babak Jalilian[1†], Stig Hill Christiansen[1†], Halldór Bjarki Einarsson[1,2], Mehdi Rasoli Pirozyan[3], Eskild Petersen[2,4] and Thomas Vorup-Jensen[1*]

Abstract

Influenza is a major challenge to healthcare systems world-wide. While prophylactic vaccination is largely efficient, long-lasting immunity has not been achieved in immunized populations, at least in part due to the challenges arising from the antigen variation between strains of influenza A virus as a consequence of genetic drift and shift. From progress in our understanding of the immune system, the mode-of-action of vaccines can be divided into the stimulation of the adaptive system through inclusion of appropriate vaccine antigens and of the innate immune system by the addition of adjuvant to the vaccine formulation. A shared property of many vaccine adjuvants is found in their nature of water-insoluble precipitates, for instance the particulate material made from aluminum salts. Previously, it was thought that embedding of vaccine antigens in these materials provided a "depot" of antigens enabling a long exposure of the immune system to the antigen. However, more recent work points to a role of particulate adjuvants in stimulating cellular parts of the innate immune system. Here, we briefly outline the infectious medicine and immune biology of influenza virus infection and procedures to provide sufficient and stably available amounts of vaccine antigen. This is followed by presentation of the many roles of adjuvants, which involve humoral factors of innate immunity, notably complement. In a perspective of the ultrastructural properties of these humoral factors, it becomes possible to rationalize why these insoluble precipitates or emulsions are such a provocation of the immune system. We propose that the biophysics of particulate material may hold opportunities that could aid the development of more efficient influenza vaccines.

Keywords: Adjuvants, Influenza vaccination, Particle size

Introduction

Seasonal influenza is one of the most common infections in humans. In general, symptoms are mild. However, elderly people and patients with a compromised immune response, or an otherwise impaired health may ultimately succumb to severe complications of the infection. For this reason, there is an important and continuous need for vaccine development, and production. Influenza vaccines only provide strain specific protection. Because of antigenic drift, vaccines are tailored to the present circulating strains each year. A change of vaccines is also needed when antigenic shift occurs, and a new pandemic arise. With the challenges in production and distribution in mind, a pan-protective influenza vaccine providing long-term protection would be a huge step forward.

In this paper, we argue that one strategy to achieve this goal is through the use of better adjuvants, in particular these inducing an immune response mimicking the natural infection.

Several decades of research have unravelled the mechanisms of the immune system, which are important in protecting against influenza virus infection. It is now clear these mechanisms prominently involve contributions from both the innate and adaptive immune system. In

* Correspondence: vorup-jensen@microbiology.au.dk
†Equal contributors
[1]Biophysical Immunology Laboratory, Department of Biomedicine, Aarhus University, DK-8000 Aarhus, Denmark
Full list of author information is available at the end of the article

clinicallyused and experimental vaccines, there is considerable uniformity in the choice of antigenic components in influenza vaccines, and hence how to guide the adaptive immune response in fighting the virus. Some vaccines include adjuvants, which largely act by stimulating the innate immune system, thereby priming a stronger response by the adaptive immune system. Interestingly, the choices of adjuvants are chemically diverse, but often with a particulate nature, prompting C.A. Janeway (1943–2003) famously to refer to these as "messy precipitates" [1].

Here, we discuss current trends in the development of adjuvants for use with influenza vaccines. In "Introduction" section, a brief outline is presented on the clinical manifestations and viral biology of influenza virus together with mechanisms of the immune system limiting the infection. In "Adaptive immunity and formulation of antigenic components in influenza vaccines" section, some of the vaccine antigens used, and their route of administration are compared. Finally, "Innate immunity and immunogenic and physicochemical properties of adjuvants" section reviews the pharmacological mode-of-action of clinicallyused, and experimental adjuvants in influenza vaccines by elaborating on the potential for adjuvant particle-size-related immunomodulatory stimuli.

Clinical manifestations of influenza virus infections

Droplet transmission and physical contact with virus-contaminated surfaces seems to be the primary means of influenza virus dissemination prior to inoculation [2]. The incubation time is approximately 1 to 3 days [3]. Cardinal manifestations of disease are malaise and headache during the prodromal period. This is followed by a sore throat, due to laryngotracheobronchitis and hyperaemic, or erythematous oral and pharyngeal mucous membranes associated with catarrhalia, rapid increase in body temperature, non-productive cough, dedolation, chills, and myalgia. The severity of the symptoms depends on the degree of immunity raised by past infections. Pre-existing conditions disposing a more severe disease include pregnancy where seasonal influenza provokes a 3–4 fold increased risk of cardiopulmonary illness, notably in the third trimester [4]. Chronic lung diseases or affected respiratory function due to respiratory muscle atrophy, cardiovascular diseases, diabetes, chronic liver and kidney diseases [5], acquired immunodeficiency [6], or obesity [7] also predispose to an aggravated course of the infection. Children infected with influenza usually present the same symptomatology as in adults, however, frequently with higher body core temperature, croup, otitis media, bronchiolitis, abdominal pain, and vomiting. Furthermore, unlike in adults, influenza-associated mortality in children appears not to be associated with an underlying medical condition [8]. Persistent fever, *i.e.*, for longer than five days, may be a consequence of bacterial co-infections with *Streptococcus pneumonia*, *Haemophilus influenza* and *Staphylococcus aureus.* These pathogens cause sinuitis, otitis, bronchitis and/or pneumonitis. Co-infections with *Staphylococci* are fulminant and even lethal [9,10]. In more general, the bacterial pathogens may cause septic shock as well as exacerbate pulmonary and cardiac diseases [11-13].

Architecture and strain diversity of the influenza virus

Influenza viruses are the only members of the *Orthomyxoviridae* family. They are classified into three different *genera*, A, B and C, based on the expression of matrix (M_1) protein, membrane (M_2) protein and nucleoprotein (NP). *Orthomyxoviridae* viruses have several biological properties in common. However, they differ significantly in their host tropism [14]. Influenza viruses of *genera* B and C principally infect humans, although they occasionally have been isolated from seals and pigs [15,16]. Influenza A viruses, on the other hand, propagate in several animal hosts, including humans, pigs, horses, minks, and in domestic and wild birds. Waterfowls are the primary reservoirs, in which the virus is hosted in the intestine. Several species act as mixing vessel between humans and birds, primarily the pig, which express receptors for both human and avian viruses in their upper respiratory tract epithelial cells. In general, influenza A viruses are nonpathogenic in birds and are classified as either low or high pathogenic avian influenza viruses (LPAI or HPAI, respectively), depending on the morbidity and mortality upon transmission to other species, including humans [17].

Subtyping of influenza viruses is based on the antigenic properties of their surface hemagglutinin (HA) and neuraminidase (NA) glycoproteins. Currently, 17 different subtypes of HA have been identified, of which the most recent (H_{17}) was identified in fruit bats [18]. Nine different subtypes of NA are known. The influenza virion (Figure 1) contains a linear, negative sense, single-stranded RNA with 7 (C *genus*) or 8 (A and B *genera*) segments, each expressing one or two of the influenza virus proteins. The segmented genome of the influenza virus facilitates genomic changes by genetic drift and/or genetic shift. Genetic drift refers to minor changes due to mutation in the genes encoding HA or NA, altering viral antigenicity. Such alterations are sufficient to permit infections in individuals with immunity to similar viruses, and drift explains the regular outbreaks of seasonal influenza. Genetic shifts are major changes as a result of reassortment of genome segments from different human and/or animal strains producing anything from slightly to completely different influenza virus genomes. In this situation little pre-existing immunity to the virus can be found in human populations, potentially leading to severe pandemics. The latter process is restricted to virus of the A *genus* [14].

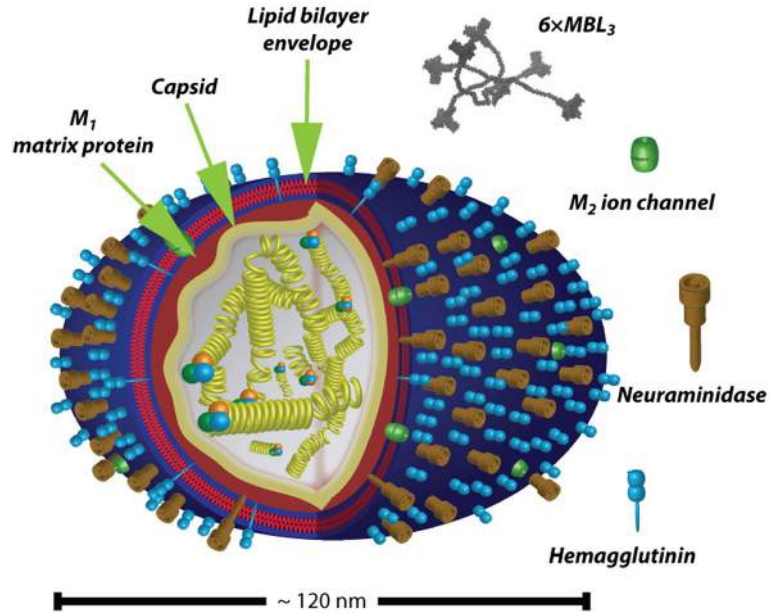

Figure 1 Architecture of the influenza virion. While the virus has often been depicted as spherical in microbiology textbooks [14], recent investigations suggest a far more pleiomorph appearance, only some particles being essentially spherical while others are tubular. The approximate length of the virion is 120 nm, possibly influenced by the organization of the RNA by the multiple ribonucleoprotein complexes [19] shown in the center of virion surrounded by the capsid and layer of matrix protein M_1. The relative abundance of the HA and NA proteins are indicated based on reports by Mitnaul *et al.* [20] and Zhang *et al.* [21] (components not to scale). Based on data from the report by Gjelstrup *et al.* [22], a 6×MBL_3 oligomer is drawn to scale relative to the size of the influenza virion.

Viral infectivity, treatment, and immunity to influenza

The requirements for influenza A virus infectivity are well studied. These viruses depend on sialic acid expression on the host tissue, which permits the attachment of the viral HA proteins. Human influenza virus mainly infects non-ciliated cells in the respiratory tract, while the avian virus infects ciliated cells [23], thereby reflecting the carbohydrate selectivity of HA. The avian viruses prefer attachment to galactose residues forming an α-(2,3)-glycosidic linkage to the sialic acid, while human viruses preferentially bind to galactose residues forming an α-(2,6)-linkage [24]. Pigs have both types of sialylations in their upper respiratory tract, while humans express α-(2,6)-galactose linked sialic acid in the upper respiratory tract and α(2,3)-galactose linked sialic acid in the lower respiratory tract [25]. NA activity is essential both to ensure the release of virus from infected cells, and to facilitate the development of the infection by providing access to the deeper layers of tissue, *i.e.* below the sialylated lung mucus [26].

Following infection with the influenza virus, inflammatory cells of the innate immune system accumulate in the mucosal membrane. The cellular response to infection involves hyperemia of the epithelium and necrosis in bronchiolar epithelial cells [27]. At least in part, this response is a consequence of the recruitment of neutrophil granulocytes to the site of inflammation and viral activation of epithelial cells [28]. The recruitment of granulocytes depends on the proteolytic cleavage of humoral factors of the innate immune system, particularly the group of plasma proteins constituting the complement system. Small fragments of these proteins, notably C5a, permeate the endothelium of adjoining blood vessels in the zone of inflammation and create a chemokine gradient guiding the granulocytes [29]. It is a classic finding that mannan-binding lectin (MBL, also known as mannose-binding lectin or mannan or mannose-binding protein, MBP), a complement-activating plasma protein, is significant in the protection against influenza infection in ferrets [30,31]. Evidence also suggests that MBL plays a similar role in infections in humans [32]. MBL recognizes a particular topological pattern of glycans on HA, thereby triggering complement activation through the lectin pathway [31,33,34]. Opsonization through the deposition of proteolytic fragments of complement component C3 allows neutrophil granulocytes and other myeloid cells to the viral particles through complement receptor (CR)3 (also known as integrin $\alpha_M\beta_2$, Mac-1, or CD11b/CD18) and CR4 (also known as integrin $\alpha_X\beta_2$, p150,95 or CD11c/CD18) [35]. Other pattern recognition molecules, such as Toll-like receptors (TLRs), recognize the single-stranded RNA transported into infected cells by the influenza virus [36], which alerts cellular parts of the immune system.

In addition to mediating direct clearance of influenza virus, the innate immune system is also important in priming a response by mechanisms of adaptive immunity. Dendritic cells (DC) transport viral antigens into the lymph nodes, where naïve T cells are converted into influenza antigen-reactive CD8+ cytotoxic T lymphocytes (CTL) or CD4+ T helper (Th) cells. T cell responses are critical for protection against influenza infection, as was established in a classic study on human volunteers infected with an unattenuated strain of influenza virus [37]. Perhaps surprisingly, a recent analysis showed that CD4+ T cells with an interferon-γ-producing Th1 phenotype, and only to a lesser extent CTLs, are particularly important in protection in humans [38]. Influenza vaccines are evaluated by their ability to react with antibodies [39]. While there is evidence that antibody titers to vaccine antigens correlate with vaccine efficacy [39], the recent identification of CD4+ Th1 cells as important in protection against influenza infection [38] could raise a question if antibody titers are a sufficiently comprehensive measure of vaccine-induced immunity to infection. At the very least, vaccine strategies permitting formation of such influenza virus antigen-reactive T cells should be carefully considered as discussed in "Adaptive immunity and formulation of antigenic components in influenza vaccines" section.

Mature naïve T cells are maturated inside the thymus. Thymic function declines, however, with age, due to a gradual replacement of thymopoietic tissue with adipose tissue [40-42]. Thus, it is not surprising that impaired formation of antigen-specific antibodies in the elderly was reported for influenza vaccination [42,43]. Although the total size of the peripheral lymphocyte pool is stable throughout life, the composition of both CD4+ and CD8+ T cells with regard to naïve and memory subpopulations changes with age [42,44]. A modest decline of naïve CD4+ lymphocytes is observed until the ages of 65–75, due to homeostatic control mechanisms, but subsequently the naïve CD4+ T cell reserve collapses [42,45]. Consistent with this, changes within the $CD4^+$ naïve and memory subsets have been shown to impair long-term $CD4^+$ T cell responses to influenza and hepatitis B vaccination [42,46,47]. These observations are particularly important in view of the essential role of these cells in protecting against the infection [38,42].

At the molecular level one of the most profound biological indicators of ageing in the human immune system is the progressive loss of expression of the co-stimulatory molecule CD28 on T cells that have undergone repeated antigen stimulations [42,48-50]. However, other mechanisms may be affected as well. In vaccinees younger than 35 years, expression of the adhesion molecule CD62L was observed to correlate with the ability to raise immunity to the hepatitis B virus following vaccination with hepatitis B surface antigen. The association between expression of the adhesion molecule CD62L (L-selectin) on $CD4^+$ naïve and central memory T cells and the formation of antigen-specific antibodies was not found for donors older than 55 years [47]. Age-related alterations in the vaccine responsiveness may consequently affect vaccinees far younger than previously thought [42,47]. Since the function of CD62L pertains to general functions of T cells, it is possible that the observations by Rosenberg *et al.* [42,47] pertain to a wider number of vaccinations than those protecting against hepatitis B virus, and this also includes influenza vaccinations.

Adaptive immunity and formulation of antigenic components in influenza vaccines

Advancements in understanding the etiology of infectious diseases and especially how antigen responses are formed through the adaptive immune system have provided means for novel ways of vaccine production and administration into the human body. The success of these accomplishments includes elimination of small pox as a human infection and efficient vaccines against other viruses providing life-long protection. Indeed, the concept of vaccination is no longer limited to prevention of infectious diseases, but is also used in modulating immune responses in autoimmune diseases [51]. With the live-attenuated small pox vaccine as an important example, vaccines broadly stimulating the immune system in a manner resembling the natural infection are far superior to most sub-component based, or otherwise engineered vaccines. By contrast, the prophylactic influenza vaccination has not achieved to induce long-lasting immunity in immunized populations [52]. To overcome this problem, the strategy has focused on challenging the adaptive immune response with influenza virus antigens tailored to the predicted upcoming seasonal or pandemic influenza virus, although the need for adequate supplies of vaccines and frequent vaccination hinder efforts to obtain sufficient protection. As an indication of load of vaccines supplied for single season, the United States of America federal Food and Drug Administration-recommended influenza vaccinations for the season 2013–2014 are listed in Table 1. It is tempting to suggest that inability to achieve long-lasting protection is in consequence of the wide use of inactivated or sub-component based formulations. However, the live-attenuated influenza vaccine FluMist (Table 1) also requires annual administration, suggesting that the biology of the virus is the real culprit in limiting vaccine efficiency. Below, we list major strategies for producing the antigenic component of influenza viruses.

Protein-based vaccines against influenza

Influenza vaccine antigens are commonly formulated either as whole inactivated virus or *in vitro*-expressed viral protein subcomponents [53].

Table 1 Influenza virus vaccines for the United States of America 2013–2014 season[a]

Seasonal influenza vaccines	Type/abbrev.	# Antigens	Route of administration	Manufacturer	Age range	Adjuvant
Afluria	Inactivated/IIV3[b]	Trivalent	Intramuscular	CSL Limited	5 ≥	None
FluLaval	Inactivated/IIV3[b]	Trivalent	Intramuscular	GlaxoSmithKline	18 ≥	None
Fluarix	Inactivated/IIV3[b]	Trivalent	Intramuscular	GlaxoSmithKline	3 ≥	None
	Inactivated/IIV4[b]	Quadrivalent	Intramuscular			None
Flublok	Recombinant/RIV3[c]	Trivalent	Intramuscular	Protein Sciences	18-49	None
Flucelvax	Cell Culture/ccIIV3[b]	Trivalent	Intramuscular	Novartis	18 ≥	None
FluMist	Live Attenuated/LAIV4[d]	Quadrivalent	Intranasal	Medimmune	2-49	None
Fluvirin	Inactivated	Trivalent	Intramuscular	Novartis	4 ≥	None
Fluzone	Inactivated/IIV3[b]	Trivalent	Intramuscular	Sanofi Pasteur	6 mo ≥[e]	None
	Inactivated/IIV4[b]	Quadrivalent	Intramuscular			None

[a]U.S. Food and Drug Administration recommends that the trivalent-formulation influenza vaccines for the U.S. 2013–2014 influenza season contain the following: (1) A/California/7/2009 (H1N1)-like virus, (2) (H3N2) virus antigenically like the cell-propagated prototype virus A/Victoria/361/2011, and (3) B/Massachusetts/2/2012-like virus. For the quadrivalent-formulation influenza vaccines for the U.S. 2013–2014 influenza season contain the above three strains and the following additional B strain: (4) B/Brisbane/60/2008-like virus. [b]IIV refers to inactivated vaccines (egg and cell-culture based). Includes trivalent (IIV3) and quadrivalent (IIV4). [c]RIV refers to recombinant HA influenza vaccine. Trivalent (RIV3). [d]LAIV refers to Live Attenuated Influenza Vaccine. Quadrivalent (LAIV4). [e]Dose dependent. Informations were found on web sites: http://www.emergency.cdc.gov/coca/ppt/2013/08_13_13_Immunizations.pdf, http://www.fda.gov/biologicsbloodvaccines/guidancecomplianceregulatoryinformation/post-marketactivities/lotreleases/ucm343828.htm (accessed on 4 September 2013).

Inactivated whole seasonal influenza vaccines are the most widely used, covering approximately 90% of human vaccine sales world-wide [54]. A new avian influenza vaccine is normally made by inoculation of the isolated virus into embryonated chicken eggs. The manufacturing process has been described in detail elsewhere [54]. Briefly, the allantoic fluids from influenza virus-inoculated embryonated eggs are collected in a fully automated process followed by a simple clarification step. The virus is recovered through multiple filtration and concentration steps and inactivated with chemicals such as formalin or β-propiolactone, typically in two steps [54]. The final influenza vaccine is trivalent with two strains of Influenza A virus (H3N2 and H1N1) and one strain of Influenza B virus to provide a suitable antigenic range that will meet the viral challenge of the season [55]. However, several problems in such manufacture remain poorly resolved. First, a stable supply of eggs is needed, which has required drastic reorganization of hen flock management [54]. Second, the egg-based viral culture is not efficient in producing high titers of virus with antigenic and genetic fidelity. Hence, there is a question of whether this procedure permits production on a scale that would be able to protect against a serious pandemic. Third, the potential susceptibility of chickens to HPAI viruses further jeopardizes the availability of eggs for vaccine production in the event of a pandemic strain arising from an HPAI virus [56].

A simpler approach to make influenza antigens in cell cultures routinely involves the synthesis of protein subcomponents of the virus using recombinant methodologies [57]. Several experimental enquiries are further exploring these possibilities by testing multiple host cell types for efficacy in producing different recombinant influenza antigens. HA was made in insect cells [58], the M_2 protein in plant cells [59] as well as *Escherichia coli*, where this protein was conjugated to the TLR-5 ligand flagellin [60], or the heat shock protein (HSP)-70 of *Mycobacterium tuberculosis* [61]. As discussed further in "Innate immunity and immunogenic and physicochemical properties of adjuvants" section, these adjuvants are necessary since the subunit antigens are generally poorly immunogenic.

In vivo-expressed influenza DNA vaccines

DNA vaccines are basically expression constructs that will produce the encoded antigen following delivery of the construct to an appropriate host cell. Compared with the production of whole viruses or viral subcomponents, DNA vaccines are easy to manufacture and extraordinarily stable when stored in the lyophilized state.

DNA vaccines have been applied as model systems to study the possibility of inducing antibodies against the HA, NP, and M1 proteins [62,63], the ability to raise CTL response, and to investigate the protection in mice, chicken, ferrets and primates using intranasal instillation, intravenous injection, intramuscular injection, or gene gun [62,64]. These experiments confirmed that influenza DNA vaccines can induce humoral and cellular responses, and the animal will get full or partial immunity to the challenge [62]. In mice, the antibody formation against HA was mostly of IgG2a isotype, but switched to IgG1 when the gene gun was used. IgG and IgA antibodies to HA were also secreted to the upper respiratory tract of vaccinated animals [65]. In primates, the titer was as high as the titer induced by human commercial influenza vaccines [66]. In mice, NP-coding DNA vaccines were able to increase the level of CD8+ CTL as well as the cellular immune response, which can give proper immunity to a

wide spectrum of influenza subtypes [64]. Furthermore, vaccination with the influenza DNA vaccine coding NP helped to induce high levels of secretion of CD4+ Th1, and to increase the levels of interferon-γ and interleukin-20 [67]. Both CD8+ CTL and CD4+ T-cells gave protection against influenza challenge [65]. In view of the recent findings that interferon-γ-secreting CD4+ Th cells are important in obtaining protection against influenza virus infection [38], DNA vaccination may carry particularly beneficial properties in shaping the right phenotypic composition of influenza virus antigen-reactive T lymphocytes. However, in spite of nearly two decades of research, influenza DNA vaccination in clinical trials has not been an unqualified success, suggesting that both choices of antigens and adjuvants as well as the means of DNA cell delivery may need reconsideration [55].

The Flumist vaccine (Table 1) with live-attenuated virus represents an important alternative to obtain in vivo expression of influenza virus antigens, this way supporting T cellular responses. In this case, an attenuated master donor virus with appropriate characteristics with regard to cold-adaptation and stability is mixed in cell cultures with a potentially epidemic wild-type virus. This procedure reassorts the RNA segments of the master donor such that it will encode the HA and NA of the wild-type virus [68].

Innate immunity and immunogenic and physicochemical properties of adjuvants

Vaccines are occasionally formulated with adjuvants to augment the potency of the antigen and presentation to the immune system. These co-administered adjuvants may enhance humoral and cellular immune responses simultaneously [69]. Adjuvants comprise a surprisingly diverse range of compounds, including mineral salts, oil-in-water emulsions, saponin-based adjuvants, liposomes, microparticles, cytokines, and polysaccharides [70]. Pandemic influenza vaccines are formulated with adjuvant since they are typically monovalent and meant to protect immunologically naïve vaccinees. Among seasonal influenza vaccination, as noted from Table 1, none of the 2013–2014 seasonal vaccinations contains adjuvants. Nevertheless, as presented further below, several experimental approaches clearly support that improvement of adjuvant efficacy may be an important route to obtaining better protecting influenza vaccines or reduce the dosage needed to obtain sufficient protection.

Historically, vaccine adjuvants were developed empirically, initially based on an assumption that the antigen adsorption onto solids would prolong the stimulus *in vivo* [71,72]. In a broad outline, their immunostimulating contributions are currently considered as relating to (1) chemical stabilization of vaccine antigens, (2) improving antigen delivery to antigen-presenting cells, (3) improving antigen processing and presentation by antigen-presenting cells, (4) stimulating the production of desirable immunomodulatory cytokines, and (5) permitting a decrease in the required dosage of the administered antigen. It is clear that the innate immune system is involved in all of these effects. In an important treatise defining the concept of innate immunity, Janeway noted that immune responses raised to soluble proteins in experimental models almost always required the further addition of "messy precipitates" [1], which apparently deliver a stimulus required for efficient formation of antigen-specific immunity. As noted in "Protein-based vaccines against influenza" section, indeed adjuvants are obligatory in vaccines based on viral subcomponents such as the pandemic influenza vaccines. Janeway concluded that this stimulus was triggered by "nonclonal recognition of nonself patterns" [1]. This is now widely recognized in the concept of adjuvants mimicking pathogen-associated molecular patterns [73,74], and supported by observations on pattern-recognition receptor agonists used as adjuvants [75]. However, the particulate nature of many adjuvants has received less attention as part of the explanation for the mechanisms of adjuvants. As explored further below, the particulate nature of many adjuvants may add an ultrastructural feature to the vaccine formulation, which is likely to activate both humoral and cellular factors of the innate immune system.

Licensed adjuvants in clinical use

Among adjuvants that have obtained a license in the European Union (Table 2), aluminum salts, oil-in-water emulsions (*e.g.*, MF59), alum-adsorbed TLR4 agonists (*e.g.*, adjuvant system [AS] 04), and liposomes (*e.g.*, Crucell), are the most widely used [80]. The list of licensed adjuvants in the United States is even more restricted, and includes only aluminum salts and AS04 [81] (Table 2).

Aluminum salts are widely used as adjuvants and are included in the hepatitis B virus, papillomavirus, and diphtheria-tetanus-pertussis vaccines [72]. The majority of aluminum salt adjuvants used in humans comprise amorphous aluminum hydroxyphosphate ($Al(OH)_x$ $(PO4)_y$), amorphous aluminum hydroxysulfate (generated from precipitation of the antigen with $AlK(SO_4)_2$ named alum), and aluminum hydroxide, which is more correctly described as aluminum oxyhydroxide, AlO(OH) [76]. These salts are insoluble in water and form particles disperse in size (Table 2).

Studies have demonstrated the apparent superiority of aluminum hydroxide-adsorbed vaccines when compared to soluble adjuvants [82]. However, aluminum salts are ineffective in providing immunity against pathogens requiring Th1 mediated immunity [83,84]. Their mode-of-action were previously considered to support antigen persistence *in vivo* by prolonging antigen release. This effect is often referred to as the "depot effect", although

Table 2 Approximate diameters and chemical constituents of particulate adjuvants used in humans for prophylactic vaccination against viral infections[a]

Adjuvant name (Provider; year licensed)	*Particle size (nm)*	*Adjuvant type*	*Chemical constituents*	*Vaccines (virus)*
Aluminum salt (Various; 1924)	1,000-20,000[b]	Mineral salts	Aluminium hydroxyphosphate *or* Aluminum hydroxysulfate *or* Aluminum oxyhydroxide	Various
MF59 (Novartis; 1997)	160[c]	Oil-in-water emulsion	Squalene, polysorbate 80, sorbitan trioleate	Fluad (seasonal influenza), Focetria (pandemic influenza), Aflunov (pre-pandemic influenza)
AS03 (GlaxoSmithKline; 2005)	< 200[d]	Oil-in-water emulsion	Squalene; polysorbate 80, α-tocopherol	Pandemrix (pandemic influenza), Prepandrix (pre-pandemic influenza)
Virosomes (Berna Biotech; 2000)	100-200[e]	Liposomes	Influenza virus (lipid) envelope	Inflexal (seasonal influenza), Epaxal (hepatitis A)
AS04 (GlaxoSmithKline; 2005)	1,000-20,000[b]	Alum-adsorbed TLR4 agonist	Aluminum oxyhydroxide, MPL	Fendrix (hepatitis B), Cervarix (human papilloma virus)

[a]Data reported are for the vaccine formulations with antigens. [b]Values are from a review by Hem & HogenEsch [76]. [c]Value from a review by O'Hagan *et al.* [77]. [d]Value from a review by Garcon *et al.* [78]. [e]Value from de Jonge *et al.* [79].

its relevance has been questioned in recent reports [85]. The aluminum salt particles may rather serve to activate macrophages and dendritic cells [72,86]. With regard to safety, aluminum salts have been commercially available for several decades [87], and are generally considered well-tolerated [88]. However, experimental evidence suggests that complexing of Al^{3+} ions with glucose-6-phosphate may interfere with the energy metabolism in a way that at least on speculative grounds might link high concentrations of aluminum to neural disorders or inflammatory syndromes [89].

Oil-in-water emulsions based on the natural lipid product squalene, *i.e.*, MF59, are licensed in most parts of Europe to be used with an updated seasonal influenza vaccine, primarily in elderly vaccinees. Moreover, MF59 and AS03 are the adjuvants of choice in pandemic influenza vaccines [74,90]. Although made from a softer material than the aluminum salts, the squalene and polysorbate mixture nevertheless in aqueous environment manage to form stable droplets as a consequence of the hydrophobic effect [77,78] and a diameter of ~100 nm [91]. As is also the case for mineral particles, the oil-in-water interface may adsorb protein from the medium, such as albumin [92].

In terms of the pharmacological mode-of-action, MF59 presumably acts by inducing a local immunostimulatory environment at the site of injection. This is characterized by enhanced antigen persistence, an increased antigen uptake by dendritic cells, and the recruitment of APCs [90,93]. Oil-in-water emulsions induce stronger antibody responses, which reduce the need for multiple doses, and lead to a combined Th1 and Th2 memory response [94]. The administration of squalene has been associated with the development of arthritis in rats [95]. Nevertheless, the evidence so far presented does not suggest significant or frequent side effects prompted by the use of squalene adjuvant in humans [96]. The H1N1 influenza vaccination Pandemrix contains squalene. Application of the vaccination was suggested to be associated with the development of narcolepsy in children [97,98], a disorder which involves the immune system [99]. However, it is unclear what role, if any, the AS03 adjuvant played in these clinical findings.

Other vaccines utilize a new class of adjuvant systems (AS04), which combine aluminum hydroxide and a proprietary form of detoxified monophosphoryl lipid A (MPL). MPL is derived from the gram-negative bacterium *Salmonella minnesota* R595 strain, and is a specific agonist of TLR4, comparable to lipopolysaccharide [100-104]. Indeed, lipopolysaccharide may also potentiate the immune response. However, frequent pyrogenic activities preclude the use of lipopolyssacharide as adjuvant for human use [72,74,83]. In contrast, the less toxic MPL is administered in vaccines for human use without any reported adverse effects [105]. AS04 directs a polarized Th1-response, as opposed to the Th2 response of aluminum salt alone. While the adjuvant activity of this formulation can mostly be ascribed to MPL, the "depot effect" of aluminum was suggested to prolong the stimulation by MPL [74,83].

Similar to the more familiar liposomes, virosomes are composed of a phospholipid bilayer, but unlike liposomes, the bilayer is unilamellar and modified with viral envelope proteins (*e.g.*, in the case of influenza-like particles with NA and HA anchored in their virosomal membrane). In this way, virosomes are designed to bind and fuse with host cells similar to their cognate viruses. Antigens anchored to the surface are degraded upon endosomal fusion within the endosome and are consequently displayed to the immune system by MHC class II receptors. In contrast, antigens encapsulated within the virosomes are transported to the cytosol during the fusion event, which enables them to enter the MHC class I pathway of antigen presentation. Hence, virosomes possess the

capability of mediating humoral as well as cell-mediated immune responses [106,107]. Currently, two commercial vaccines utilizing the virosome technology have acquired a license: Epaxal® against hepatitis A and Inflexal® against influenza. Both are proven to be effective immunogens with unique adjuvant properties [108].

New generation of adjuvants for influenza vaccines

Novel vaccine adjuvants are designed to favour stronger responses as well as the development of Th1, Th2, or CTL-mediated immunity. Cationic liposomes are such strong activators of the immune system. As already mentioned above, selective cellular responses may be required to offer efficient immunity to influenza [109]. To achieve this goal, genetic adjuvants and cytokines may be efficient. In general, genetic adjuvants are constituted by plasmid vectors encoding immunomodulatory products, such as cytokines [110]. Interestingly, novel directions in the design of genetic adjuvants include the use of DNA motifs such as CpG or HSPs from *Mycobacterium*.

Cationic liposomes are potent stimulators of the immune system [111,112]. While there is a considerable literature on experimental use of such liposomes as adjuvant, it is only recently that promising clinical trials have been conducted [113]. At least two influenza vaccines with cationic liposomes as adjuvants have been tested in clinical trials [114,115]; one addressing the complications mentioned in "Viral infectivity, treatment, and immunity to influenza" section of raising protective immunity in the elderly vaccinees [115]. The cationic adjuvant formulation no. 1 (CAF01) consists of dimethyldioctadecylammonium and α,α'-trehalose-6,6′-dibehenate (TDB) [116]. TDB is a synthetic analogue of trehalose 6,6′-dimycolate, which itself possess an unwanted toxicity. However, by preserving the *Mycobacterium*-like lipid structure in TDB, the CAF01 formulation makes it possible to raise an immune response to antigens from *Mycobacterium*, such as the early-secreted antigenic target 6 kDa (ESAT-6). The mode-of-action of the adjuvant seems to involve the TLR-independent Syk/Card9-dependent pathway [116], apparently through direct binding to the C-type lectin receptor Mincle expressed in macrophages [117]. These findings points to an interesting principle in the choice of appropriate adjuvants also explored below, namely efficient adjuvants as a source of an innate immune response similar to those induced by the target microbial organism. As a tool to direct T cellular response the CAF01 cationic lipid composition appears to produce a Th1 response [118], but examples of cationic lipids stimulating Th2 response are also reported [118,119].

Unmethylated bacterial CpG motifs are commonly used recombinant adjuvants that can induce innate immune response to DNA vaccines. Because CpG motifs in vertebrates are often methylated, bacterial CpG motifs are recognized as pathogen-associated molecular patterns by the human immune system, typically by TLR-9 after receptor-mediated endocytosis [120-122]. CpG motifs enhance both humoral and cellular immune responses to the encoded vaccine antigen, skewing the cellular response towards Th1 phenotype [123]. Recently, CpG DNA formed an important part in DNA vaccine protection against *Mycobacterium* tuberculosis, with ability of the adjuvant to augment the lung infiltrate of interferon-γ producing T lymphocytes [124]. This finding is not, however, independent of the microbial challenge or applied vaccine antigen. Wu *et al.* showed that addition of CpG DNA may even weaken the protective activity of the influenza M_2 protein vaccine [125].

In three independent studies, *Mycobacterium*-dependent protein-1, HSP 70, and ESAT-6, respectively, were used as potential genetic adjuvants for the avian influenza H5 DNA vaccine [61,126,127]. HSPs are chaperones and play an important role in protein folding and prevention of protein aggregation or misfolding. Previous studies have shown the high potential of HSPs as genetic adjuvants in DNA-based vaccination, probably due to their capacity to stabilize weak antigens, permitting the delivery to APCs, notably DCs [128]. When fused to vaccine antigens, HSPs or heat shock cognate proteins can elicit CD8+ CTL response *in vivo* and *in vitro* [129]. Optimal results are obtained if they are directly fused with the vaccine gene of interest [61,130,131]. Rasoli *et al.* tested a potential enhancement of immunogenicity of an avian influenza virus DNA vaccine, where the H5 gene was fused with the HSP-70 gene [61].

Adjuvants as particulate material and immunogenicity

Many commonly applied adjuvants precipitate in aqueous environment and remain stable as particles once administered suggesting this property to be important. With doubts being cast on the "depot" effect as rationalizing the effect of adjuvant [85], it remains enigmatic precisely why "messy precipitates" as adjuvants are such a provocation of the immune system. As detailed in an excellent review by Fox *et al.* [132], the physicochemical properties of particulate materials affect, however, many aspects of vaccine efficacy. Indeed, as noted above, other physicochemical properties such as surface charge of the particulate material has received interest, while the size of these particles are not often mentioned even though it is an intrinsic property of precipitates.

We propose that the colloidal nature of several adjuvants (Table 2) influence the immune system through three highly interconnected routes.

First, the deposition of soluble proteins of the innate immune system on particle surfaces stimulates in many cases a proinflammatory response. Notably, these proteins include components of the complement system, which

may amplify interactions with receptors on cells of the innate immune system. In this situation, peptides released by the complement activation make the adjuvants proinflammatory "by-standers", which influence the vaccine response indirectly by activating leukocytes. Second, both the deposition of complement as well as a spontaneous deposition of other proteins on the adjuvant particle surface, such as the abundant plasma proteins fibrinogen or albumin may generate cues for recognition by receptors expressed on leukocytes. This is a less indirect route of stimulating leukocytes to vaccine antigen responses since such protein-coated adjuvants directly interact with the leukocytes involved in the process. Third, the biophysical characteristics of particulate material, *e.g.*, size and surface charge, may dramatically influence cellular uptake and response [133]. This phenomenon relates to both the rigidity of the cell membrane, and the accompanying molecular interactions permitting receptor recognition of ligands on the particulate surfaces Figure 2. As reviewed below, here it appears that size *per se* is an important factor in the direct interactions between the adjuvant and leukocytes.

The complement system is constituted by approximately 40 soluble plasma proteins and receptors. In essence, the function of complement involves the capability of the soluble proteins to transform into a surface-bound state with deposition on target surfaces, *e.g.*; the cell walls of bacterial or fungal organisms, envelopes or capsids of viruses, or even decayed host tissue or apoptotic cells. The pathways of activation have been detailed elsewhere [134]. Briefly, three distinct mechanisms initiate the deposition of complement. The classical pathway *(i)* is activated by binding of the complement component (C) C1 complex to IgG or IgM antibodies. Followed by proteolytic activation of C4 and C2, which generate the surface-bound fragments C4b and C2a and the small soluble fragments C4a and C2b, an enzyme C4bC2a is formed, which converts C3 into surface-bound C3b and the soluble fragment C3a. A similar process, named the lectin pathway *(ii)*, may be

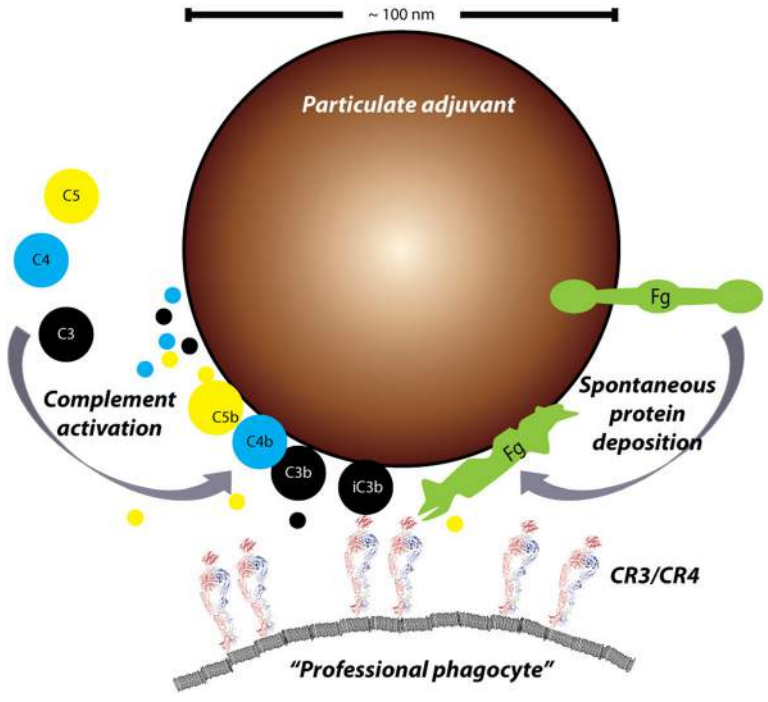

Figure 2 The sources and consequences of plasma protein deposition on particulate adjuvants. Deposition of complement is well-described for liposomes and is likely to happen on the surface lipid adjuvants as well [142]. The deposition of complement on aluminum oxide particles is less characterized [148]. As clear from the schematic, a particle with a diameter of ~100 nm presents certain space and topological restraints, which may influence both the complement activation and actually capacity for carrying deposited protein as detailed elsewhere [134]. Following activation of the complement components C3, C4, and C5 these are covalently bound to target surfaces concomitantly with the proteolytic release of small peptides from the molecules (indicated with colors). This release depends on the pathway of complement activation and may hence create a signature for adjuvants. In this scenario, which does not explicitely involve the vaccine antigen, the adjuvants act as by-standers creating a milieu of immunostimulatory peptides. Proteolytic processing of the C3b fragment creates the iC3b fragments, which is ligand for both CR3 and CR4 and may thus support phagocytosis by "professional phagocytes" [161] through the connection of these receptors with cytoskeleton. In addition to complement, surface-adsorbed fibrinogen is a ligand for CR3 and CR4, probably in part because of the structural denaturation of the protein as a consequence of the surface adsorption, which enhances the interaction with these receptors [155,156]. Sizes are indicated approximately to scale based on data presented in Refs. [134,166,167].

initiated by binding of MBL to suitable carbohydrates or by binding of ficolins to certain acetylated compounds [135]. Finally, the alternative pathway *(iii)* is based on the ability of C3 to deposit spontaneously on nearly all biological surfaces. Host cells may catalyze the removal of C3 and other complement components from their cell surface. By contrast, many microbial cells do not harbour such mechanisms, and are hence susceptible to complement attack. Following the covalent deposition of C3b, a complex with the proteolytic part of activated Factor B (termed Bb) is formed. Unlike C4bC2a enzyme, the C3bBb enzyme permits a positive amplification loop since the deposition of more C3b creates more enzymes. Further proteolytic degradation *in situ* generates the iC3b and C3d fragments, which are ligand for complement receptors (CR)2 and CR3. Also, the C4bC2a and C3bBb enzymes enables the recruitment of the large C5b to the surface, while releasing the small C5a peptide to the environment. C5a is a strong activator of the endothelium of blood vessels, and central in the recruitment of many inflammatory cells to the site of complement activation.

Complement has long been known to play a quintessential role of in raising a strong antibody response to antigens [136], now more fully understood with the help of intravital fluorescent microscopy of the cellular processes involved in the lymph node [137,138]. A part of the benefit from complement activation may derive from the covalent coupling of a proteolytic fragment of C3 (C3d) to antigens, this way supporting the uptake by B cells through CR2. This has already been explored as a so-called "molecular adjuvant" in experimental studies by engineered coupling of this fragment onto target antigens, including influenza vaccine antigens [139-141].

A less appreciated route of complement influencing the function of adjuvants involves direct activation of complement. Indeed, it is well established that lipid vesicles in the kind of liposomes may activate the complement system [142,143]. The *in vivo* significance of this phenomenon is well-known in the field of drug delivery. Such activation accelerates the clearance of the liposome from free circulation through capture by hepatic macrophages in a process, which is very similar to the fate of viral particles opsonised by complement. More recently, it has become clear that poloxamers, a type of pluronic block co-polymers, also activate the complement system as well as more widely affects cellular functions when administered [144,145]. Poloxamers have been tested in the context of experimental DNA vaccines to influenza virus [146]. The benefit from this addition was probably in part obtained by improving DNA drug delivery [146]. Nevertheless, it is tempting to suggest that complement activation by poloxamers also contributed to the immunogenicity due to the complement system's many influences on the inflammatory response. Interestingly, these poloxamers as well as drug delivery liposomes and lipidic adjuvants used in the clinic (Table 2) attain diameters of 100–200 nm [77-79,146], similar to the dimensions of influenza virus particles with a diameter of ~120 nm (Figure 1) [19]. This is a conspicuous property of both the adjuvant and viral particles since Pedersen *et al.* [147] reported that nanoparticles with structural features similar to molecular initiators of complement activation produced stronger responses than particles with either smaller or larger sizes than these initiators. At least in serum from some donors the strongest activation was clearly found for dextran-coated polystyrene or iron oxide particles with diameters of 100–250 nm, apparently pending a sufficient titer of anti-dextran IgM. This effect was attributed to perturbations in the ultrastructure of IgM with cross-sectional diameters in the order of 20–30 nm [134], when IgM bound epitopes on the curved surface of the particles. With regard to aluminium salts and phosphate adjuvants, these are composed of small (~50 nm) primary particles, similar in size to the lipid adjuvants. The antigen-precipitated particles are, however, far larger than those generated from lipid adjuvants, typically with diameters ~1,000-20,000 nm [76]. This would seem to preclude complement activation through the processes addressed by Pedersen et *al.* [147]. Furthermore, while aluminium salt particles activate complement [148], there is evidence that at least hydrated aluminium surfaces adsorbed complement in a manner not generating the typical proteolytic cleavage products associated with activation [149]. This could point to significant differences between particulate adjuvants in their interaction with the complement proteins and hence in their immunomodulatory capacity and capabilities.

Obviously, the topology of particles is only one source of properties that may tune the ability to activate complement. By altering the interligand distance from 6 nm up 14 nm, an almost 1,000-fold increase in the dissociation constant was observed for the binding of the MBL oligomers to these surfaces [22]. This disproportional response, with a two-fold alteration in ligand density causing a 1,000-fold lowering of the affinity, was interpreted to reflect the critical difference between binding patterns of dimensions comparable to the size of MBL and those even just moderately exceeding these dimensions. As recently demonstrated by Pacheco *et al.* [150] for complement activation through particle surface-bound IgG, there is a complex interplay between size of the particles and amount of bound ligand for C1, *i.e.*, the IgG Fc parts, in regulating the strength of the activation [150]. Similar to the findings by Pedersen *et al.* [147], particles with a diameter of 500 nm appeared more efficient in activating complement than larger particles with a diameter of 4,000 nm. From careful quantification of the surface-bound IgG and multiple experiments varying the amount of IgG, Pacheco *et al.* hypothesized that an essential trigger of

complement activation is assembly of the C1 complex via binding to multiple, closely apposed Fc parts [150]. C1 and MBL share several biochemical properties, in particular with regard to their ultrastructure and ability of both proteins to form polyvalent interactions. With this in mind, the critical role of polyvalency for strong MBL bonding to ligand-presenting surfaces [22], supports Pacheco *et al.* hypothesis [150].

As already noted in "Viral infectivity, treatment, and immunity to influenza" section, complement activation is an important part of immunity to influenza virus. The ability of adjuvant to trigger such a response is consequently mimicking conditions that could well be essential to enable full priming of the adaptive immune system, which is required to obtain antigen recognition. Importantly, in this scenario, the influence of complement activation is mediated by the adjuvant particles acting as "by-standers" creating a milieu of inflammation-stimulating complement peptides. More specifically, the generation of the smaller peptide fragments from C3, C4 and C5 may arguably create signatures of the type of complement activation induced. It may be significant that the adjuvant mimic the complement activation signature of the natural infection, which vaccination sought to prevent. For instance, liposomes appear to trigger a response through the alternative pathway [151] implying that primarily C3a and C5a are generated in this process. By contrast, as mentioned above, influenza virus is most likely activating complement through all pathways [152] with a prominent role of the lectin pathway, thereby suggesting the additional presence of C4a and C2b fragments. Yet, the influences of these peptidic signatures are only incompletely understood. As a valuable comparison on how small differences in proteolytic activities may change the profile of cleavage products, a recent report demonstrated vast alterations in the cleavage of soluble protein, and their cutaneous deposition during inflammation. This emerged as a consequence of genetic ablation in mice of a single protease, namely MMP-2 [153]. By analogy, we propose that regulating the adjuvant-triggered pathway of complement activation, and hence the proteolytic activities, potentially could quantitatively and qualitatively improve the outcome of vaccination.

An even simpler route to immune activation through the interaction between adjuvant surfaces and body fluid proteins is derived from the spontaneous surface deposition of notably albumin and fibrinogen [154]. Such spontaneous deposition on particle surfaces has been observed to affect or even destroy the structure of the adsorbed protein in particle-size-dependent manner [155]. Denatured fibrinogen is a ligand for CR3 and CR4 [156]. Hence, the surfaces of particulate adjuvants play an important role in permitting receptor-mediated contacts between adjuvants and leukocytes, probably in some cases by manufacturing a high density of cues for receptor binding on the particle surface. Such interactions are extremely strong [34] and may cause receptor signalling through CR3 leading to stimulation of cytokine production [157]. Obviously, the processes discussed above are initiated by simple contact of the colloidal adjuvant with protein-containing fluids, notably blood or interstitial fluids, which seems unavoidable with the chosen routes of vaccine administration. As outlined above and also noted from other studies [158], the transition of soluble proteins onto surfaces offers a wealth of complex quantitative influences, which may well manipulate those microenvironments-developing immune responses. Even so, it is an interesting observation that both past and present investigations into the adjuvant properties have largely ignored these processes and focused on the later cellular responses, such as modulated receptor expression and activation of the inflammasome. As noted by Fox *et al.* [132] this does not capture the full picture of the processes enabling the adjuvants to make such stimulations.

It is a classic observation that receptor-mediated endocytosis both have upper and lower limits with regard to the size range of particulate material that may enter the cell through a given mechanism [159,160]. Pinocytosis and receptor-mediated endocytosis brings in to the cytoplasm relatively small entities such as macromolecules or viral particles, apparently through a shared use of clathrin [159]. Receptor-mediated endocytosis is most efficient with particles taking *radii* of 25–30 nm with a sharp cut in efficiency for *radii* smaller than ~22 nm [160]. These smaller particles may still enter the cells through pinocytosis albeit less efficiently. By contrast, phagocytosis enables uptake of particles larger than 500 nm in a process involving reorganization of the actin cytoskeleton. This process is typically mediated by Fc receptors, or the integrins CR3 and CR4 expressed on "professional phagocytes" [161], which includes macrophages/dendritic cells, monocytes, and granulocytes [159,161]. On top of the size-selectivity in terms of the actual cellular process mediating the uptake, it is now clear that both micro- and nanoparticulate material influence these processes through their shape [162,163]. This influence appears to derive from the ability of the cell membrane to form a phagocytic cup covering the particle [164].

In the context of adjuvants, it is of considerable interest that human B cells are unable to phagocytose particulates but may endocytose smaller particles [165]. This makes the large aluminium hydroxide particles unlikely to directly enter the cytosol of B cells, while the C3d-tagged antigens would easily do so. By contrast, the aluminum hydroxide particles can be phagocytozed by "professional phagocytes", which during the intracellular storage may release the antigen from aluminium hydroxide matrix and permitting presentation of antigen by myeloid cells

in the lymph nodes to CD4+ T cells. In this way, simple differences in size of the particulate adjuvant and modification of molecular adjuvant tags on the antigen could potentially qualitatively and quantitatively change the subsets of leukocytes involved in the formation of an immune response. While the size-difference between macromolecules and aluminium hydroxide particles are striking and simple to relate to the known capacity of certain types of cellular endocytosis, the lipid adjuvants with sizes intermediate between these extremes are far more difficult to assign similar discrete mechanisms. Indeed, based on theoretical calculations and the well-known ability of macrophages to clear liposomes [142,160], their size regimen (Table 2) seems to indicate that both B cells and myeloid cells would be able endocytose or phagocytose these types particulates. At least on speculative grounds, this would suggest that minor differences in the size of these adjuvants could tilt the immune response towards either endocytosis or phagocytosis-mediated types of uptake hence altering immunological outcome of vaccination.

Conclusions

Vaccination to protect against influenza infection is a field of great socio-economic and healthcare importance. The dual targeting of vaccine formulations, engaging both the innate and adaptive arms of the immune system, is crucial for efficacy. The TLR recognition of certain adjuvants is well documented and may hence serve as the prototype example for the claim that adjuvants are essentially enhancers of the innate immune response. The humoral part of the innate immune system, namely the complement system, may, however, well be equally important. In addressing the precise mechanisms of interactions between the adjuvants and the molecular environment of the body, we have stressed that in particular the size of adjuvants may fundamentally regulate their properties with regard to stimulating the immune response. The biology of influenza A viruses, notably their genetic flexibility, is significantly limiting the prospect of generating a single, omnipotent vaccine formulation. On the other hand, the conservative choice of adjuvants seems to ask the question if not more sophisticated strategies would now be of value, here perhaps in particular benefitting from the available scientific insight on mechanisms of the innate immune system. We propose that biophysical properties of the adjuvant formulation, in particular the dimensions of particulate materials, offer attractive opportunities to augment the immune response elicited.

Abbreviations

APC: Antigen-presenting cell; AS: Adjuvant system; CAF01: Cationic adjuvant formulation no. 1; CR: Complement receptor; CTL: Cytotoxic T lymphocyte; DC: Dendritic cell; DNA: Deoxyribonucleic acid; ESAT-6: Early-secreted antigenic target 6 kDa; HA: Hemagglutinin; HPAI: High pathogenic avian influenza virus; HSP: Heat shock protein; Ig: Immunoglobulin; LPAI: Low pathogenic avian influenza virus; M: Matrix protein; MBL: Mannan-binding lectin; MPL: Monophosphoryl lipid A; NA: Neuroaminidase; NP: Nucleoprotein; RNA: Ribonucleic acid; TDB: α,α′-trehalose 6,6′-dibehenate; Th: T helper cell; TLR: Toll-like receptor.

Competing interests

The authors hereby declare that they have no competing interests.

Authors' contributions

BJ, SHC, EP and TV-J organized and wrote sections and edited the final manuscript. BJ prepared Figure 1 and SHC tabulated the information found in Tables 1 & 2. HBE wrote a draft of "Clinical manifestations of influenza virus infections" section and contributed to the writing of "Adaptive immunity and formulation of antigenic components in influenza vaccines" section. MRP contributed to the writing of "New generation of adjuvants for influenza vaccines" section. All authors read and approved the final manuscript.

Acknowledgements

The authors thank Drs. Tina Yen-Ting Chen and Carina A. Rosenberg for critical reading and revision of the manuscript and Dr. Uffe Skov Sørensen for valuable suggestions concerning the writing on endocytosis of antigens and adjuvants. TV-J, BJ, and HBE were supported by the Lundbeck Foundation through the "The Lundbeck Foundation Nanomedicine Centre for Individualized Management of Tissue Damage and Regeneration". TV-J and EP were in receipt of support from the Karen Elise Jensen Foundation.

Author details

[1]Biophysical Immunology Laboratory, Department of Biomedicine, Aarhus University, DK-8000 Aarhus, Denmark. [2]Department of Clinical Medicine, Aarhus University, Aarhus, Denmark. [3]Inflammation and Infection Research Centre, School of Medical Sciences, University of New South Wales, Sydney, Australia. [4]Department of Infectious Medicine (Q), Aarhus University Hospital, Aarhus, Denmark.

Received: 15 July 2013 Accepted: 10 September 2013
Published: 6 November 2013

References

1. Janeway CA Jr: **Approaching the asymptote? Evolution and revolution in immunology.** *Cold Spring Harbor symposia on quantitative biology* 1989, **54**(Pt 1):1–13.
2. Bridges CB, Kuehnert MJ, Hall CB: **Transmission of influenza: implications for control in health care settings.** *Clinical infectious diseases: an official publication of the Infectious Diseases Society of America* 2003, **37:**1094–1101.
3. Lessler J, Reich NG, Brookmeyer R, Perl TM, Nelson KE, Cummings DA: **Incubation periods of acute respiratory viral infections: a systematic review.** *The Lancet infectious diseases* 2009, **9:**291–300.
4. Neuzil KM, Reed GW, Mitchel EF, Simonsen L, Griffin MR: **Impact of influenza on acute cardiopulmonary hospitalizations in pregnant women.** *American journal of epidemiology* 1998, **148:**1094–1102.
5. Barker WH, Mullooly JP: **Pneumonia and influenza deaths during epidemics: implications for prevention.** *Archives of internal medicine* 1982, **142:**85–89.
6. Lin JC, Nichol KL: **Excess mortality due to pneumonia or influenza during influenza seasons among persons with acquired immunodeficiency syndrome.** *Archives of internal medicine* 2001, **161:**441–446.
7. Kwong JC, Campitelli MA, Rosella LC: **Obesity and respiratory hospitalizations during influenza seasons in Ontario, Canada: a cohort study.** *Clinical infectious diseases: an official publication of the Infectious Diseases Society of America* 2011, **53:**413–421.
8. Finelli L, Fiore A, Dhara R, Brammer L, Shay DK, Kamimoto L, Fry A, Hageman J, Gorwitz R, Bresee J, Uyeki T: **Influenza-associated pediatric mortality in the United States: increase of staphylococcus aureus coinfection.** *Pediatrics* 2008, **122:**805–811.
9. Rothberg MB, Haessler SD, Brown RB: **Complications of viral influenza.** *The American journal of medicine* 2008, **121:**258–264.
10. Petersen E, Keld DB, Ellermann-Eriksen S, Gubbels S, Ilkjaer S, Jensen-Fangel S, Lindskov C: **Failure of combination oral oseltamivir and inhaled zanamivir antiviral treatment in ventilator- and ECMO-treated critically ill patients**

with pandemic influenza A (H1N1)v. *Scandinavian journal of infectious diseases* 2011, **43:**495–503.
11. Rohde G, Wiethege A, Borg I, Kauth M, Bauer TT, Gillissen A, Bufe A, Schultze-Werninghaus G: **Respiratory viruses in exacerbations of chronic obstructive pulmonary disease requiring hospitalisation: a case–control study.** *Thorax* 2003, **58:**37–42.
12. Mamas MA, Fraser D, Neyses L: **Cardiovascular manifestations associated with influenza virus infection.** *International journal of cardiology* 2008, **130:**304–309.
13. Warren-Gash C, Smeeth L, Hayward AC: **Influenza as a trigger for acute myocardial infarction or death from cardiovascular disease: a systematic review.** *The Lancet infectious diseases* 2009, **9:**601–610.
14. Murray PR, Rosenthal KS, Pfaller MA: *Medical Microbiology*. 7th edition. Oxford: Elsevier Saunders; 2013.
15. Guo YJ, Jin FG, Wang P, Wang M, Zhu JM: **Isolation of influenza C virus from pigs and experimental infection of pigs with influenza C virus.** *J Gen Virol* 1983, **64**(Pt 1):177–182.
16. Osterhaus AD, Rimmelzwaan GF, Martina BE, Bestebroer TM, Fouchier RA: **Influenza B virus in seals.** *Science* 2000, **288:**1051–1053.
17. Webster RG, Bean WJ, Gorman OT, Chambers TM, Kawaoka Y: **Evolution and ecology of influenza A viruses.** *Microbiological reviews* 1992, **56:**152–179.
18. Tong S, Li Y, Rivailler P, Conrardy C, Castillo DA, Chen LM, Recuenco S, Ellison JA, Davis CT, York IA, *et al*: **A distinct lineage of influenza A virus from bats.** *Proc Natl Acad Sci USA* 2012, **109:**4269–4274.
19. Harris A, Cardone G, Winkler DC, Heymann JB, Brecher M, White JM, Steven AC: **Influenza virus pleiomorphy characterized by cryoelectron tomography.** *Proc Natl Acad Sci USA* 2006, **103:**19123–19127.
20. Mitnaul LJ, Matrosovich MN, Castrucci MR, Tuzikov AB, Bovin NV, Kobasa D, Kawaoka Y: **Balanced hemagglutinin and neuraminidase activities are critical for efficient replication of influenza A virus.** *Journal of virology* 2000, **74:**6015–6020.
21. Zhang Y, Lin X, Wang G, Zhou J, Lu J, Zhao H, Zhang F, Wu J, Xu C, Du N, *et al*: **Neuraminidase and hemagglutinin matching patterns of a highly pathogenic avian and two pandemic H1N1 influenza A viruses.** *PloS one* 2010, **5:**e9167.
22. Gjelstrup LC, Kaspersen JD, Behrens MA, Pedersen JS, Thiel S, Kingshott P, Oliveira CL, Thielens NM, Vorup-Jensen T: **The role of nanometer-scaled ligand patterns in polyvalent binding by large mannan-binding lectin oligomers.** *J Immunol* 2012, **188:**1292–1306.
23. Matrosovich MN, Matrosovich TY, Gray T, Roberts NA, Klenk HD: **Human and avian influenza viruses target different cell types in cultures of human airway epithelium.** *Proc Natl Acad Sci USA* 2004, **101:**4620–4624.
24. Stevens J, Blixt O, Tumpey TM, Taubenberger JK, Paulson JC, Wilson IA: **Structure and receptor specificity of the hemagglutinin from an H5N1 influenza virus.** *Science* 2006, **312:**404–410.
25. Shinya K, Ebina M, Yamada S, Ono M, Kasai N, Kawaoka Y: **Avian flu: influenza virus receptors in the human airway.** *Nature* 2006, **440:**435–436.
26. Calfee DP, Peng AW, Hussey EK, Lobo M, Hayden FG: **Safety and efficacy of once daily intranasal zanamivir in preventing experimental human influenza A infection.** *Antiviral therapy* 1999, **4:**143–149.
27. Arndt U, Wennemuth G, Barth P, Nain M, Al-Abed Y, Meinhardt A, Gemsa D, Bacher M: **Release of macrophage migration inhibitory factor and CXCL8/interleukin-8 from lung epithelial cells rendered necrotic by influenza A virus infection.** *Journal of virology* 2002, **76:**9298–9306.
28. Lam WY, Yeung AC, Chu IM, Chan PK: **Profiles of cytokine and chemokine gene expression in human pulmonary epithelial cells induced by human and avian influenza viruses.** *Virology journal* 2010, **7:**344.
29. Garcia CC, Weston-Davies W, Russo RC, Tavares LP, Rachid MA, Alves-Filho JC, Machado AV, Ryffel B, Nunn MA, Teixeira MM: **Complement C5 activation during influenza A infection in mice contributes to neutrophil recruitment and lung injury.** *PloS one* 2013, **8:**e64443.
30. Burnet FM, Mc CJ: **Inhibitory and activating action of normal ferret sera against an influenza virus strain.** *Aust J Exp Biol Med Sci* 1946, **24:**277–282.
31. Anders EM, Hartley CA, Jackson DC: **Bovine and mouse serum beta inhibitors of influenza A viruses are mannose-binding lectins.** *Proc Natl Acad Sci USA* 1990, **87:**4485–4489.
32. Chang WC, White MR, Moyo P, McClear S, Thiel S, Hartshorn KL, Takahashi K: **Lack of the pattern recognition molecule mannose-binding lectin increases susceptibility to influenza A virus infection.** *BMC immunology* 2010, **11:**64.
33. Job ER, Deng YM, Tate MD, Bottazzi B, Crouch EC, Dean MM, Mantovani A, Brooks AG, Reading PC: **Pandemic H1N1 influenza A viruses are resistant to the antiviral activities of innate immune proteins of the collectin and pentraxin superfamilies.** *J Immunol* 2010, **185:**4284–4291.
34. Vorup-Jensen T: **On the roles of polyvalent binding in immune recognition: perspectives in the nanoscience of immunology and the immune response to nanomedicines.** *Advanced drug delivery reviews* 2012, **64:**1759–1781.
35. Gil M, McCormack FX, Levine AM: **Surfactant protein A modulates cell surface expression of CR3 on alveolar macrophages and enhances CR3-mediated phagocytosis.** *The Journal of biological chemistry* 2009, **284:**7495–7504.
36. Lund JM, Alexopoulou L, Sato A, Karow M, Adams NC, Gale NW, Iwasaki A, Flavell RA: **Recognition of single-stranded RNA viruses by toll-like receptor 7.** *Proc Natl Acad Sci USA* 2004, **101:**5598–5603.
37. McMichael AJ, Gotch FM, Noble GR, Beare PA: **Cytotoxic T-cell immunity to influenza.** *The New England journal of medicine* 1983, **309:**13–17.
38. Wilkinson TM, Li CK, Chui CS, Huang AK, Perkins M, Liebner JC, Lambkin-Williams R, Gilbert A, Oxford J, Nicholas B, *et al*: **Preexisting influenza-specific CD4+ T cells correlate with disease protection against influenza challenge in humans.** *Nature medicine* 2012, **18:**274–280.
39. Hardy S, Eichelberger M, Griffiths E, Weir JP, Wood D, Alfonso C: **Confronting the next pandemic–workshop on lessons learned from potency testing of pandemic (H1N1) 2009 influenza vaccines and considerations for future potency tests, Ottawa, Canada, July 27–29, 2010.** *Influenza and other respiratory viruses* 2011, **5:**438–442.
40. Douek DC, McFarland RD, Keiser PH, Gage EA, Massey JM, Haynes BF, Polis MA, Haase AT, Feinberg MB, Sullivan JL, *et al*: **Changes in thymic function with age and during the treatment of HIV infection.** *Nature* 1998, **396:**690–695.
41. Fagnoni FF, Vescovini R, Passeri G, Bologna G, Pedrazzoni M, Lavagetto G, Casti A, Franceschi C, Passeri M, Sansoni P: **Shortage of circulating naive CD8(+) T cells provides new insights on immunodeficiency in aging.** *Blood* 2000, **95:**2860–2868.
42. Rosenberg C: *Investigation of the immune responses induced after immunizatuion against the intracellular microorganisms Toxoplasma gondii and Hepatitis B virus (Ph.D. thesis).* Aarhus University, Dept of Biomedicine; 2012.
43. Castle SC: **Clinical relevance of age-related immune dysfunction.** *Clinical infectious diseases: an official publication of the Infectious Diseases Society of America* 2000, **31:**578–585.
44. Aspinall R, Andrew D: **Thymic involution in aging.** *Journal of clinical immunology* 2000, **20:**250–256.
45. Goronzy JJ, Lee WW, Weyand CM: **Aging and T-cell diversity.** *Experimental gerontology* 2007, **42:**400–406.
46. Kang I, Hong MS, Nolasco H, Park SH, Dan JM, Choi JY, Craft J: **Age-associated change in the frequency of memory CD4+ T cells impairs long term CD4+ T cell responses to influenza vaccine.** *J Immunol* 2004, **173:**673–681.
47. Rosenberg C, Bovin NV, Bram LV, Flyvbjerg E, Erlandsen M, Vorup-Jensen T, Petersen E: **Age is an important determinant in humoral and T cell responses to immunization with hepatitis B surface antigen.** *Human vaccines & immunotherapeutics* 2013, **9:**1466-1476.
48. Effros RB, Boucher N, Porter V, Zhu X, Spaulding C, Walford RL, Kronenberg M, Cohen D, Schachter F: **Decline in CD28+ T cells in centenarians and in long-term T cell cultures: a possible cause for both in vivo and in vitro immunosenescence.** *Experimental gerontology* 1994, **29:**601–609.
49. Vallejo AN: **CD28 extinction in human T cells: altered functions and the program of T-cell senescence.** *Immunological reviews* 2005, **205:**158–169.
50. Weng NP, Akbar AN, Goronzy J: **CD28(−) T cells: their role in the age-associated decline of immune function.** *Trends in immunology* 2009, **30:**306–312.
51. Jalilian B, Einarsson HB, Vorup-Jensen T: **Glatiramer acetate in treatment of multiple sclerosis: a toolbox of random co-polymers for targeting inflammatory mechanisms of both the innate and adaptive immune system?** *International journal of molecular sciences* 2012, **13:**14579–14605.
52. Cox RJ, Brokstad KA, Ogra P: **Influenza virus: immunity and vaccination strategies. Comparison of the immune response to inactivated and live, attenuated influenza vaccines.** *Scandinavian journal of immunology* 2004, **59:**1–15.
53. Swayne DE, Beck JR: **Heat inactivation of avian influenza and Newcastle disease viruses in egg products.** *Avian Pathol* 2004, **33:**512–518.

54. Matthews JT: **Egg-based production of influenza vaccine: 30 years of commercial experience.** *The Bridge* 2006, **36:**17–24.
55. Lambert LC, Fauci AS: **Influenza vaccines for the future.** *The New England journal of medicine* 2010, **363:**2036–2044.
56. Singh N, Pandey A, Mittal SK: **Avian influenza pandemic preparedness: developing prepandemic and pandemic vaccines against a moving target.** *Expert reviews in molecular medicine* 2010, **12:**e14.
57. Sedova ES, Shcherbinin DN, Migunov AI, Smirnov Iu A, Logunov D, Shmarov MM, Tsybalova LM, Naroditskii BS, Kiselev OI, Gintsburg AL: **Recombinant influenza vaccines.** *Acta naturae* 2012, **4:**17–27.
58. Lin SC, Huang MH, Tsou PC, Huang LM, Chong P, Wu SC: **Recombinant trimeric HA protein immunogenicity of H5N1 avian influenza viruses and their combined use with inactivated or adenovirus vaccines.** *PloS one* 2011, **6:**e20052.
59. Nemchinov LG, Natilla A: **Transient expression of the ectodomain of matrix protein 2 (M2e) of avian influenza A virus in plants.** *Protein expression and purification* 2007, **56:**153–159.
60. Huleatt JW, Nakaar V, Desai P, Huang Y, Hewitt D, Jacobs A, Tang J, McDonald W, Song L, Evans RK, *et al*: **Potent immunogenicity and efficacy of a universal influenza vaccine candidate comprising a recombinant fusion protein linking influenza M2e to the TLR5 ligand flagellin.** *Vaccine* 2008, **26:**201–214.
61. Rasoli M, Omar AR, Aini I, Jalilian B, Syed Hassan SH, Mohamed M: **Fusion of HSP70 gene of Mycobacterium tuberculosis to hemagglutinin (H5) gene of avian influenza virus in DNA vaccine enhances its potency.** *Acta virologica* 2010, **54:**33–39.
62. Donnelly J, Friedman A, Ulmer J, Liu M: **Further protection against antigenic drift of influenza virus in a ferret model by DNA vaccination.** *Vaccine* 1997, **15:**865–868.
63. Donnelly JJ, Friedman A, Martinez D, Montgomery DL, Shiver JW, Motzel SL, Ulmer JB, Liu MA: **Preclinical efficacy of a prototype DNA vaccine: enhanced protection against antigenic drift in influenza virus.** *Nature medicine* 1995, **1:**583–587.
64. Ulmer JB, Donnelly JJ, Parker SE, Rhodes GH, Felgner PL, Dwarki VJ, Gromkowski SH, Deck RR, DeWitt CM, Friedman A, *et al*: **Heterologous protection against influenza by injection of DNA encoding a viral protein.** *Science* 1993, **259:**1745–1749.
65. Justewicz DM, Morin MJ, Robinson HL, Webster RG: **Antibody-forming cell response to virus challenge in mice immunized with DNA encoding the influenza virus hemagglutinin.** *Journal of virology* 1995, **69:**7712–7717.
66. Donnelly JJ, Ulmer JB, Liu MA: **Immunization with DNA.** *J Immunol Methods* 1994, **176:**145–152.
67. Ulmer JB, Fu TM, Deck RR, Friedman A, Guan L, DeWitt C, Liu X, Wang S, Liu MA, Donnelly JJ, Caulfield MJ: **Protective CD4+ and CD8+ T cells against influenza virus induced by vaccination with nucleoprotein DNA.** *Journal of virology* 1998, **72:**5648–5653.
68. Gomez Lorenzo MM, Fenton MJ: **Immunobiology of influenza vaccines.** *Chest* 2013, **143:**502–510.
69. Vogel FR: **Improving vaccine performance with adjuvants.** *Clin Infect Dis* 2000, **30:**S266–S270.
70. Aucouturier J, Dupuis L, Ganne V: **Adjuvants designed for veterinary and human vaccines.** *Vaccine* 2001, **19:**2666–2672.
71. de Veer M, Meeusen E: **New developments in vaccine research–unveiling the secret of vaccine adjuvants.** *Discov Med* 2011, **12:**195–204.
72. Marrack P, McKee AS, Munks MW: **Towards an understanding of the adjuvant action of aluminium.** *Nat Rev Immunol* 2009, **9:**287–293.
73. McCartney S, Vermi W, Gilfillan S, Cella M, Murphy TL, Schreiber RD, Murphy KM, Colonna M: **Distinct and complementary functions of MDA5 and TLR3 in poly(I:C)-mediated activation of mouse NK cells.** *The Journal of experimental medicine* 2009, **206:**2967–2976.
74. Coffman RL, Sher A, Seder RA: **Vaccine adjuvants: putting innate immunity to work.** *Immunity* 2010, **33:**492–503.
75. Desmet CJ, Ishii KJ: **Nucleic acid sensing at the interface between innate and adaptive immunity in vaccination.** *Nat Rev Immunol* 2012, **12:**479–491.
76. Hem SL, Hogenesch H: **Relationship between physical and chemical properties of aluminum-containing adjuvants and immunopotentiation.** *Expert review of vaccines* 2007, **6:**685–698.
77. O'Hagan DT, Ott GS, Nest GV, Rappuoli R, Giudice GD: **The history of MF59 ((R)) adjuvant: a phoenix that arose from the ashes.** *Expert review of vaccines* 2013, **12:**13–30.
78. Garcon N, Vaughn DW, Didierlaurent AM: **Development and evaluation of AS03, an adjuvant system containing alpha-tocopherol and squalene in an oil-in-water emulsion.** *Expert review of vaccines* 2012, **11:**349–366.
79. de Jonge J, Schoen P, ter Veer W, Stegmann T, Wilschut J, Huckriede A: **Use of a dialyzable short-chain phospholipid for efficient solubilization and reconstitution of influenza virus envelopes.** *Biochimica et biophysica acta* 2006, **1758:**527–536.
80. Mbow ML, De Gregorio E, Valiante NM, Rappuoli R: **New adjuvants for human vaccines.** *Curr Opin Immunol* 2010, **22:**411–416.
81. Rappuoli R, Mandl CW, Black S, De Gregorio E: **Vaccines for the twenty-first century society.** *Nat Rev Immunol* 2011, **11:**865–872.
82. Gupta RK, Siber GR: **Comparison of adjuvant activities of aluminium phosphate, calcium phosphate and stearyl tyrosine for tetanus toxoid.** *Biologicals* 1994, **22:**53–63.
83. Didierlaurent AM, Morel S, Lockman L, Giannini SL, Bisteau M, Carlsen H, Kielland A, Vosters O, Vanderheyde N, Schiavetti F, *et al*: **AS04, an aluminum salt- and TLR4 agonist-based adjuvant system, induces a transient localized innate immune response leading to enhanced adaptive immunity.** *J Immunol* 2009, **183:**6186–6197.
84. Kuroda E, Coban C, Ishii KJ: **Particulate adjuvant and innate immunity: past achievements, present findings, and future prospects.** *Int Rev Immunol* 2013, **32:**209–220.
85. Hutchison S, Benson RA, Gibson VB, Pollock AH, Garside P, Brewer JM: **Antigen depot is not required for alum adjuvanticity.** *FASEB journal: official publication of the Federation of American Societies for Experimental Biology* 2012, **26:**1272–1279.
86. Lambrecht BN, Kool M, Willart MA, Hammad H: **Mechanism of action of clinically approved adjuvants.** *Curr Opin Immunol* 2009, **21:**23–29.
87. Brewer JM: **(How) do aluminium adjuvants work?** *Immunol Lett* 2006, **102:**10–15.
88. Edelman R: **Vaccine adjuvants.** *Rev Infect Dis* 1980, **2:**370–383.
89. Shoenfeld Y, Agmon-Levin N: **'ASIA' - autoimmune/inflammatory syndrome induced by adjuvants.** *J Autoimmun* 2011, **36:**4–8.
90. O'Hagan DT, Ott GS, De Gregorio E, Seubert A: **The mechanism of action of MF59 - an innately attractive adjuvant formulation.** *Vaccine* 2012, **30:**4341–4348.
91. Bernewitz R, Guthausen G, Schuchmann HP: **NMR on emulsions: characterisation of liquid dispersed systems.** *Magnetic resonance in chemistry: MRC* 2011, **49**(Suppl 1):S93–S104.
92. Cheetangdee N, Oki M, Fukada K: **The coalescence stability of protein-stabilized emulsions estimated by analytical photo-centrifugation.** *Journal of oleo science* 2011, **60:**419–427.
93. Dupuis M, Murphy TJ, Higgins D, Ugozzoli M, van Nest G, Ott G, McDonald DM: **Dendritic cells internalize vaccine adjuvant after intramuscular injection.** *Cell Immunol* 1998, **186:**18–27.
94. Ott G, Barchfeld GL, Chernoff D, Radhakrishnan R, van Hoogevest P, Van Nest G: **MF59. Design and evaluation of a safe and potent adjuvant for human vaccines.** *Pharm Biotechnol* 1995, **6:**277–296.
95. Carlson BC, Jansson AM, Larsson A, Bucht A, Lorentzen JC: **The endogenous adjuvant squalene can induce a chronic T-cell-mediated arthritis in rats.** *The American journal of pathology* 2000, **156:**2057–2065.
96. Durando P, Icardi G, Ansaldi F: **MF59-adjuvanted vaccine: a safe and useful tool to enhance and broaden protection against seasonal influenza viruses in subjects at risk.** *Expert opinion on biological therapy* 2010, **10:**639–651.
97. Partinen M, Saarenpaa-Heikkila O, Ilveskoski I, Hublin C, Linna M, Olsen P, Nokelainen P, Alen R, Wallden T, Espo M, *et al*: **Increased incidence and clinical picture of childhood narcolepsy following the 2009 H1N1 pandemic vaccination campaign in Finland.** *PloS one* 2012, **7:**e33723.
98. Nohynek H, Jokinen J, Partinen M, Vaarala O, Kirjavainen T, Sundman J, Himanen SL, Hublin C, Julkunen I, Olsen P, *et al*: **AS03 adjuvanted AH1N1 vaccine associated with an abrupt increase in the incidence of childhood narcolepsy in Finland.** *PloS one* 2012, **7:**e33536.
99. Mahlios J, De la Herran-Arita AK, Mignot E: **The autoimmune basis of narcolepsy.** *Current opinion in neurobiology* 2013:767-773.
100. Hirschfeld M, Ma Y, Weis JH, Vogel SN, Weis JJ: **Cutting edge: repurification of lipopolysaccharide eliminates signaling through both human and murine toll-like receptor 2.** *J Immunol* 2000, **165:**618–622.
101. Tapping RI, Akashi S, Miyake K, Godowski PJ, Tobias PS: **Toll-like receptor 4, but not toll-like receptor 2, is a signaling receptor for Escherichia and Salmonella lipopolysaccharides.** *J Immunol* 2000, **165:**5780–5787.

102. Evans JT, Cluff CW, Johnson DA, Lacy MJ, Persing DH, Baldridge JR: **Enhancement of antigen-specific immunity via the TLR4 ligands MPL adjuvant and Ribi.529.** *Expert review of vaccines* 2003, **2:**219–229.
103. Martin M, Michalek SM, Katz J: **Role of innate immune factors in the adjuvant activity of monophosphoryl lipid A.** *Infect Immun* 2003, **71:**2498–2507.
104. Tiberio L, Fletcher L, Eldridge JH, Duncan DD: **Host factors impacting the innate response in humans to the candidate adjuvants RC529 and monophosphoryl lipid A.** *Vaccine* 2004, **22:**1515–1523.
105. Verstraeten T, Descamps D, David MP, Zahaf T, Hardt K, Izurieta P, Dubin G, Breuer T: **Analysis of adverse events of potential autoimmune aetiology in a large integrated safety database of AS04 adjuvanted vaccines.** *Vaccine* 2008, **26:**6630–6638.
106. Chen WC, Huang L: **Non-viral vector as vaccine carrier.** *Adv Genet* 2005, **54:**315–337.
107. Daemen T, de Mare A, Bungener L, de Jonge J, Huckriede A, Wilschut J: **Virosomes for antigen and DNA delivery.** *Advanced drug delivery reviews* 2005, **57:**451–463.
108. Immordino ML, Dosio F, Cattel L: **Stealth liposomes: review of the basic science, rationale, and clinical applications, existing and potential.** *Int J Nanomedicine* 2006, **1:**297–315.
109. Flower DR: **Chapter 9 - towards the systematic discovery of immunomodulatory adjuvants.** *Immunomic Discovery of Adjuvants and Candidate Subunit Vaccines, Immunocomics Reviews* 2013:155–180.
110. Lillehoj HS, Ding X, Dalloul RA, Sato T, Yasuda A, Lillehoj EP: **Embryo vaccination against Eimeria tenella and E. acervulina infections using recombinant proteins and cytokine adjuvants.** *J Parasitol* 2005, **91:**666–673.
111. Solmesky LJ, Shuman M, Goldsmith M, Weil M, Peer D: **Assessing cellular toxicities in fibroblasts upon exposure to lipid-based nanoparticles: a high content analysis approach.** *Nanotechnology* 2011, **22:**494016.
112. Landesman-Milo D, Goldsmith M, Leviatan Ben-Arye S, Witenberg B, Brown E, Leibovitch S, Azriel S, Tabak S, Morad V, Peer D: **Hyaluronan grafted lipid-based nanoparticles as RNAi carriers for cancer cells.** *Cancer letters* 2013, **334:**221–227.
113. Korsholm KS, Andersen PL, Christensen D: **Cationic liposomal vaccine adjuvants in animal challenge models: overview and current clinical status.** *Expert review of vaccines* 2012, **11:**561–577.
114. Smith LR, Wloch MK, Ye M, Reyes LR, Boutsaboualoy S, Dunne CE, Chaplin JA, Rusalov D, Rolland AP, Fisher CL, *et al*: **Phase 1 clinical trials of the safety and immunogenicity of adjuvanted plasmid DNA vaccines encoding influenza A virus H5 hemagglutinin.** *Vaccine* 2010, **28:**2565–2572.
115. *Safety and Immunogenicity Study of Intramuscular CCS/C-adjuvanted Influenza Vaccine in Elderly.* [http://clinicaltrials.gov/ct2/show/NCT00915187?term=NCT00915187&rank=1]
116. Christensen D, Agger EM, Andreasen LV, Kirby D, Andersen P, Perrie Y: **Liposome-based cationic adjuvant formulations (CAF): past, present, and future.** *Journal of liposome research* 2009, **19:**2–11.
117. Schoenen H, Bodendorfer B, Hitchens K, Manzanero S, Werninghaus K, Nimmerjahn F, Agger EM, Stenger S, Andersen P, Ruland J, *et al*: **Cutting edge: mincle is essential for recognition and adjuvanticity of the mycobacterial cord factor and its synthetic analog trehalose-dibehenate.** *J Immunol* 2010, **184:**2756–2760.
118. Christensen D, Henriksen-Lacey M, Kamath AT, Lindenstrom T, Korsholm KS, Christensen JP, Rochat AF, Lambert PH, Andersen P, Siegrist CA, *et al*: **A cationic vaccine adjuvant based on a saturated quaternary ammonium lipid have different in vivo distribution kinetics and display a distinct CD4 T cell-inducing capacity compared to its unsaturated analog.** *Journal of controlled release: official journal of the Controlled Release Society* 2012, **160:**468–476.
119. Schellack C, Prinz K, Egyed A, Fritz JH, Wittmann B, Ginzler M, Swatosch G, Zauner W, Kast C, Akira S, *et al*: **IC31, a novel adjuvant signaling via TLR9, induces potent cellular and humoral immune responses.** *Vaccine* 2006, **24:**5461–5472.
120. Hemmi H, Kaisho T, Takeda K, Akira S: **The roles of toll-like receptor 9, MyD88, and DNA-dependent protein kinase catalytic subunit in the effects of two distinct CpG DNAs on dendritic cell subsets.** *J Immunol* 2003, **170:**3059–3064.
121. Weeratna RD, Brazolot Millan CL, McCluskie MJ, Davis HL: **CpG ODN can re-direct the Th bias of established Th2 immune responses in adult and young mice.** *FEMS Immunol Med Microbiol* 2001, **32:**65–71.
122. Hemmi H, Takeuchi O, Kawai T, Kaisho T, Sato S, Sanjo H, Matsumoto M, Hoshino K, Wagner H, Takeda K, Akira S: **A toll-like receptor recognizes bacterial DNA.** *Nature* 2000, **408:**740–745.
123. Heeg K, Zimmermann S: **CpG DNA as a Th1 trigger.** *Int Arch Allergy Immunol* 2000, **121:**87–97.
124. Silva BD, da Silva EB, Do Nascimento IP, dos Reis MCG, Kipnis A, Junqueira-Kipnis AP: **MPT-51/CpG DNA vaccine protects mice against mycobacterium tuberculosis.** *Vaccine* 2009, **27:**4402–4407.
125. Wu F, Yuan XY, Li J, Chen YH: **The co-administration of CpG-ODN influenced protective activity of influenza M2e vaccine.** *Vaccine* 2009, **27:**4320–4324.
126. Jalilian B, Omar A, Bejo M, Alitheen N, Rasoli M, Matsumoto S: **Development of avian influenza virus H5 DNA vaccine and MDP-1 gene of mycobacterium bovis as genetic adjuvant.** *Genetic Vaccines and Therapy* 2010, **8:**4.
127. Oveissi S, Omar AR, Yusoff K, Jahanshiri F, Hassan SS: **DNA vaccine encoding avian influenza virus H5 and Esat-6 of mycobacterium tuberculosis improved antibody responses against AIV in chickens.** *Comp Immunol Microbiol Infect Dis* 2010, **33:**491–503.
128. Noessner E, Gastpar R, Milani V, Brandl A, Hutzler PJS, Kuppner MC, Roos M, Kremmer E, Asea A, Calderwood SK, Issels RD: **Tumor-derived heat shock protein 70 peptide complexes are cross-presented by human dendritic cells.** *J Immunol* 2002, **169:**5424–5432.
129. Udono H, Yamano T, Kawabata Y, Ueda M, Yui K: **Generation of cytotoxic T lymphocytes by MHC class I ligands fused to heat shock cognate protein 70.** *Int Immunol* 2001, **13:**1233–1242.
130. Li J, Ye ZX, Li KN, Cui JH, Cao YX, Liu YF, Yang SJ: **HSP70 gene fused with hantavirus S segment DNA significantly enhances the DNA vaccine potency against hantaviral nucleocapsid protein in vivo.** *Vaccine* 2007, **25:**239–252.
131. Qazi KR, Wikman M, Vasconcelos NM, Berzins K, StaÃähl S, FernaÃÅndez C: **Enhancement of DNA vaccine potency by linkage of plasmodium falciparum malarial antigen gene fused with a fragment of HSP70 gene.** *Vaccine* 2005, **23:**1114–1125.
132. Fox CB, Kramer RM, Barnes VL, Dowling QM, Vedvick TS: **Working together: interactions between vaccine antigens and adjuvants.** *Ther Adv Vaccines* 2013, **1:**7–20.
133. Dufort S, Sancey L, Coll JL: **Physico-chemical parameters that govern nanoparticles fate also dictate rules for their molecular evolution.** *Advanced drug delivery reviews* 2012, **64:**179–189.
134. Vorup-Jensen T, Boesen T: **Protein ultrastructure and the nanoscience of complement activation.** *Advanced drug delivery reviews* 2011, **63:**1008–1019.
135. Holmskov U, Thiel S, Jensenius JC: **Collections and ficolins: humoral lectins of the innate immune defense.** *Annual review of immunology* 2003, **21:**547–578.
136. Carroll MC, Isenman DE: **Regulation of humoral immunity by complement.** *Immunity* 2012, **37:**199–207.
137. Gonzalez SF, Degn SE, Pitcher LA, Woodruff M, Heesters BA, Carroll MC: **Trafficking of B cell antigen in lymph nodes.** *Annual review of immunology* 2011, **29:**215–233.
138. Heesters BA, Chatterjee P, Kim YA, Gonzalez SF, Kuligowski MP, Kirchhausen T, Carroll MC: **Endocytosis and recycling of immune complexes by follicular dendritic cells enhances B cell antigen binding and activation.** *Immunity* 2013, **38:**1164–1175.
139. Fearon DT, Locksley RM: **The instructive role of innate immunity in the acquired immune response.** *Science* 1996, **272:**50–54.
140. Watanabe I, Ross TM, Tamura S, Ichinohe T, Ito S, Takahashi H, Sawa H, Chiba J, Kurata T, Sata T, Hasegawa H: **Protection against influenza virus infection by intranasal administration of C3d-fused hemagglutinin.** *Vaccine* 2003, **21:**4532–4538.
141. Mkrtichyan M, Ghochikyan A, Movsesyan N, Karapetyan A, Begoyan G, Yu J, Glenn GM, Ross TM, Agadjanyan MG, Cribbs DH: **Immunostimulant adjuvant patch enhances humoral and cellular immune responses to DNA immunization.** *DNA and cell biology* 2008, **27:**19–24.
142. Moghimi SM, Hunter AC, Andresen TL: **Factors controlling nanoparticle pharmacokinetics: an integrated analysis and perspective.** *Annual review of pharmacology and toxicology* 2012, **52:**481–503.
143. Szebeni J, Muggia F, Gabizon A, Barenholz Y: **Activation of complement by therapeutic liposomes and other lipid excipient-based therapeutic products: prediction and prevention.** *Advanced drug delivery reviews* 2011, **63:**1020–1030.

144. Batrakova EV, Kabanov AV: **Pluronic block copolymers: evolution of drug delivery concept from inert nanocarriers to biological response modifiers.** *Journal of controlled release: official journal of the Controlled Release Society* 2008, **130:**98–106.
145. Hamad I, Hunter AC, Moghimi SM: **Complement monitoring of pluronic 127 gel and micelles: suppression of copolymer-mediated complement activation by elevated serum levels of HDL, LDL, and apolipoproteins AI and B-100.** *Journal of controlled release: official journal of the Controlled Release Society* 2013, **170:**167–174.
146. Hartikka J, Geall A, Bozoukova V, Kurniadi D, Rusalov D, Enas J, Yi JH, Nanci A, Rolland A: **Physical characterization and in vivo evaluation of poloxamer-based DNA vaccine formulations.** *The journal of gene medicine* 2008, **10:**770–782.
147. Pedersen MB, Zhou X, Larsen EK, Sorensen US, Kjems J, Nygaard JV, Nyengaard JR, Meyer RL, Boesen T, Vorup-Jensen T: **Curvature of synthetic and natural surfaces is an important target feature in classical pathway complement activation.** *J Immunol* 2010, **184:**1931–1945.
148. Klein CP, de Groot K, Vermeiden JP, van Kamp G: **Interaction of some serum proteins with hydroxylapatite and other materials.** *Journal of biomedical materials research* 1980, **14:**705–712.
149. Tengvall P, Askendal A, Lundstrom I: **Studies on protein adsorption and activation of complement on hydrated aluminium surfaces in vitro.** *Biomaterials* 1998, **19:**935–940.
150. Pacheco PM, Le B, White D, Sulchek T: **Tunable complement activation by particles with variable size and Fc density.** *Nano LIFE* 2013, **3:**1341001–1341012.
151. Moghimi SM, Hamad I, Andresen TL, Jorgensen K, Szebeni J: **Methylation of the phosphate oxygen moiety of phospholipid-methoxy(polyethylene glycol) conjugate prevents PEGylated liposome-mediated complement activation and anaphylatoxin production.** *FASEB journal: official publication of the Federation of American Societies for Experimental Biology* 2006, **20:**2591–2593.
152. Thielens NM, Tacnet-Delorme P, Arlaud GJ: **Interaction of C1q and mannan-binding lectin with viruses.** *Immunobiology* 2002, **205:**563–574.
153. auf dem Keller U, Prudova A, Eckhard U, Fingleton B, Overall CM: **Systems-level analysis of proteolytic events in increased vascular permeability and complement activation in skin inflammation.** *Science signaling* 2013, **6:**rs2.
154. Heimlich JM, Regnier FE, White JL, Hem SL: **The in vitro displacement of adsorbed model antigens from aluminium-containing adjuvants by interstitial proteins.** *Vaccine* 1999, **17:**2873–2881.
155. Deng ZJ, Liang M, Monteiro M, Toth I, Minchin RF: **Nanoparticle-induced unfolding of fibrinogen promotes Mac-1 receptor activation and inflammation.** *Nature nanotechnology* 2011, **6:**39–44.
156. Vorup-Jensen T, Carman CV, Shimaoka M, Schuck P, Svitel J, Springer TA: **Exposure of acidic residues as a danger signal for recognition of fibrinogen and other macromolecules by integrin alphaXbeta2.** *Proc Natl Acad Sci USA* 2005, **102:**1614–1619.
157. Nakashima Y, Sun DH, Trindade MC, Maloney WJ, Goodman SB, Schurman DJ, Smith RL: **Signaling pathways for tumor necrosis factor-alpha and interleukin-6 expression in human macrophages exposed to titanium-alloy particulate debris in vitro.** *The Journal of bone and joint surgery American volume* 1999, **81:**603–615.
158. Schuck P, Zhao H: **The role of mass transport limitation and surface heterogeneity in the biophysical characterization of macromolecular binding processes by SPR biosensing.** *Methods Mol Biol* 2010, **627:**15–54.
159. Aderem A, Underhill DM: **Mechanisms of phagocytosis in macrophages.** *Annual review of immunology* 1999, **17:**593–623.
160. Zhang S, Li J, Lykotrafitis G, Bao G, Suresh S: **Size-Dependent Endocytosis of Nanoparticles.** *Adv Mater* 2009, **21:**419–424.
161. Rabinovitch M: **Professional and non-professional phagocytes: an introduction.** *Trends in cell biology* 1995, **5:**85–87.
162. Huang C, Zhang Y, Yuan H, Gao H, Zhang S: **Role of nanoparticle geometry in endocytosis: laying down to stand up.** *Nano letters* 2013.
163. Tollis S, Dart AE, Tzircotis G, Endres RG: **The zipper mechanism in phagocytosis: energetic requirements and variability in phagocytic cup shape.** *BMC systems biology* 2010, **4:**149.
164. Swanson JA: **Shaping cups into phagosomes and macropinosomes.** *Nature reviews Molecular cell biology* 2008, **9:**639–649.
165. Li J, Barreda DR, Zhang YA, Boshra H, Gelman AE, Lapatra S, Tort L, Sunyer JO: **B lymphocytes from early vertebrates have potent phagocytic and microbicidal abilities.** *Nature immunology* 2006, **7:**1116–1124.
166. Doolittle RF, Yang Z, Mochalkin I: **Crystal structure studies on fibrinogen and fibrin.** *Ann N Y Acad Sci* 2001, **936:**31–43.
167. Xie C, Zhu J, Chen X, Mi L, Nishida N, Springer TA: **Structure of an integrin with an alphal domain, complement receptor type 4.** *The EMBO journal* 2010, **29:**666–679.

doi:10.1186/2052-8426-1-2
Cite this article as: Jalilian *et al.*: Properties and prospects of adjuvants in influenza vaccination - messy precipitates or blessed opportunities? *Molecular and Cellular Therapies* 2013 **1**:2.

Regarding MD/PhD student, Translational Molecular Medicine
Halldór Bjarki Einarsson, GP 10 program, Aarhus University

The work described in the PhD dissertation was carried out at the Spinal Unit Aarhus University Hospital, Department of Biomedicine, Aarhus University and Yale University School of Medicine. In addition, the Graduate School's integrated MD/PhD program at Aarhus University (GP Biomedicine) was followed. The PhD dissertation is based on a monograph with incorporated 7 interconnected studies. Supplementary work performed during the course of the MD/PhD program is included under appendix. A summary, including declaration concerning the monograph has been signed by the PhD student and the main supervisor.

I. ***Monograph:*** New Resorption Pathways in Polycaprolactone Degradation; roles of Mononuclear and Multinucleated Giant Cells

Aim: to study target effects of multinucleated giant cells on the foreign body material polycaprolactone (PCL). Hypothesis: degradation of PCL by hydrolysis is further directed by resorption mediated by mononuclear and multinucleated giant cells. Methods: in this study we used human peripheral blood mononuclear cells (PBMCs) from healthy donors (n=3). Both monocytes and T lymphocytes were isolated by negative selection, i.e. tube-based magnetic separation with Dynabeads®. Monocytes were either seeded on PCL at fusiogenic density in monoculture or in co-culture with T lymphocytes at the ratio 2:1. Beta 2/CD18 integrin facilitated cell-to-material attachment and migration capabilities were analyzed by time-resolved immunofluorometric assay and confocal imaging. We prepared foreign body PCL constructs (MW = 50 kDa, Perstorp, UK), by mold design for dynamic mechanical analysis as Bose ElectroForce 3200 was used after 21 days of fusiogenic PBMC culturing. Then new sets of PCL constructs was produced by electrospinning, both pure constructs and additionally with incorporated 1 µm fluorescent carboxyl polymer microspheres, as to enable qualitative (confocal and electron scanning microscopy) and quantitative (flow cytometry) analysis for the PCL cell mediated degradation itself. Parallel to this *in vitro* study, we performed a paired *in vivo* cranial bone defect model study, on female Landrace pigs (n=3) as to investigate for multinucleated giant cell and T lymphocyte recruitment at the site of PCL implantation. Results: our *in vivo* data indicate formation of granulomas associated to implanted PCL scaffolds. These granulomas are composed of syncytium or tartrate-resistant acid phosphatase (TRAP) negative multinucleated giant cells and CD3 receptor positive cells, suggesting fusion of macrophages, hence formation of foreign body giant cells and T lymphocyte recruitment. By our *in vitro* study we show an increased release of the 1µm fluorescent microspheres from the electrospun PCL constructs into the microenvironment, post 7 days of multinucleated giant cell culturing. This phenomenon is even further enhanced after the addition of T lymphocytes at the ratio 2:1 into the culture system. Moreover, we find a significant increase in the shedding of CD18 by the multinucleated giant cells when those are exposed and attached to PCL compared to non-material exposure. These results indicate the immunogenicity of PCL in addition to the observed complement activation. Our data show that the shedding ultimately can result in CD18 binding to extracellular matrix (ECM) compounds left behind during cell migration. The results are in an alignment with our dynamic mechanical analysis data, which indicate increased material stiffness after 21 days of multinucleated giant cell culturing. Conclusion: degradation of PCL by hydrolysis is further directed by resorption and phagocytosis prior to complement component opsonization mediated by mononuclear (pre-cursors) and multinucleated giant cells. This effect is enhanced in the presence of T lymphocytes. We conclude that the initial increased material stiffness after 21 days of cell culturing, is a result of material attached ECM and due to the adhesion molecules.

Supplementary work; pre-graduate MD/PhD period

II. ***Paper:*** Cui W, Cuartas E, Ke J, Zhang Q, Einarsson HB, Sedgwick JD, Li J, Vignery A. CD200 and its receptor, CD200R, modulate bone mass via the differentiation of osteoclasts. Proc Natl Acad Sci USA. 2007; 104(36):14436-41

Aim: to identify undescribed components of the machinery of macrophage fusion. Hypothesis: we postulated that the CD200-CD200R axis might play a role in the fusion of macrophages. Methods: $CD200^{-/-}$ mice were produced by homologous recombination, as described by Hoek et al (1). Bone-marrow derived macrophages and osteoclasts were generated from 6- to 12-week old $CD200^{-/-}$, and $CD200^{+/+}$ mice were prepared as before (2). Data (n=3-6) were generated by immunohistochemical analysis, light and confocal microscopy imaging, micro CT and bone densitometry, flow cytometry, RT-PCR in addition to western blotting. To identify previously undescribed components of the machinery of macrophage fusion, we submitted fusing alveolar macrophages from rats to genome-wide microarray analysis. Results: We found that the expression of CD200 was potently induced *de novo* in macrophages at the onset of fusion, and that osteoclasts deficient in CD200 had a defect in multinucleation and in signaling downstream of receptor activator of NF-κB (RANK), which are essential for osteoclastogenesis. We also found that CD200-deficient mice had a lower number of osteoclasts and a higher bone density than wild-type mice. Conclusion: together, our observations indicate that the CD200-CD200R axis plays a central role in the fusion of macrophages and the formation of osteoclasts. As stated in the manuscript: WC, EC, JK, QZ, HBE, and JL performed research and like indicated by the research year thesis HBE's contribution is a part of his PhD dissertation.

Supplementary work; post-graduate MD/PhD period

III. ***Paper:*** Greisen SR, Einarsson HB, Hvid M, Hauge E, Deleuran B, Kragstrup TW. Spontaneous generation of functional osteoclasts from synovial fluid mononuclear cells as a model of inflammatory osteoclastogenesis. Manuscript submitted to Acta Pathologica, Microbiologica et Immunologica Scandinavica

Aim: to provide a simple model for investigating inflammatory osteoclastogenesis. Hypothesis: we hypothesized that synovial fluid mononuclear cells (SFMCs) isolated from inflamed peripheral joints of patients with rheumatoid arthritis (RA) and spondyloarthritis (SpA) possess the ability to spontaneously develop into functional osteoclasts *ex vivo*. Methods: we used healthy human control PBMCs isolated from buffy coats. For both culture setups, controls (n=6) and SFMCs (n=12) were exposed to RANK ligand and M-CSF at the same concentration levels as described in the monograph. Post 21 days of culturing, cells were analyzed for pheno- and genotypic osteoclast characteristics, by TRAP-staining and light microscopy imaging, followed by qPCR and ELISA. Furthermore, the *in vitro* generated osteoclast-like cell resorption capabilities were determined by investigating for lacunae formations after pre-cursor cell seeding on dentin plates. Results: to evaluate osteoclast activity and differentiation we measured TRAP and MMP-9 secretion in the SFMC cultures at different time points. Both TRAP and MMP-9 secretion increased significantly (all $p < 0.05$). By adding RANKL and M-CSF to the SFMC cultures potentiated the spontaneous formation of multinucleated TRAP positive osteoclasts from 10.2% [3.3%-10.5%] to 14.2% [13.3%-16.3%] and significantly increased TRAP secretion ($p = 0.028$) which moreover was the tendency for the secretion of MMP-9. In addition to the evident SFMC induced dentin resorption, mRNA of the calcitonin receptor, cathepsin K and the β_3 chain of the $\alpha_v\beta_3$ integrin complex were all present in the SFMC lysates. Conclusion: in this study we provide a method for studying inflammatory genesis of osteoclasts and appreciate the method as a suitable *ex vivo* model for testing treatments regulating or mediators potentiating osteoclast formation and activity.

Other supplementary work; post-graduate MD/PhD period

IV. ***Paper:*** Jalilian B, Christiansen SH, Einarsson HB, Mehdi R, Petersen E, Vorup-Jensen T. Properties and prospects of adjuvants in influenza vaccination – messy precipitates or blessed opportunities? Molecular and Cellular Therapies, 2013 Vol. 1,2

V. ***Paper:*** Jalilian B, Einarsson HB, Vorup-Jensen T. Glatiramer acetate in treatment of multiple sclerosis: a toolbox of random co-polymers for targeting inflammatory mechanisms of both the innate and adaptive immune system? Int J Mol Sci. 2012; 13(11): 14579-605

1) Down-regulation of the macrophage lineage through interaction with OX2 (CD200). Hoek RM, Ruuls SR, Murphy CA, Wright GJ, Goddard R, Zurawski SM, Blom B, Homola ME, Streit WJ, Brown MH, Barclay AN, Sedgwick JD. Science. 2000 Dec 1;290(5497):1768-71.

2) Li H, Cuartas E, Cui W, Choi Y, Crawford TD, Ke HZ, Kobayashi KS, Flavell RA, Vignery A. IL-1 receptor-associated kinase M is a central regulator of osteoclast differentiation and activation. J Exp Med. 2005 Apr 4;201(7):1169-77.

Declaration concerning the monograph

Contributions by others

Department of Orthopaedic Surgery, Aarhus University Hospital
Jonas Jensen, MD, PhD designed and launched the animal study. Furthermore, he performed the surgery. Laboratory technicians Anette Baatrup, Jane Pauli and Anna Bay Nielsen helped with improvements and editing of protocols, qPCR, in addition to assistance in regard to preparation and sectioning of tissue samples.

Aarhus University School of Engineering
Associate professor Jens V. Nygaard & Anders Frisk Mortensen, M.Eng, contributed considerably to the dynamic mechanical analysis study.

Aarhus University School of Dentistry
Associate professor David Christian Evar Kraft & laboratory technician Sussi Madsen provided the dentin plates.

The Interdisciplinary Nanoscience Center (iNANO), Aarhus University
Assistant professor Menglin Chen & Søren Roesgaard Nielsen, M.Sci, PhD student provided the electrospun PCL fibers and contributed to the SEM imaging.

Department of Biomedicine, Aarhus University
Associate professor Morten Schallburg Nielsen performed the 3D-confocal and IMARIS imaging. Associate professor Mette Bjerre (Clinical Medicine), laboratory technicians Bettina Winther Grumsen & Anette Thomsen (The FACS Core Facility) all supported the project in a pivotal manner by technical help and laboratory bench work assistance, concerning both TRIFMA and flow cytometry.

Summary of the PhD student's share of the work
The PhD candidate, Halldór Bjarki Einarsson, has formulated the hypothesis and aims of the monograph, with the application of appropriate methodology. Moreover, the PhD student was centrally involved in all laboratory aspects of the studies, performing the great majority of these demanding techniques himself, either alone or in collaboration with his co-workers as specified above. Identification of scientific difficulties, as well as planning of the experimental work and interpretation of the gained data, was primarily done by the PhD student himself. The monograph was solely written by the PhD student.

Sincerely yours
24th of February 2015

Main supervisor
Professor Cody Eric Bünger, MD, DMSc
Department of Orthopaedics, Spine Unit
Aarhus University Hospital, Denmark

24th of February 2015

PhD student
Halldór Bjarki Einarsson, MD
Orthopaedic Research Laboratory
Aarhus University Hospital, Denmark